Fractionation and Purification of Syringaldehyde and Vanillin from Oxidation of Lignin

Dissertation presented to Faculdade de Engenharia da Universidade do Porto for the PhD degree in Chemical and Biological Engineering

by

Maria Inês Ferreira da Mota

Supervisor: Dr. Paula Cristina de Oliveira Rodrigues Pinto

Co-supervisor: Prof. Dr. Alírio Egídio Rodrigues

Laboratory of Separation and Reaction Engineering - Associate Laboratory LSRE-LCM

Department of Chemical Engineering, Faculty of Engineering, University of Porto

March 2017

FEUP, LSRE-LCM - Universidade do Porto

Inês Mota gratefully acknowledges her Ph.D. scholarship (SFRH/BD/91582/2012) from Fundação para a Ciência e Tecnologia (FCT). This work was financially supported by: Project POCI-01-0145-FEDER- 006984 – Associate Laboratory LSRE-LCM funded by FEDER through COMPETE2020 - Programa Operacional Competitividade e Internacionalização (POCI) – and by national funds through FCT - Fundação para a Ciência e a Tecnologia.

Acknowledgments

Começo por agradecer ao meu co-orientador, o professor Alírio Rodrigues, pela oportunidade que me deu de integrar na sua equipa. Serei sempre grata por todos os conhecimentos e ensinamentos que me transmitiu durante estes 4 anos e que me permitiram crescer profissionalmente e aprender.

Não existem palavras no mundo que descrevam a enorme gratidão que tenho pela minha orientadora, Drª. Paula Pinto, que me pescou e me ajudou a concretizar um sonho. Para além de uma excelente orientadora, foi sempre minha amiga e muito disponível para me apoiar neste percurso. Os seus conselhos, dedicação, paciência e entusiasmo foram essenciais a este trabalho e deram-me ânimo e vontade de continuar em frente a ultrapassar as dificuldades. Desbravamos juntas muito terreno, ultrapassamos muitos desafios e aqui está o fruto do nosso trabalho!

Ao professor José Miguel Loureiro, agradeço de coração a sua paciência e disponibilidade para me ajudar, orientar e ensinar. As suas aulas de gabinete despertam-me a curiosidade para muitos assuntos e foram essenciais para o meu trabalho e crescimento.

À Mafalda, ao Alexandre e ao Rui agradeço todo o precioso apoio que me deram e observações pertinentes que me ajudaram a enriquecer o meu trabalho.

Aos meus amigos e colegas de gabinete e de laboratório que me ajudaram de muitas maneiras diferentes e tornam os meus dias mais agradáveis e felizes! À minha companheira de gabinete, de laboratório, de pausas para café, de reclamações, de tristezas e de risadas, à Carina. Obrigada pela tua alegria contangiante e pela tua paciência e apoio, pois não é fácil aturar uma sindicalista!

Um agradecimento com muito carinho aos meus amigos mais chegados e família, em especial, os meus primos, maninha e cunhadinho: vocês são dos tesouros mais importantes que eu tenho e a vossa presença e apoio são essenciais na minha vida. Maninha, serás sempre a minha musa e a minha alma gémea.

Ao meu Zezito, obrigada por estares ao meu lado sempre com muito carinho, paciência e compreensão. Sou uma privilegiada de te ter na minha vida pois ela fica mais preenchida e feliz.

Por fim, agradeço às pessoas mais importantes da minha vida, aos meus Pais. Não tenho palavras para descrever todo o apreço e gratidão que tenho por vocês, que sempre me deram amor incondicional, que sempre me deram apoio em todas as minhas decisões e caminhos e que sempre se sacrificaram para, acima de tudo, eu e a minha irmã sermos felizes e mulheres concretizadas. Ida e Manuel, vocês são a minha inspiração, os meus modelos a seguir! Foram vocês que me ensinaram a lutar pelos sonhos e a ultrapassar os desafios com um sorriso no rosto. A vocês devo tudo o que tenho e a vocês dedico todas as minhas conquistas!

Dedico a tese aos meus Pais e Irmã

Abstract

The present work is within the scope of valorising lignin-rich side streams resulting from lignocellulosic biomass processing in order to obtain purified fractions of added value phenolic compounds, in particular, vanillin and syringaldehyde.

The main goal is to contribute with new insights for the integrated oxidation and separation process suggested by the LA LSRE-LCM in the 90's. In this regard, the studies developed herein can be divided in two main parts:

- Studies with synthetic solutions prepared with some of the phenolic compounds present in oxidized lignin solutions (vanillin, syringaldehyde, vanillic and syringic acids, among others) in order to i) assess the feasibility of employing non-polar resins to adsorb vanillin and syringaldehyde and ii) study the recovery and concentration of the adsorbed phenolic compounds using ethanolic solutions; Finally, evaluate the potential of employing a supercritical fluid chromatographic process with CO_2 to separate vanillin and syringldehyde from other phenolic monomers;

- Demonstration of the integration of membrane separation, adsorption/desorption and supercritical fluid chromatographic processes starting with an oxidized kraft black liquor solution.

Mono-component equilibrium adsorption batch studies of vanillin, syringaldehyde and respective acids in aqueous solution, were performed onto macropourous styrene-divinylbenzene resins (XAD16N and SP700). The adsorption equilibrium isotherms for three different temperatures were found for each compound and equilibrium data fitted by Langmuir, Bi-Langmuir and Freundlich models. Fixed bed studies with SP700 resin were performed for each compound at different temperatures and feed concentrations and experimental results described with the axial dispersion model and linear driving force approximation to represent the intraparticle mass transfer.

In order to overcome the disadvantage of desorbing the phenolic compounds with water, which proved to be a time consuming process, adsorption/desorption studies with ethanol:water (90:10, % V/V) were performed for different temperatures and vanillin and syringaldehyde feed concentrations with the SP700 resin. The breakthrough curves obtained were described by a similar mathematical model used in the adsorption experiments performed in aqueous medium. Moreover, fixed bed desorption studies employing ethanol:water (90:10, % V/V) solutions were conducted after loading the SP700 bed with aqueous solutions of vanillin, syringaldehyde, and vanillic and syringic acids.

A three-stage membrane fractionation sequence of an oxidized industrial kraft liquor diluted and enriched in some of the phenolic compounds of interest was carried out with the molecular weight cut-off tubular ceramic membranes of 50, 5 and 1 kDa. The main goal was to obtain a final permeate stream depleted in the higher molecular weight lignin fragments and richer in the phenolic monomers of interest. The efficiency of each stage was analysed regarding the permeate flux obtained and membrane intrinsic and fouling resistances observed. Each stream of the fractionation process (feed, permeates and retentantes) was characterized regarding total non-volatile solids, ashes and phenolic compounds quantified by HPLC-UV, in order to obtain the respective membrane apparent rejection coefficients and evaluate the composition changes in each stream.

The permeates obtained after 5 and 1 kDa membrane stage processing were loaded onto a bed packed with SP700 prior to pH value correction with H_2SO_4 from 10 to 8. The SP700 resin bed was saturated with the permeate 1 kDa and adsorption/desorption cycles with the permeates 5 and 1 kDa. The adsorbed coumpounds were recovered with an ethanol:water (90:10, % V/V) solution and the composition of the final eluates obtained characterized in the same parameters used in membrane processing.

A final stage of the ethanolic eluates purification was evaluated using CO_2 supercritical fluid chromatography employing the best set of operating conditions previously established with synthetic solutions among temperature, flowrate, amount of methanol and formic acid as the co-solvent and additive, respectively.

Resumo

O presente trabalho insere-se no âmbito da valorização de correntes secundárias ricas em lenhina resultantes do processamento de biomassa lenhocelulósica com o propósito de se obter fracções purificadas de compostos fenólicos com valor acrescentado, em particular, vanilina e seringaldeído.

O principal objetivo é contribuir com novos conhecimentos científicos para o processo integrado de oxidação e separação sugerido pelo LA LSRE-LCM nos anos 90. Desta forma, os estudos aqui desenvolvidos podem ser divididos em duas partes principais:

- Estudos com soluções sintéticas preparadas com alguns dos compostos fenólicos presentes em soluções de lenhina oxidadas (vanilina, seringaldeído, ácidos vanílico e seríngico, entre outros) para: i) avaliar a viabilidade do uso de resinas não polares para adsorver vanilina e seringaldeído e ii) estudar a recuperação e concentração dos compostos fenólicos adsorvidos recorrendo a soluções etanólicas; Finalmente, avaliar o potencial de aplicar um processo de cromatografia supercrítica com CO_2 para separar a vanilina e o seringaldeído de outros monómeros fenólicos;

- Demonstração da integração dos processos de separação por membranas, adsorção / dessorção e cromatografia supercrítica partindo de uma solução de licor negro kraft oxidada, diluída;

Estudos monocomponente de equilíbrio de adsorção de vanilina, seringaldeído e respectivos ácidos foram realizados em sistema descontínuo e meio aquoso sobre resinas macroporosas de estireno-divinilbenzeno (SP700 e XAD16N). Obtiveram-se as isotérmicas de equilíbrio de adsorção a três temperaturas para cada composto e os dados de equilíbrio foram descritos com os modelos de Langmuir, Bi-Langmuir e Freundlich. Para cada composto, realizaram-se estudos em leito fixo a diferentes temperaturas e concentrações de alimentação com a resina SP700 e os resultados experimentais foram descritos com o modelo dispersão axial e aproximação de força motriz linear para descrever a resistência à transferência de massa intraparticular.

De forma a ultrapassar a desvantagem de desorção dos compostos fenólicos com água, que revelou ser um processo moroso, realizaram-se estudos de adsorção/desorção com etanol:água (90:10, % V/V) a diferentes temperaturas e concentrações de alimentação de vanilina e seringaldeído com a resina SP700. As curvas de ruptura obtidas foram descritas com um modelo matemático semelhante ao usado nos ensaios realizados em meio aquoso. Mais ainda, foram efetuados estudos de desorção em leito fixo com uma solução de etanol:água (90:10, % V/V) após saturação do leito com soluções aquosas de vanilina, seringaldeído e ácidos vanílico e seríngico.

Uma sequência de fraccionamento por membrana de licor kraft industrial previamente oxidado, diluído e enriquecido em alguns dos compostos fenólicos de interesse foi efetuado em três etapas

com membranas cerâmicas tubulares de peso molecular de corte de 50, 5 e 1 kDa. O principal objectivo foi obter uma corrente final de permeado empobrecida em fragmentos de lenhina de maior peso molecular e rica nos monómeros fenólicos de interesse. A eficiência de cada etapa foi analisada quanto ao fluxo de permeado obtido e aos coeficientes de resistência intrínseca da membrana e gerada por fouling calculados. Cada corrente obtida do fraccionamento de membranas (alimentação, permeados e concentrados) foi caracterizada em relação aos sólidos totais não voláteis, cinzas e compostos fenólicos quantificados por HPLC-UV, de forma a obter os respectivos coeficientes de rejeição aparentes da membrana e avaliar as alterações de composição em cada corrente do processo.

Os permeados obtidos após as etapas de processamento com as membranas de 5 e 1 kDa foram alimentados num leito empacotado com a resina SP700 após correcção do valor de pH com H_2SO_4 de 10 para 8. Foi efectuado um ensaio de saturação do leito com o permeado 1 kDa e ciclos de adsorção/desorção com os permeados 5 e 1 kDa. Os compostos adsorvidos foram recuperados com uma solução de etanol:água (90:10, % V/V) e os respectivos eluatos caracterizados nos mesmos parâmetros usados no processamento de membranas.

Uma etapa final de purificação dos eluatos etanólicos obtidos foi avaliada recorrendo a cromatografia supercrítica com CO_2 aplicando o conjunto de condições operacionais previamente estabelecidos com soluções modelo entre as quais, temperatura, caudal, quantidade de metanol e ácido fórmico adicionados como co-solvente e aditivo, respectivamente.

Table of contents

List of Figures

Chapter 1

Chapter 2

Chapter 3

Chapter 4

Chapter 5

Chapter 6

Chapter 7

Appendices

List of Tables

Chapter 2

Chapter 3

Chapter 4

Chapter 5

Chapter 6

Appendices

List of symbols

Nomenclature

a_S	specific surface area of the resin	(m^2 g^{-1})
A_m	membrane surface area.	(m^2)
$C_{i,e}$	equilibrium concentration of species '*i*' in the bulk solution	(g L^{-1})
$C_{j,e}$	equilibrium concentration of species '*j*' in the bulk solution	(g L^{-1})
$C_{i,0}$	initial concentration of species '*i*' (batch bottle point method)	(g L^{-1})
$C_{i,feed}$	concentration at column inlet for the species '*i*'	(g L^{-1})
C_i	concentration in the bulk fluid phase for the species '*i*'	(g L^{-1})
$C_{P,i}$	concentration of the solute in the permeate	(g L^{-1})
$C_{R,i}$	concentration of the solute in the retentate	(g L^{-1})
d_p	particle diameter	(m)
D_{ax}	axial dispersion coefficient	(m^2 min^{-1})
$D_{pe,i}$	effective pore diffusivity	(m^2 min^{-1})
$D_{m,i}$	molecular diffusivity	(m^2 min^{-1})
f_h	dry particle to wet particle mass ratio	($g_{dry\ resin}$ g^{-1}_{resin})
J_P	permeate flux	(m^3 s^{-1} m^{-2})
J_w	water permeate flux	(m^3 s^{-1} m^{-2})
K_{Lin}	equilibrium distribution coefficient for Linear isotherm	(L $g^{-1}_{dry\ resin}$)
$K_{L,i}$	Langmuir equilibrium constant for species '*i*'	(L g^{-1})
$K_{L1,i}$	Langmuir equilibrium constant for species '*i*' and adsorption site 1	(L g^{-1})
$K_{L2,i}$	Langmuir equilibrium constant for species '*i*' and adsorption site 2	(L g^{-1})
$K_{L1,j}$	Langmuir equilibrium constant for species '*j*' and adsorption site 1	(L g^{-1})
$K_{L2,j}$	Langmuir equilibrium constant for species '*j*' and adsorption site 2	(L g^{-1})
$K_{F,i}$	Freundlich constant for species '*i*'	(g $g^{-1}_{dry\ resin}$) (L g^{-1})$^{1/n}$
K_x	Langmuir equilibrium constant	(L g^{-1})
K_x^o	equilibrium constant	(L g^{-1})
k_s	overall effective mass transfer coefficient (which includes intraparticle and film mass resistances).	(min^{-1})
k_f	external film mass transfer coefficient	(m min^{-1})
k_{LDF}	linear driving force kinetic rate constant	(min^{-1})
L_b	bed length	(m)

L_p	Membrane permeability	(m^3 s^{-1} m^{-2} Pa^{-1})
n	Freundlich exponent	(dimensionless)
Pe	Peclet number	(dimensionless)
$q_{i,e}$	adsorbed phase concentration of species 'i' at equilibrium with $C_{i,e}$	(g $g^{-1}_{dry\ resin}$)
$q_{m,i}$	maximum adsorption capacity of species 'i'	(g $g^{-1}_{dry\ resin}$)
$q_{i,feed}$	adsorbed phase concentration of species 'i' in equilibrium with $C_{i,feed}$	(g $g^{-1}_{dry\ resin}$)
$q_{ads,exp}$	experimental adsorbed phase concentration	(g $g^{-1}_{dry\ resin}$)
$q_{ads,pred}$	predicted adsorbed phase concentration	(g $g^{-1}_{dry\ resin}$)
$q_{des,exp}$	experimental desorbed phase concentration	(g $g^{-1}_{dry\ resin}$)
$\frac{dq_i^*}{dC_i}$	slope of the adsorption equilibrium isotherm	-
q_i	average adsorbed phase concentration of species 'i' in the adsorbent particles	(g $g^{-1}_{dry\ resin}$)
q_i^*	adsorbed phase concentration of species 'i' in equilibrium with the bulk concentration C_i	(g $g^{-1}_{dry\ resin}$)
Q	feed flowrate	(m^3 min^{-1})
Q_P	permeate flowrate measured for a certain TMP	(m^3 s^{-1})
R_m	membrane hydraulic resistance	(m^{-1})
R_T	total membrane resistance	(m^{-1})
R_f	fouling resistance	(m^{-1})
$R_{f,irrev}$	irreversible fouling resistance	(m^{-1})
$R_{f,rev}$	reversible fouling resistance	(m^{-1})
R_i	apparent rejection coefficient	(%)
r_p	radius of the resin particle	(m)
r_{pores}	pore radius	(Å)
R	ideal gas constant	(kJ mol^{-1} K^{-1})
Re	Reynolds number	(dimensionless)
Sh	Sherwood number	(dimensionless)
Sc	Schmidt number	(dimensionless)
t	time	(min)
T	absolute temperature	(K)
$t_{st,exp}$	experimental stoichiometric time	(min)
$t_{st,pred}$	predicted stoichiometric time	(min)
u_i	interstitial velocity	(m min^{-1})

TMP	transmembrane pressure	(Pa)
V_p	volume of pores	(mL g^{-1})
V	solution volume (batch bottle point method)	(L)
V_b	volume of the bed	(m^3)
$V_{m,i}$	molar volume of solute at its normal boiling point	(cm^3 mol^{-1})
VCF	volume concentration factor	
V_F	feed solution volume amount	(L)
V_R	retentate volume amount	(L)
W	weight of dry resin (batch bottle point method)	($g_{dry\ resin}$)
z	axial position	(m)

Greek letters

$\Delta H_{isosteric}$	isosteric enthalpy of adsorption	(kJ mol^{-1})
ΔH	adsorption enthalpy	(kJ mol^{-1})
ε_P	particle porosity	(L_{pores} $L^{-1}_{particle}$)
ε_b	bed porosity	
μ	viscosity of the solution	(cP)
μ_s	viscosity of the solution used in each membrane stage	(Pa s)
ρ_{app}	particle apparent density	($g_{wet\ resin}$ $L^{-1}_{wet\ resin}$)
ρ	density of the solution	(g cm^{-3})
τ	tortuosity factor	(dimensionless)
ν	kinematic viscosity	(cSt)
ϕ	association factor of the solvent	(dimensionless)
Ω	linear driving force shape factor	(dimensionless)
κ	nominal constant equal to 0.004 cSt s^{-1} for viscometer series 50 and 0.008 cSt s^{-1} for viscometer series 75	(cSt s^{-1})

Subscripts and superscripts

NC	number of species
i, j	species

List of acronyms

OV	acetovanillone
OS	acetosyringone
p*K*a	acid dissociation constant
ATPS	aqueous two-phase systems
ashes	ash content
BV	bed volume
CO_2	carbon dioxide
cp	critical point
K_D	distribution ratio or partition coefficient
α	extraction selectivity
α_{ij}	extraction selectivity between solute i and j
ferAc	ferulic acid
fV	formylvanillin
GPC	gel permeation chromatography
***p*-OHB**	*p*-hydroxybenzaldehyde
IL	ionic liquid
ILs	ionic liquids
IKL	industrial kraft liquor
LLE	liquid-liquid extraction
LDF	linear driving force
PDVB/PAEM IPN	macroporous polydivinylbenzene / polyacrylethylenediamine interpenetrating polymer networks
MV	methyl vanillate
MTBE	methyl-tert-butyl ether
MIP	molecularly imprinted polymers
MWCO	Molecular weight cut-off
NF	nanofiltration
SSR	sum of square residuals
PEBA	polyether-polyamide block-copolymer
P_{50kDa}	permeate stream obtained from processing with 50kDa membrane
P_{5kDa}	permeate stream obtained from processing with 5kDa membrane
P_{1kDa}	permeate stream obtained from processing with 1kDa membrane
R_{50kDa}	retentate stream obtained from processing with 50kDa membrane
R_{5kDa}	retentate stream obtained from processing with 5kDa membrane
R_{1kDa}	retentate stream obtained from processing with 1kDa membrane

SRMBR	perstraction silicon rubber membrane bioreactor
SFE	supercritical fluid extraction
ScCO2E	SFE with CO_2
sc-CO2	supercritical carbon dioxide
S	syringaldehyde
SA	syringic acid
SPE	solid-phase extraction
TBP	tributyl phosphate carrier
TP	low molecular weight phenolate/phenolic compounds
TS	total non-volatile solids
UF	ultrafiltration
V	vanillin
VA	vanillic acid

1. Introduction

In this chapter the driving force for the development of this study is presented, from the perspective of multistock biorefineries and pulp mills operating with hardwood lignins and its valorisation processes. In this scope, an integrated separation process emerges as the required key piece for the sustainable production of added value compounds from lignin oxidation. Herein, the main goals of this thesis are presented along with a brief description of each chapter.

1.1. Relevance and motivation

Nowadays, industries worldwide are developing new strategies towards environmental and economical sustainable processes to provide efficient biomass conversion into bio-based chemicals, platform chemicals, fuels and energy (1).

Lignin-rich side streams resulting from processing lignocellulosic biomass are promising feedstocks to produce materials, fuels and chemicals (2, 3). Oxidative depolymerisation of lignin is one of many existing processes (2) and yields several added value functionalized phenolic compounds (4), such as vanillin and syringaldehyde (2, 4, 5). These aldehydes are important ingredients for flavour and fragrance industry (6-8) and intermediates of fine chemicals or drugs such as 3,4,5-trimethoxybenzaldehyde (9) or levodopa (10).

Several favourable economic and environmental aspects point out the use of lignocellulosic biomass as an interesting source for obtaining valuable fine chemicals by means of controlled oxidation. Pulp and paper industries generate large amounts of lignin-based material that are mainly handled in a destructive way for energy production. Pulp and paper industry generate pulping (or black) liquor currently used for energy production and inorganic chemicals recovery. A single average size Portuguese mill produces the amount of liquor necessary to produce 240 000 tons of lignin per year. Diverging 0.1% of liquor from a *Eucalyptus globulus* mill will not compromise the actual use for this stream and it represents about 4 000 tons of liquor containing 240 tons of lignin available to be converted into valuable chemicals. Considering the average yields achieved by the LA LSRE-LCM team with oxidative depolymerisation of lignin, 1.2% and 2.8% for vanillin and syringaldehyde, respectively (4), about 2.9 tons of vanillin and 6.7 tons of syringaldehyde can be produced. The market price for these two compounds is about $11/kg (11) for Vanillin and $22/kg (12) for syringaldehyde, which would account for a total of 179 thousands

of dollars. These numbers can be increased if besides the production of vanillin and syringaldehyde, other compounds of interest are also recovered (e.g. oligomers).

Pulp and paper industry in Portugal was pioneering in the use of *E. globulus* wood as raw material for pulp, representing an important economic sector. Considering that its lignin is mainly composed by syringyl units (80S:20G) (13), and that the raw materials of biorefineries are hardwood residues, syringaldehyde should be considered as one of the main valuable chemicals produced from these lignins, followed by vanillin. Accordingly, a feasible and efficient sequential process of separation is critical for the maximum recovery of both compounds, as well as oligomers from the reaction mixture, in an integrated process.

The scope of my PhD work is to study the process conditions for the separation of vanillin and syringaldehyde from the other oxidation products of hardwood lignins, by means of three sequential processes (membrane separation, adsorption and supercritical fluid chromatography), to obtain high purity fractions of each compound.

Since the 90's that the LA LSRE-LCM team develops work on the chemical production of vanillin and syringaldehyde from kraft lignin oxidation (2, 4, 13-24). Some studies on membrane separation and adsorption processes of vanillin have already been developed by LSRE-LCM group (17, 19-21). Based on these studies, the team designed a sequence of processes aiming the integration of membrane and ion exchange processes with the reaction process of the lignin (25). This work intends to gather new information that will contribute to obtain more knowledge about the feasibility of the integration of these separation processes. Within this work plan a complete study implementing an integrated sequence of processes with the real oxidized lignin solution will be attempted for the first time. Additionally, obtaining new valuable compounds from lignin oxidative depolymerisation, such as syringaldehyde, will be considered and the evaluation of the potential of supercritical fluid chromatography for obtaining purified fractions of each phenolic aldehyde will be initiated within this project.

This study will contribute to the scientific knowledge and advances on finding the suitable combination of processes to separate and purify products from lignin oxidation. It will bring new and valuable information about the viability of developing an industrially environmental integrated process of reaction and separation for the recovery of high added value compounds from lignin, thus meeting the emerging demand on biobased products.

1.2. Objectives and outline

This work addresses the study of integration of three distinct separation and purification processes to streams of lignin oxidative depolymerisation in order to obtain more refined fractions of vanillin and syringaldehyde. A forecast of the intended sequence to study is depicted in Figure 1.1 encompassing membrane separation process with tubular ceramic membranes, adsorption process with a polymeric adsorbent and a final purification stage with supercritical fluid chromatography (SFC-CO_2). It is expected to obtain valuate information about the potential of integration of these separation and purification processes in the perspective of obtaining highly purified fractions of each aldehyde.

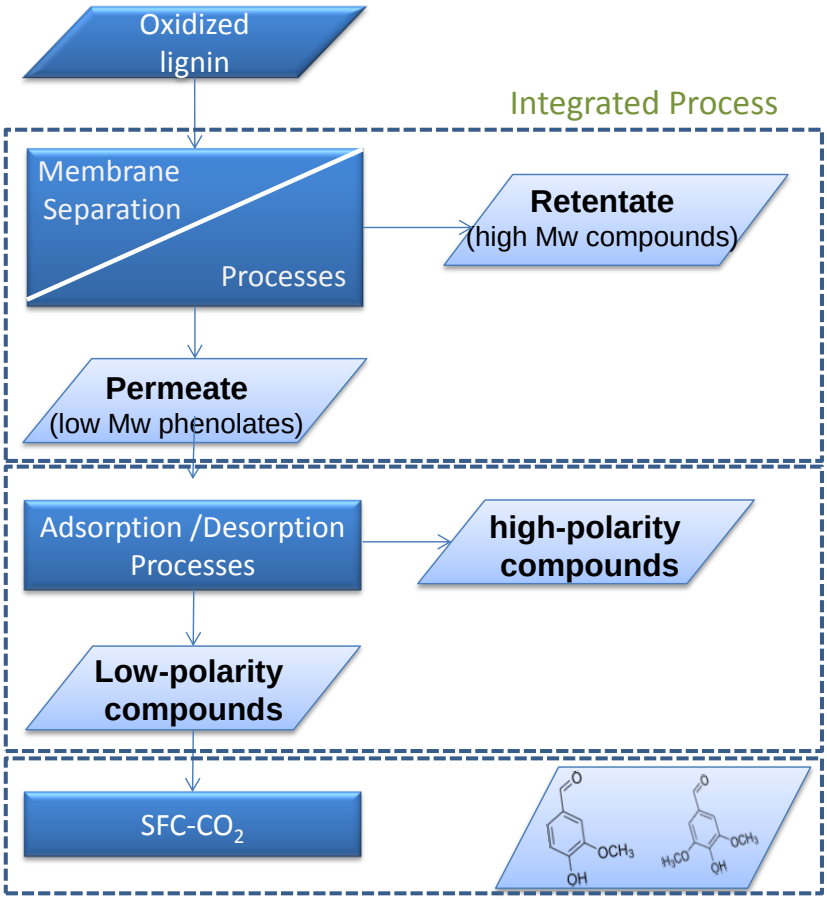

Figure 1.1 Forecast of the integrated sequence of processes to study

In **Chapter 2** it is summarized relevant literature from international peer reviewed publications and patents dealing with core processes and applications implemented aiming syringaldehyde and vanillin separation from real oxidation mixtures. Literature since the early years of the 20th century

is summarized covering several separation technologies encompassing liquid-liquid extraction, supercritical fluid extraction, distillation, crystallization, membrane separation, and adsorption. The combination of the different processes addressed in the literature aiming the purification of vanillin and syringaldehyde is discussed.

Chapters 3 and 4 describe the adsorption/desorption studies performed with model solutions of vanillin and syringaldehyde. **Chapter 3** addresses adsorption studies performed with aqueous solutions of vanillin, syringaldehyde, vanillic acid and syringic acid. Batch equilibrium studies with vanillin and syringaldehyde are performed to select the most suitable adsorbent among SP700 and XAD16N. SP700 is selected to pursue with batch equilibrium studies with vanillic and syringic acids. Single adsorption equilibrium isotherms for each compound at different temperatures are fitted with Langmuir, Bi Langmuir and Freundlich models. Fixed bed studies with each phenolic compound in aqueous solution are performed as well. A mathematical model considering a plug flow with axial dispersion, linear driving force rate equations to describe mass transfer inside the resin, no temperature gradients and constant porosity along the bed is implemented to describe the adsorption/desorption histories of concentration at the outlet of the fixed bed experiments. Binary adsorption studies with vanillin and syringaldehyde are performed as well and the extended Bi-Langmuir model implemented.

Chapter 4 evaluates the adsorption of the phenolic aldehydes in ethanol:water (90:10, % V/V), in the perspective of using an ethanolic solution for recovery of the aldehydes. In this chapter is also shown the advantage of applying an ethanol:water (90:10, % V/V) solution for the recovery of the phenolic compounds from lignin oxidation mixture. The high level of concentration achieved with this strategy and the type of solvent used is favourable for any further processing step, such as crystallization or spray drying.

Chapter 5 addresses the implementation of a membrane separation to process an oxidized industrial kraft liquor diluted and enriched in some phenolic compounds of interest. A membrane fractionation sequence employing ceramic membranes with cut-offs 50 kDa, 5 kDa and 1 kDa is applied and the different retentate and permeate streams characterized regarding molecular weight using GPC, total solids, ashes and total phenolate compounds quantified by HPLC-UV. The efficiency of the membrane process is evaluated in terms of understanding the relevance of reversible and irreversible fouling on the membrane productivity observed.

In **Chapter 6**, the final permeates obtained in the second and third membrane stages, P5kDa and P1kDa, pursues with adsorption and desorption studies onto a bed with SP700 resin after adjusting

the pH value to approximately 7.5-8.0. The complete saturation of the bed is performed with P1kDa feed stream in order to understand the maximum adsorption achieved for vanillin and syringaldehyde. The phenolic compounds are recovered with an ethanol:water (90:10, % V/V) solution and the efficiency of the adsorption process evaluated. Herein, cycles of adsorption/desorption of the bed are performed as well in order to investigate the regeneration of the SP700 resin in the perspective of its reutilization, key factor for the development of a viable industrial adsorption process.

In this chapter, the potential of SFC technology to recover purified fractions of vanillin and syringaldehyde is also evaluated. Preliminary experiments with model solutions are applied first and afterwards with a real solution after being treated by membrane and adsorption processes.

Finally, overall conclusions and suggestions for future work are presented in **Chapter 7**.

1.3. References

1. Kamm, B. and Kamm, M. (2004) Principles of biorefineries. Appl. Microbiol. Biotechnol., 64: 137-145.
2. Pinto, P. C. R., Borges da Silva, E. A. and Rodrigues, A. E. (2012) Lignin as source of fine chemicals: vanillin and syringaldehyde: In Biomass Conversion. Chinnappan Baskar, Shikha Baskar and Ranjit S. Dhillon. Springer Berlin Heidelberg: London, United kingdom, 381-420.
3. Eckert, C., Liotta, C., Ragauskas, A., Hallett, J., Kitchens, C., Hill, E. and Draucker, L. (2007) Tunable solvents for fine chemicals from the biorefinery. Green Chem., 9: 545-548.
4. Pinto, P. C. R., Costa, C. E. and Rodrigues, A. E. (2013) Oxidation of lignin from *Eucalyptus globulus* pulping liquors to produce syringaldehyde and vanillin. Ind. Eng. Chem. Res., 52: 4421-4428.
5. Zakzeski, J., Bruijnincx, P. C. A., Jongerius, A. L. and Weckhuysen, B. M. (2010) The catalytic valorization of lignin for the production of renewable chemicals. Chem. Rev., 110: 3552-3599.
6. Hocking, M. B. (1997) Vanillin: synthetic flavoring from spent sulfite liquor. J. Chem. Educ., 74: 1055-1059.

7. Ibrahim, M. N. M., Sriprasanthi, R. B., Shamsudeen, S., Adam, F. and Bhawani, S. A. (2012) A concise review of the natural existence, synthesis, properties, and applications of syringaldehyde. BioResour., 7: 1-23.

8. Holladay, J. E., Bozell, J. J., White, J. F. and Johnson, D. (2007) Volume II: Results of screening for potential candidates from biorefinery lignin: In Top Value-added Chemicals from Biomass availabe from http://www.pnl.gov/main/publications/external/ technical_reports/PNNL-16983.pdf (accessed 07-04-2016).

9. Erofeev, Y. V., Afanas'eva, V. L. and Glushkov, R. G. (1990) Synthetic routes to 3,4,5-trimethoxybenzaldehyde (review). Pharm. Chem. J., 24: 501-510.

10. Bjørsvik, H.-R. and Liguori, L. (2002) Organic processes to pharmaceutical chemicals based on fine chemicals from lignosulfonates. Org. Process Res. Dev., 6: 279-290.

11. Walton, N. J., Mayer, M. J. and Narbad, A. (2003) Vanillin. Phytochemistry, 63: 505-515.

12. *Integrated Forest Biorefineries, Challenges and Opportunities*, in *RSC Green Chemistry No. 18*, 2013, edited by Lew P. Christopher, The Royal Society of Chemistry, Cambridge, United Kingdom.

13. Costa, C. A. E., Pinto, P. C. R. and Rodrigues, A. E. (2014) Evaluation of chemical processing impact on E. globulus wood lignin and comparison with bark lignin. Ind. Crop. Prod., 61: 479-491.

14. Mathias, Á. L. (1993) Produção de vanilina a partir da lenhina: estudo cinético e do processo, Ph.D. thesis, Chemical Engineering Department, Faculty of Engineering of University of Porto, Porto, Portugal.

15. Mathias, Á. L., Lopretti, M. I. and Rodrigues, A. E. (1995) Chemical and biological oxidation of Pinus pinaster lignin of the production of vanillin. J. Chem. Technol. Biotechnol., 64: 225-234.

16. Mathias, Á. L. and Rodrigues, A. E. (1995) Production of vanillin by oxidation of pine kraft lignins with oxygen. Holzforschung, 49: 273.

17. Fargues, C., Mathias, Á. L. and Rodrigues, A. (1996) Kinetics of vanillin production from kraft lignin oxidation. Ind. Eng. Chem. Res., 35: 28-36.

18. Fargues, C., Mathias, Á. L., Silva, J. and Rodrigues, A. (1996) Kinetics of vanillin oxidation. Chem. Eng. Technol., 19: 127-136.

19. Žabková, M., Otero, M., Minceva, M., Zabka, M. and Rodrigues, A. E. (2006) Separation of synthetic vanillin at different pH onto polymeric adsorbent Sepabeads SP206. Chem. Eng. Process., 45: 598-607.

20. Žabková, M., Borges da Silva, E. A. and Rodrigues, A. E. (2007) Recovery of vanillin from Kraft lignin oxidation by ion-exchange with neutralization. Sep. Purif. Technol., 55: 56-68.

21. Žabková, M., Borges da Silva, E. A. and Rodrigues, A. E. (2007) Recovery of vanillin from lignin/vanillin mixture by using tubular ceramic ultrafiltration membranes. J. Membr. Sci., 301: 221-237.

22. Araújo, J. D. P., Grande, C. A. and Rodrigues, A. E. (2009) Structured packed bubble column reactor for continuous production of vanillin from Kraft lignin oxidation. Catal. Today, 147, Supplement: S330-S335.

23. Araújo, J. D. P., Grande, C. A. and Rodrigues, A. E. (2010) Vanillin production from lignin oxidation in a batch reactor. Chem. Eng. Res. Des., 88: 1024-1032.

24. Pinto, P. C. R., Borges da Silva, E. A. and Rodrigues, A. E. (2011) Insights into oxidative conversion of lignin to high-added-value phenolic aldehydes. Ind. Eng. Chem. Res., 50: 741-748.

25. Borges da Silva, E. A., Zabkova, M., Araujo, J. D., Cateto, C. A., Barreiro, M. F., Belgacem, M. N. and Rodriques, A. E. (2009) An integrated process to produce vanillin and lignin-based polyurethanes from Kraft lignin. Chem. Eng. Res. Des., 87: 1276-1292.

2. State of the art[1]

In this chapter a literature survey about the main research advances in the recovery of vanillin and syringaldehyde coming from oxidation of lignin is addressed, covering various separation methodologies namely liquid-liquid extraction, supercritical fluid extraction, distillation, crystallization, membrane separation, and adsorption.

Studies in this area started in the early years of the 20th century, but in the last decades several processes have been suggested, mainly for vanillin separation. In the last section, an overview of integration of these separation processes is presented aiming to meet the final product requirements. Finding the ultimate industrially feasible process is still a necessary task. The most promising technologies and sequence of processes proposed in literature are highlighted in this chapter.

[1] This chapter is based on the paper

Mota, I. F., Pinto, P. C. R., Loureiro, J. M., Rodrigues, A. E. (2016) Recovery of Vanillin and Syringaldehyde from Lignin Oxidation: A Review of Separation and Purification Processes. Sep. Purif. Rev., 45: 227-259.

2.1. Introduction

Lignin is one of the main structural components of lignocellulosic materials accounting for 15% to 30% of their dried weight. Its structure is based on phenylpropane units involved in alkyl-aryl ether linkages, some of them carrying phenolic hydroxyl groups. The delignification of the materials is the fundamental process of both wood pulping in pulp and paper industries and deconstruction of lignocellulosic materials in biorefineries, thus generating side streams with high lignin content. The main application for these lignins still is for energy production and, in the case of kraft pulping industries, inorganic chemicals recovery.

Lignin has a large number of other applications as active agent in dispersing, binding, and emulsifying formulations, in phenolic resins, polyurethane foams, among others (1-6). Through oxidation of lignin under controlled conditions high added value compounds such as vanillin and syringaldehyde (Figure 2.1) can be produced. However, a complex mixture is obtained resulting from side-reactions and incomplete depolymerisation (7, 8). Discovering the suitable combination of purification methods is still a challenge to overcome.

Vanillin (Figure 2.1.a) is widely used as flavouring and fragrance agent in food products, cosmetics as well as a starting material for the synthesis of several second-generation fine chemicals (9, 10). Vanillin has potential to be used as a food preservative since it possesses antioxidant and antimicrobial properties (11, 12). Nowadays 85% of vanillin world supply is synthesized from oil derived guaiacol and the remaining 15% come from softwood lignin (13). Only about 1% of the global demand for vanillin is assured by natural vanillin and its market value is very high ranging from 1200 to 4000 USD per kilogram (14).

Synthetic vanillin constitutes an interesting alternative since it is cheaper (11-20 USD per kilogram (14, 15)), does not depend of natural conditions to yield considerably amounts and has a wide range of applications. Vanillin can be produced through means of bioconversion of lignin (16-18), phenolic stilbenes (19), isoeugenol and eugenol (20), creosol (21), ferulic acid (22-24), glucose (25), and vanillic acid (26, 27). This subject has been extensively reviewed (28, 29). Fermentation of ferulic acid is the only existing commercial profitable biocatalytic route for vanillin (30, 31), which is explored by Solvay Rhodia. Vanillin can also be produced by chemical synthesis route being coniferin, guaiacol, eugenol, ferulic acid and lignin the possible starting materials (28). Borregaard (Norway) is the single industrial producer of vanillin from the lignosulfonate oxidation path (31).

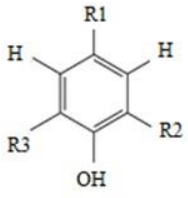

	Compound	R1	R2	R3
a)	Vanillin	-CHO	$-OCH_3$	-H
b)	Vanillic acid	-COOH	$-OCH_3$	-H
c)	Syringic acid	-COOH	$-OCH_3$	$-OCH_3$
d)	Syringaldehyde	-CHO	$-OCH_3$	$-OCH_3$
e)	*p*-Hydroxybenzaldehyde	-CHO	-H	-H
f)	Acetovanillone	$-COCH_3$	$-OCH_3$	-H
g)	Acetosyringone	$-COCH_3$	$-OCH_3$	$-OCH_3$

Figure 2.1 Functionalized phenolic monomers that can be found in lignin oxidized reaction mixtures.

Syringaldehyde (Figure 2.1.d) is also used as ingredient by flavour and fragrance industry and as a precursor of second generation fine chemicals and drugs such as 3,4,5-trimethoxybenzaldehyde, a building block of the antibacterial agent trimethoprim (9). Vanillin is also a precursor of 3,4,5-trimethoxybenzaldehyde (9) but syringaldehyde has the advantage of having already two methoxyl groups. This aldehyde can be synthesized from gallic acid (32), pyrogallol (33), vanillin (34, 35) or *p*-cresol (13, 36-38). Oxidation of lignin has also been studied to obtain syringaldehyde (39-45). The market value for this compound is about 22 USD per kilogram (15).

Literature is extensive regarding the oxidative conversion of lignin from different origins into functionalized phenolic monomers. A variety of oxidation methods have been proposed and some reviews about the subject have been recently published (31, 46).

Alkaline oxidation of lignin using air with or without the presence of a catalyst is the most revisited process. Studies from the very beginning of the 40´s and several patents (47-52) were published. More recently, modifications and improvements have been disclosed, bringing new highlights in unexplored aspects of the reaction engineering and products (31, 45, 53-57), as well as separation issues (31, 56, 58-61). Vanillin yields obtained from this process are usually in the range 4-20% w/w_{lignin} and for syringaldehyde is 5-16% w/w_{lignin} (10, 31, 39, 42-45, 51, 53, 54, 62-64). The centennial company Borregaard is the single producer of vanillin by means of oxidation of lignosulfonates with oxygen (31). Acidic lignin oxidation has also been suggested by some authors (65-67), achieving similar final yields to the aforementioned method.

Several studies of electrochemical oxidation of lignin, reporting different electrode materials and configurations, have been published (68-72) and patented (73-77).

The potential of other lignin oxidation processes and using new catalysts have been proposed employing photocatalysis (78), ionic liquids (ILs) (79, 80), mesoporous materials (81) and vanadium-based catalysis (82, 83) .

It is important to notice that despite the oxidation methods used, the lignin source has great influence on the obtained yields of vanillin and syringaldehyde and other phenolics like *p*-hydroxybenzaldehyde, vanillic acid, acetovanillone, syringic acid (Figure 2.1) (43). Studying the industrial viability of the aforementioned processes is still a necessary task.

2.1.1. Physical-chemical properties of vanillin, syringaldehyde and other relevant phenolic monomers present in oxidized lignin solution

As already stated before, through oxidation of lignin a complex solution with functionalized phenolic monomers is produced along with products from incomplete depolymerisation such as sugars and derivatives, organic acids and inorganic compounds. Table 2.1 presents physical and chemical properties of some phenolic compounds present in oxidized solutions from hardwood lignin. Most of these compounds have similar molecular weights, acid dissociation constants in water, densities and melting points (84-89). Due to these similarities, the purification of each monomer is not effective. This is the subject of many research studies and attempts to obtain highly purified fractions of each monomer in an easy and cost effective manner. Vanillin has been the main monomer studied and syringaldehyde is beginning to earn considerable interest as well on the perspective of its production from renewable sources.

Vanillin, syringaldehyde, acetovanillone and acetosyringone have very similar molecular weights and acid dissociation constants hampering their separation by membrane separation processes or other techniques based on their acidity differences (84-87, 89, 90).

The heats of dissolution for vanillin (21.8 kJ mol^{-1}) and syringaldehyde (33.3 kJ mol^{-1}) (91) are not different enough to allow an efficient separation, as for example by crystallization. The maximum differences of solubility are achieved for low temperatures and concentrations of 1-11 g L^{-1} (92).

Table 2.1 Physical-chemical properties of some monomeric phenolic compounds present in lignin oxidation reaction media

	MM (g mol^{-1})	T_{melt} (^{o}C)	T_{boil} (^{o}C)	ρ (g cm^{-3})	Dipole moment (D)	$LogP_{OW}$	p*Ka* @ 25 °C	Solubility (g L^{-1})
V	152.2 (84, 86, 87)	81-83 (84, 86, 87)	285 @ 101.3KPa (84, 86, 87) 154 @ 1.3 KPa[86]	1.056 (84, 86, 87)	3.57[97] Benzene: 2.87[98, 99] Dioxan: 3.39[98]	1.188[90]	Water: 7.40[85, 89] Ethanol: 12.37[85] Methanol: 11.81[85] EW 50:50 % V/V: 8.50[85]	Water: 9.0[93]; 14.2±1.4*; 6.9@25 °C[90]; 11[90]; ≈10@25 °C [94]; soluble in hot water[86] EW 10:90 % V/V: 13.5[93]; Soluble in 1:2 vanillin/ethanol[86] Freely soluble in chloroform, ether, soluble in glycerin and hot water[86]
S	182.2 (86, 87)	110-113 (86-88)	192-193 @ 19 KPa[87, 88]	1.01 (88)	-	1.315[90]	Water: 7.34[85]	Water: 9.5@25 °C[90]; 6.2[90];4.37±0.09* Very sparklingly soluble in water[86] Soluble in alcohol, ether, chloroform, hot benzene[86, 88]
VA	168.15 (86, 87)	207-211.5 (84, 86, 87, 95)	353.4 @ 101.3KPa[95]	1.351 (95)	-	1.334[90]	Water: 4.42[85]	Water: 3.8@25 °C[90]; 2.3[90]; 1.5@25°C[94]; ≈1.53@25 °C [94]; 3.06±0.04* Soluble in 860 parts of water (weight basis)[84] Soluble in 100 parts of water is 0.12[84]; Very soluble in alcohol; soluble in ether;[84, 86]
SA	198.2 (87)	205 – 209 (100) 204.5 (87)	192[87] 192-193 @ 6.7 KPa[87, 100] 363 @ 101.3 KPa [90]	1.335 (90)	-	1.129[90]	Water: 4.34[85]	Water: 5.8@25 °C[90]; 1.5[90]; 2.02±0.06*
***p*-OHB**	122.1 (86, 87)	116-117 (86, 87)	191 @ 6.7 KPa (100)	1.129 (87)	4.19[86]; Dioxan 4.19[98]; Benzene 3.957[99]	1.392[90]	Water: 7.61[96]; 8.4[86]	Water: 4.1@25 °C[90]; 2.5[90] Freely soluble in alcohol, ether[86] slightly soluble in benzene[86]
OV	166.2 (87)	112-115 (87)	297[87]; 234[87] 263-265[95]	1.158 (95)	-	1.389[90]	Water: 7.81[85]	Slightly soluble in cold water[86]; soluble in hot water[86] Soluble in alcohol, benzene, chloroform, and ether[86] Practically insoluble in petroleum ether[86]
OS	196.2 (90)	117-127 (90)	124-127[100]	1.172 (95)	-	1.23[90]	Water: 7.88[85]	Water: 8.7@25 °C[90]; 6.3[90] Soluble in ethanol and ethyl ether[95] Slightly soluble in chloroform [95]

V: Vanillin; **S**: Syringaldehyde; **VA**: Vanillic acid; **SA**: Syringic acid; ***p*-OHB**: *p*-Hydroxybenzaldehyde; **OV**: Acetovanillone; **OS**: Acetosyringone; **EW:** Ethanol:water; **MM:** Molar Mass; T_{melt}: Melting temperature; T_{boil}: Boiling temperature; ρ: Density; p*Ka*: Acid dissociation constant; $LogP_{OW}$: Logarithm of the ratio of concentration of a certain compound in octanol and in water. *Value experimentally determined through HPLC-UV quantification of the dissolved amount in a saturated aqueous solution;

Vanillin and syringaldehyde vapour pressures at 192 ºC, 55 torr and 14 torr (91) respectively, do not allow a prompt separation by distillation or rectification. Additionally, special attention must be given when employing distillation or any other separation techniques that require the use of high temperatures since these compounds have limited thermal stability.

In the next sections, a review on the processes suggested in literature for isolation and purification of vanillin and syringaldehyde from aqueous solutions containing other similar compounds will be addressed. The main advances of each process as well as drawbacks are highlighted and, whenever possible, exploring and referencing studies using real oxidation mixture instead of model mixtures will be made. The suggested methods for vanillin and syringaldehyde purification usually comprise separation sequences which are presented in the last section as possible approaches, some of them not yet tested, to meet the final products requirements.

2.2. Extraction processes

2.2.1. Liquid-liquid extraction (LLE)

LLE is the process of solute(s) transfer from one liquid to another liquid phase, involving the contact between two partially or completely immiscible liquids, formation of distinct layers caused by differences of density and separation and collection of the extract and raffinate streams (101).

The distribution ratio or partition coefficient (K_D) and the selectivity factor (α) are two parameters of great importance in LLE. K_D is assigned to the distribution of a certain solute between the extract and raffinate streams after equilibrium, being calculated as the ratio between the concentrations in these two streams. Table 2.2 and Table 2.3 present selected literature data on *K* for vanillin or for other phenolics, respectively. Although for vanillin there are data for simple aliphatic alkanes, alkenes, nitriles, organochloride solvents, amides, and ionic liquids, with electrolytes or carriers, for other phenolics such as vanillic acid, syringic acid and syringaldehyde, the literature is more scarce. Table 2.4 presents K_D and α for bicomponent mixtures of phenolics and for a real mixture from depolymerisation.

Table 2.2 Distribution coefficients of vanillin aqueous solutions for different solvents

Solvent	K_D	pH	T (ºC)	C_V (mol L^{-1})	Ref.
Isopropanol	1.50	-	-	-[(a)]	(102)
Butanol	27	-	-	-	(103)
	14.16	-	-	-	(104)
	27	1-4	-	-	(105)
	0.75	11-14	-	-	
	0.20	-	-	-[(a)]	(102)
Butanol:water (50:50, % V/V)	7.00	-	30	1 $x10^{-3}$	(106)
Pentanol	22.50	-	-	-	(104)
Hexanol	30.5	1-4	-	-	(105)
	0.21	11-14	-	-	
Heptanol	24.6	1-4	-	-	(105)
	0.18	11-14	-	-	
Octanol	20.5		-	-	(107)
	20.3	1-4	-	-	(105)
	0.15	11-14	-	-	(105)
	14.8		25	-	(108)
	16.6	-	-	-	(109)
	15.4	-	25	1 $x10^{-3}$	(110)
	9.8-15.5	-	25-45	5 $x10^{-3}$	(111)
	21.5-51.6	-	25	1 $x10^{-3}$ [(b)]	(110)
2-Octanol:TBP (50:50, % V/V)	2512	1	25	3.3$x10^{-4}$	(112)
Hexane	0.2	-	-	-	(107)
Hexane:water (50:50, % V/V)	0.049	-	30	1 $x10^{-3}$	(106)
50% Hexane + 50% TBP	65	1	25	3.3$x10^{-4}$	(112)
Heptane – Octylamine	~50-600	~8-9.5	20	5 $x10^{-2}$ [(c)]	(113)
Decane:TBP (50:50, % V/V)	3311	1	25	3.3$x10^{-4}$	(112)
Kerosene:50% (50:50, % V/V)	1413	1	25	3.3$x10^{-4}$	(112)
Benzene	3.75, 6.3	-		-	(104, 107)
Toluene	4.64, 4.1	-		-	(104, 107)
Toluene:Water (50:50, % V/V)	4.14	-		6.6$x10^{-3}$	(114)
Chloroform	26.5	-		-	(107)
Chloroform:water (50:50, % V/V)	22.1	-	30	1 $x10^{-3}$	(106)
Dichloromethane	19.20	-		-	(104)
Trichloromethane	20.22	-		-	(104)
1,2-Dichloroethane	20.2	-		-	(107, 115)
	13.10	-		-	(104)

Table 2.2 (cont.)

Solvent	K_D	pH	T (ºC)	C_V (mol L^{-1})	Ref.
Tetraalkylammonium chloride	50-100	-		-	(103)
Ethyl acetate	21.75	-		-	(104)
Butyl acetate	28.2	-		-	(116)
Acetic ether	24.8	-	30	1×10^{-3}	(106)
Diethyl ether	6.25	-		-	(104)
Di-isopropyl ether	2.75	-		-	(104)
Methyl isobutyl ketone	29.20	-	-	-	(104)
	0.16	11	-	-	
Pure pyridine	4.88	-	-	-[(a)]	(102)
Pyridine bases	2.03				
Pyrrolidine	5.67				
Morpholine	0.14				
Pyridine bases	5.67				
Diethylamine	0.14				
Isopropylamine	0.01				
Isopropylamine	0.01				
Octylamine	>600	-	-		(113)
25% $[C_2mim]Cl$ - 15% K_3PO_4 ATPS	36.49	-	25	-	(117)
25% $[C_4mim]Cl$ - 15% K_3PO_4 ATPS	19.26- 98.08	-	15-55	3.3×10^{-3} - 4.9×10^{-2}	(117)
25% $[C_4mim][N(CN)_2]$ - 15% K_3PO_4 ATPS	31.87	-	25	6.6×10^{-3}	(117)
25% $[C_4mim]Br$ - 15% K_3PO_4 ATPS	25.66		25	6.6×10^{-3}	(117)
25% $[C_4mim][CH_3SO_4]$ - 15% K_3PO_4 ATPS	14.63-36.19	-	15-55	3.3×10^{-3} - 3.3×10^{-2}	(117)
25% $[C_6mim]Cl$ -15% K_3PO_4 ATPS	49.59	-	25	6.6×10^{-3}	(117)
25% $[C_7mim]Cl$ - 15% K_3PO_4 ATPS	42.39	-	25	6.6×10^{-3}	(117)
25% $[C_{10}mim]Cl$ - 15% K_3PO_4 ATPS	2.72	-	25	6.6×10^{-3}	(117)
25% $[C_7H_7mim]Cl$ - 15%K_3PO_4 ATPS	21.31-98.69	-	15-55	3.3×10^{-3} - 4.9×10^{-2}	(117)
40% $[OHC_2mim]Cl$ - 15% K_3PO_4 ATPS	22.95	-	25	2.6×10^{-3}	(117)
40, 50% ACN - 10, 20% disaccharide ATPS	3.5-7.1	5.97-7.06	25	2.6×10^{-3}	(118)
40,50% ACN-10,20% monosaccharide ATPS	3.5-9.7	5.69-7.00	-	2.6×10^{-3}	(118)
50% MeOH - 15% K_3PO_4 ATPS	166 ± 61	-	-	-	(119)
50% MeOH - 15% K_2HPO_4 ATPS	358 ± 8	-	-	-	(119)
KH_2PO_4 / K_2HPO_4 ATPS	14.1 ± 0.5	-	-	-	(119)
50% EtOH - 15% K_3PO_4 ATPS	351 ± 19	-	-	-	(119)
50% EtOH - 15% KH_2PO_4/K_2HPO_4 ATPS	15 ± 1	-	-	-	(119)
50% 1-Propanol - 15% K_3PO_4 ATPS	74 ± 1	-	-	-	(119)

Table 2.2 (cont.)

Solvent	K_D	pH	T (ºC)	C_V (mol L^{-1})	Ref.
50% 1-Propanol-15% K_2HPO_4 ATPS	78 ± 6	-	-	-	(119)
50% 1-Propanol-15% KH_2PO_4/K_2HPO_4 ATPS	34 ± 4	-	-	-	(119)
50% 2-Propanol-15% K_3PO_4 ATPS	122 ± 3	-	-	-	(119)
50% 2-Propanol-15% K_2HPO_4 ATPS	114 ± 3	-	-	-	(119)
50% 2-Propanol -15% KH_2PO_4 / 50% 2-Propanol-15% KH_2PO_4/K_2HPO_4 ATPS	15 ± 2	-	-	-	(119)
Water-Acetone-CO_2	2.5	-	40	-	(120)
(liquid-Liquid-Vapor)	2.35	-	60	-	

a) Prepared mixture contains 3.4% V, 2.4% NaOH, 14.2% Na_2SO_4, 2.9% Na_2CO_3 and 77.1% H_2O; **b)** With electrolytes; **c)** With different concentrations of octylamine;

C_V: Vanillin concentration; **TBP:** Tributyl phosphate carrier; TBP is a suitable complexing agent for vanillin recovery from aqueous solutions since it increases the extraction efficiency; **ATPS:** Aqueous two-phase systems; **ACN:** acetonitrile; **EtOH:** Ethanol;

Ionic Liquids: [C_2mim]Cl: 1-Ethyl-3-methylimidazolium chloride; **[C_4mim]Cl:** 1-Butyl-3-methylimidazolium chloride; **[C_4mim]Br:** 1-Butyl-3-methylimidazolium bromide; **[C_4mim][CH_3SO_4]:** 1-Butyl-3-methylimidazolium methylsulfate; **[C_4mim][$N(CN)_2$]:** 1-Butyl-3-methylimidazolium dicyanamide; **[C_6mim]Cl:** 1-Hexyl-3-methylimidazolium chloride; **[C_7mim]Cl:** 1-Heptyl-3-methylimidazolium chloride; **[C_{10}mim]Cl:** 1-Decyl-3-methylimidazolium chloride; **[amim]Cl:** 1-Allyl-3-methylimidazolium chloride; **[C_7H_7mim]Cl:** 1-Benzyl-3-methylimidazolium chloride; **[OHC_2mim]Cl:** 1-Hydroxyethyl-3-methylimidazolium chloride

The capability of separation between two solutes is described by the selectivity factor α_{ij} between solutes *i* and *j*, assessed by the ratio between the partition coefficients of solute *i* (K_{Di}) and solute *j* (K_{Dj}). Therefore, α_{ij} is strongly dependent on the magnitude of the distribution ratios. Whenever the selectivity factor is significantly different than one, a good separation between the two targeted solutes is accomplished. The separation efficiency can be adjusted by using different solvents and aqueous phases (101). Additionally, the formation of complexes can also increase the extraction efficiency, since they promote an increase on α_{ij} and on mass transfer. This is particularly important when dealing with very dilute solutions, which is the case of vanillin and other phenolic monomers in the oxidized lignin medium (121-123). Some examples applied to recover vanillin such as complexation with bisulphite (61, 122) as well as the use of other complexing agents (112, 113) will be later on described.

LLE can be performed in batchwise or continuous and in co-, counter- or cross-current modes. The equipment arrangement (e.g. spray tower, baffle plate, mechanically stirred tower with paddles, reciprocating discs) is also very important since it can exert influence on solute transfer due to changes in the interfacial area within the extractor (101).

Table 2.3 Distribution coefficients for other phenolic compounds (in aqueous solution) resulting from lignin oxidation

	Extracting system	K_D	T (ºC)	C (mol L^{-1})	Other components added	Ref.
S	Butanol:water (50:50, % V/V)	28.5	30	1 $x10^{-3}$	-	(106)
	Acetic ether:water (50:50, % V/V)	12.4	30	1 $x10^{-3}$	-	(106)
	Chloroform:water (50:50, % V/V)	38.4	30	1 $x10^{-3}$	-	(106)
	Hexane:water (50:50, % V/V)	0.28	30	1 $x10^{-3}$	-	(106)
VA	Octanol	15.1-26.3	25-45	0.005	-	(111)
		26.9	-	-	-	(124)
		25.1	-	-	-	(125)
		26.3		0.001	-	(110)
		31.9-51.6	25	0.001	1M, 3M LiCl or NaCl or KCl	
	PEG300+Na_2SO_4+Water	15.5±0.3	25	-		(126)
	PEG300+Na_2SO_4+ 5%[C4mim]Cl+Water	46.0±3.2	25	-		
***p*-OHB**	1-Octanol	22.9	25	-	-	(108)
		38.0	-	-	-	(124)
	Butanol:water (50:50, % V/V)	10.6	30	30	1 $x10^{-3}$	(106)
	Acetic ether:water (50:50, % V/V)	19.7	30	1 $x10^{-3}$	-	(106)
	Chloroform:water (50:50, % V/V)	0.73	30	1 $x10^{-3}$	-	(106)
	Hexane:water (50:50, % V/V)	0.063	30	1 $x10^{-3}$	-	(106)
SA	1-Octanol	12.9	25	0.001		(110)
		11.0				(124)
		13.5	-	-		(125)
		13.0-18.4	25	0.001	1M, 3M LiCl or NaCl or KCl	(110)
	PEG300 + Na_2SO_4	16.9	25			(126)
	23% PEG300 + 12% Na_2SO_4 + 5% [C4mim]Cl	50.2	25			

VA: Vanillic acid; ***p*-OHB:** *p*-Hydroxybenzaldehyde; **SA:** Syringic acid; **Ionic liquid [C_4mim]Cl:** 1-Butyl-3-methylimidazolium chloride; **PEG** - Polyethylene glycol.

Table 2.4 Distribution coefficients and selectivity factors of phenolic compounds in mixtures

Compounds	Extracting system	K_{D1}	K_{D2}	α_{12}	Observations	Ref.
V (1) and *p*-OHB (2)	Benzene	0.17	2.1	0.08	25 ºC, 0.5 g/each	(127)
	20% X222 and 80% Benzene	0.21	4.3	0.05		
S (1) and *p*-OHB (2)	Benzene	0.14	2.1	0.07	25 ºC, 0.25 g of SYR, 0.5 g of *p*-OHB	(127)
	20% X222 and 80% Benzene	0.38	4.3	0.09		
	50% X222 and 50% Benzene	1.3	11.7	0.11		
V (1) and S (2)	95% X222 and 5% Ether	2.5	7.5	0.33	25 ºC, 0.5 g of VAN, 0.25 g of SYR	(127)
	95% X222 and 5% Isopropylether	4.3	11.3	0.38		
V (1) and ferAC (2)	Diethyl-ether	3.6	0.1	36	pH 7, 30 ºC	(128)
	n-Hexane	0.09	0.001	90		
	Ethyl acetate	16.8	0.2	84		
	Butyl-acetate	21.0	0.4	52.5		
	2-Ethyl-1-Hexanol	7.0	0.005	1400		
	Butyl acetate	~16	-	-	pH 8, 30 ºC	
		~10	-	-	pH 9, 30 ºC	
		~5	-	-	pH 10, 30 ºC	
		~2	-	-	pH 11, 30 ºC	
		~0	-	-	pH 12, 30 ºC	
Mixture of monomers [a]	Diethyl ether	-	-	0.42*	-	(129)
	Dichloromethane	-	-	0.51*		
	Toluene	-	-	0.72*		
	Ethyl acetate	-	-	0.35*		
	4-Methyl-furan	-	-	0.54*		

V: Vanillin; **S:** Syringaldehyde; ***p*-OHB:** *p*-Hydroxybenzaldehyde; **ferAc** - Ferulic acid; **X222** – Shell X222 solvent mixture; **a)** Coming from acidified aqueous phase of base catalysed depolymerisation reaction of a lignin-rich feedstock containing catechol, 3-methoxy catechol, phenol, 4-methyl catechol, vanillin, guaiacol, syringaldehyde, acetovanillone, syringol, 4-ethyl catechol; ***** Ratio between total mass of extracted and identified monomers and the total mass of rich fraction

Microreactors are known for their superior heat and mass transfer characteristics, enhanced surface-to-volume ratio, steady laminar flow and elevated shear rates. In an attempt to take advantage of these characteristics, the performance of microreactors for extracting vanillin from aqueous solutions has been evaluated (114, 130). Fries *et al.* (114) revealed that the extraction efficiency of vanillin with toluene in rectangular microchannels is higher than in conventional toluene batch extraction, which is due to the higher mass transfer of the segmented flow patterns in comparison with stratified ones. Assmann and von Rohr (130) demonstrated that the incorporation of an inert gas can improve mass transfer from 6.0 – 12 s^{-1} to 6.5 – 17 s^{-1} at flow velocities above 0.08 m s^{-1}.

Many LLE methods have been described in literature and also in patents as a starting stage to obtain a crude extract of vanillin from oxidized lignin solutions or from other media such as fermentation broth. However, other low molecular weight phenolics are also co-extracted and therefore further refinement by other separation methods, such as a new solvent extraction step, distillation and/or crystallization must be carried out.

Studies on extraction of vanillin and homologous have been conducted with organic solvents such as benzene (107, 127, 131-134), toluene (52, 107, 114, 129, 130, 135), ethyl acetate (129, 136), hexane (107), heptane (113), 4-methyl-furan (129), chloroform (67, 107), dichloromethane (129) and diethyl ether (129, 137), many of which were used for analytical purposes (53, 54, 57, 138-140). The main drawback when applying the abovementioned solvents is the initial step of acidification (with H_2SO_4 or CO_2) of the alkaline oxidized lignin medium which entails elevated costs due to the large amounts of acid consumed in the process. An additional disadvantage, consequence of the lignin precipitation, would be the partial dragging of the phenolic monomers, such as vanillin.

Since the precipitated lignin is removed before the extraction, the vanillin recovery yields could be compromised. Craig and Logan (135) recommended the filtration of the precipitated lignin, followed by washing of the solids with water. The collected filtrate and washing solutions can then be gathered together and solvent extracted. Tarabanko *et al.* (116) disclosed an improved extraction methodology in two steps at moderate pHs (7-9), minimizing the formation of precipitated lignin, and using extracting agents with distribution ratios for vanillin above 10 (e.g. esters or alcohols).

LLE yields reported in the literature for vanillin from model solutions and from real lignin and oxidized lignin solutions with several solvents are summarized in Table 2.5 and Table 2.6, respectively. These data must be carefully compared due to the different calculation bases and different sources of lignin and processes. Furthermore, some data available in literature are the outcome of a set of separation methods (e.g. extraction, distillation, crystallization) and not only

one extraction process, leading to alteration of the yield and purity when compared with those obtained by a single extraction step.

Many organic solvents, such as alcohols or ionic liquids, as well as binary and ternary mixtures, have been studied for extracting vanillin (from Table 2.2 to Table 2.4). Some authors have demonstrated that temperature (111, 120), pH (104), and initial vanillin concentration (117) influence the partition coefficient K_D. The increase of pH had a considerable negative impact in the distribution coefficient of vanillin (Table 2.2) as well as for other solvents such as butyl acetate – water mixtures (128). For some octanol-water systems the increase of temperature decreased the distribution coefficient for vanillin and vanillic acid (111). The same trend was demonstrated for vanillin employing the aliphatic alcohols such as butanol, heptanol, hexanol and octanol (105).

Table 2.5 Yields of extraction of vanillin from model aqueous solutions

Solvent	Yield (%)	Ref.
Chloroform	85-100	(140)
Ethyl ether	96-100	(140)
Benzene	40-50	(115)
***n*-Butyl alcohol[a]**	59.4	(121)
***sec*-Butyl alcohol[a]**	46.7	(121)
Ciclohexanol[a]	33.5	(121)
Benzyl alcohol[a]	34	(121)
***n*-Amyl alcohol[a]**	17.4	(121)
***sec*-Amyl alcohol[a]**	5.5	(121)
50% Hexane + 50% TBP[b]	84.44	(112)
50% Decane + 50% TBP[b]	99.99	(112)
50% Octan-2-ol + 50% TBP[b]	98.06	(112)
50% Kerosene + 50% TBP[b]	97.73	(112)
ATPS: 40% ACN+20% Sugar[c]	85 - 91	(118)
ATPS 50% ACN+10% Sugar[c]	75 - 89	(118)
ATPS: 50% Alcohol+15% Inorganic salt[d]	98.37-99.94	(119)

ACN: Acetonitrile; **ATPS: A**queous two-phase systems**; a)** 5-6 g L^{-1} vanillin and 25 g L^{-1} NaOH, 3 extraction stages; **b)** pH 1 and 25 ºC and 0.05 $g_{vanillin}$ L^{-1}; **c)** 25 ºC, 0.4 $g_{vanillin}$ mL^{-1}; **d)** 25 ºC, 1 $g_{vanillin}$ L^{-1}; **TBP:** Tributyl phosphate carrier.

Table 2.6 Extracting agents and data on vanillin or other relevant compounds recovery from real mixtures

Targeted compound	Source	Extracting agent / agents	Extraction data			Other information	Ref.
			N	R %	K_D		
V	Alkaline oxidation of sulphite liquor	Benzene	-	-	-	Overall yield 2-3 % w/w_{lignin} Vanillin purity 92% and 63%	(131)
V	Alkaline oxidation of sulphite liquor	Benzene	-	-	-	Final solution of 2.7 – 4.7 $g_{Vanillin} \cdot L^{-1}_{Liquor}$	(132)
V	Alkaline oxidation of sulphite liquor	Benzene	-	-	-	Yield: 8-9.9 % $w_{vanillin}$ / w_{solids}	(133)
V	Alkaline oxidation of sulphite liquor	Tertiary butyl alcohol	1	65.5	1.9	-	(141)
		Butanol	1	35.5	0.55	-	
NaV	Alkaline oxidation of sulphite liquor with 30% of solids content	Isopropanol or propanol	1-5	75 – 99%	-	-	(62)
V	Alkaline oxidation of sulphite liquor	Isopropanol	-	-	1.00	-	(102)
		Butanol			0.20		
		Pure pyridine			2.85		
		Pyridine bases			9.00		
		pyrrolodine			1.22		
V	Oxidized kraft black liquor	1L aqueous Na_2SO_4 ($3g.L^{-1}$) + 5L butanol + SO_2	1	-	2.38	-	(122)
o-V			1	-	3.4		
V & S	Oxidized kraft lignin	Butanol and aqueous alkali salt solution	-	-	-	Composition: 90.4% V; 1.3% o-VAN; 0.3% S, *p*-OHB. 0.3%; G < 1.0%	(122)
V	Bioconversion of ferulic acid	Methyl-tert-butyl ether (MTBE)	-	-	-	Final extract containing 37% w/w of vanillin	(23)
V	Crude vanillin obtained from ferulic acid containing about19.3-19.4 %w of vanillin present is evaporated in the presence of water) (the ethyl acetate	Dichloromethane	-	-	-	V purity: 98.5% (NR) 98% (R) Overall yield: 85% (NR) 94% (R)	(136)
		Isopropyl acetate	-	-	-	V purity: 99% (NR / R) Overall yield: 80% (NR) 83% (R) V purity: 98.7% (NR) Overall yield: 35% (NR)	
V, S & S-OL	Organosolv lignin	Methanol (in the presence of CO_2)	-	-	-	Composition: 1% S-OL, 0.82% V, 1.96% S	(142)

V: Vanillin; **NaV:** Sodium vanillate; ***o*-V:** *ortho*-Vanillin; **S:** Syringaldehyde; **S-OL:** Syringol; ***p*-OHB:** *p*-Hydroxybenzaldehyde; **G:** Guaicaol; **MTBE:** Methyl-tert-butyl ether; **N:** Number of stages, **%R:** Percentage of removal; K_D**:** Partition coefficient; **R:** With washing and recycling a portion of the V from the mother liquors; **NR:** not washing nor recycling a portion of the V from the mother liquors. *****The solvent (ethyl acetate) is initially evaporated in the presence of water, then LLE with dichloromethane or isopropyl acetate at pH 8-9. Afterwards the aqueous phase containing vanillin is precipitated at atmosphere pressure, 20 ºC and pH between 4 and 7.5

Some organic solvents exhibit very low K_D such as hexane (0.2), di-isopropylether (2.75) or toluene (4.1) (Table 2.2). Despite the low K_D for hexane, it can yield pure crystalline vanillin (81). Some solvents having K_D for vanillin between 25-30 are chloroform, butyl acetate, butanol and methyl isobutyl ketone. The best partition coefficient K_D to extract vanillin was found for 50:50 (V/V %) mixture decane:tributyl phosphate carrier (TBP) (K_D = 3311) (112), followed by 50:50 (V/V %) 2-octanol:TBP mixture (K_D = 2512) (112), octylamine (K_D > 600) (113) and heptane-octylamine mixture ($K_D \approx 600$) (113). Other binary systems containing 15% K_2HPO_4 in ethanol and in methanol also revealed good K_D values, 460 and 358, respectively (119).

Studies employing LLE multicomponent model solutions are scarce. Table 2.4 summarizes the values of K_D and α for binary systems and for one real mixture. From the data collected it is possible to conclude that the K_D values for vanillin and syringaldehyde are very low (< 0.1) comparatively with *p*-hydroxybenzaldehyde in LLE with benzene, mixtures of benzene and a complex hydrocarbon solvent (X222, Shell). The same is observed for solvent mixtures of X222 with 5% diethyl ether (0.33) or isopropyl ether (0.38). Vigneault *et al.* (129) found selectivity factors in the range 0.35-0.72 (Table 2.4) for monomers from a depolymerisation mixture using different organic solvents.

The selectivity for vanillin relative to ferulic acid is also the subject of some studies with major interest for the biosynthesis of vanillin from ferulic acid. Through the data gathered in Table 2.4 it is possible to observe that the relative selectivity factor for vanillin is higher than 36. The solvent exhibiting the highest affinity is 2-ethyl-1-hexanol (1400). However, solvents such as ethyl acetate and butyl acetate combine high vanillin K_D (16.8 and 21.0, respectively) and high selectivity factors (84 and 52.5, respectively). Although *n*-hexane has selectivity for vanillin (α_{ij} of 90), the vanillin K_D value is very low (0.09).

LLE with alcohols was suggested by many authors as a means to avoid the acidification stage to convert vanillate (produced in the alkaline oxidation) to vanillin. Some examples go back to the middle of the last century: propanol (62), isopropanol (62), *t*-butanol (141), and butanol (121, 122, 143). Other immiscible alcohols have been also referenced as shown in Table 2.5. More recently Kaygorodov *et al.* (105) demonstrated the potential of C_6-C_8 aliphatic alcohols to extract vanillin. From Table 2.2 to Table 2.4 it is include some literature data regarding K_D and α values employing alcohols as the extracting agent.

Studies on vanillin extraction from model solutions with different alcohols showed K_D ranging from 14 to 30.5, with hexanol providing the highest K_D. Octanol was extensively studied for vanillin (Table 2.2) and for other functionalized phenolic monomers (Table 2.3). According to the published data, at 25 ºC, K_D was higher for vanillic acid (26.5), followed by *p*-hydroxybenzaldehyde (22.9), vanillin (15.38), and syringic acid (12.5). One can infer that octanol

is not an advantageous choice to selectively extract vanillin from a mixture of lignin products due to the lower K_D in this solvent comparatively to other phenolic compounds.

Additional studies have been performed in order to improve the selectivity and performance of this solvent to extract vanillin by adding electrolytes such as LiCl, NaCl and KCl (Table 2.2). LiCl was the one with greatest influence on K_D value leading to increases of 3.35-fold, 1.94-fold and 1.47-fold for vanillin, vanillic acid and syringic acid, respectively, in comparison with single octanol.

Alberda (102) showed that amine derivative solvents in alkaline media had better performance for extracting vanillin than the alcohols isopropyl and butanol (Table 2.2 and Table 2.3). For real oxidized mixtures (Table 2.6) pyridine bases manifested a K_D of 9.

Concerning extraction yields of vanillin from model aqueous solutions in several solvents, Table 2.5 presents the most relevant data. In the literature that goes back to early decades of the last century, propanol (62, 121) and isopropanol (62) reveal to be better than higher alcohols. From the overall reported data, conventional organic solvents have some important disadvantages such as low K_D (e.g. hexane, toluene), toxicity (e.g. benzene), solubility of the extractants in water (e.g. butanol, benzene, butyl acetate) and low efficiency associated with low recovery yields (e.g. some alcohols described in Table 2.5 provide low vanillin recovery yields (<35%) and poor phase separation (e.g. benzene)). Some solvents having reasonable distribution coefficient (e.g. chloroform, octanol) have shown low selectivity for vanillin. Other solvents (e.g. diethyl ether, dichloroethane, carbon tetrachloride) have been studied and proved to be unsuitable for the purpose of vanillin recovery (115, 144).

The formation of vanillin complexes with octylamine (113) or with tributyl phosphate (TBP) (112) has been proposed as a procedure to enhance extraction efficiency of vanillin. Tarabanko *et al.* (113) suggested octylamine in heptane as a way to improve the selectivity for vanillin due to the additional solvent affinity for phenolic groups besides the carbonyl groups. Herein, the vanillin reacts with the octylamine forming a Schiff base which is subsequently extracted into the heptane phase. The authors demonstrated that at the optimum pH (8-10), K_D reaches to about 600 (Table 2.2).

Recently Zidi and Jamrah (112) reported an improved solvent extraction process for vanillin at low pH, using decane:TBP and 2-octanol:TBP (50:50, % V/V) in kerosene aiming to develop a stable supported liquid membrane system which led to K values about 5.5-fold and 4.2-fold, respectively, higher than those obtained by Tarabanko *et al.* (113).

Many vanillin LLE studies have been performed, in particular to avoid prior acidification or concentration steps of the lignin rich media. The distribution ratio of vanillin, selectivity and yield have been improved by complexing agents (112, 113) and electrolytes (102). Attempts to overcome

stripping and/or extractant recovery problems are being made resorting to aqueous two-phase systems (ATPS) and ILs. In the following sub-sections 2.2.2 to 2.2.5 other studied approaches will be addressed.

Bisulphitation is the conversion of vanillin and other compounds carrying carbonyl groups into water-soluble bisulphite complexes by reaction with SO_2 (48, 121, 122, 131, 134, 145). This process is the basis for extractive bisulphitation of vanillin as reported by Major and Nicolle (122).

The purification of vanillin using the bisulphite technique is an ancient method. One of the first reports dates back to 1904 (137), proposing a first step of evaporation, then a CO_2 acidification followed by LLE with ethyl ether and then bisulphitation. Several other authors have been working on bisulphitation with numerous variants and improvements. The sequence of processes encompassing a bisulphitation step proposed by Sandborn (121) is shown in Figure 2.2.

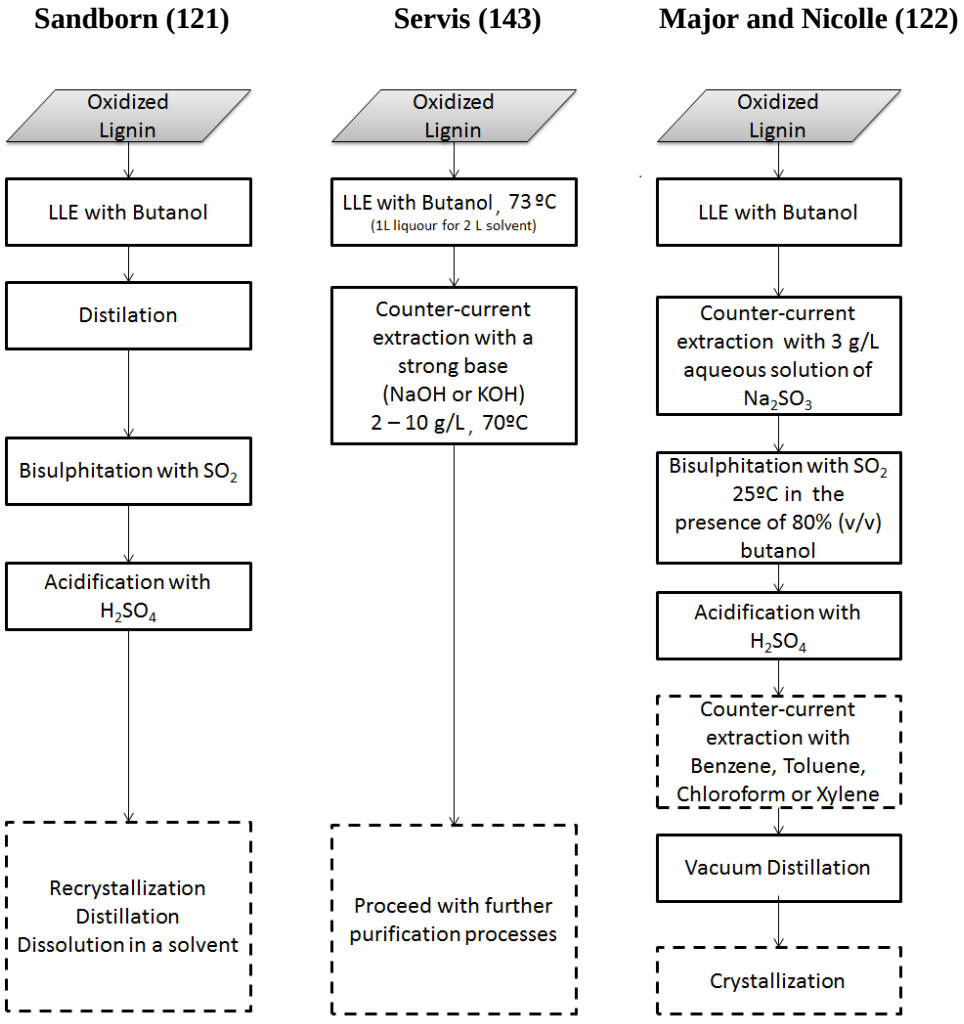

Figure 2.2 Comparison between Sandborn (121) , Servis (143) and Major and Nicolle (122) proposed extraction processes to yield pure vanillin. The dashed rectangles indicate additional techniques recommended by the authors.

After solvent extraction of the oxidized liquor with butanol, the author proposed a distillation step and the treatment of the crude vanillin extract by a bisulphitation process with SO_2 coming from sulphurous acid (H_2SO_3) followed by further purification processes. Some improvements were studied and suggested by other researchers (122, 143, 146).

Servis (143) (Figure 2.2) upgraded the method of Sandborn (121) by replacing the distillation stage of the aqueous-butanol extract with a counter-current extraction by means of a weak aqueous solution containing about 2-10 g L^{-1} of NaOH or KOH, saving steam costs and avoiding vanillin losses with heating.

Later on, Major and Nicolle (122) introduced the extractive bisulphitation by the formation of bisulphite complexes in the presence of an extracting solvent (e.g. butanol). The sequence of purification proceeded as disclosed in Figure 2.2.

2.2.2. Aqueous two-phase solvent systems (ATPS)

Studies of ATPS for separation and purification of several high added value biomolecules are increasing remarkably (117-119, 147-149) due to their versatility, high efficiency, selectivity, and fast mass transfer rates, being relatively simple to implement at industrial scale. Nonetheless, some drawbacks must be overcome depending on the type of ATPS such as chemical changes of the targeted compound that compromise its added value, high viscosity of some polymer-based systems, and high cost. Some studies regarding the application of ATPS for vanillin recovery have been performed with a wide diversity of systems using inorganic salts, sugars and ionic liquids (IL) (117-119) as depicted in Table 2.2. IL-ATPS-based systems are discussed in detail later.

The partition of aqueous solutions of vanillin with ATPS composed by an alcohol and an inorganic salt was investigated by Reis *et al.* (119). Vanillin distribution coefficients were obtained for ATPS composed by a 50% alcohol solution and 15% of an inorganic salt solution at 25 ºC and atmospheric pressure. The authors demonstrated that vanillin preferentially migrates to the alcohol-rich phase and the highest *K* obtained was corresponding to the ATPS composed by 50% ethanol and 15% K_2HPO_4 solution. The other distribution coefficients obtained are shown in Table 2.2. Vanillin recovery yields for all ATPS studied were between 98.4% and 99.9% (Table 2.5).

Cardoso *et al.* (118) have demonstrated the potential of carbohydrate-acetonitrile-based ATPS for extracting vanillin. Carbohydrates can be suitable substitutes to the conventional salts inducing an effect similar to the salting-out due to their hydration capacity, also known as “sugaring-out” effect. Several carbohydrates were considered in this study such as monosaccharides (glucose, mannose,

galactose, xylose, arabinose and fructose) and the disaccharides sucrose and maltose. It was shown that vanillin has more affinity for the acetonitrile phase and its distribution coefficient is influenced by the hydration capacity of each sugar given by the number of hydroxyl groups and stereochemistry. The authors managed to attain vanillin recovery yields of 75% and 91% in just one step (118). The maximum K was attained using mannose (9.8) and xylose (8.7). Table 2.2 summarizes the conditions and the different K values obtained by Cardoso *et al.* (118).

2.2.3. Ionic liquids (ILs)

ILs have been indicated as holding great potential for recovering several biomolecules of interest namely amino acids (150) proteins (151), alkaloids (152), among others (153, 154). ILs constitute a fascinating approach due to their interesting physical and chemical properties such as low volatility, flammability and vapour pressure, extraordinary solvation capability, high thermal stability and selectivity (154, 155). Some ILs have good affinity for organic compounds and their polarity, hydrophobicity, viscosity, and other physical and chemical properties can be easily tuned as desired (154). On the other hand, some ILs can be toxic and/or manifest incompatibilities with certain materials (121), among other disadvantages (156, 157).

The potential for ILs in the extraction of vanillin has been considered as an alternative to organic solvents by Cláudio *et al.* (117). Vanillin distribution coefficients *K* were assessed on IL-based ATPS systems composed by imidazolium-based ILs, water and the inorganic salt K_3PO_4, studying the influence of anionic and cationic structure of the IL, equilibrium temperature (15-55 ºC) and vanillin concentration (0.5-7.2 g L^{-1}). Vanillin has preference for the IL-rich phase due to favourable interactions and due to the lower surface tension of the IL phase. The authors showed that vanillin extraction is more efficient for IL with *salting-in* inducing behaviour (low charge density ions). Therefore all distribution coefficients are higher than the unit, ranging from 2.7 to 98.7, as summarized in Table 2.2.

The highest distribution coefficient for studies performed at 25 ºC and 1.0 g L^{-1} of vanillin, the most studied condition, was obtained for $[C_6mim]Cl$ (49.59, see Table 2.2).

Cost, desired purity, water content, type of by-products and recycling/reuse issues are some of the variables that should be carefully studied in each application when considering an industrial application of ILs (157). The development of green ILs is still a task to overcome and their recovery to reuse also requires more research efforts (154, 155). There are no studies for LLE of syringaldehyde employing ILs or IL-based ATPS systems.

2.2.4. Gas-expanded liquid extraction and other gas liquid extraction processes

Eckert *et al.* (142) studied the extraction of vanillin, syringaldehyde and other low molecular weight compounds through gas-expanded liquid extraction. Methanol is used to dissolve an organosolv lignin and the solution is next loaded into an equilibrium cell where CO_2 is added to promote precipitation of the higher molecular weight lignin fractions. During this precipitation process, three phases are generated, and the low-molecular weight compounds, soluble in the liquid-phase, are collected by means of a high pressure valve. Starting from an organosolv lignin solution in methanol the authors manage to extract 1% syringol, 0.82% vanillin and 1.96% syringaldehyde (at 13 bar and 25 ºC).

Adrian *et al.* (120) developed a method for extracting thermally sensitive high value compounds by using two miscible liquids (at atmospheric pressure, e.g. water and water-soluble organic solvent such as an alcohol or a carboxylic acid) into two liquid phases by pressurization with CO_2 at near critical conditions. This phenomenon is also designated as *salting-out* with a gas (123). A ternary system water-acetone-CO_2 in high pressure liquid-liquid-vapour equilibrium was studied for partition of vanillin at 40 ºC (26 - 70 bar) and 60 ºC (37 - 89 bar). Vanillin preferentially migrated to the organic phase and the maximum *K* attained was 2.5 for 40 ºC. For 60 ºC the *K* was 2.35 revealing that the temperature has low impact on the vanillin *K*.

Although gas expanded liquid extraction involves lower operational pressures than supercritical systems, the energy required for compression of gases must be considered for the development of a sustainable and green process.

2.2.5. CO_2 extractions in supercritical conditions

Supercritical carbon dioxide (sc-CO_2) fluid extraction is a particular case of LLE distinguished by operating with CO_2 at temperature and pressure above the critical point (cp), presenting higher diffusivity (it can penetrate into the matrix as easily as a gas) and, at the same time, lower density, viscosity and surface tension than an organic solvent (158, 159).

Phenolic compounds can be highly soluble in CO_2 (97, 160) depending of intra- and intermolecular interactions amongst the compounds present in the feed mixture. The type and position of the aromatic ring substituents have great influence on the solubilities in sc-CO_2 soluble compounds. On one way, the intermolecular hydrogen bonding strengthens the solute-solute interaction thereby drastically reducing their solubility. On the other hand, different effects from the intramolecular

hydrogen bonds can be used to separate isomers. Skerget *et al.* (97) performed a study about solid-liquid phase transitions and equilibrium sc-CO_2 solubilities of vanillin, *o*-vanillin, ethylvanillin and *o*-ethylvanillin. All of these compounds possess three functional groups: aldehyde and hydroxyl in *ortho* or *para* position and an alkoxy group in the *meta* position. In this work it was demonstrated that the presence of a hydroxyl group in the *ortho* position favours the solubility and, therefore, *o*-vanillin and *o*-ethylvanillin are more soluble than the respective isomers while methoxyl or ethoxyl group at *meta* position does not influence the solubility. The authors disclosed solubility data at 40 ºC, 60 ºC and 80 ºC covering a pressure range from 80 to 310 bar and concluded that efficient separation among isomers can be accomplished at 40 ºC and 300 bar.

Vanillin extraction from different sources like vanilla beans (161), oxidized lignin solutions (138, 162-165), and broths of bioconversion of ferulic acid (166) has been reported. Some studies were also performed with vanillin model solutions to understand the solubility properties, extraction capabilities and other relevant vanillin-CO_2 system characteristics (97, 167-170).

sc-CO_2 fluid extraction was first implemented for the withdrawal of flavour and aroma compounds from vegetable matter. Vitzthum and Hubert (171) in 1980 proposed a two-step extraction process for vanillin extraction from vanilla pods: a first extraction with dry sc-CO_2 for 4 hours at 403.5 bar and 45 ºC, followed by wet CO_2 extraction for 6 hours at conditions bellow the critical point (65.9 bar and 25 ºC). The extraction yield was considerably low (10%) as well as the vanillin purity in the extract (28%) starting with a feed containing 3%. Nonetheless, this work gave an optimistic tone for applying this technology in a final stage of vanillin extraction.

In the perspective of vanillin purification, Makin (164) disclosed CO_2 fluid extraction at supercritical conditions to extract impurities from a crude vanillin originated from paper mill waste liquors. At moderate conditions (60 min, 52.7 bar, 40 ºC) about 85% of the vanillin could be recovered with about 93 wt% purity, starting from a crude extract containing 82 wt% of vanillin. The authors also have theoretically established that with multistage counter-current CO_2 extraction (4 extraction cycles) of this crude extract it would be possible to obtain vanillin at 99.4-99.8 % purity. However, the higher the final purity in vanillin, the lower is the yield of vanillin recovered.

Klemola and Tuovinen (138) applied sc-CO_2 fluid extraction to obtain vanillin from neutralized oxidized lignin media, as an alternative to conventional LLE. Vanillin dissolved in CO_2 was recovered by means of fractionation promoted by gradually decreasing pressure and temperature, obtaining a vanillin rich fraction in the low CO_2 soluble compounds fraction and another fraction composed of highly CO_2 soluble compounds. With the extraction conditions shown in Table 6, 96.8-98 % of vanillin yields and purities between 88-91% were obtained. These authors (138) also suggested multiple stages of crystallization after sc-CO_2 fluid extraction and a sequential extraction of neutralized oxidized lignin with toluene and sc-CO_2 followed by one crystallization stage.

Coenen and Konrad (163) recommended a multi-step extraction of vanillin comprising: 1) CO_2 extraction with temperature below the supercritical temperature and pressure in the range of supercritical pressure, 2) gas scrubbing with Na_2SO_3 aqueous solution, 3) acidification with H_2SO_4 and 4) heating the solution up to 50 ºC to yield purer vanillin in the order of 91.3%.

Recently, Assmann *et al.* (162) presented a microfluidic reactor as a new improvement for extracting vanillin from lignin oxidation products by sc-CO_2 (the conditions proposed are summarized in Table 2.7). The extraction by the supercritical phase comprises contacting the aqueous solution of vanillin using a segmented flow in a microchannel. The major advantages of this technology are the increase of surface to volume ratio and heat and mass transfers at well-controlled conditions (130, 168). Vanillin aqueous solution distribution coefficients in sc-CO_2 at 40 ºC increased from 0.012 to 0.222 in the range 81 to 111 bar, which is consistent with the increase of fluid density inflicted by the pressure rise (168).

Many benefits come from employing supercritical fluid extraction (SFE) processes. However, this technology has some disadvantages that can seriously compromise its industrial application and sustainability. The main drawbacks are the fact that SFE is a very expensive technology, consequence of the special conditions required for the high pressure. Furthermore, although this method requires considerably less energy than the conventional purification methods, the crude vanillin solution must contain at least 50 wt% vanillin in order to be commercially affordable (164).

Table 2.7 Conditions for CO_2 fluid extraction aiming the recovery of vanillin or other compounds from different materials

Target material	Type extraction	T (ºC)	P (bar)	Extracting agent flow (A)	Solution flow (B)	Ratio A/B	Yield (%)	Purity (%)	Ref
Crushed vanilla pods	Batch	1st stage: 45 2nd stage: 25	1st stage: 403.5 2nd stage: 65.9	-	-	-	10	28	(171)
Cryo grinded vanilla beans	Batch	31 - 37	100-130	-	-	2 – 62 $g_{CO2}\ g^{-1}_{vanilla\ bean}$	95	74 – 97	(161)
Crude vanillin synthetized from glycoxylic acid	Batch	55	250	20 $kg_{CO2}\ h^{-1}$	-	-	99.8	95.66	(172)
		55	200	22 $kg_{CO2}\ h^{-1}$	-	-	95.7	95.03	
Crude ethylvanillin synthetized from glycoxylic acid	Batch	50	250	25 $kg_{CO2}\ h^{-1}$	-	-	98.5	95.31	(172)
Crude vanillin synthesized from eugenol or from wood-derived products	Batch	32-50	40.5-101	-	-	10-30	76.2-90.8	82.2-92.9	(164)
Oxidized sulphite liquor	Batch	60	150	-	-	700	96.8	88	(138)
	Batch	60	230	-	-	800	98	91	
	Batch	60	350	-	-	-	98	90	
Oxidized sulphite liquor	Counter-current extraction	27	100	4.65 $kg_{CO2}\ h^{-1}$	0.95 $kg_{liquor}\ h^{-1}$	-	91*	91.3*	(163)
Oxidized lignin solution	Counter-current extraction	53	220	25 $kg_{CO2}\ h^{-1}$	-	-	97.8	93.28	(162)
		39.8 – 59.3	81-121	120 $\mu L_{CO2}\ min^{-1}$	50 $\mu L\ min^{-1}$	2.4	-	-	

***** Vanillin yield and purity are the result of combining a first stage with sc-CO_2 fluid extraction in the conditions mentioned in the table and pH value of 5.6, a second stage comprising of solvent scrubbing with Na_2SO_3 aqueous solution (75 g L^{-1}) performed for 5 hours operated at same temperature and pressure as in the extraction stage, an acidification to a pH value of 3.5 with sulphuric acid and a final heating stage of the solution up to 50 ºC.

2.3. Crystallization, precipitation and evaporation

Crystallization is commonly used as a final stage of purification of several food or pharmaceutical products (173). This technology consists in a solid-fluid separation in which crystalline particles are produced from a homogeneous fluid phase. The processing conditions must allow good separation between phases (173, 174) and produce pure crystals of a compound at elevated yield while preserving their biological activity, flavour and/or odour (173).

Usually, water, alcohols or solvent mixtures are employed to promote crystallization. If water is the additional solvent then the separation process is designated as *watering-out*. When an organic solvent is added to an aqueous salt solution the process is named as *salting-out* (173).

In order to understand the dominant process variables in the crystallization mechanism of vanillin, several studies with model solutions have been published giving more enlightenment about the influence of solvents, nucleation and presence of additives in vanillin crystallization and purity levels attained (175-178). The propanol:water systems are the most studied because they are widely used in industry (175-178).

Most of the works referring to vanillin, suggest crystallization as the preferred final stage for vanillin purification. Proposed methods to deal with more complex mixtures are based on the differences of solubility either due to solvent composition or/and temperature changes. This task can be very arduous since the mixture would contain very similar compounds with tiny differences of solubility. Table 2.8 presents some examples of crystallization processes to recover functionalized phenolic monomers from the oxidized lignin reaction media. So far, proposed vanillin purification processes employing crystallization manage to accomplish a vanillin purity ranging from 96 to 99.6 % and yields above 83%.

Water, methanol and acetone (pure or solvent aqueous mixtures) are the most common solvents suggested in the purification of vanillin and other relevant compounds (138, 179, 180)). Aqueous ethanol solutions were also employed by Liu *et al.* (172). Fractional precipitations with aqueous solutions of zinc or magnesium salts have also been suggested (179, 181).

Crude vanillin refinement through crystallization was proposed in 1962 by Schoeffel (179) involving two main stages of dissolution in aqueous methanol and one in water. The supernatant of the first crystallization stage was also treated to recover vanillin by a multi-step sequence which was later on simplified by Gitchel *et al.* (181) using successive treatment of the crystallization mother liquors with alkali-metal hydroxide and zinc salt solutions to yield its respective insoluble salt, followed by bisulphitation and distillation, yielding similar vanillin purities.

Table 2.8 Examples of crystallization processes proposed to recover functionalized phenolic monomers from the oxidized lignin reaction media

Solvents / steps employed	Target solutions	Target compound(s)	Achieved purity	Achieved yield	Ref.
Sequential LLE and precipitations with magnesium salts	Supernatant after crystallization with 40% aqueous methanol	V	97	-	(179)
Sequential addition of alkali-metal hydroxide and zinc salt	Mother liquors (40% methanol) containing 90% V, 6% *p*-OHB, 2% 5-fV and 2% OV	5-fV (stage 1)	80%	-	(181)
		V (stage 2)	72%	-	
		V (stage 3)	96%	-	
Hot hydrocarbon extraction with AMSCO LEP[a] solvent (W-3) containing parafins (51%), C5-C6 naphthenes (24%), C8-C12 aromatics (18%) and dinaphthenes (6%) and crystallization promoted by dropping the temperature to 20 ºC	Oily phase of the distillation residue from previous extraction of oxidized sulphite liquor (containing about 65% vanillin)	V	93.2%	83%.	(182)
Water	Oxidized sulphite liquor after sc-CO_2 extraction	V	Stage 1: 8.32% Stage 2: 99.58	-	(138)
		OG	Stage 1: 1.24% Stage 2: 0.25	-	
		S	Stage 1: 0.05% Stage 2: 0.02%	-	
	Oxidized sulphite liquor after toluene and sc-CO_2 extractions	V	97.54%	-	
		OG	2.19	-	
		S	0.01	-	
Ethanol	Crude vanillin synthesized from glycoxylic acid and submitted to SFE	V	99.99	94	(172)
	Crude ethylvanillin synthesized from glycoxylic acid and submitted to SFE	EV	99.96	94	
20% Ammonia aqueous solution and sulphuric acid	Extract obtained after bisulphite extraction of oxidized aspen wood	V	97-98%	> 90%	(61)
		S	98.5-99%		

a) AMSCO LEP is a hydrocarbon solvent; **V:** Vanillin; **5-fV:** 5-Formyl vanillin; **OG:** Acetoguaiacol; **EV:** Ethylvanillin; **OV:** Acetovanillin; ***p*-OHB:** *p*-Hydroxybenzaldehyde

In order to substitute the complex purification steps suggested at that time to yield a highly purified fraction of vanillin, Diddams and Renaud (182) proposed extractions with a hot hydrocarbon solvent at 70 ºC and a cooling step to 20 ºC to precipitate vanillin. In one of the examples given by the authors in their patent (182) the average vanillin content is 93.2% after 13 extraction cycles with hydrocarbon solvent performed to the vanillin enriched phase after methanol stripping, reaching a total extraction yield of 83%.

Separating vanillin from syringaldehyde through one single step of crystallization is a difficult process and sequential precipitation processes such as the ones suggested by Schoeffel (179) and Gitchel (181) can be a very arduous task. Creighton *et al.* (134) isolated syringaldehyde with good yields by means of one-stage precipitation with ethanol and gradual addition of ammonia. Vanillin was recovered at low yields from the resulting supernatant by evaporation, extraction with ether, and precipitation by a new addition of ammonia. Similar approaches were followed by Zhang *et al.* (183) and Deng (184). Based on the same principles, Tarabanko *et al.* (61) accomplished vanillin and syringaldehyde purification: after LLE and bisulphite extraction of oxidized aspen wood, ammonia aqueous solution is applied to selectively precipitate syringaldehyde. The filtered syringaldehyde crystals are then mixed with water, acidified, washed and dried yielding 98.5-99 % of purity. The acidification of the ammonia-derivative supernatant, along with the water washings obtained from the syringaldehyde crystallization step, led to vanillin crystals of 97-98 % purity.

Tarabanko *et al.* (61) proposed an additional separation method for syringaldehyde and vanillin based on LLE or crystallization after treating the initial mixture with aqueous-potassium carbonate solutions. Potassium vanillate and potassium syringate enhance solubility differences and consequently allow a more efficient LLE or crystallization.

Evaporation used to concentrate dilute solutions also produces crystals that can be washed and separated from the slurry through centrifugation or filtration. Some authors have suggested evaporation of the lignin solution prior (62) or after (61) LLE, or any other separation method, as a means to concentrate the solution/extract.

2.4. Membrane separation

Membrane separation is a process where a feed stream passes through a semipermeable barrier and is separated into two streams (permeate and retentate streams - Figure 2.3.a) while at the same time the transport of some compounds is selectively restricted.

(A) (B)

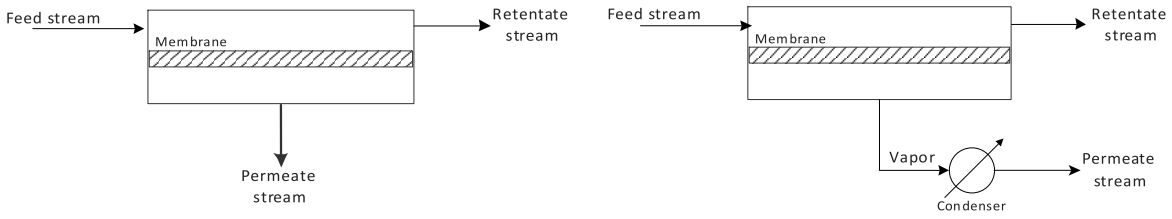

Figure 2.3 Conventional membrane separation (A) and pervaporation coupled with sample condensation (B) schematics.

Regarding the type of operational driving force, membrane processes can be classified in: i) pressure driven operations (microfiltration, ultrafiltration (UF), nanofiltration (NF), reverse osmosis, gas separation); ii) concentration driven operations (dialysis, osmosis and forward osmosis); iii) operations with electric potential gradient (electrodialysis, membrane electrolysis and electrophoresis); and iv) operations with temperature gradient (membrane distillation and pervaporation). The main advantages associated with membrane separation processes are their low energy requirements when comparing with other separation methods and, in some cases, good fractionation capability without resorting to any reagent or solvent as in LLE process. Pervaporation (Figure 2.3.b) has an additional advantage over distillation since it allows the separation of compounds with similar boiling points in mild conditions with less energy consumption. The use of membrane contactor processes has the benefit of being easily controlled with independent liquid fluid dynamics and possessing good mass transfer due to high contact areas.

In the perspective of separation and purification of oxidized lignin streams, subsection 2.4.1 summarizes studies related with pressure driven processes encompassing ultrafiltration (UF) (60) and nanofiltration (NF) (185). For vanillin recovery from fermented broths, pervaporation (186-188) and membrane contactors (128) have been proposed as well, and is addressed in subsections 2.4.2 and 2.4.3, respectively.

2.4.1. Ultra and Nanofiltration

Membrane separation has been long suggested by many authors as a way to fractionate and concentrate components from lignocellulosic-derived streams (189-194). UF is the most extensively separation process studied being applied to hemicellulose separation from lignin rich streams (194) or to fractionate lignin (189, 191, 195, 196) or for lignin concentration as an alternative to acid precipitation (197); NF has also been studied in a sequential process for small organic molecules or inorganic chemicals elimination (194, 195).

To our knowledge just one study is related with the application of membranes to the real oxidized lignin solution. This study was performed by Werhan *et al.* (185) on the ethyl acetate extract of the oxidized reaction medium as summarized in Table 2.9. Among the 4 tested membranes, PuraMem S380 showed the best performance due to the higher rejections to dimers (83%) and trimers (93%) comparatively to monomers (38%).

Koncsag and Kirwan (198) demonstrated the feasibility of a sequence of UF and NF membranes and (or) applying direct NF membrane for treating the depolymerised lignin and separate dilignols and trilignols from other higher molecular weight molecules resulting from enzymatic hydrolysis.

In a perspective of process development for separation of vanillin from lignin oxidation mixture, Žabková *et al.* (60) studied the performance of ceramic UF to recover vanillin from a solution of vanillin and commercial lignin. Different molecular weight cut-off membranes (1, 5 and 15 kDa) were tested for the experimental conditions summarized in Table 2.9. For all tested membranes lignin was retained above 85% and vanillin transported in the permeate stream. As expected, the membrane with the lowest cut-off retained more lignin but with the disadvantage of having the lowest permeate flux, with no noticeable effect of pH on lignin retention. However, for the membrane with the highest cut-off, the change in pH value from near 8.5 to 12.6 promoted a decrease of the retention coefficient of lignin of about 9%, which is disadvantageous for the targeted separation.

Table 2.9 Membrane separation applied to complex mixtures for vanillin recovery

Solution or medium	Membrane				Membrane separation conditions						Ref
	Commercial designation	Composition	MWCO (Da)	Type	Q_{feed} (L h^{-1})	C_{feed} (g L^{-1})	pH	TMP (bar)	T (ºC)	Rejection (%)	
V and VA	DuraMem™ 500 [a]	PI	500	NF	-	0.25	-	20	-	V: 13.8-17.9; MV: 16.8-18.2	(185)
	DuraMem™ 900 [a]	PI	900	NF						V ≈0 /MV: ≈0-1.2	
	PuraMem™ 280 [a]	PI	280	NF						V: 24.7-25.8 / MV: 41.5-42.3	
	PuraMem™ S380 [a]	PI	600	NF						V: 26.2-31.7 / MV: 26.5-31.1	
	Selro® MPF44 [b]	PDMS on PAN	250	NF						V: ≈0-2.5 / MV: ≈0-2.8	
Ethyl acetate extract of oxidized lignin (average weight ≈ 1150 g mol^{-1})	DuraMem™ 500 [a]	PI	500	NF	-	5	-	20	-	Mon: 15.7 / Dim: 77.5 / Trim: 88.8	
	DuraMem™ 900 [a]	PI	900	NF						Mon: 23.2 / Dim: 80.9 / Trim: 91.8	
	PuraMem™ 280 [a]	PI	280	NF						Mon: 8.0 / Dim: 77.3 / Trim: 86.6	
	PuraMem™ S380 [a]	PI	600	NF						Mon: 38.4 / Dim: 83.2 / Trim: 93.2	
V and commercial lignin (60K g mol^{-1})	Filtanium 1KDa [c]	TiO_2	1000	UF	130	V: 6 / Lignin: 60	8.5	1.55	25	V: ≈0 / Lignin: 95.1	(60)
					120		12.5			V: ≈0 / Lignin: 97.2	
	Filtanium 5KDa [c]	TiO_2	5000	UF	120	V: 5 / Lignin: 60	12.5	1.55	25	V: ≈0 / Lignin: 96.8	
	Kerasep 15KDa [d]	Al_2O_3- TiO_2	15000	UF	109	V: 0.5 / Lignin: 5	8.5	1.30	25	V: ≈0 / Lignin: 91.6	
					102	V: 2 / Lignin: 20	8.5			V: ≈0 / Lignin: 95.8	
					102	V: 2 / Lignin: 20	12.5			V: ≈0 / Lignin: 87.3	
					101	V: 6 / Lignin: 60	8.5			V: ≈0 / Lignin: 94.3	
					101	V: 6 / Lignin: 60	12.5			V: ≈0 / Lignin: 86.5	

a) Supplier Evonik MET; **b)** Supplier Koch; **c)** Supplier Tami Industries; **d)** Supplier Orelis; **MWCO:** Molecular weight cut-off; **NF:** Nanofiltration; **UF:** Ultrafiltration; **PI:** Cross-linked polyimide (integral asymmetric); **SIL:** Silicone-coated polyimide (thin-film composite membrane); **PDMS:** Polydimethylsiloxane; **PAN:** Polyacrylonitrile; **V:** Vanillin; **MV:** Methyl vanillate; **Mon:** Monomers; **Dim:** Dimers; **Tri:** Trimers

2.4.2. Pervaporation

In pervaporation a dense, non-porous membrane acts as a selective barrier between the liquid-phase feed and the vapour-phase permeate (199) which is continuously desorbed by means of vacuum or carrier gas stream (200). The transport through membrane is based on a solution-diffusion mechanism with an intense solute-membrane interaction (200) .

Pervaporation is a suitable process for volatile compounds of low molecular size and with great potential for organic-water and organic-organic separations. Therefore it constitutes a very promising technology for the purification of vanillin or syringaldehyde.

Pervaporation coupled with crystallization have been attempted by Zhang *et al.* (201) to recover phenol crystals in very dilute concentrations from aqueous solutions giving also good insights of using a similar type of apparatus to purify vanillin and syringaldehyde.

Pervaporation process has been suggested in literature as a process to recover and/or purify vanillin from synthetic or bioconversion production routes and/or increase vanillin productivity (186-188). Böddeker *et al.* (187) suggested using PEBA (polyether-polyamide block-copolymer) in membrane pervaporation process for recovering vanillin from the bioconversion of eugenol/isoeugenol and managed to attain a final product with more than 99% in vanillin. The feasibility of integrating a pervaporation process with the fermentation of ferulic acid was demonstrated by Brazinha *et al.* (186). At the fermentation pH 7.2, vanillin is neutral while the main co-products, vanillic acid and ferulic acid are ionized. The authors take advantage of this difference to recover vanillin by pervaporation with simultaneous intensification of the fermentation. Additionally, it was demonstrated that vanillin production by photocatalysis of ferulic acid can be coupled with pervaporation to increase productivity since the synthesized vanillin is continuously removed (188, 202, 203).

2.4.3. Membrane contactor processes and perstraction

Nowadays, new membrane systems and membrane contactors are emerging in a perspective of process intensification. The main concept of this type of systems is based upon the establishment of an interface for mass transfer and/or reaction between two phases by means of a solid, microporous, hydrophilic or hydrophobic polymeric matrix. Some examples of membrane contactor systems are membrane strippers, membrane scrubbers, membrane extractors, supported liquid membranes, membrane distillation, osmotic distillation, membrane emulsifiers and phase

transfer catalysis. The main principles, advantages and applications are well summarized in literature (204, 205).

Sciubba *et al.* (128) suggested a new process for treating fermented broths by hollow fibre membrane contactor technology where the membrane behaves as a physical interface to "couple" solvent extraction with the bioreactor. Based on the previous evaluation of partition coefficients of vanillin and ferulic acid in several solvents and analysis of the mass transfer coefficients (128), the authors managed to selectively remove vanillin in detriment of ferulic acid during the bioconversion favouring vanillin production.

Perstraction or pertraction is a separation process where certain solutes from a liquid feed stream migrate through a membrane, either a nonporous polymer or a liquid, and are simultaneously stripped to a liquid solution. Perstraction silicon rubber membrane bioreactor (SRMBR) was studied by Wu *et al.* (206) for continuous vanillin recovery from the bioconversion of clove oil. This is a perstraction process employing a nonporous membrane process driven by diffusion mechanism, which is also suitable for incorporating in pervaporation bioreactors for separation of volatile organic compounds (207-209).

Recently, Stiefel *et al.* (210) designed an electrochemical membrane reactor with a nanofiltration ceramic membrane aiming to obtain higher recovery of low molecular weight compounds with improved membrane production rates and permeate fluxes.

2.5. Adsorption

2.5.1. General considerations

Adsorption is based on the interactions between the solid and the molecules in the fluid phase. Several adsorbent-adsorbate interactions can be involved (e.g. van der Waals, acid-base interaction, ionic hydrogen bond, π-bond, covalent bond) and give rise to either physical adsorption or chemisorption. In the perspective of the recovery of an adsorbate and adsorbent regeneration, the interaction should allow desorption and recovery.

Adsorption constitutes a good substitute to organic solvent extraction of vanillin with the main advantage of direct application on oxidized lignin solution which is usually a diluted solution of functionalized phenolic monomers (211).

Hence, the number of separation stages can be markedly reduced and the overall process can become more attractive due to the combined possibility to recover, purify and concentrate in food graded adsorbents.

Literature is mostly related with studying the potential of a particular adsorbent using vanillin model solutions. Thus, these studies lack explaining the competition among vanillin and the other compounds present in the oxidation mixture, many of which have very similar physical and chemical properties.

The next subsections provide a detailed review of literature about the type of ionic and non-ionic adsorbents applied with the purpose of recovering functionalized phenolic monomers from the mixture of oxidized lignin. Data related with model compounds solutions will also be presented because they positively contribute to the assessment of the potential of a given adsorbent.

2.5.2. Ion exchange

Ion exchange resins are polymer matrixes with functional group(s) that can act as cation or as anion exchangers, depending on their negative or positive charge, and are classified into as strong or weak exchangers. Existing literature using ion-exchange resins in pure phenolics and natural extracts is considerable (212-215). This type of resins has been also studied in the perspective of process intensification in the bioconversion of isoeugenol (216) or lignocellulose hydrolysates to vanillin (217).

On the perspective of vanillin and syringaldehyde recovery, cation exchange process is applied to neutralize the compounds resulting from alkaline oxidation of lignin, thus avoiding the large consumption of acid that would be required by direct acidification of the solution. In accordance, Forss *et al.* (218) have demonstrated a saving of 60% of the required acid. However, a prior step for separation of high molecular weight fractions of lignin is required to avoid operational problems due to lignin precipitation with pH decrease.

Table 2.10 summarizes the applications of ion exchange resins in the recovery of vanillin from oxidized lignin media. The main type of ion exchange resins studied is of cationic nature, strongly or weakly acidic. It is important to note that the majority of studies with the real oxidized lignin medium are focused exclusively in vanillin. Depending on the lignin source, a variety of low molecular weight phenolic aldehydes and phenolic acids are also produced. Since some of these compounds have polarities and properties similar to vanillin, they will probably be also adsorbed,

although some differentiation from vanillin would be possible due to eventual differences on adsorption rates.

The first reported work with vanillin adsorption employing ion-exchange is relative to Töppel's US patent 2897238 (219) in 1959 where it was attempted to improve cationic exchangers to promptly adsorb compounds with a carbonyl group, namely aldehydes and ketones by charging a polystyrene sulfonic acid cation exchanger with hydroxylammonium chloride solution, enhancing the interaction of the carbonyl group of vanillin through the ammonia group. Vanillin was then eluted with 3 M hydrochloric acid solution. This was of major importance at that time once it allowed the use of cheaper and physical-chemical stable cationic resins for vanillin adsorption.

Logan (220) considered the application of a weak cation exchange process for the same purpose. The additional goals were to sharply decrease the acid needs for neutralization of the phenolates, provide the recovery and reuse of the free or combined sodium present in the mixture and, at the same time, regenerate the resin to its hydrogen form by employing sulphurous acid or soluble bisulphite. Two weak cation exchange resins were studied: Amberlite® IRC-50 (from Rohm and Haas) with carboxylic acid exchange centres and Duolite C-63 (from Chemical Processing Company) with phosphoric acid exchange centres. Examples given by the author patent are focused in the sodium recovery and its re-utilization in lignin oxidation or other processes. Thus, no results regarding the efficiency of employing these resins in the recovery of vanillin are mentioned.

Forss *et al.* (211, 218) explored various cation-exchange resins to simultaneously recover the sodium vanillate and regenerate the resin, as depicted in Table 2.10. Dowex® 50W-X2 and Dowex® 50W-X8 showed the highest adsorption capacities of 5.4 and 5.5 $kg_{NaV}\ m^{-3}_{resin}$, respectively. Both resins have a microporous PS-DVB matrix and a strong sulfonic acid functional group with Na^+ as counter ion. After initial activation with 3 M NaOH, the oxidized mixture was applied into the packed bed and the elution of the products was attempted with water or a combination of sodium carbonate solutions and water. A separation of lignin, sodium and low molecular weight phenolics was possible because of their different elution orders, achieving a final enriched vanillin fraction. When changing the elution solution to sodium carbonate aqueous solution, the authors concluded that it only slightly influenced the elution of oxidized lignin but the adsorption of the oxidation products increased. However the elution time and, consequently, the elution volume also increased.

Table 2.10 Summary of applications of the ion-exchange resins on the recovery of functionalized phenolic monomers

Reference	Stecker *et al.* (74)	Žabková *et al.* (59)	Fargues *et al.* (54)	Logan (220)	Logan (220)	Schmitt *et al.* (72)
Commercial name and type	Amberlite® IR402 (OH)	Amberlite IR120H	Duolite C20	Duolite C-63	Amberlite IRC-50	Dowex monosphere 550a OH
	Rohm & Hass	Rohm & Hass	Rohm & Haas	Chemical processing company	Rohm & Haas	Dow
	Anion exchange resin	Cation exchange resin	Cation exchange resin	Cation exchange resin	Cation exchange resin	Anion exchange resin
	Strong base	Strong acid	Strong acid	Weak acid	Weak acid	Strong base
Matrix	PS-DVB copolymer	PS-DVB Styrene DVB copolymer (8%DVB, gel type)	PS-DVB Styrene DVB copolymer	n.k.	n.k.	Polystyrene divinylbenzene
Functional group	Quaternary ammonium	Sulfonic	Sulfonates	Phosphoric acid	Carboxylic acid	Tetraalkylammonium
Total exchange capacity (given by supplier)	0.95 eq L^{-1} minimum (OH^- form)	1.8 eqH^+ L^{-1}	2.00 eqNa^+ L^{-1}	n.k.	n.k.	1.10 eq L^{-1}
			APPLICATION DESCRIPTION			
Counter ion	OH^-	H^+	Na^+	H^+	H^+	OH^-
Targeted solute	NaV	NaV	NaV	NaV and other low MW phenolates		NaV
Targeted solution / mixture	Alkaline oxidized lignin solution obtained from electrochemical oxidation	V in NaOH solution (0.033 eq L^{-1} V in 0.03 eq L^{-1} NaOH)	V solutions prepared in 1 M NaOH	Alkaline oxidized lignin		V from alkaline electrochemical oxidation of kraft lignin
Resin activation / regeneration	n.k.	n.k.	n.k.	Acid sodium bisulphite Solution		n.k.
Elution	2% HCl aqueous solution in MeOH	n.k.	Water	n.k.	n.k.	EtOAc:AcOH (1:8)
Operational pH	-	8	-	>13	>13	-
T (K)	Room temperature	293	293	348	348	-
Capacity	-	0.0053 eq $g^{-1}_{dry\ resin}$ ($\Leftrightarrow$~806 mgV $g^{-1}_{dry\ resin}$)	0.518 mgV $g^{-1}_{dry\ resin}$	n.k.	n.k.	-

Table 2.10 (cont.)

Reference	**Forss *et al.* (218)**						
	Dowex-50W X2 200-400 mesh	Dowex-50W X8 200-400 mesh	Dowex-50W X12 200-400 mesh	Dowex-50W X16 200-400 mesh	Amberlite 200	AG-MP-50 200-400 mesh	Amberlite-CG-50 200 mesh
	Dow	Dow	Dow	Dow	Dow	Bio-Rad	Dow
Commercial name and type	Cation exchange resin	Cation exchange resin	Cation exchange resin	Cation exchange resin	Cation exchange resin	Cation exchange resin	Cation exchange resin
	Lower cross-linked strong acid cation resin	Strong acid cation resin containing 8% DVB	Strong acid	Strong acid	Strong acid	Strong acid	Weak acid
Matrix	Microporous copolymer of styrene and DBV	Microporous copolymer of styrene and DBV	n.k.	n.k.	Macroporous	Macropourous	Macroporous metacrylic
Functional group	Sulfonic acid	Sulfonic acid	Sulfonic acid	Sulfonic acid	Sulfonic acid	Sulfonic acid	Carbonic acid
Total exchange capacity (given by supplier)	0.6 $eqH^+ L^{-1}$	1.7 $eqH^+ L^{-1}$	n.k.	n.k.	n.k.	1.5 $eqH^+ L^{-1}$	0.01 $eqH^+ g^{-1} min^{-1}$
	APPLICATION DESCRIPTION						
Counter ion	Na^+	Na^+	Na^+	Na^+	Na^+	Na^+	Na^+
Targeted solute	NaV						
Targeted solution / mixture	Alkaline oxidized spent sulphite liquor						
Resin activation / regeneration	NaOH 3 M	NaOH 3 M	NaOH 3 M	NaOH 3 M	-	NaOH 3 M	NaOH 3 M
Elution	Water	Water	Water	Water	Water	Water	Water
Operational pH	>12	>12	>12	>12	>12	>12	>12
T (K)	n.k.	n.k.	n.k.	n.k.	n.k.	n.k.	n.k.
Capacity	5.4 $kg_{NaV} m^{-3}_{resin}$	5.5 $kg_{NaV} m^{-3}_{resin}$	n.k.	1.3 $kg_{NaV} m^{-3}_{resin}$	2.4 $kg_{NaV} m^{-3}_{resin}$	2.0 $kg_{NaV} m^{-3}_{resin}$	2.0 $kg_{NaV} m^{-3}_{resin}$

n.k. – Not known; **a)** Only the resin Amberlite 200 is shipped in Na^+ form. The other resins were initially activated with 3 M NaOH solution; Summary of the characteristics of the different resins is the result of information gathered from supplier technical data and information given by the author. **PS:** Polystyrene; **DVB:** Divinylbenzene; **V**: Vanillin; **NaV**: Sodium vanillate; **MW**: Molecular weight

For Dowex® 50W-X2 resin, the recovery yields of vanillin were in the range 73.2-95.4 %, according to the initial feed volume while for Dowex® 50W, X8 recoveries in the order of 95% were achieved, as well as a considerable enrichment of vanillin (initially 4.3% to a final value of 21.3%) (211). An additional advantage presented within this work is the reduction of the amount of sulphuric acid necessary to neutralize the enriched sample: from 5.0 kg of H_2SO_4 / kg of vanillin to 1.1 kg of H_2SO_4 / kg of vanillin (which represents only 22% of the initial amount of acid consumed to neutralize the oxidized spent sulphite liquor) (211).

Fargues *et al.* (54) employed a cationic resin Duolite C20 from Rohm and Haas to recover vanillin from the oxidized media. Some data obtained by these authors are summarized in Table 2.10. This resin presented an adsorption capacity of 0.518 mg $g^{-1}_{dry\ resin}$ at 20 ºC.

The application of a strong cationic resin in H^+ form for the recovery of vanillin directly from the alkaline solution was explored by Žabková *et al.* (59) testing Amberlite® IR120 (Rohm and Haas). The authors reported a capacity of 806 mg $g^{-1}_{dry\ resin}$, which is considerably higher to the capacity obtained by Fargues *et al.* (54). This study demonstrated that the concentration of vanillin and sodium, as well as pH have great impact in the performance of the ion exchange process and, therefore, these factors must be carefully considered for its application in real oxidation lignin solutions. The novelty was the evaluation and modelling of the process of vanillate conversion to vanillin in alkaline lignin solution by an ion-exchange process. Since the pH changes during this process, lignin and partially depolymerised lignin must be previously separated from the other compounds in order to avoid precipitation of the solution. In this study, a preliminary fractionation by UF of the oxidation mixture to remove the polymeric/oligomeric lignin was suggested as a solution to overcome the precipitation problem, besides the inherent advantage of the fractionation by itself.

Recently, Stecker *et al.* (74) suggested an anion exchange process for vanillin, acetovanillone, vanillic acid and guaiacol produced by alkaline electrochemical oxidation of lignin. The authors highlighted the advantage of using the continuous process to remove vanillin during the electrochemical oxidation step, as an intensification approach. This possibility was demonstrated by employing the anion exchange resin Amberlite® IRA402 OH (Dow) where vanillin and the other adsorbed monomers were eluted with 2% hydrochloric acid in methanol solutions. A global recovery yield of about 2.5 wt% (based on the starting kraft lignin) was accomplished. It is important to mention that this yield is the result of 5 cycles of electrochemical oxidation. Other anion exchange resins were evaluated regarding their vanillin desorption rates from model alkaline solutions such as Dowex Monosphere® 550A OH (Dow), Reillex® HPQ Cl^- (Sigma Aldrich), Ambersep® 900 OH and Amberlite® IRA910 Cl (Dow). Therefore, batch experiments with 50 mg of vanillin in NaOH 1 M per g of resin (for each resin listed above) were performed and eluted with 10% HCl in methanol solution. The resins with the highest recovery rate were Dowex®

Monosphere 550A OH and Amberlite® IRA 402 OH with 90.5 wt% and 86.6 wt% of vanillin recovery, respectively. For the other tested resins, the recovery achieved was in the range 60-70%.

Schmitt *et al.* (72) studied the recovery of vanillin by adsorption on a strong basic anion resin using ethyl acetate:acetic acid (80:20, % V/V) as the eluent solvent. They have demonstrated that the inclusion of an adsorption step after electrochemical oxidation of kraft lignin can improve vanillin recovery from 1 wt% (with conventional separation methods) to 1.3 wt% (lignin basis) and simultaneously, avoid the drawbacks associated with the conventional separation technics such as lignin precipitation and the use of environmental harmful chemicals.

2.5.3. Mineral adsorbents: zeolites

Zeolites are microporous crystalline solids with a three-dimensional framework and well-defined and regular channels and cavities of molecular dimensions, based on TO_4 tetrahedron structure, where T is an aluminium or silicon atom. These adsorbents are found as natural minerals or can be produced by synthesis and modification allowing modulating pore size, hydrophilicity and acidity (221) for a wide range of industrial applications (222). Studies for developing zeolites with high affinity for organic molecules are gaining considerable interest (223).

Several authors have demonstrated that high Si/Al ratios are responsible for turning the zeolites with a hydrophobic character and consequently increase the adsorption capacity for aromatics (e.g. phenol or vanillin) (223-225). Moreover, the water adsorption decreases as well as the competition between water and other solutes such as phenol for the occupation of the active sites (224). Pore size is also a very important feature of zeolites, acting upon the adsorption capacity of a given compound (225).

The application of zeolites appears commonly associated with wastewater treatment for removal of phenols (223-225) and with the removal of inhibitors from lignocellulosic biomass hydrolysates (224). Ranjan *et al.* (224) demonstrated the selective removal of some fermentation inhibitors, such as vanillin, in the perspective of their recovery and intensification of bioethanol production. Desorption studies revealed that the adsorption processes are of reversible nature.

The application of a fixed bed packed with a zeolite to recover vanillin from a fermented spent liquor was first advanced by Derouane and Powell (226). Zeolite Beta, Zeolite ZSM-20 or dealuminated Zeolite Y were the materials proposed as suitable adsorbents for vanillin recovery from acidified oxidation mixture due to wide pores (enough to admit vanillin molecules (>0.7 nm)), high capacity, and low polarity. The requisites for these characteristics are a high SiO_2/Al_2O_3

ratio (about 10/35 to 100) and low sodium content. Fixed bed adsorption and desorption temperatures recommended were in the range of 0-100 ºC and 20-80 ºC, respectively, and ethanol was suggested as a suitable desorption solvent. However, this document lacks of application data about the performance of the different zeolites for recovering vanillin and their behaviour towards other vanillin-related compounds and impurities.

2.5.4. Non-ionic adsorbents

Non-ionic adsorbent materials are mostly based on activated carbon and synthetic cross-linked polymeric adsorbents of hydrophobic nature and, in some cases, carrying functional groups (227). Attempts to find out suitable non-ionic adsorbents for selective adsorption of vanillin molecules have been made on a variety of solutions with model compounds (58, 228-234) or real complex solutions such as alkaline oxidized lignin (235), lignocellulose hydrolysates (217) or fermented broths coming from ferulic acid or eugenol conversions to vanillin (216, 236).

2.5.4.1. *Polymeric resins*

Polymeric resins are usually polystyrene-divinylbenzene copolymers, polymethacrylate polymers, divinylbenzene-ethylvinylbenzene copolymers, or vinylpyridine polymers. Besides the properties provided by the synthetic polymer itself, the surface can be derivatized thus creating a wide diversity of surface polarities. A wide range of synthetic resins can be found in the market. The use of macroporous resins in food and pharmaceutical sectors is viable due to the low or non-existent toxicity and to the moderated temperatures required for regeneration of these resins (237). Usually, the total desorption of compounds can be easily accomplished with organic solvents such as ethanol (229, 232).

Regarding the hyper-cross-linked resins, some authors manage to synthesize and modify their own resins focusing on the adsorption of vanillin. This is the case of the anisole-modified polystyrene resin obtained by Jin and Huang (234), the resin modified with acetylaniline groups (238) and the hydrophobic / hydrophilic macroporous polydivinylbenzene / polyacrylethylenediamine interpenetrating polymer networks (PDVB/PAEM IPN) disclosed by Xiao *et al.* (232).

A wide variety of cross-linked polymeric resins of hydrophobic nature were evaluated regarding their performance in the recovery of vanillin. Such resins have also been used for recovering vanillin continuously and directly from different fermentation broths during its production, thereby increasing the vanillin production yields (216, 217, 236, 239). Wang *et al.* (240) studied the use of several macroporous resins to recover vanillin from fermentation broth and the maximum adsorption capacity reported was 89.6 mg g^{-1}_{resin} with a desorption yield of 66.4%.

To our knowledge, few studies have been carried out with real mixtures of oxidized lignin (226, 235, 241) and most of them display insufficient information about the performance of resins used for added value aldehydes such as vanillin and syringaldehyde.

Overall results showed that the application of non-ionic resins for recovering mostly vanillin is possible. One example is the work of Wu *et al.* (241) demonstrating the recovery of 93.6% of the vanillin from the oxidized liquors of acidic sulphite pulping. Another successful example was published by Wang *et al.* (235) evaluating the performance of a macroporous resin for the isolation of vanillin and syringaldehyde from an oxygen delignification liquor, as depicted in Table 2.11. The authors managed to recover 96.2% and 94.7% of vanillin and syringaldehyde, respectively, using ethyl ether as elution solvent. Reporting the sum of vanillin, syringaldehyde and other compounds (mainly acetosyringone) to 100% in the desorbed solution, the relative proportion of each compound was: vanillin 37.5%, syringaldehyde 31.9% and others 30.6%.

Table 2.11 summarizes the main results of different studies of adsorption and desorption, mainly for model solutions. It is important to highlight that the maximum adsorption capacities listed are obtained from different experimental conditions (initial feed concentrations, pH values, temperatures, solution volume and resin quantity) and therefore, these variables must be taken into consideration when comparing the different data.

Among all types of resins tested, so far one of the resins that exhibited higher adsorption capacity towards vanillin was the one synthesized by Jin and Huang (234) accounting for 337.8–358.4 mg g^{-1}. The authors produced an anisole-modified hyper-cross-linked polystyrene resin type which has the particularity of binding the phenolic hydroxyl group through the anisole oxygen atom, stating this as the main reason for the enhanced vanillin adsorption in spite of its lower superficial area comparatively to other resins reported in literature, such as H103 described in the next paragraph.

Table 2.11 Non-ionic resins, conditions and maximum adsorption capacities for the separation of functionalized phenolic monomers from the oxidized lignin reaction media

Adsorbate	Resin characteristics			Conditions			q_m (mg g^{-1})	Eluting and/or regenerating agent	Ref.
	Type	a_S (m^2 g^{-1})	Average pore diameter size (Å)	T (K)	pH	Max Ce (mg L^{-1})			
V and S from an oxygen delignification liquor	D101	400-550	90-100	290	4.5	6.08 – 7.28	4.10-4.92	Ethyl ether (elution); 10% NaCl + 0.2% NaOH for 30 min (regeneration)	(235)
V in water	SP206	556	200-300	293-333	5.3	53	114.63	Regeneration with 0.1% NaOH	(58)
V in NaOH aqueous solution	SP206	556	200-300	293	6.5	91	≈106* ≈91*		
V in water	Cross-linked styrene H103	1000-1100	85-89	293	6	400-700	416 [a]	Absolute ethanol (elution) - 95.6% recovery	(42)
V in water	Anisole-modified hyper-cross-linked HJ-J08	884.5	26.2	300-320	-	450	337.8 – 358.4	-	(234)
V in water	Cross-linked styrene H103	900-1100	85-89	293-328	-	30	73.015	-	(233)
V in water	PDVB /PAEMIPN [b]	-	-	293-308	-	-	73.44 – 102.73	Vanillin recovery: 20% ethanol (60.6%); 40% ethanol (70.0%); 60% ethanol (80.9%); 80% ethanol (87.8%); 100% ethanol (71.4%); 80% ethanol with 1% HCl (82.3%); 80% ethanol with 5% HCl (73.5%)	(232)
p-OHB in water	Poly(styrene-co-divinylbenzene) resin [c]	987.8	-	298	-	500	245.7-282.5	-	(242)

V: Vanillin; **S**: Syringaldehyde; ***p*-OHB**: *p*-Hydroxybenzaldehyde; **T**: Temperature; Max Ce: Maximum equilibrium concentration in adsorption experiments; q_m: Maximum adsorption capacity; **a)** Column exhausting studies, saturated adsorption capacity; **b)** Hydrophobic-hydrophilic macroporous polydivinylbenzene/polyacrylethylenediamine interpenetrating polymer networks, **c)** Modified with 2% resorcinol; **Resin D101**: Medoresin Corporation, Tianjin, China; **Sepabeads SP206**: Mitsubishi Chemical Corporation; **Resin H103**: Chemical Factory of Nankai University, Tianjin, China. * Values estimated from the literature source

The macroporous resin H103 was tested towards its capacity of adsorbing vanillin by Zhang *et al.* (229) and Samah *et al.* (233). Different results were obtained by the two teams probably due to the different experimental approaches. In fixed bed experiments, Zhang *et al.* (229) managed to obtain adsorption capacity of 416 mg g^{-1} for a feed vanillin solution of 1 g L^{-1} at room temperature and pH 6. Samah *et al.* (233) conducted batch experiments with 100 mL of vanillin solution varying its concentration till a maximum equilibrium concentration of 30 mg L^{-1} for 0.5 g to 5 g of resin. The vanillin maximum adsorption capacity obtained was about 73 mg g^{-1}, almost 6-fold lower than the capacity observed by Zhang *et al.* (229).

Temperature and pH were two variables studied in the work developed by both authors. Regarding the capacity of the resin H103, Samah *et al.* (233) reported low influence of temperature while Zhang *et al.* (229) observed an increase of the adsorption capacity with the increase on this parameter. Nonetheless, after a careful analysis of the data obtained by both authors it is possible to conclude that these results agree: for lower vanillin equilibrium concentration (<30 mg L^{-1}), the same behaviour was obtained, with practically no changes in the adsorption capacity with the temperature change. Zhang *et al.* (229) studied higher equilibrium concentration range and for values higher than 75 mg L^{-1}, temperature had great impact on the adsorption capacity by favouring the adsorption. Concerning the effect of temperature, Žabková *et al.* (58) observed that the process of adsorption was exothermic for SP206 resin and thus, the adsorption capacity decreased with the increase of temperature.

The influence of pH on adsorption in non-polar resins has been studied by several authors (58, 229, 233). The common observation is a decrease on adsorption while increasing pH values from 3 to 8, which becomes more accentuated when pH reaches 10. This behaviour is attributed to changes on the charge of vanillin molecule for different pH values due to the presence of a hydroxyl group. Vanillin is a weak acid with dissociation constant (p*K*a) of 7.4 (85) and within pH 2 to 6 it is neutral. Thus, in this pH range the adsorption of vanillin onto non-polar resins is practically not affected. For higher pH values (> 7.4), vanillin molecules become negatively charged, decreasing their affinity for non-polar resins. These studies are clear evidence that the conditions and methodologies used to study the performance of an resin towards a certain solute are important.

From the Žabková *et al.* (58) work, it was possible to conclude that the maximum adsorption capacity of vanillin in water for SP206 at pH 5.3 and temperatures ranging from 293 K to 333 K was 114.6 mg $g^{-1}_{\text{dry resin}}$. Using a similar resin (SP207), Zhou and Wang (243) managed to recover all the vanillin adsorbed (at pH value of 6 and room temperature) employing 4.5 bed volumes of absolute ethanol.

Vanillin desorption from cross-linked polymeric resins was assessed by some authors using different solvents as depicted in Table 2.11. As for adsorption, desorption rate is very different

according to the type of resin or the elution solvent and conditions applied. Values for desorption rate reported in literature range from 80% to 100% (229, 232, 236).

A resin with both hydrophobic and hydrophilic character was synthesized by Xiao et al. (192). This ambivalent macroporous PDVB/PAEM IPN adsorbs by both hydrogen bonding and π–π interactions. The best desorption rate (87.8%) was achieved with a solvent composed by 80% of ethanol and 20% of water (Table 2.11). The addition of small amounts of acid (e.g. 1-5% HCl) led to a slight decrease in the desorption rate.

2.5.4.2. *Activated carbon*

Activated carbon materials are made by thermal decomposition of various carbonaceous materials followed by an activation process (244, 245), and consist of small hydrophobic layers with disordered, irregular and heterogeneous surfaces containing hydrophilic functional groups. Usually they have extremely high adsorption capacities, mainly due to their high surface area, pore volume, and porosity. The surface area is very heterogeneous and can hold a high diversity of surface charges and surface groups making them a very versatile adsorbent (246).

Since the main application of this type of adsorbents is the removal of contaminants from wastewaters, high temperature, hot water or chemical regeneration is used allowing recoveries of 95% of the initial adsorption capacity (247). However, these regeneration techniques cannot be used considering the perspective of the recovery of thermally unstable compounds and some studies with desorption using solvents are now emerging (248). Table 2.12 summarizes data regarding the adsorption onto activated carbon of some functionalized phenolic monomers from oxidized lignin media.

The emerging interest of developing sustainable biorefinery processes (associated with reducing wastes and make them profitable), led to a set of studies using other by-products as natural adsorbents such as lignin (249), bark (250), wood (251), sawdust (252), cork (253), olive husks (230), fruit shells (254, 255), among many others as reviewed by Ahmaruzzaman (256) and Soto *et al.* (227). In their extensive reviews related with the adsorption of phenolic compounds, the main types of adsorbents tested for separation/purification are presented for phenolic compounds (model and real solutions) but none of the adsorbents are specific for adsorption of vanillin and syringaldehyde.

Table 2.12 Maximum adsorption capacities for adsorption of phenolic compounds in aqueous solution onto activated carbon adsorbents with relevance for the separation and purification of functionalized phenolic monomers from the oxidized reaction media

	Activated carbon characteristics		Experimental conditions			q_m	Ref.
Adsorbate	**Type**	**a_S ($m^2 g^{-1}$)**	**T (K)**	**pH**	**Max Ce (mg L^{-1})**	**(mg g^{-1})**	
V	AC[1]	≈ 1000	298 318	3.2 – 3.5	700	191.41 204.29	(230)
	cAC[2]	≈ 1000	298 318	3.2 – 3.5	1100	93.18 121.72	(230)
VA	AC[1]	≈ 1000	298 318	3.2 – 3.5	1400	148.23 171.46	(230)
	cAC[2]	≈ 1000	298 318	3.2 – 3.5	1200	56.31 85.10	(230)
	cAC[3]	1370	293	8	2000	240	(231)
***p*-OHB**	AC[1]	≈ 1000	298 318	3.2 – 3.5	1400	101.01 104.55	(230)
	cAC[2]	≈ 1000	298 318	3.2 – 3.5	1600	39.39 59.85	(230)
	AC[4]	967	293-313	3.4 – 3.7	350	≈220-226*	(228)
SA	AC[4]	967	293-313	3.4 – 3.7	400	≈260-320*	(228)

T: Temperature; **Max Ce:** Maximum equilibrium concentration in adsorption experiments; **q_m**: Maximum adsorption capacity; **V**: Vanillin; **VA**: Vanillic acid; ***p*-OHB**: *p*-Hydroxybenzaldehyde; **SA**: Syringic acid

AC: Activated carbon; **cAC** – Commercial activated carbon; 1 – Olive husk, 2 - Acticarbon CX (Ceca SA, France), 3 - TE80® (Pica, Vierzon, France), 4 – Bituminous coal;

***** Values estimated from the literature source

In spite of these studies on recoveries from activated carbon, polymeric adsorbents would be preferred for vanillin and syringaldehyde recovery from oxidation mixtures due to their better mechanical resistance, diversity of structures and easiness of regeneration with simultaneous recovery (257-259).

2.5.4.3. *Molecular imprinting technology*

Molecularly imprinted polymers (MIP) are usually obtained by polymerizing functional and cross-linking monomers, surrounding template molecules and consequently obtaining a cross-linked three dimensional network polymer with selective binding properties, after removing the template molecules. Thus, this process has the advantage of creating binding sites with specific shape, size and functionalities that selectively retain the desired targeted molecules (260, 261).

The range of applications of this technology includes separation processes (e.g. chromatography, adsorption, extraction, liquid membranes) (262, 263) but many others have been reported (264-267). MIP have been used for separation of several molecules (262, 263, 268) including the development of sensors for vanillin quantitative analysis from food matrices (269) or its colorimetric detection (270).

The development of molecular imprinting methods and different polymerization techniques to increase MIP capacity and specificity for vanillin has been also the focus of some studies (180, 271-273). So far, methacrylic acid (272, 273), dimethacrylate acid (271) and acrylamide (271) were the functional monomers proposed, using ethylene glycol dimethacrylate acid as cross-linker, to produce the MIP for vanillin capture. Vanillin itself (272, 273) and syringaldehyde (271) were used as template during the MIP synthesis.

Puzio *el al.* (271) used syringaldehyde for MIP synthesis and determined the imprinting factors for vanillin (7.4) and other similar phenolics such as ethylvanillin (2.4), acetovanillone (2.3), vanillic acid (1.7), syringaldehyde (1.4), among others. The MIP obtained was applied to real samples and the authors managed to accomplish 80% vanillin recovery from vanilla pods, red wine spiked with vanillin and artificial or natural vanillin sugar.

2.6. Combination of separation processes

Oxidized lignin medium consists of a complex mixture of oligomers and other low molecular weight phenolics such as vanillin, syringaldehyde, acetovanillone, *p*-hydroxybenzaldehyde, and several phenolic acids like vanillic acid and syringic acid (31, 67). Due to chemical and physical similarities of these compounds, separation and purification would not be possible in one single separation process and, therefore, a separation train is needed.

In this chapter, processes to obtain purified monomers from oxidized reaction medium of lignin were reviewed. The majority of published literature is related with vanillin purification. Figure 2.4 summarizes the main sequence of processes described in literature to process oxidized lignin mixtures, encompassing LLE, membrane separation, adsorption, distillation and crystallization.

Vanillin and syringaldehyde represent a very small fraction of the oxidized lignin medium. So, evaporating the extract to concentrate these compounds would be ineffective because other compounds would be concentrated to higher levels. As it has already been stated, applying other techniques such as acidification of the oxidized medium and further extraction with volatile organic solvents requires high volumes of chemicals, compromises the environmental sustainability of the process, and is being discouraged for industrial applications. Direct extraction of the oxidized medium with water immiscible alcohols, like *n*-butyl or isopropyl alcohol, has serious limitations on sodium vanillate and other phenolates solubilities.

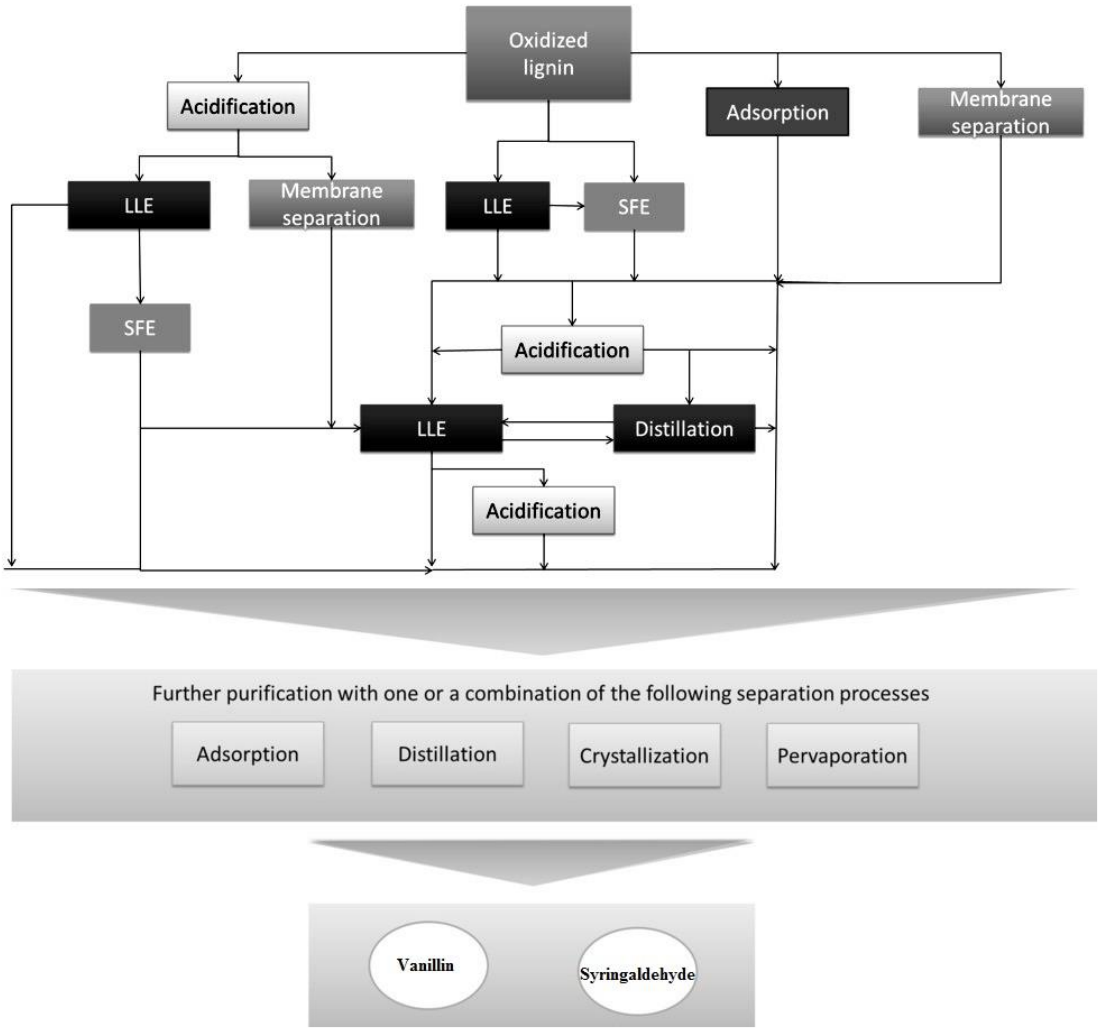

Figure 2.4 Overview of separation and purification processes to obtain purified fractions of vanillin and syringaldehyde.

Membrane separation can be used as one of the first processes to simplify the complex oxidation mixture, by separating the unreacted lignin and fragments of high molecular weight from the monomers of interest. A membrane separation sequence or membrane cascades (274) can be very successful for this purpose, overcoming some current well-known limitations such as low fluxes, fouling and unfavourable rejections. However, other techniques must be coupled to downstream processing. Adsorption constitutes a good subsequent step to membrane separation once it can be effectively applied to dilute solutions; however, it is based on the polarity of molecules and, for higher degree of purification, other processes must be combined.

Crystallization and distillation should be restricted to a final stage of the process, in the presence of low volume and high concentration of the desirable compound. Crystallization usually requires several stages, some of them involving derivatizations, in order to accomplish high purity on vanillin and syringaldehyde. On the other hand, distillation requires high temperatures and degradation of the compounds of interest can occur. Vacuum distillation (with or without an inert) (129, 164), fractional distillation (275), carrier steam distillation (276) and azeotropic distillation (277, 278) have been recommended to obtain a purified vanillin product. After distillation, other processes such as LLE or crystallization are often required.

A sequence of processes seems to be the key factor to get close to the target for a sustainable process development aiming to recover vanillin and syringaldehyde from the other low molecular weight phenolics. Hence, several authors contributed with some insights about what would be the combination and correct sequence to achieve enriched vanillin or syringaldehyde fractions. However, few authors have effectively implemented and studied the sequential process proposed.

This subsection summarizes some suggestions of sequential separations. Some sequences have been previously described in this document such as the ones summarized in Figure 2.2 comprising a bisulphitation step coupled with other processes such as distillation, crystallization and other LLE.

Bryan (279) presented a US Patent sequence aiming vanillin purification by combining several LLE with vacuum distillation and crystallization as shown in Figure 2.5. The drawbacks associated with this sequence are the operating costs, reagents consumption and numerous stages involved in the process.

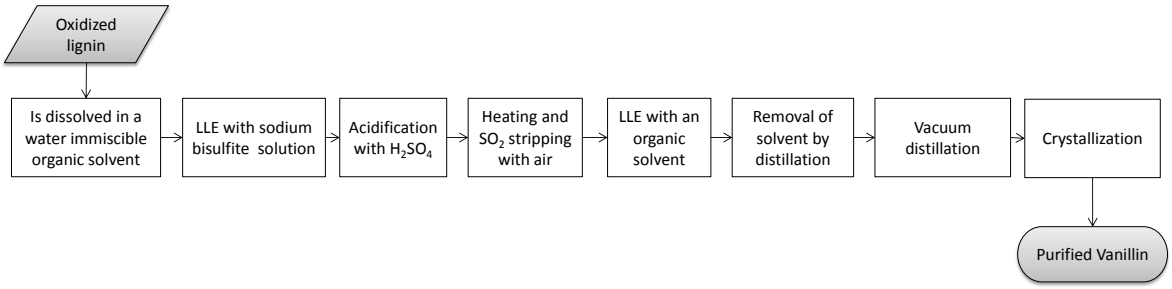

Figure 2.5 Sequence proposed by Bryan (279).

Klemola and Tuovinen (138) was one of the few teams that studied purification sequences on oxidized sulphite liquor. Sequences encompass LLE or/and SFE after neutralization of the liquor and one or more crystallization stages. Figure 2.6 summarizes two of the sequences studied by the authors along with the detailed composition of each stream obtained. As previously stated, the sequence has the particularity of gradually decrease pressure and temperature during SFE and also recycles some of the fractions back to the beginning of the extraction. Thus, compounds are gradually fractionated and those having lower or higher solubility in CO_2 than vanillin are separated before or after vanillin recovery, respectively. The highest vanillin content (99.58%) obtained was for the sequence employing SFE and two crystallization stages.

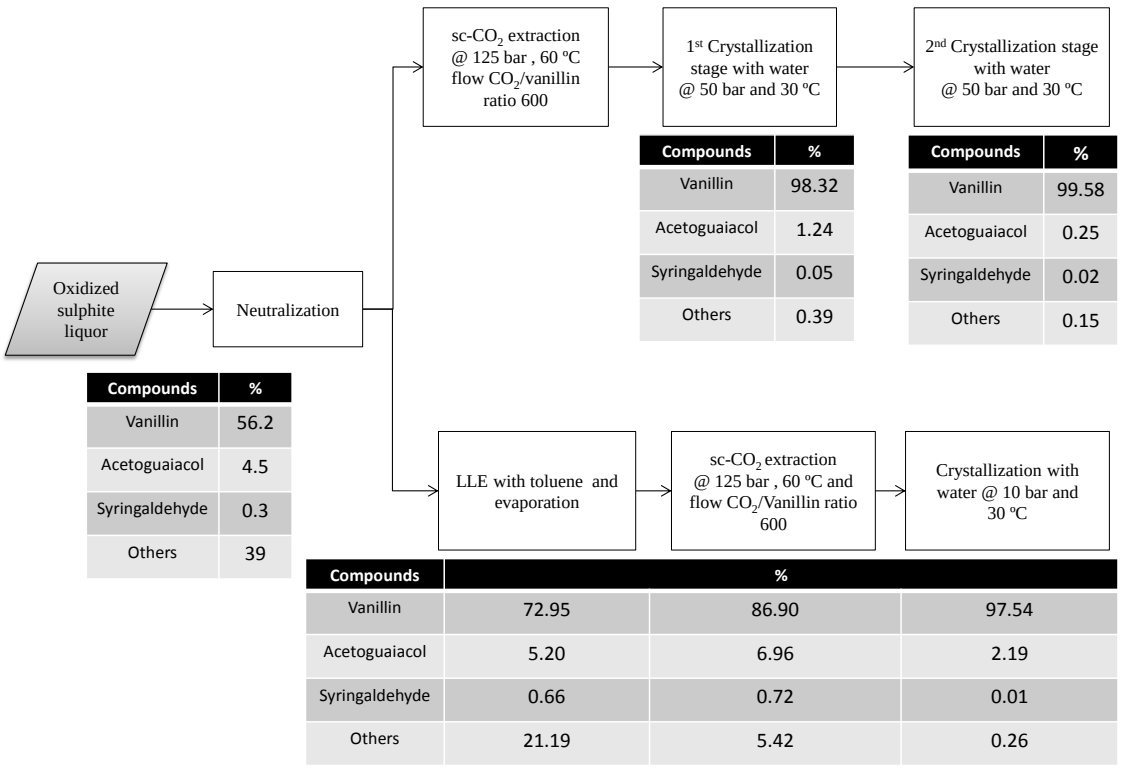

Compounds	%
Vanillin	56.2
Acetoguaiacol	4.5
Syringaldehyde	0.3
Others	39

Compounds	%
Vanillin	98.32
Acetoguaiacol	1.24
Syringaldehyde	0.05
Others	0.39

Compounds	%
Vanillin	99.58
Acetoguaiacol	0.25
Syringaldehyde	0.02
Others	0.15

Compounds	%		
Vanillin	72.95	86.90	97.54
Acetoguaiacol	5.20	6.96	2.19
Syringaldehyde	0.66	0.72	0.01
Others	21.19	5.42	0.26

Figure 2.6 Sequence proposed by Klemola and Tuovinen (138).

Fargues *et al.* (54) suggested a sequence of processes for obtaining a refined vanillin extract. This work is focused on cationic-exchange process using Duolite C20 to perform a first separation. The overall sequence (Figure 2.7) includes the acidification with H_2SO_4, LLE with benzene and addition of sodium bisulphite aqueous solution for further vanillin re-extraction. After acidification with H_2SO_4 and SO_2 stripping with air, the crude vanillin is further purified by vacuum distillation followed by crystallization. This proposal was not tested and therefore it lacks more information regarding vanillin recovery and purity at each stage. Additionally, their proposal has the drawback of employing benzene which is a carcinogenic agent.

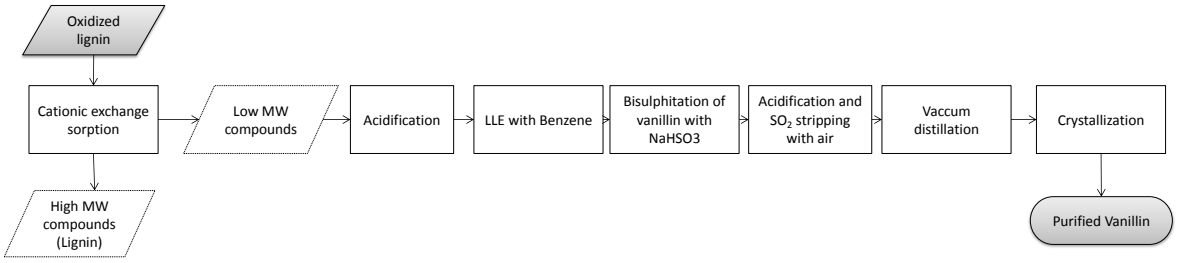

Figure 2.7 Sequence proposed by Fargues *et al.* (54).

In a different approach, Vigneault *et al.* (129) published a sequence of processes for a first fractionation to simplify the complex mixture so that, in a second phase, the distillation and crystallization processes would be more effective (depicted in Figure 2.8). Initially, water is removed by means of adiabatic flash separators and the resulting mixture is acidified and extracted with ethyl acetate, evidenced by the authors to be a solvent with good performance for extracting the compounds of interest. The monomers-rich fraction passes onto a silica adsorption column aiming to retain oligomers and the eluate is then submitted to vacuum distillation between 25 ºC and 164 ºC producing 4 distinct fractions. The last distilled fraction (110 ºC and 164 ºC) includes vanillin and syringaldehyde. The liquid chromatography with silica gel of this distillate produces a vanillin enriched fraction and a second fraction which, after crystallization, led to an enriched fraction of syringaldehyde.

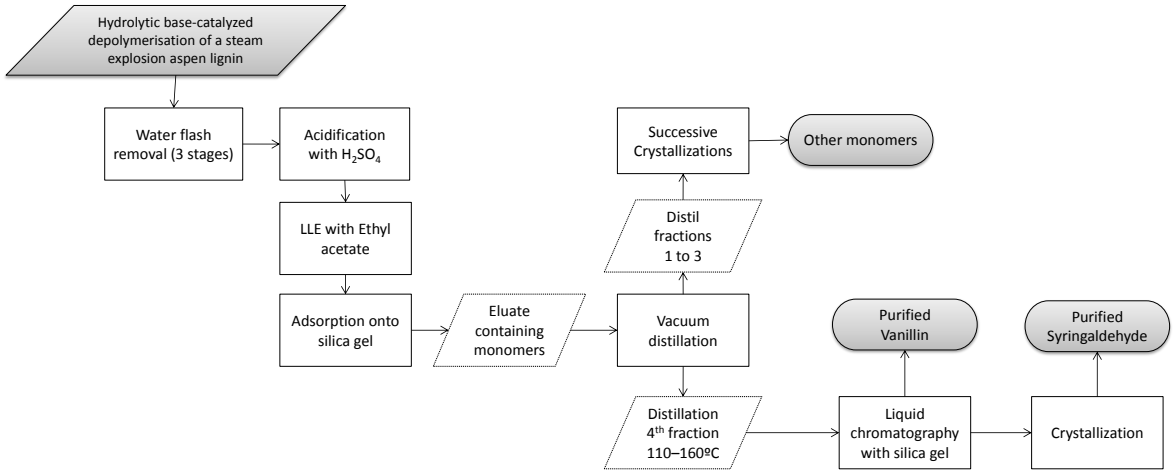

Figure 2.8 Sequence proposed by Vigneault *et al.* (129).

Borges da Silva *et al.* (56) designed a sequence of processes based on previous work of the team aiming the integration of membrane separation and ion exchange processes (Figure 2.9) with the reaction process of the lignin to give vanillin. It embraces an initial step of UF employing a sequence of tubular ceramic membranes with cut-offs of 5 kDa and 1 kDa, starting with the membrane with the highest cut-off. This combination would allow the fractionation of the alkaline reaction medium producing two valuable streams: one with high molecular weight compounds (mainly depolymerised lignin) and a second one with low molecular weight compounds including vanillin. The fraction with the low molecular weight compounds will proceed straightforward to a cation exchange process employing a protonated resin recovering vanillin in its neutral form. To finalize the separation and purification process the authors suggest the application of a final step of crystallization, by any known method described in literature.

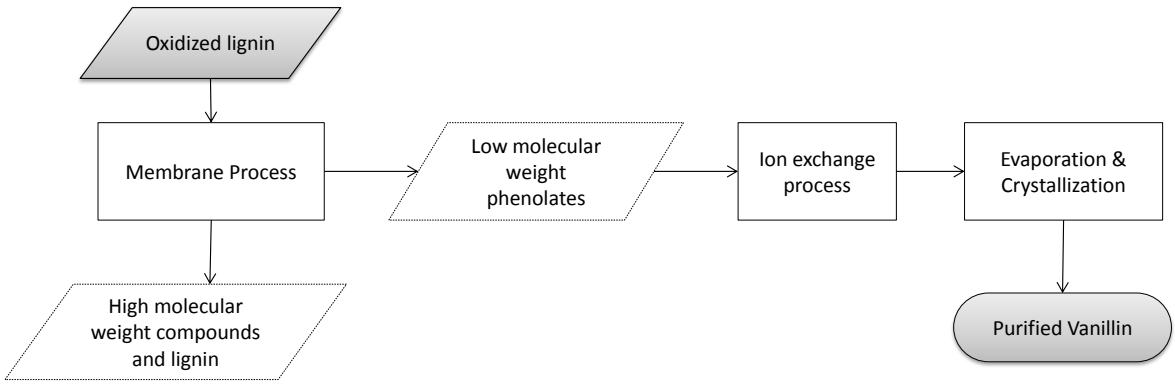

Figure 2.9 Sequence proposed by Borges da Silva *et al.* (56).

2.7. Final remarks

A detailed description of separation and purification processes applied to vanillin, syringaldehyde and other phenolic aldehydes of interest were summarized within this review. Considerable effort has been devoted for long time to design processes to work-up the complex mixture resulting from lignin oxidation. The interest on this subject has reappeared in the last years, driven by the recognition of lignin simultaneously as an important side stream from biorefinery activity and an important source of phenolic compounds. Consequently, the focus of this review was on processes for extraction and purification to successfully recover functionalized phenolic monomers resulting from lignin oxidative depolymerisation. Some of the available literature is focused on vanillin isolation and purification from real alkaline oxidized lignin solutions but most of the studies deal with model solutions to simulate the real mixture and/or demonstrate the potential of using a particular separation technique for recovering a fraction of pure vanillin.

The final purification stage of crude vanillin and syringaldehyde is very hard to accomplish because it contains compounds with similar physical and chemical properties. Although some separation processes manage to successfully recover vanillin from lignin containing solutions, most of them are very laborious, are high energy consuming, use environmentally harmful solvents and encompass great losses of material. It is crucial to provide separation processes that efficiently and effectively recover vanillin and syringaldehyde and, at the same time, being economic and environmentally safe, allow the industrial application of the aldehydes.

In recent years, non-ionic macroreticular polymeric resins for this end have gained considerable interest. Although this type of resins have lower adsorption capacity for most of the organic compounds than the activated carbon adsorbents, the extensive variation of functionality, porosity and surface area open new perspectives for its use on separation of vanillin and syringaldehyde. MIP studies also indicate that this technology can be very promising to be applied in oxidized lignin media with the advantage of being specifically moulded to capture vanillin or other desired phenolics with great levels of selectivity and affinity. The development of new resistant and anti-fouling membranes or cascade processes also appear interesting approaches to simplify the lignin oxidized reaction media and turn the application of a second separation technique (e.g. adsorption) more efficient and focused.

2.8. References

1. Lora, J. and Glasser, W. (2002) Recent industrial applications of lignin: A sustainable alternative to nonrenewable materials. J. Polym. Environ., 10: 39-48.
2. Çetin, N. S. and Özmen, N. (2002) Use of organosolv lignin in phenol–formaldehyde resins for particleboard production: I. Organosolv lignin modified resins. Int. J. Adhes. Adhes., 22: 477-480.
3. Braun, J. L., Holtman, K. M. and Kadla, J. F. (2005) Lignin-based carbon fibers: Oxidative thermostabilization of kraft lignin. Carbon, 43: 385-394.
4. Hatakeyama, H., Kosugi, R. and Hatakeyama, T. (2008) Thermal properties of lignin-and molasses-based polyurethane foams. J Therm Anal Calorim, 92: 419-424.
5. Stewart, D. (2008) Lignin as a base material for materials applications: Chemistry, application and economics. Ind. Crop. Prod., 27: 202-207.
6. Xu, G., Yang, J.-H., Mao, H.-H. and Yun, Z. (2011) Pulping black liquor used directly as a green and effective source for neat oil and as an emulsifier of catalytic cracking heavy oil. Chem. Technol. Fuels Oils, 47: 283-291.
7. Gierer, J. and Imsgard, F. (1977) The reactions of lignins with oxygen and hydrogen peroxide in alkaline media. Svensk papperstidning 80: 510-518.
8. Gierer, J., Imsgard, F. and Norén, I. (1977) Studies on the degradation of phenolic lignin units of the β-aryl ether type with oxygen in alkaline media. Acta Chem. Scand. B, 31: 561-572.
9. Erofeev, Y. V., Afanas'eva, V. L. and Glushkov, R. G. (1990) Synthetic routes to 3,4,5-trimethoxybenzaldehyde (review). Pharm. Chem. J., 24: 501-510.
10. Bjørsvik, H.-R. and Minisci, F. (1999) Fine chemicals from lignosulfonates. 1. Synthesis of vanillin by oxidation of lignosulfonates. Org. Process Res. Dev., 3: 330-340.
11. Burri, J., Graf, M., Lambelet, P. and Löliger, J. (1989) Vanillin: more than a flavouring agent - a potent antioxidant. J. Sci. Food Agric., 48: 49-56.
12. Davidson, P. M. and Naidu, A. S. (2000) Phyto-phenols: In Natural Food Antimicrobial Systems. A.S. Naidu. CRC Press: Florida, United State of America, 265-294.
13. Thiel, L. and Hendricks, F. (2004) Study into the establishment of an aroma and fragrance fine chemicals value chain in south africa, part three: aroma chemicals derived from petrochemical feedstocks, Tender number T79/07/03. Government Tender Bulletins. National Economic Development and Labor Council, availabe from http://www.thedti.gov.za/industrial_development/docs/fridge/Aroma_Part3.pdf (accessed 26/07/2013).

14. Walton, N. J., Mayer, M. J. and Narbad, A. (2003) Vanillin. Phytochemistry, 63: 505-515.

15. *Integrated Forest Biorefineries, Challenges and Opportunities*, in *RSC Green Chemistry No. 18*, 2013, edited by Lew P. Christopher, The Royal Society of Chemistry, Cambridge, United Kingdom.

16. Kirk, T. K. and Farrell, R. L. (1987) Enzymatic "combustion": The microbial degradation of lignin. Annu. Rev. Microbiol., 41: 465-501.

17. Martínez, Á. T., Speranza, M., Ruiz-Dueñas, F. J., Ferreira, P., Camarero, S., Guillén, F., Martínez, M. J., Gutiérrez, A. and Río, J. C. d. (2005) Biodegradation of lignocellulosics: microbial, chemical, and enzymatic aspects of the fungal attack of lignin. International Microbiology, 8: 195-204.

18. Bugg, T. D. H., Ahmad, M., Hardiman, E. M. and Rahmanpour, R. (2011) Pathways for degradation of lignin in bacteria and fungi. Nat. Prod. Rep., 28: 1883-1896.

19. Kamoda, S., Terada, T. and Saburi, Y. (1997) Purification and some properties of lignostilbene-alpha; beta-dioxygenase isozyme IV from *Pseudomonas paucimobilis* TMY1009. Biosci. Biotechnol. Biochem., 61: 1575-1576.

20. Rabenhorst, J. and Hopp, R. (1991) Process for the preparation of vanillin, US Patent 5017388 (21-05-1991).

21. van den Heuvel, R. H. H., Fraaije, M. W., Laane, C. and van Berkel, W. J. H. (2001) Enzymatic synthesis of vanillin. J. Agric. Food. Chem., 49: 2954-2958.

22. Rosazza, J. P. N., Huang, Z., Dostal, L., Volm, T. and Rousseau, B. (1995) Review: Biocatalytic transformations of ferulic acid: An abundant aromatic natural product. J. Ind. Microbiol., 15: 457-471.

23. Muheim, A., Müller, B., Münch, T. and Wetli, M. (1998) Process for the production of vanillin, EP Patent 0885968 (23-12-1998).

24. Lesage-Meessen, L., Delattre, M., Haon, M. and Asther, M. (1999) Methods for bioconversion of ferulic acid to vanillic acid or vanillin and for the bioconversion of vanillic acid to vanillin using filamentous fungi, US Patent 5866380 A (02-02-1999).

25. Li, K. and Frost, J. W. (1998) Synthesis of vanillin from glucose. J. Am. Chem. Soc., 120: 10545-10546.

26. Lesage-Meessen, L., Haon, M., Delattre, M., Thibault, J. F., Ceccaldi, B. C. and Asther, M. (1997) An attempt to channel the transformation of vanillic acid into vanillin by controlling methoxyhydroquinone formation in Pycnoporus cinnabarinus with cellobiose. Appl. Microbiol. Biotechnol., 47: 393-397.

27. Li, T. and Rosazza., J. P. (2000) Biocatalytic synthesis of vanillin. Appl. Environ. Microbiol., 66: 684-687.

28. Rao, S. R. and Ravishankar, G. A. (2000) Vanilla flavour: production by conventional and biotechnological routes. J. Sci. Food Agric., 80: 289-304.

29. Priefert, H., Rabenhorst, J. and Steinbüchel, A. (2001) Biotechnological production of vanillin. Appl. Microbiol. Biotechnol., 56: 296-314.

30. Schrader, J., Etschmann, M. M. W., Sell, D., Hilmer, J. M. and Rabenhorst, J. (2004) Applied biocatalysis for the synthesis of natural flavour compounds – current industrial processes and future prospects. Biotechnol. Lett., 26: 463-472.

31. Pinto, P. C. R., Borges da Silva, E. A. and Rodrigues, A. E. (2012) Lignin as source of fine chemicals: vanillin and syringaldehyde: In Biomass Conversion. Chinnappan Baskar, Shikha Baskar and Ranjit S. Dhillon. Springer Berlin Heidelberg: London, United Kingdom, 381-420.

32. McCord, W. M. (1931) A new method for the preparation of syringic aldehyde. J. Am. Chem. Soc., 53: 4181-4183.

33. Pearl, I. A. (1948) Synthesis of syringaldehyde. J. Am. Chem. Soc., 70: 1746-1748.

34. Pepper, J. M. and MacDonald, J. A. (1953) The synthesis of syringaldehyde from vanillin. Can. J. Chem., 31: 476-483.

35. Rao, D. V. and Stuber, F. A. (1983) An efficient synthesis of 3,4,5-trimethoxybenzaldehyde from vanillin. Synthesis, 4: 308.

36. Manchand, P. S., Belica, P. S. and Wong, H. S. (1990) Synthesis of 3,4,5-trimethoxybenzaldehyde. Synth. Commun., 20: 2659-2666.

37. Ya-Fei, J., Zhi-Min, Z. and Xian-Yong, W. (2002) Synthesis of 3,4,5-trimethoxybenzaldehyde from p-cresol. Synth. Commun., 32: 2809-2814.

38. Tripathi, A. K., Sama, J. K. and Taneja, S. C. (2010) An expeditious synthesis of syringaldehyde from *para*-cresol. Indian J. Chem., Sect B, 49: 379-381.

39. Wu, G., Heitz, M. and Chornet, E. (1994) Improved Alkaline Oxidation Process for the Production of Aldehydes (Vanillin and Syringaldehyde) from Steam-Explosion Hardwood Lignin. Ind. Eng. Chem. Res., 33: 718-723.

40. Villar, J. C., Caperos, A. and García-Ochoa, F. (2001) Oxidation of hardwood kraft-lignin to phenolic derivatives with oxygen as oxidant. Wood Sci. Technol., 35: 245-255.

41. Sales, F. G., Maranhão, L. C. A., Lima Filho, N. M. and Abreu, C. A. M. (2006) Kinetic evaluation and modeling of lignin catalytic wet oxidation to selective production of aromatic aldehydes. Ind. Eng. Chem. Res., 45: 6627-6631.

42. Zhang, J., Deng, H. and Lin, L. (2009) Wet aerobic oxidation of lignin into aromatic aldehydes catalysed by a perovskite-type oxide: $LaFe_{1-x}Cu_xO_3$ (x=0, 0.1, 0.2). Molecules, 14: 2747-2757.

43. Pinto, P. C. R., Borges da Silva, E. A. and Rodrigues, A. E. (2011) Insights into oxidative conversion of lignin to high-added-value phenolic aldehydes. Ind. Eng. Chem. Res., 50: 741-748.

44. Santos, S. G., Marques, A. P., Lima, D. L. D., Evtuguin, D. V. and Esteves, V. I. (2011) Kinetics of Eucalypt lignosulfonate oxidation to aromatic aldehydes by oxygen in alkaline medium. Ind. Eng. Chem. Res., 50: 291-298.

45. Pinto, P. C. R., Costa, C. E. and Rodrigues, A. E. (2013) Oxidation of lignin from *Eucalyptus globulus* pulping liquors to produce syringaldehyde and vanillin. Ind. Eng. Chem. Res., 52: 4421-4428.

46. Zakzeski, J., Bruijnincx, P. C. A., Jongerius, A. L. and Weckhuysen, B. M. (2010) The catalytic valorization of lignin for the production of renewable chemicals. Chem. Rev., 110: 3552-3599.

47. Salvesen, J. R., Brink, D. L., Diddams, D. G. and Owzarski, P. (1948) Process for making vanillin, US Patent 3686322 (13-01-1948).

48. Fisher, J. H. and Marshall, H. (1951) Method of producing vanillin, US Patent 2576752 (27-11-1951).

49. Fisher, J. H. and Marshall, H. B. (1951) Method of producing vanillin, US Patent 2576753 (27-11-1951).

50. Marshall, H. B. and Sankey, C. A. (1951) Methods of pulping ligno-cellulose materials and simultaneously producing oxidation products therefrom, CA Patent 470916 (16-01-1951).

51. Bryan, C. C. (1954) Manufacture of vanillin from lignin, US Patent 2692291 (19-10-1954).

52. Craig, D. and Logan, C. D. (1962) Method of producing vanillin and other useful products from lignosulfonic acid compounds, US Patent 3054659 (18-09-1962).

53. Mathias, Á. L. and Rodrigues, A. E. (1995) Production of vanillin by oxidation of pine kraft lignins with oxygen. Holzforschung, 49: 273.

54. Fargues, C., Mathias, Á. L. and Rodrigues, A. (1996) Kinetics of vanillin production from kraft lignin oxidation. Ind. Eng. Chem. Res., 35: 28-36.

55. Kuznetsov, B. N. (1996) Application of catalysts for producing organic compounds from plant biomass. React. Kinet. Catal. Lett., 57: 217-225.

56. Borges da Silva, E. A., Žabková, M., Araújo, J. D., Cateto, C. A., Barreiro, M. F., Belgacem, M. N. and Rodrigues, A. E. (2009) An integrated process to produce vanillin and lignin-based polyurethanes from kraft lignin. Chem. Eng. Res. Des., 87: 1276-1292.

57. Araújo, J. D. P., Grande, C. A. and Rodrigues, A. E. (2010) Vanillin production from lignin oxidation in a batch reactor. Chem. Eng. Res. Des., 88: 1024-1032.

58. Žabková, M., Otero, M., Minceva, M., Zabka, M. and Rodrigues, A. E. (2006) Separation of synthetic vanillin at different pH onto polymeric adsorbent Sepabeads SP206. Chem. Eng. Process., 45: 598-607.

59. Žabková, M., Borges da Silva, E. A. and Rodrigues, A. E. (2007) Recovery of vanillin from Kraft lignin oxidation by ion-exchange with neutralization. Sep. Purif. Technol., 55: 56-68.

60. Žabková, M., Borges da Silva, E. and Rodrigues, A. (2007) Recovery of vanillin from lignin/vanillin mixture by using tubular ceramic ultrafiltration membranes. J. Membr. Sci., 301: 221-237.

61. Tarabanko, V. E., Chelbina, Y. V., Kudryashev, A. V. and Tarabanko, N. V. (2013) Separation of vanillin and syringaldehyde produced from lignins. Sep. Sci. Technol., 48: 127-132.

62. Bryan, C. C. (1955) Propanol extraction of sodium vanillinate, US Patent 2721221 (18-10-1955).

63. Xiang, Q. and Lee, Y. Y. (2001) Production of oxychemicals from precipitated hardwood lignin. Appl. Biochem. Biotechnol., 91-93: 71-80.

64. Tarabanko, V. E., Petukhov, D. V. and Selyutin, G. E. (2004) New mechanism for the catalytic oxidation of lignin to vanillin. Kinet. Catal., 45: 569-577.

65. Labat, G. and Gonçalves, A. (2008) Oxidation in Acidic Medium of Lignins from Agricultural Residues. Appl. Biochem. Biotechnol., 148: 151-161.

66. Partenheimer, W. (2009) The aerobic oxidative cleavage of lignin to produce hydroxyaromatic benzaldehydes and carboxylic acids via metal/bromide catalysts in acetic acid/water mixtures. Adv. Synth. Catal., 351: 456-466.

67. Voitl, T. and Rohr, P. R. v. (2010) Demonstration of a process for the conversion of Kraft lignin into vanillin and methyl vanillate by acidic oxidation in aqueous methanol. Ind. Eng. Chem. Res., 49: 520-525.

68. Smith, C., Utley, J. P. and Hammond, J. (2011) Electro-organic reactions. Part 60[1]. The electro-oxidative conversion at laboratory scale of a lignosulfonate into vanillin in an FM01 filter press flow reactor: preparative and mechanistic aspects. J. Appl. Electrochem., 41: 363-375.

69. Smith, C., Utley, J. P., Petrescu, M. and Viertler, H. (1989) Biomass electrochemistry: Anodic oxidation of an organo-solv lignin in the presence of nitroaromatics. J. Appl. Electrochem., 19: 535-539.

70. Moodley, B., Mulholland, D. and Brookes, H. (2011) The electro-oxidation of lignin in Sappi Saiccor dissolving pulp mill effluent. Water SA, 37: 33-40.

71. Parpot, P., Bettencourt, A. P., Carvalho, A. M. and Belgsir, E. M. (2000) Biomass conversion: attempted electrooxidation of lignin for vanillin production. J. Appl. Electrochem., 30: 727-731.

72. Schmitt, D., Regenbrecht, C., Hartmer, M., Stecker, F. and Waldvogel, S. R. (2015) Highly selective generation of vanillin by anodic degradation of lignin: a combined approach of electrochemistry and product isolation by adsorption. Beilstein Journal of Organic Chemistry, 11: 473-480.

73. Stecker, F., Fischer, A., Kirste, A., Waldvogel, S., Regenbrecht, C. and Schmitt, D. (2014) Method for producing vanillin, WO Patent 2014006106 (9-01-2014).

74. Stecker, F., Fischer, A., Kirste, A., Voitl, A., Wong, C. H., Waldvogel, S., Regenbrecht, C., Schmitt, D. and Hartmer, M. F. (2014) Method for obtaining vanillin from aqueous basic compositions containing vanillin, WO Patent 2014006108 A1 (09-01-2014).

75. Stecker, F., Malkowsky, I. M., Fischer, A., Waldvogel, S. R. and Regenbrecht, C. (2013) Method for producing vanillin by electrochemical oxidation of aqueous lignin solutions or suspensions, US Patent 2013/0040031 A1 (14-Feb-2013).

76. Utley, J. and Smith, C. (1988) Electrochemical treatment of lignins, US Patent 4786382 (22-11-1988).

77. Smith, C. Z. and Utley, J. H. P. (1987) Electrochemical treatment of lignins, WO Patent 1987003014 A1 (21-05-1987).

78. Tonucci, L., Coccia, F., Bressan, M. and d'Alessandro, N. (2012) Mild photocatalysed and catalysed green oxidation of lignin: a useful pathway to low-molecular-weight derivatives. Waste Biomass Valorization, 3: 165-174.

79. Stärk, K., Taccardi, N., Bösmann, A. and Wasserscheid, P. (2010) Oxidative depolymerization of lignin in ionic liquids. ChemSusChem, 3: 719-723.

80. Zakzeski, J., Jongerius, A. L. and Weckhuysen, B. M. (2010) Transition metal catalyzed oxidation of Alcell lignin, soda lignin, and lignin model compounds in ionic liquids. Green Chem., 12: 1225-1236.

81. Badamali, S. K., Luque, R., Clark, J. H. and Breeden, S. W. (2013) Unprecedented oxidative properties of mesoporous silica materials: towards microwave-assisted oxidation of lignin model compounds. Catal. Commun., 31: 1-4.

82. Hanson, S. K., Baker, R. T., Gordon, J. C., Scott, B. L. and Thorn, D. L. (2010) Aerobic oxidation of lignin models using a base metal vanadium catalyst. Inorg. Chem., 49: 5611-5618.

83. Hanson, S. K., Wu, R. and Silks, L. A. P. (2012) C-C or C-O bond cleavage in a phenolic lignin model compound: selectivity depends on vanadium catalyst. Angew. Chem. Int. Ed., 51: 3410-3413.

84. Perry, R. H. and Green, D. W. (1998) Perry's Chemical Engineers'Handbook. Seventh edition, McGraw Hill: New York, United State of America.

85. Ragnar, M., Lindgren, C. T. and Nilvebrant, N.-O. (2000) *pKa*-values of guaiacyl and syringyl phenols related to lignin. J. Wood Chem. Technol., 20: 277-305.

86. *The Merck Index: An Encyclopedia of Chemicals, Drugs, and Biologicals*, 2001, Thirteen edition, M. J. O'Neil , A. Smith, P.E. Heckelman and S. Budavari eds, Merck & Co Inc, Whitehouse Station. New Jersey, United States of America.

87. Haynes, W. M. and Lide, D. R. (2004) The CRC Handbook of Chemistry and Physics. Eighty-fifth edition, CRC: Florida, United State of America.

88. Syringaldehyde (CAS 134-96-3): Market Research Report 2011. Business Analytic Center.

89. Kumar, R., Sharma, P. K. and Mishra, P. S. (2012) A Review on the vanillin derivatives showing various biological activities. Int. J. PharmTech Res., 4: 266-279.

90. Royal Society of Chemistry, *ChemSpider - search and share chemistry* (2014), retrieved from: http://www.chemspider.com (accessed 17/02/2016).

91. Mark, H. (1972) Kirk-Othmer Encyclopedia of Chemical Technology. Volume 21, Second edition, John Wiley & Sons: London, United Kingdom.

92. Tarabanko, N. V., Pervishina, A., Kuznetsov, B. N. and Koropachinskaya, N. V. (1998) The new methods of the vanillin and syringaldehyde separation. Chem. Plant Raw Mat. (Russia), 3: 93-97.

93. Mange, C. E. and Ehler, O. (1924) Solubilities of vanillin. Ind. Eng. Chem., 16: 1258-1260.

94. Noubigh, A., Mgaidi, A., Abderrabba, M., Provost, E. and Fürst, W. (2007) Effect of salts on the solubility of phenolic compounds: experimental measurements and modelling. J. Sci. Food Agric., 87: 783-788.

95. Hangzhou weiku information & Technology Co. Ltd, *Look for Chemicals* (2008), retrieved from: http://www.lookchem.com (accessed 30/10/2014).

96. National Center for Biotechnology Information, *PubChem - Open Chemistry database* (2004), retrieved from: http://pubchem.ncbi.nlm.nih.gov (accessed 30/10/2014).

97. Škerget, M., Čretnik, L., Knez, Ž. and Škrinjar, M. (2005) Influence of the aromatic ring substituents on phase equilibria of vanillins in binary systems with CO_2. Fluid Phase Equilib., 231: 11-19.

98. Lindberg, J. J. (1960) Dipole moments of guaicol derivatives. Acta Chem. Scand., 14: 379-384.

99. Yaws, C. L. (2009) Thermophysical properties of chemicals and hydrocarbons. William Andrew Publishing: New York, United States of America.

100. *Chemical Book* (2008), retrieved from: http://www.chemicalbook.com (accessed 30/10/2014).

101. Humphrey, J. L. and Keller, G. E. (1997) Separation process technology. McGraw-Hill: New York, United States of America.

102. Alberda, G. (1959) Process for the extraction of alkali metal salts of vanillin or its higher homologues from alkaline process liquors, US Patent 2871270 (27-01-1959).

103. Tarabanko, V. E., Ivanchenko, N. M., Kudryashev, A. V. and Gulbis, G. R. (1996) Vanillin extraction from alkaline solutions. Russ. J. Appl. Chem., 69: 580-582.

104. Lamprecht, G. and Blochberger, K. (2009) Protocol for isolation of vanillin from ice cream and yoghurt to confirm the vanilla beans origin by ^{13}C-EA-IRMS. Food Chem., 114: 1130-1134.

105. Kaygorodov, K. L., Chelbina, Y. V., Tarabanko, V. E. and Tarabanko, N. V. (2010) Extraction of vanillin by aliphatic alcohols. J. Siberian Federal University: Chemistry 3, 228-233.

106. Pan, J., Fu, J., Deng, S. and Lu, X. (2015) Distribution coefficient of products from lignin oxidative degradation in organic-water systems. Fuel Processing Technology, 140: 262-266.

107. Korenman, Y. I. (1992) Distribution Ratios of Organic Compounds. Voronez University Press: Voronezh, Russia.

108. Jin, L. J., Wei, Z., Dai, J. Y., Guo, P. and Wang, L. S. (1998) Prediction of partitioning properties for benzaldehydes by various molecular descriptors. Bull. Environ. Contam. Toxicol., 61: 1-7.

109. Miller, D. M. (1991) Evidence that interfacial transport is rate-limiting during passive cell membrane permeation. Biochim. Biophys. Acta, 1065: 75-81.

110. Noubigh, A., Abderrabba, M. and Provost, E. (2009) Salt addition effect on partition coefficient of some phenolic compounds constituents of olive mill wastewater in 1-octanol-water system at 298.15 K. J. Iran. Chem. Soc., 6: 168-176.

111. Noubigh, A., Mgaidi, A. and Abderrabba, M. (2010) Temperature effect on the distribution of some phenolic compounds: An experimental measurement of 1-octanol/water partition coefficients. J. Chem. Eng. Data, 55: 488-491.

112. Zidi, C. and Jamrah, A. (2013) Kinetic and stability studies on phenol and vanillin facilitated transport through a Supported Liquid Membrane. Int. J. Innov. Res. Sci. Eng. Technol., 2: 7360-7368.

113. Tarabanko, V. E., Chelbina, Y. V., Sokolenko, V. A. and Tarabanko, N. V. (2007) A study of vanillin extraction by octylamine. Solvent Extr. Ion Exch., 25: 99-107.

114. Fries, D. M., Voitl, T. and von Rohr, P. R. (2008) Liquid extraction of vanillin in rectangular microreactors. Chem. Eng. Technol., 31: 1182-1187.

115. Kamaldina, O. and Massov, Y. (1959) Production of vanillin from lignosulfonates. TsBTI TsINIS: Moscow.

116. Tarabanko, V. E., Ivanchenko, N. M., Kudryashev, A. V., Gulbis, G. R. and Kuznetsov, B. N. (1996) Method for extraction of vanillin, RU Patent 2065434 (20-08-1996).

117. Cláudio, A., Freire, M., Freire, C., Silvestre, A. and Coutinho, J. (2010) Extraction of vanillin using ionic-liquid-based aqueous two-phase systems. Sep. Purif. Technol., 75: 39-47.

118. Cardoso, G. B., Mourão, T., Pereira, F. M., Freire, M. G., Fricks, A. T., Soares, C. M. F. and Lima, Á. S. (2013) Aqueous two-phase systems based on acetonitrile and carbohydrates and their application to the extraction of vanillin. Sep. Purif. Technol., 104: 106-113.

119. Reis, I. , Santos, S., Santos, L., Oliveira, N., Freire, M., Pereira, J., Ventura, S., Coutinho, J., Soares, C. and Lima, Á. (2012) Increased significance of food wastes: selective recovery of added-value compounds. Food Chem., 135: 2453-2461.

120. Adrian, T., Freitag, J. and Maurer, G. (1999) High pressure multiphase equilibria in aqueous systems of carbon dioxide, a hydrophilic organic solvent and biomolecules. Fluid Phase Equilib., 158–160: 685-693.

121. Sandborn, L. T. (1938) Process of making vanillin, US Patent 2104701 (04-01-1938).

122. Major, F. W. and Nicolle, F. M. A. (1977) Vanillin recovery process, US Patent 4021493 (03-05-1977).

123. Tarabanko, V. E., Chelbina, Y. V., Kaygorodov, K. L., Tarabanko, N. V. and Koropachinskaya, N. V. *Study of vanillin extraction from solutions of lignin oxidation*. In *Proceedings of International solvent extraction Conference, Tucson, Arizona, United States of America.* 2008.

124. Kamaya, Y., Fukaya, Y. and Suzuki, K. (2005) Acute toxicity of benzoic acids to the crustacean *Daphnia magna*. Chemosphere, 59: 255-261.

125. Nakamura, K., Da, Y.-Z., Jikihara, T. and Fujiwara, H. (1995) Thermochemical aspects of partition. A study on the novel hydrophobic parameters of multiply-substituted benzoic acids. Bull. Chem. Soc. Jpn., 68: 782-786.

126. Almeida, M. R., Passos, H., Pereira, M., Lima, Á. S., Coutinho, J. A. P. and Freire, M. G. (2014) Ionic liquids as additives to enhance the extraction of antioxidants in aqueous two-phase systems. Sep. Purif. Technol., 128: 1-10.

127. Bland, D. E., Hillis, W. E. and Williams, E. J. (1951) Prediction curves for counter-current separations : application to lignin aldehydes. Australian Journal of Scientific Research, Series A: Physical Sciences (Aust. J. Sci. Res. A), 5: 346-367.

128. Sciubba, L., Di Gioia, D., Fava, F. and Gostoli, C. (2009) Membrane-based solvent extraction of vanillin in hollow fiber contactors. Desalination, 241: 357-364.

129. Vigneault, A., Johnson, D. K. and Chornet, E. (2007) Base-catalyzed depolymerization of lignin: separation of monomers. Can. J. Chem. Eng., 85: 906-916.

130. Assmann, N. and von Rohr, P. R. (2011) Extraction in microreactors: intensification by adding an inert gas phase. Chem. Eng. Process., 50: 822-827.

131. Sandborn, L. T., Salvesen, J. R. and Howard, G. C. (1936) Process of making vanillin, US Patent 2057117 (13-10-1936).

132. Hilbbert, H. and Tomlinson, G. H. J. (1937) Manufacture of vanillin from waste sulphite pulp liquor, US Patent 2069185 (26-01-1937).

133. Schulz, L. (1940) Manufacture of vanillin, US Patent 2187266 (16-01-1940).

134. Creighton, R. H. J., McCarthy, J. L. and Hibbert, H. (1941) Aromatic aldehydes from spruce and maple woods. J. Am. Chem. Soc., 63: 312-312.

135. Craig, D. and Logan, C. D. (1962) Method of producing vanillin and other useful products, US Patent 3054825 (18-09-62).

136. Vibert, M., Cochennec, C. and Etchebarne, A. (2013) Method for purifying vanillin by liquid-liquid extraction, WO Patent 2013087795 A1 (20-06-2013).

137. Grafe, V. (1904) Untersuchungen über die Holzsubstanz vom chemisch-physiologischen Standpunkte. Monatshefte für Chemie, 25: 987-1029.

138. Klemola, A. and Tuovinen, J. (1989) Method for the production of vanillin, US Patent 4847422 (11-7-1989).

139. Mathias, Á. L., Lopretti, M. I. and Rodrigues, A. E. (1995) Chemical and biological oxidation of Pinus pinaster lignin of the production of vanillin. J. Chem. Technol. Biotechnol., 64: 225-234.

140. Pinto, P. C. R., Borges da Silva, E. A. and Rodrigues, A. E. (2010) Comparative study of solid-phase extraction and liquid−liquid extraction for the reliable quantification of high value added compounds from oxidation processes of wood-derived lignin. Ind. Eng. Chem. Res., 49: 12311-12318.

141. Sankey, C. A. and Marshall, H. B. (1949) Separation of vanillin from alkaline solutions, US Patent 2489200 (22-1-1949).

142. Eckert, C., Liotta, C., Ragauskas, A., Hallett, J., Kitchens, C., Hill, E. and Draucker, L. (2007) Tunable solvents for fine chemicals from the biorefinery. Green Chem., 9: 545-548.

143. Servis, R. (1946) Process of making vanillin, US Patent 2399607 (30-04-1946).

144. Я.А., М. *Факторы, влияющие на бисульфитацию ванилина в процессе экстракции*. Сб. тр. ВНИИГС, 1959. **VII**, 157-162.

145. Massov, Y. *A. Bisulfitation of vanillin during its extraction*. In Sbornic trudov VNIIGS, 1959. **VII**, 157-162.

146. Töppel, O. (1961) Verfahren zur reindarstellung von vanillin, DE Patent 1119244B (14-12-1961).

147. Mokhtarani, B., Karimzadeh, R., Amini, M. H. and Manesh, S. D. (2008) Partitioning of Ciprofloxacin in aqueous two-phase system of poly(ethylene glycol) and sodium sulphate. Biochem. Eng. J., 38: 241-247.

148. Porto, C. S., Porto, T. S., Nascimento, K. S., Teixeira, E. H., Cavada, B. S., Lima-Filho, J. L. and Porto, A. L. F. (2011) Partition of lectin from *Canavalia grandiflora* Benth in aqueous two-phase systems using factorial design. Biochem. Eng. J., 53: 165-171.

149. Malpiedi, L. P., Romanini, D., Picó, G. A. and Nerli, B. B. (2009) Purification of trypsinogen from bovine pancreas by combining aqueous two-phase partitioning and precipitation with charged flexible chain polymers. Sep. Purif. Technol., 65: 40-45.

150. Ventura, S. P. M., Neves, C. M. S. S., Freire, M. G., Marrucho, I. M., Oliveira, J. and Coutinho, J. A. P. (2009) Evaluation of anion influence on the formation and extraction

capacity of ionic-liquid-based aqueous biphasic systems. J. Phys. Chem. B, 113: 9304-9310.

151. Dreyer, S., Salim, P. and Kragl, U. (2009) Driving forces of protein partitioning in an ionic liquid-based aqueous two-phase system. Biochem. Eng. J., 46: 176-185.

152. Li, S., He, C., Liu, H., Li, K. and Liu, F. (2005) Ionic liquid-based aqueous two-phase system, a sample pretreatment procedure prior to high-performance liquid chromatography of opium alkaloids. J. Chromatogr. B: Anal. Technol. Biomed. Life Sci., 826: 58-62.

153. Li, Z., Pei, Y., Wang, H., Fan, J. and Wang, J. (2010) Ionic liquid-based aqueous two-phase systems and their applications in green separation processes. TrAC, Trends Anal. Chem., 29: 1336-1346.

154. Han, D. and Row, K. H. (2010) Recent applications of ionic liquids in separation technology. Molecules, 15: 2405-2426.

155. Park, S. and Kazlauskas, R. J. (2003) Biocatalysis in ionic liquids – advantages beyond green technology. Curr. Opin. Biotechnol., 14: 432-437.

156. Abu-Eishah, S. I., *Chapter 11: Ionic Liquids Recycling for Reuse*, in *Ionic Liquids - Classes and Properties*, 2011, Scott T. Handy editor. InTech, available from: http://www.intechopen.com/books/ionicliquids-classes-and-properties/ionic-liquids-recycling-for-reuse.

157. Wagner, M. and Hilgers, C. (2008) Quality aspects and other questions related to commercial ionic liquid production: In Ionic liquids in synthesis. Peter Wasserscheid and Thomas Welton eds. Wiley -VCH: Weinheim, Vol 1, 27-28.

158. Taylor, L. T. (1996) Supercritical fluid extraction. Wiley-Interscience Publication: New York, United States of America.

159. Reverchon, E. and De Marco, I. (2006) Supercritical fluid extraction and fractionation of natural matter. J. Supercrit. Fluids, 38: 146-166.

160. Fornari, T., Chafer, A., Stateva, R. P. and Reglero, G. (2005) A new development in the application of the group contribution associating equation of state to model solid solubilities of phenolic compounds in sc-CO_2. Ind. Eng. Chem. Res., 44: 8147-8156.

161. Nguyen, K., Barton, P. and Spencer, J. S. (1991) Supercritical carbon dioxide extraction of vanilla. J. Supercrit. Fluids, 4: 40-46.

162. Assmann, N., Werhan, H., Ładosz, A. and Rudolf von Rohr, P. (2013) Supercritical extraction of lignin oxidation products in a microfluidic device. Chem. Eng. Sci., 99: 177-183.

163. Coenen, H. and Konrad, R. (1990) Process for the extraction of vanillin, US Patent 4898990 (06-02-1990).

164. Makin, E. C. (1984) Purification of vanillin, US Patent 4474994 (02-10-1984).

165. Hocking, M. B. (1997) Vanillin: synthetic flavoring from spent sulfite liquor. J. Chem. Educ., 74: 1055-1059.

166. Heald, S., Myers, S., Walford, T., Robbins, K. and Hill, C. (2013) Preparation of vanillin from microbial transformation media by extraction by means supercritical fluids or gases, US Patent 8563292 B2 (22-10-2013).

167. Wells, T., Foster, N. R. and Chaplin, R. P. (1992) Diffusion of phenylacetic acid and vanillin in supercritical carbon dioxide. Ind. Eng. Chem. Res., 31: 927-934.

168. Assmann, N., Kaiser, S. and Rudolf Von Rohr, P. (2012) Supercritical extraction of vanillin in a microfluidic device. J. Supercrit. Fluids, 67: 149-154.

169. Liu, J., Kim, Y. and McHugh, M. A. (2006) Phase behavior of the vanillin–CO_2 system at high pressures. J. Supercrit. Fluids, 39: 201-205.

170. Hybertson, B. M. (2007) Solubility of the sesquiterpene alcohol patchoulol in supercritical carbon dioxide. J. Chem. Eng. Data, 52: 235-238.

171. Vitzthum, O. and Hubert, P. (1980) Process for the production of spice extracts, US Patent 4198432 (15-04-1980).

172. Liu, Y., Liu, C., Wu, Y., Li, Y., Chen, C., Zheng, X. and Wei, G. (2010) Carbon dioxide supercritical extraction method for vanillic aldehyde or ethyl vanillin raw product, CN Patent 101386570A (29-09-2010).

173. Seader, J. D., Henley, E. J. and Roper, K. (2010) Separation process principles - chemical and biochemical operations. Third edition, John Wiley & Sons, Inc.: New Jersey, United States of America.

174. Ulrich, J. and Stelzer, T. (2000) Crystallization: In Kirk-Othmer Encyclopedia of Chemical Technology. John Wiley & Sons, Inc.: London, United Kingdom.

175. Pino-García, O. and Rasmuson, Å. C. (2004) Influence of additives on nucleation of vanillin: experiments and introductory molecular simulations. Cryst. Growth Des., 4: 1025-1037.

176. Hussain, K., Thorsen, G. and Malthe-Sørenssen, D. (2001) Nucleation and metastability in crystallization of vanillin and ethyl vanillin. Chem. Eng. Sci., 56: 2295-2304.

177. Zhao, H., Xie, C., Xu, Z., Wang, Y., Bian, L., Chen, Z. and Hao, H. (2012) Solution rystallization of vanillin in the presence of a liquid–liquid phase separation. Ind. Eng. Chem. Res., 51: 14646-14652.

178. Du, Y., Wang, H., Du, S., Wang, Y., Huang, C., Qin, Y. and Gong, J. (2016) The liquid–liquid phase separation and crystallization of vanillin in 1-propanol/water solution. Fluid Phase Equilib., 409: 84-91.

179. Schoeffel, E. W. (1962) Vanillin purification, US Patent 3049566 (14-08-1962).

180. Ibrahim, M. N. M., Sipaut, C. S. and Yusof, N. N. M. (2009) Purification of vanillin by a molecular imprinting polymer technique. Sep. Purif. Technol., 66: 450-456.

181. Gitchel, W. B., Diddams, D. G. and Hoffman, C. A. (1971) Method of recovering vanillin from crystallization liquors, US Patent 3600442 (17-08-1971).

182. Diddams, D. G. and Renaud, N. E. (1972) Process for purifying vanillin, US Patent 3686322 (22-08-1972).

183. Zhang, Z., Zhang, H., Deng, C., Zhong, Q., Yang, J. and Gao, J. (1998) Method for producing vanillin and syringaldehyde by catalytic oxidation of alkali lignin of sugercane residue, CN Patent 1201778 (16-12-1998).

184. Deng, H. (2013) Method for preparing syringaldehyde by oxidative degradation of lignin, CN Patent 102146025 B (05-06-2013).

185. Werhan, H., Farshori, A. and Rudolf von Rohr, P. (2012) Separation of lignin oxidation products by organic solvent nanofiltration. J. Membr. Sci., 423–424: 404-412.

186. Brazinha, C., Barbosa, D. S. and Crespo, J. G. (2011) Sustainable recovery of pure natural vanillin from fermentation media in a single pervaporation step. Green Chem., 13: 2197-2203.

187. Böddeker, K. W., Gatfield, I. L., Jähnig, J. and Schorm, C. (1997) Pervaporation at the vapor pressure limit: vanillin. J. Membr. Sci., 137: 155-158.

188. Camera-Roda, G., Augugliaro, V., Cardillo, A., Loddo, V., Palmisano, G. and Palmisano, L. (2013) A pervaporation photocatalytic reactor for the green synthesis of vanillin. Chem. Eng. J., 224: 136-143.

189. Evju, H. (1979) Process for preparation of 3-methoxy-4-hydroxybenzaldehyde, US Patent 4151207 (24-04-1979).

190. Jönsson, A.-S., Nordin, A.-K. and Wallberg, O. (2008) Concentration and purification of lignin in hardwood kraft pulping liquor by ultrafiltration and nanofiltration. Chem. Eng. Res. Des., 86: 1271-1280.

191. Toledano, A., García, A., Mondragon, I. and Labidi, J. (2010) Lignin separation and fractionation by ultrafiltration. Sep. Purif. Technol., 71: 38-43.

192. Sainio, T., Kallioinen, M., Nakari, O. and Mänttäri, M. (2013) Production and recovery of monosaccharides from lignocellulose hot water extracts in a pulp mill biorefinery. Bioresour. Technol., 135: 730-737.

193. Sevastyanova, O., Helander, M., Chowdhury, S., Lange, H., Wedin, H., Zhang, L., Ek, M., Kadla, J. F., Crestini, C. and Lindström, M. E. (2014) Tailoring the molecular and thermo–mechanical properties of kraft lignin by ultrafiltration. J. Appl. Polym. Sci., 131: 1-11.

194. Arkell, A., Olsson, J. and Wallberg, O. (2014) Process performance in lignin separation from softwood black liquor by membrane filtration. Chem. Eng. Res. Des., 92: 1792-1800.

195. Keyoumu, A., Sjödahl, R., Henriksson, G., Ek, M., Gellerstedt, G. and Lindström, M. E. (2004) Continuous nano- and ultra-filtration of kraft pulping black liquor with ceramic filters: A method for lowering the load on the recovery boiler while generating valuable side-products. Ind. Crop. Prod., 20: 143-150.

196. Toledano, A., Serrano, L., Garcia, A., Mondragon, I. and Labidi, J. (2010) Comparative study of lignin fractionation by ultrafiltration and selective precipitation. Chem. Eng. J., 157: 93-99.

197. Uloth, V. C. and Wearing, J. T. (1988) Kraft lignin recovery: acid precipitation versus ultrafiltration. I. Laboratory test results. Pulp and paper Canada, 90: 67-71.

198. Koncsag, C. I. and Kirwan, K. (2012) A membrane screening for the separation/concentration of dilignols and trilignols from solvent extracts. Sep. Purif. Technol., 94: 54-60.

199. Wankat, P. C. (1994) Rate-controlled separations. Blackie Academic & Professional: London, United Kingdom.

200. Schäfer, T. and Crespo, J. (2007) Aroma Recovery by Organophilic Pervaporation: In Flavours and Fragrances. RalfGünter editor Berger. Springer Berlin Heidelberg: Heidelberg, Germany, 427-437.

201. Zhang, X., Li, C., Hao, X., Feng, X., Zhang, H., Hou, H. and Liang, G. (2014) Recovering phenol as high purity crystals from dilute aqueous solutions by pervaporation. Chem. Eng. Sci., 108: 183-187.

202. Camera-Roda, G., Santarelli, F., Augugliaro, V., Loddo, V., Palmisano, G., Palmisano, L. and Yurdakal, S. (2011) Photocatalytic process intensification by coupling with pervaporation. Catal. Today, 161: 209-213.

203. Camera-Roda, G. and Santarelli, F. (2012) Design of a pervaporation photocatalytic reactor for process intensification. Chem. Eng. Technol., 35: 1221-1228.

204. Drioli, E., Criscuoli, A. and Curcio, E. (2005) Membrane Contactors: Fundamentals, Applications and Potentialities. Elsevier: Boston, United States of America.

205. Pabby, A. K. and Sastre, A. M. (2013) State-of-the-art review on hollow fibre contactor technology and membrane-based extraction processes. J. Membr. Sci., 430: 263-303.

206. Wu, Y.-T., Feng, M., Ding, W.-W., Tang, X.-Y., Zhong, Y.-H. and Xiao, Z.-Y. (2008) Preparation of vanillin by bioconversion in a silicon rubber membrane bioreactor. Biochem. Eng. J., 41: 193-197.

207. Hoover, K. C. and Hwang, S.-T. (1982) Pervaporation by a continuous membrane column. J. Membr. Sci., 10: 253-271.

208. Nakao, S.-i., Saitoh, F., Asakura, T., Toda, K. and Kimura, S. (1987) Continuous ethanol extraction by pervaporation from a membrane bioreactor. J. Membr. Sci., 30: 273-287.

209. Cho, C.-W. and Hwang, S.-T. (1991) Continuous membrane fermentor separator for ethanol fermentation. J. Membr. Sci., 57: 21-42.

210. Stiefel, S., Lölsberg, J., Kipshagen, L., Möller-Gulland, R. and Wessling, M. (2015) Controlled depolymerization of lignin in an electrochemical membrane reactor. Electrochemistry Communications, 61: 49-52.

211. Forss, K. G., Talka, E. T. and Fremer, K. E. (1986) Isolation of vanillin from alkaline oxidized spent sulfite liquor. Ind. Eng. Chem. Prod, Res, Dev,, 25: 103-108.

212. van Blaricom, L. E., Gray, K. R. and Ward, F. G. (1955) Adsorption of lignosulfate from solution with porous ion exchange resin, US Patent 2727029 (13-12-1955).

213. Ku, Y., Lee, K. C. and Wang, W. (2004) Removal of phenols from aqueous solutions by purolite A-510 resin. Sep. Sci. Technol., 39: 911-923.

214. Raman, G., Jayaprakasha, G. K., Cho, M., Brodbelt, J. and Patil, B. S. (2005) Rapid adsorptive separation of citrus polymethoxylated flavones in non-aqueous conditions. Sep. Purif. Technol., 45: 147-152.

215. Carmona, M., Lucas, A. D., Valverde, J. L., Velasco, B. and Rodríguez, J. F. (2006) Combined adsorption and ion exchange equilibrium of phenol on Amberlite IRA-420. Chem. Eng. J., 117: 155-160.

216. Zhao, L.-Q., Sun, Z.-H., Zheng, P. and He, J.-Y. (2006) Biotransformation of isoeugenol to vanillin by *Bacillus fusiformis* CGMCC1347 with the addition of resin HD-8. Process Biochem., 41: 1673-1676.

217. Nilvebrant, N.-O., Reimann, A., Larsson, S. and Jönsson, L. (2001) Detoxification of lignocellulose hydrolysates with ion-exchange resins. Appl. Biochem. Biotechnol., 91-93: 35-49.

218. Forss, K. G., Fremer, K. E. and Talka, E. T. (1981) Method for the isolation of vanillin from lignin in alkaline solutions, US Patent 4277626 (07-07-1981).

219. Toppel, O. (1959) Method for the separation of carbonyl compounds, US Patent 2897238 (28-07-1959).

220. Logan, C. D. (1965) Cyclic process for recovering vanillin and sodium values from lignosulfonic waste liquors by ion exchange, US Patent 3197359 (27-07-1965).

221. Parida, S. K., Dash, S., Patel, S. and Mishra, B. K. (2006) Adsorption of organic molecules on silica surface. Adv. Colloid Interface Sci., 121: 77-110.

222. Rouquerol, J., Rouquerol, F. and Sing, K. S. W. S. (1999) Adsorption by Powders and Porous Solids: Principles, Methodology and Applications. First edition, Academic Press: London, United Kingdom.

223. Chaouati, N., Soualah, A. and Chater, M. (2013) Adsorption of phenol from aqueous solution onto zeolites Y modified by silylation. Comptes Rendus Chimie, 16: 222-228.

224. Ranjan, R., Thust, S., Gounaris, C. E., Woo, M., Floudas, C. A., von Keitz, M., Valentas, K. J., Wei, J. and Tsapatsis, M. (2009) Adsorption of fermentation inhibitors from lignocellulosic biomass hydrolyzates for improved ethanol yield and value-added product recovery. Microporous Mesoporous Mater., 122: 143-148.

225. Damjanović, L., Rakić, V., Rac, V., Stošić, D. and Auroux, A. (2010) The investigation of phenol removal from aqueous solutions by zeolites as solid adsorbents. J. Hazard. Mater., 184: 477-484.

226. Derouane, E. G. and Powell, R. A. (1987) Vanillin extraction process using large pore, high silica/alumina ratio zeolites, US patent 4652684 (24-03-1987).

227. Soto, M. L., Moure, A., Domínguez, H. and Parajó, J. C. (2011) Recovery, concentration and purification of phenolic compounds by adsorption: A review. J. Food Eng., 105: 1-27.

228. García-Araya, J. F., Beltrán, F. J., Álvarez, P. and Masa, F. J. (2003) Activated carbon adsorption of some phenolic compounds present in agroindustrial wastewater. Adsorption, 9: 107-115.

229. Zhang, Q.-F., Jiang, Z.-T., Gao, H.-J. and Li, R. (2008) Recovery of vanillin from aqueous solutions using macroporous adsorption resins. Eur. Food Res. Technol., 226: 377-383.

230. Michailof, C., Stavropoulos, G. G. and Panayiotou, C. (2008) Enhanced adsorption of phenolic compounds, commonly encountered in olive mill wastewaters, on olive husk derived activated carbons. Bioresour. Technol., 99: 6400-6408.

231. Richard, D., Delgado-Núñez, M. L. and Schweich, D. (2009) Adsorption of complex phenolic compounds on active charcoal: Adsorption capacity and isotherms. Chem. Eng. J., 148: 1-7.

232. Xiao, G.-Q., Xie, X.-L. and Xu, M.-C. (2009) Adsorption performances for vanillin from aqueous solution by the hydrophobic - hydrophilic macroporous polydivinylbenzene / polyacrylethylenediamine IPN resin. Acta Phys.-Chim. Sin., 25: 97-102.

233. Samah, R. A., Zainol, N., Yee, P. L., Pawing, C. M. and Abd-Aziz, S. (2013) Adsorption of vanillin using macroporous resin H103. Adsorpt. Sci. Technol., 31: 599-610.

234. Jin, X. and Huang, J. (2013) Adsorption of vanillin by an anisole-modified hyper-cross-linked polystyrene resin from aqueous solution: equilibrium, kinetics, and dynamics. Adv. Polym. Tech., 32: E221-E230.

235. Wang, Z., Chen, K., Li, J., Wang, Q. and Guo, J. (2010) Separation of vanillin and syringaldehyde from oxygen delignification spent liquor by macroporous resin adsorption. Clean, 38: 1074-1079.

236. Hua, D., Ma, C., Song, L., Lin, S., Zhang, Z., Deng, Z. and Xu, P. (2007) Enhanced vanillin production from ferulic acid using adsorbent resin. Appl. Microbiol. Biotechnol., 74: 783-790.

237. Geng, X., Ren, P., Pi, G., Shi, R., Yuan, Z. and Wang, C. (2009) High selective purification of flavonoids from natural plants based on polymeric adsorbent with hydrogen-bonding interaction. J. Chromatogr. A, 1216: 8331-8338.

238. Xiao, G., Long, L., Wang, J. and Xu, M. (2011) Synthesis of the Hypercrosslinked Resin Modified by Acetylaniline and Its Adsorption Performances for Vanillin. Chinese Polymer Materials Science & Engineering, 27: 160-164

239. Stentelaire, C., Lesage-Meessen, L., Oddou, J., Bernard, O., Bastin, G., Ceccaldi, B. C. and Asther, M. (2000) Design of a fungal bioprocess for vanillin production from vanillic acid at scalable level by *Pycnoporus cinnabarinus*. J. Biosci. Bioeng., 89: 223-230.

240. Wang, C.-l., LI, S.-l., Zhou, Q.-l., Zhang, M., Zeng, J.-h. and Zhang, Y. (2005) Extraction of vanillin in fermented broth by macroporous adsorption resin. Jingxi Huagong (Fine Chemicals), 22: 458-460.

241. Wu, X., Zhang, N.-z. and Qi, C.-h. (2003) Enrichment of vanillin with adsorbent resin in the oxidative liquorsof acidic sulphite pulping. China Pulp & Paper Industry, 24: 21.

242. Huang, J., Yang, L., Zhang, Y., Pan, C. and Liu, Y.-N. (2013) Resorcinol modified hypercrosslinked poly(styrene-co-divinlybenzene) resin and its adsorption equilibriums, kinetics and dynamics towards *p*-hydroxylbenzaldehyde from aqueous solution. Chem. Eng. J., 219: 238-244.

243. Zhou, Q.-l. and Wang, H.-l. (2008) Study on Separation and Purification of Total Vanillin by Adsorbing Resin. Acta Agriculturae Jiangxi, 28.

244. Crittenden, B. D. and Thomas, W. J. (1998) Adsorption Technology and Design. First edition, Butterworth and Heinemann: Oxford, United Kingdom.

245. Ruthven, D. M. (1984) Principles of Adsorption and Adsorption Processes. John Willey and Sons: New York, United States of America.

246. Cooney, D. O. (1999) Adsorption design for wastewater treatment. Lewis Publishers: Florida, United States of America.

247. Berčič, G., Pintar, A. and Levec, J. (1996) Desorption of phenol from activated carbon by hot water regeneration. Desorption isotherms. Ind. Eng. Chem. Res., 35: 4619-4625.

248. Rodrigues, L. A., Sousa Ribeiro, L. A., Thim, G. P., Ferreira, R. R., Alvarez-Mendez, M. O. and Coutinho, A. R. (2013) Activated carbon derived from macadamia nut shells: an effective adsorbent for phenol removal. J. Porous Mater., 20: 619-627.

249. Fu, K., Yue, Q., Gao, B., Sun, Y. and Zhu, L. (2013) Preparation, characterization and application of lignin-based activated carbon from black liquor lignin by steam activation. Chem. Eng. J., 228: 1074-1082.

250. Brás, I., Lemos, L., Alves, A. and Pereira, M. F. R. (2005) Sorption of pentachlorophenol on pine bark. Chemosphere, 60: 1095-1102.

251. Wu, F.-C., Tseng, R.-L. and Juang, R.-S. (2005) Preparation of highly microporous carbons from fir wood by KOH activation for adsorption of dyes and phenols from water. Sep. Purif. Technol., 47: 10-19.

252. Srinivasakannan, C. and Zailani Abu Bakar, M. (2004) Production of activated carbon from rubber wood sawdust. Biomass Bioenergy, 27: 89-96.

253. Cardoso, B., Mestre, A. S., Carvalho, A. P. and Pires, J. (2008) Activated carbon derived from cork powder waste by KOH activation: Preparation, characterization, and VOCs adsorption. Ind. Eng. Chem. Res., 47: 5841-5846.

254. Tongpoothorn, W., Sriuttha, M., Homchan, P., Chanthai, S. and Ruangviriyachai, C. (2011) Preparation of activated carbon derived from *Jatropha curcas* fruit shell by simple thermo-chemical activation and characterization of their physico-chemical properties. Chem. Eng. Res. Des., 89: 335-340.

255. Gottipati, R. and Mishra, S. (2013) Preparation of microporous activated carbon from Aegle marmelos fruit shell by KOH activation. Can. J. Chem. Eng., 91: 1215-1222.

256. Ahmaruzzaman, M. (2008) Adsorption of phenolic compounds on low-cost adsorbents: a review. Adv. Colloid Interface Sci., 143: 48-67.

257. Ravi, V. P., Jasra, R. V. and Bhat, T. S. G. (1998) Adsorption of phenol, cresol isomers and benzyl alcohol from aqueous solution on activated carbon at 278, 298 and 323 K. J. Chem. Technol. Biotechnol., 71: 173-179.

258. Kammerer, D. R., Saleh, Z. S., Carle, R. and Stanley, R. A. (2007) Adsorptive recovery of phenolic compounds from apple juice. Eur. Food Res. Technol., 224: 605-613.

259. He, Z. and Xia, W. (2008) Preparative separation and purification of phenolic compounds from *Canarium album L.* by macroporous resins. J. Sci. Food Agric., 88: 493-498.

260. Spégel, P., Schweitz, L. and Nilsson, S. (2002) Molecularly imprinted polymers. Anal. Bioanal. Chem., 372: 37-38.

261. Chen, L., Xu, S. and Li, J. (2011) Recent advances in molecular imprinting technology: current status, challenges and highlighted applications. Chemical Society Reviews, 40: 2922-2942.

262. Feng, Q.-Z., Zhao, L.-X., Yan, W., Lin, J.-M. and Zheng, Z.-X. (2009) Molecularly imprinted solid-phase extraction combined with high performance liquid chromatography for analysis of phenolic compounds from environmental water samples. J. Hazard. Mater., 167: 282-288.

263. Mhaka, B., Cukrowska, E., Tse Sum Bui, B., Ramström, O., Haupt, K., Tutu, H. and Chimuka, L. (2009) Selective extraction of triazine herbicides from food samples based on a combination of a liquid membrane and molecularly imprinted polymers. J. Chromatogr. A, 1216: 6796-6801.

264. Ramström, O. and Mosbach, K. (1999) Synthesis and catalysis by molecularly imprinted materials. Curr. Opin. Chem. Biol., 3: 759-764.

265. Alexander, C., Davidson, L. and Hayes, W. (2003) Imprinted polymers: artificial molecular recognition materials with applications in synthesis and catalysis. Tetrahedron, 59: 2025-2057.

266. Hunt, C. E., Pasetto, P., Ansell, R. J. and Haupt, K. (2006) A fluorescence polarisation molecular imprint sorbent assay for 2,4-D: a non-separation pseudo-immunoassay. Chem. Commun., 1754-1756.

267. Lépinay, S., Ianoul, A. and Albert, J. (2014) Molecular imprinted polymer-coated optical fiber sensor for the identification of low molecular weight molecules. Talanta, 128: 401-407.

268. Li, W. and Li, S. (2007) Molecular Imprinting: A Versatile Tool for Separation, Sensors and Catalysis: In Oligomers - Polymer Composites - Molecular Imprinting. R. G. Berger editor. Springer Berlin Heidelberg: London, United Kingdom, Volume 206, 191-210.

269. Ávila, M., Zougagh, M., Escarpa, A. and Ríos, Á. (2007) Supported liquid membrane-modified piezoelectric flow sensor with molecularly imprinted polymer for the determination of vanillin in food samples. Talanta, 72: 1362-1369.

270. Peng, H., Wang, S., Zhang, Z., Xiong, H., Li, J., Chen, L. and Li, Y. (2012) Molecularly imprinted photonic hydrogels as colorimetric sensors for rapid and label-free detection of vanillin. J. Agric. Food. Chem., 60: 1921-1928.

271. Puzio, K., Delépée, R., Vidal, R. and Agrofoglio, L. A. (2013) Combination of computational methods, adsorption isotherms and selectivity tests for the conception of a mixed non-covalent–semi-covalent molecularly imprinted polymer of vanillin. Anal. Chim. Acta, 790: 47-55.

272. Zhang, Y., Ding, J. and Gong, S. (2013) Preparation of molecularly imprinted polymers for vanillin via reversible addition-fragmentation chain transfer suspension polymerization. J. Appl. Polym. Sci., 128: 2927-2932.

273. Zhang, Y. and Yao, X. (2014) Preparation of molecularly imprinted polymer for vanillin via seed swelling and suspension polymerization. Polym. Sci. Ser. B, 56: 538-545.

274. Caus, A., Braeken, L., Boussu, K. and Van der Bruggen, B. (2009) The use of integrated countercurrent nanofiltration cascades for advanced separations. J. Chem. Technol. Biotechnol., 84: 391-398.

275. Marshall, H. B. and Vincent, D. L. (1978) Production of syringealdehyde from hardwood waste pulping liquors, US Patent 4075248 (21-02-1978).

276. Bauer, K., Brandt, H. W. and Schroter, J. (1978) Carrier-vapor distillation, US Patent 4090922 (23-05-1978).

277. Jones, T., Finnan, J. L. and Arvizzigno, J. (1996) Process for separation of vanillin by means of azeotropic distillation with dibenzyl ether, US Patent 5510006 (23-04-1996).

278. Jones, T., Finnan, J. L. and Arvizzigno, J. (1998) Process for separation of vanillin from other chemicals by means of azeotropic distillation with dibenzyl ether and mixtures of vanillin and dibenzyl ether used in such process, US Patent 5772909 (30-06-1998).

279. Bryan, C. C. (1950) Vanillin purification by distillation, US Patent 2506540 (02-05-1950).

3. Adsorption studies of vanillin, syringaldehyde, vanillic acid and syringic acid in aqueous solution onto macroporous polymeric resins[1]

In this chapter adsorption studies with aqueous solutions of vanillin, syringaldehyde, vanillic acid and syringic acid onto nonpolar resins are presented.

Herein, macroporous polymeric resins XAD16N and SP700 are characterized regarding particle size, solid density, apparent density and particle porosity by means of laser dispersion, helium pycnometry and mercury intrusion porosimetry, respectively.

Vanillin and syringaldehyde adsorption equilibrium experiments onto both resins are performed employing the batch bottle point method for three different temperatures 283/288, 298 and 333 K. Due to the adsorptive capacity towards vanillin, SP700 resin is selected to pursue with adsorption equilibrium studies with the phenolic acids. Batch experimental results are fitted to Langmuir, Freundlich and Bi-Langmuir isotherm models.

Dynamic studies in fixed bed columns with the four compounds for different feed concentrations and temperatures are shown in this chapter. A mathematical model comprising the Bi-Langmuir equilibrium isotherm, axial dispersed plug flow, intraparticle mass transfer resistance expressed with linear driving force approximation with no temperature gradients and constant porosity along the bed is used to describe the adsorption/desorption concentration histories at the outlet of the fixed bed.

[1] This chapter is based on the papers

Mota, I. F., Pinto, P. C. R., Loureiro, J. M., Rodrigues, A. E. (2016) Adsorption of vanillin and syringaldehyde onto a macroporous polymeric resin. Chem. Eng. J., 288: 869-879.

Mota, I. F., Barbosa, S., Pinto, P. C. R., Loureiro, J. M., Rodrigues, A. E., Adsorption of vanillic and syringic acids onto a macroporous polymeric resin and recovery with ethanol:water (90:10, % V/V) solution (draft in preparation).

3.1. Introduction

Vanillin, syringaldehyde, vanillic acid and syringic acid are some of the low molecular weight compounds obtained through oxidation of lignin (1, 2). Each one of them has interesting applications on pharmaceutical, fragrance and flavour industries (3-8). The interest for vanillic and syringic acids is very recent and thus, syringaldehyde and, in particular, vanillin have been the phenolic compounds resulting from lignin depolymerisation more extensively investigated.

Several separation and purification sequences to obtain purified fractions of vanillin and syringaldehyde from oxidized lignin media frequently include a stage of solid–liquid adsorption as already described in Chapter 2 State of the art. The majority of adsorption studies report the recovery of functionalized phenolic monomers from oxidized lignin medium by ion exchange resins being particularly focused on vanillin (9-11). The application of zeolites has also been evaluated by Derouane and Powell (12) .

No report of adsorption studies conducted for mono-component aqueous solutions of syringaldehyde was found. There is only one study in literature reporting the recovery of syringaldehyde from an oxygen delignification spent liquor with a polymeric resin (13).

In respect to the phenolic acids, studies of adsorption are restricted to activated carbon and have already been summarized in Table 2.12 (14-16).

The main studies with model vanillin aqueous solutions are focused on the potential of ionic resins (17, 18). Recently, the application of polymeric resins to recover vanillin gained considerable interest (13, 14, 19-23) for many reasons: adsorption of phenolic compounds onto nonpolar resins is feasible due to the existence of both hydrophobic and hydrophilic groups in the molecule; the pH is maintained constant along the process avoiding precipitation; these resins are chemically stable and inert, being suitable for applications under a wide variety of conditions; the phenolic compounds recovery and resin regeneration can be performed simultaneously in one step; and the resin adsorptive properties can be modelled by the surface hydrophobicity, surface area and porosity (24). The acid dissociation constant *pKa* of the adsorbate also determines the adsorption capacity (25). The highest adsorption is achieved for the neutral form of the compounds.

Phenolic compounds adsorption onto nonpolar resins is commonly explained by the occurrence of weak physical interactions mainly of the van der Waals forces type (e.g. permanent dipole-induced dipole or induced dipole-induced dipole) (25-27). Since the phenolic compounds have hydrogen donors, some authors have studied the effect of functional groups (e.g. phenolic hydroxyl or carbonyl, acetyl, amine or methoxy groups) in polymeric resins as promoters of hydrogen bonding to improve the adsorption capacity for these compounds (28-32).

In this chapter adsorption studies of vanillin and syringaldehyde in aqueous solutions were performed employing the polymeric resins SP700 and XAD16N. The resin SP700, with larger surface area and greater adsorptive capabilities was chosen to perform further studies with vanillic acid and syringic acid. Initially, the resins were characterized regarding solid density, apparent density, particle size and moisture content. Afterwards, batch adsorption studies of each phenolic compound in aqueous solution were assessed for different temperatures and data fitted to Langmuir, Freundlich and Bi-Langmuir equilibrium isotherms. Fixed bed studies onto SP700 were performed for different feed concentrations and temperatures and a mathematical model was used to predict the breakthrough curves.

3.2. Experimental description

3.2.1. Chemicals and adsorbents

Model solutions of vanillin (Sigma-Aldrich, purity ≥ 98%), syringaldehyde (Sigma-Aldrich, purity ≥ 98%), vanillic acid (Sigma-Aldrich, purity ≥ 97%) and syringic acid (Sigma-Aldrich, purity ≥ 95%) were prepared in deionized water and filtered through a 0.2 μm nylon membrane (Whatman®) by means of a diaphragm vacuum pump (Vacuubrand GMBH, Germany) and ultrasonic degassed (Liarre, model Starsonic 35, Italy).

Batch adsorption studies (described in 3.2.5) were conducted with two styrene–divinylbenzene-based synthetic resins: Sepabeads SP700 purchased from Mitsubishi chemical and Amberlite XAD16N from Sigma-Aldrich. Their physical and chemical properties will be summarized in Table 3.1 – section 3.4.

Each adsorbent was washed prior to use with several solutions encompassing deionized water, methanol (Merck), methanol acidified with 0.1% formic acid (Chem-Lab). The procedure is detailed in 3.2.3.

The resin SP700 was selected to pursue with fixed bed studies (described in 3.2.6). Deionized water and 0.1 M $NaHCO_3$ (BDH Laboratories) were used as solvent in fixed bed studies and in column regeneration, respectively.

3.2.2. Analytical method (HPLC-UV)

The phenolic compounds concentration was determined by high performance liquid chromatography with ultraviolet detection (HPLC-UV). A Knauer HPLC system (Germany) equipped with a Smartline 5000 online degasser, a Smartline 1000 quaternary pump, and a Smartline 2600 UV – DAD was used. The analytical column was an ACE 5 C_{18}-pentafluorophenyl group (250 x 3.0 mm, 5 µm) with a guard column of the same material. The detection length was set to 280 nm and the volume of injection loop was 20 µL. Standard solutions and samples were filtered before injection using a 0.2 µm syringe filter (VWR). For multi-component analysis the separation was performed at 30 ºC at 0.6 mL min^{-1} using an elution gradient composed by two eluents previously filtered through a 0.20 µm pore size nylon filter (Whatman®): A) methanol:water (5:95, % V/V) and B) methanol:water (95:5, % V/V), both acidified with formic acid (0.1% V/V). The following elution gradient was used: [0-3.30] min 90% A; 6.70 min 80% A; [6.70-20] min 80% A; 35 min 50% A; 38.3 min 0% A, [38.3-41.7] min 0% A; 45 min 90% A; [45-55] min 90% A. For mono-component analysis, chromatograms were run at room temperature and 0.4 mL min^{-1} at isocratic elution of eluents A and B 50:50, % V/V.

3.2.3. Initial resin preparation and cleaning

Each resin was initially handled to remove any contaminant or monomers prior to use. Thus, the resins were brought into contact with a set of different solutions, in batch mode, at room temperature. Initially, the resins were rinsed with deionized water and placed with fresh deionized water in an orbital shaker (IKA®HS 260, Germany) at 160 rpm for about 0.5 h. This step was repeated one more time. The resins were then rinsed with methanol and placed in an orbital shaker at 160 rpm with methanol for about 0.5 h. The methanol was replaced by acidified methanol (0.1% formic acid) and shaken at 160 rpm for 0.5 h. Afterwards, each resin was rinsed with deionized water and acidified deionized water (0.1% formic acid) was added. The mixture was agitated for 0.5 h and this step was repeated twice using deionized water.

3.2.4. Physical and chemical characterization of the resins

The resins were characterized concerning particle size, solid density, apparent density, particle porosity and water content. After being cleaned and prepared as described in 3.2.3, moisture content was assessed by weighting a known amount of resin before and after drying it at 105 ºC. A dry to wet resin volume ratio was assessed by measuring the volume occupied by a certain amount of resin before and after drying at 105 ºC. This analysis allowed converting the apparent density and volume of pores into wet volume of resin and comparing the experimental values with the values given by the supplier.

Particle size distribution was determined by laser dispersion using a particle size analyser (Coulter, LS230) and samples were used in wet form.

Helium pycnometry analysis was performed with previously dried resin at 105 ºC to obtain the solid (or skeletal) density. This analysis measures the change in pressure of a certain amount of compressed helium gas filling a reference chamber with a known volume expanding into a second chamber containing the material to be analysed. Helium readily diffuses into small pores, accessing larger pores than its atomic diameter of 3 Å (33).

In opposition to helium gas that readily penetrates into very fine pores, mercury is a non-wetting liquid that does not penetrate pores under atmospheric pressure. Thus, an external pressure must be applied in order to force the mercury to enter in a pore. Taking into account these principles, apparent density and volume pore size distribution can be assessed. A Quantachrome PoreMaster apparatus (Boynton Beach, FL, USA) at 20 ºC was used in the analysis. It was assumed mercury density, surface tension and contact angle of 13.579 g mL^{-1}, 480 erg cm^{-2} and 140º, respectively. The porosimetry analysis was performed from 20 psi to 59000 psi and covered pore diameters in the range between 3.6 nm and 10.6 μm. Samples were previously dried at 105 ºC. It was used penetrometers of 50 g in mercury weight and about 0.4 g (dried weight) of sample.

Particle porosity and volume of pores were estimated by the following expressions:

$$\rho_{app} = \frac{1}{a}\left(1-\varepsilon_P\right)\rho_S \qquad \textbf{Equation 3.1}$$

$$V_P = \frac{1}{a\rho_{app}} - \frac{1}{\rho_S} \qquad \textbf{Equation 3.2}$$

where, ρ_S ($g_{dry\ resin}\ L^{-1}_{dry\ resin}$) is the solid density, ρ_{app} ($g_{wet\ resin}\ L^{-1}_{wet\ resin}$) is the particle apparent density, ε_P ($L_{pores}\ L^{-1}_{particle}$) is the particle porosity and V_p ($L_{pores}\ g^{-1}_{dry\ resin}$) is the volume of pores;

a ($g_{dry\ resin}\ L_{wet\ resin}\ g^{-1}_{wet\ resin}\ L^{-1}_{dry\ resin}$) is the factor to convert apparent density from $g_{wet\ resin}\ L^{-1}_{wet\ resin}$ to $g_{dry\ resin}\ L^{-1}_{dry\ resin}$: 0.348 and 0.377 for SP700 and XAD16N, respectively.

3.2.5. Batch adsorption studies

Mono-component batch experiments for vanillin and syringaldehyde were conducted with 0.04 L of 4 g L^{-1} and/or 6 g L^{-1} solutions of each compound. Different amounts of resin (SP700 or XAD16N) were used, ranging from 0.1 to 0.5 g of dry weight. Batch samples were shaken in a thermostatic water bath shaker (GLF model 3018, Germany) for 72 h at the desired temperature, in order to ensure that the equilibrium was met. Adsorption equilibrium isotherms onto each adsorbent was measured for three different temperatures 283/288K, 298K and 313K employing the batch bottle point method.

The resin SP700 was selected to perform further batch adsorption studies with vanillic and syringic acids. Assays were performed for three different temperatures 283/288K, 298K and 313K with 0.1 L of a feed solution with concentrations ranging from 1 - 2.25 g L^{-1} and 0.5 - 0.9 g L^{-1} for vanillic acid and syringic acid, respectively. It was used amounts of resin between 0.1 to 0.5 g of dry weight. Samples were shaken in a rotary shaker (IKA®KS4000, Germany) at 190 rpm for 24 h.

Each sample was immediately filtered through a syringe filter with 0.2 μm. The initial feed concentration and equilibrium concentrations of adsorption were quantified by HPLC-UV as described in 3.2.2. pH was monitored (VWR model pH110) and no significant change was observed during the adsorption experiments (around 4.5-4.9 for vanillin, 5.7-6.2 for syringaldehyde, 3.3-3.5 for vanillic acid and 3.5-3.6 for syringic acid).

The adsorbed phase concentration of species 'i' at equilibrium ($q_{i,e}$, g $g^{-1}_{dry\ resin}$) is calculated from a mass balance between the adsorbent and liquid phases:

$$q_{i,e} = \frac{(C_{i,0} - C_{i,e})V}{W} \qquad \textbf{Equation 3.3}$$

where $C_{i,0}$ (g L^{-1}) corresponds to the initial concentration of species 'i' in the solution; $C_{i,e}$ (g L^{-1}) is the equilibrium concentration of species 'i' in the solution; V (L) is the solution volume; and W ($g_{dry\ resin}$) is the weight of dry resin.

Binary batch experiments with vanillin and syringaldehyde were conducted as well, with 0.04 L of 2.12 g L^{-1} of vanillin and 2.62 g L^{-1} of syringaldehyde at 298 K, employing different resin amounts between 0.1 and 0.3 g of dry resin. The pH was monitored and it remained constant around 4.5.

3.2.6. Fixed bed adsorption studies

Fixed bed adsorption studies onto SP700 were carried out in a jacketed glass column (Götec, Germany) of 5.6 cm length and 1 cm internal diameter. Bed porosity (ε_b) of 0.35 and Peclet number (*Pe*) of 98 were estimated by tracer experiments using blue dextran as described elsewhere (34). One bed volume (BV) corresponds to the bed void volume of approximately 1.54 mL. Aqueous vanillin or syringaldehyde solutions were pumped into the column with a Smartline Pump 1000 (Knauer, Germany) and isothermal conditions were assured with a thermostatic water bath (Lauda). Mono-component experiments were performed for different temperatures (298 and 313 K) and feed concentrations (0.4, 1 and 4 g L^{-1}) at fixed flowrate (approximately 5 mL min^{-1}). For the mono-component adsorption studies with the phenolic acids, similar experiments were performed for temperatures 288 K, 298 K and 313 K, feed concentrations ranging from 0.16 to 1.40 g L^{-1} at fixed flowrate of approximately 5.25 mL min^{-1}. Binary experiments were performed at 298 K and fixed flowrate of approximately 5 mL min^{-1}.

The column was fed with the solution at fixed or constant temperature and samples were collected at the column outlet, diluted and quantified by HPLC-UV as described in 3.2.2.

The experimental ($t_{st,exp}$, min) and predicted ($t_{st,pred}$, min) stoichiometric times were obtained by Equation 3.4 and Equation 3.5, respectively (35, 36), for constant feed flowrate:

$$t_{st,\exp} = \int_0^{\infty} \left(1 - \frac{C_i}{C_{i,\,feed}}\right) dt \qquad \textbf{Equation 3.4}$$

$$t_{st,\,pred} = \frac{L_b}{u_i}\left[1 + \left(\frac{1-\varepsilon_b}{\varepsilon_b}\right)\left(\frac{q_{i,\,feed}\,\rho_{app}\,f_h}{C_{i,\,feed}}\right)\right] \qquad \textbf{Equation 3.5}$$

where $C_{i,feed}$ (g L^{-1}) is the concentration at column inlet for the species 'i', C_i (g L^{-1}) is the concentration at column outlet for the species 'i' and time t (min), $q_{i,feed}$ (g $g^{-1}_{dry\ resin}$) is the adsorbed phase concentration for the species 'i' in equilibrium with $C_{i,feed}$, f_h ($g_{dry\ resin}$ $g^{-1}_{wet\ resin}$) is the dry particle to wet particle mass ratio, L_b (m) is the bed length and u_i (m min^{-1}) is the interstitial velocity and was calculated as following (37):

$$u_i = \frac{Q}{A\varepsilon_b} \qquad \textbf{Equation 3.6}$$

where Q (m^3 min^{-1}) is the feed flowrate and A (m^2) is the cross sectional area of the bed.

For the determination of $t_{st,exp}$, it was calculated the area under the plot $1\text{-}C_i/C_{i,feed}$ versus time employing the trapezoidal rule.

The experimental adsorbed ($q_{ads,exp}$, g $g^{-1}_{dry\ resin}$) and desorbed ($q_{des,exp}$, g $g^{-1}_{dry\ resin}$) phase concentrations were assessed from global mass balances to the adsorption and desorption steps, Equation 3.7 and Equation 3.8, respectively (38):

$$q_{ads,\exp} = \frac{QC_{i,feed}t_{st,\exp}}{V_b\left(1-\varepsilon_b\right)\rho_{app}f_h} - \frac{\varepsilon_b C_{i,feed}}{\left(1-\varepsilon_b\right)\rho_{app}f_h} \qquad \textbf{Equation 3.7}$$

$$q_{des,\exp} = \frac{\int_0^t QC_i dt}{V_b\left(1-\varepsilon_b\right)\rho_{app}f_h} - \frac{\varepsilon_b C_{i,feed}}{\left(1-\varepsilon_b\right)\rho_{app}f_h} \qquad \textbf{Equation 3.8}$$

where V_b (m^3) is the volume of the bed.

It was calculated the ratio between $q_{des,exp}$ and $q_{ads,exp}$ corresponding to the removal percentage in each adsorption/desorption cycle performed.

After each run, the column was regenerated by eluting about 45 BV with 0.1 M $NaHCO_3$ solution and rinsing with deionized water until pH 5.5 – 6 (about 1100 BV), thus, assuring the removal of any residual phenolic compound.

3.3. Mathematical modelling

3.3.1. Adsorption equilibrium isotherms

Langmuir, Bi-Langmuir and Freundlich models were studied to describe the adsorption equilibrium isotherm data obtained for each phenolic compound in aqueous solution onto SP700 and XAD16N resins.

The Langmuir isotherm (39) defines monolayer adsorption onto homogeneous surface containing a finite number of adsorption sites of uniform energy with no interaction occurring among the adjacent adsorbed molecules. The adsorption is considered reversible and the maximum adsorption corresponds to the saturation of the monolayer of molecules adsorbed on the adsorbent surface. Graphically it is observed a plateau which corresponds to an equilibrium saturation point where no further adsorption takes place once the sites are occupied with the adsorbates. It can be described by the following Equation 3.9, considering liquid-solid adsorption:

$$q_{i,e} = \frac{q_{m,i} K_{L,i} C_{i,e}}{1 + K_{L,i} C_{i,e}}$$ **Equation 3.9**

where $q_{m,i}$ (g $g^{-1}_{dry\ resin}$) is the maximum adsorption capacity for component 'i' and $K_{L,i}$ (L g^{-1}) is the Langmuir equilibrium constant for component 'i'.

The Bi-Langmuir isotherm was first suggested by Graham (40) and considers the adsorption onto a surface composed by patches of two different homogeneous surfaces that behave independently. On each type of site, the same Langmuir principles of local adsorption and no adsorbate - adsorbate interactions are applied. It can be described by the following Equation 3.10, considering liquid-solid adsorption (41) and two independent local Langmuir isotherms:

$$q_{i,e} = \frac{q_{m1,i} K_{L1,i} C_{i,e}}{1 + K_{L1,i} C_{i,e}} + \frac{q_{m2,i} K_{L2,i} C_{i,e}}{1 + K_{L2,i} C_{i,e}}$$ **Equation 3.10**

where $q_{m1,i}$ and $q_{m2,i}$ (g $g^{-1}_{dry\ resin}$) are the two maximum adsorption capacities for component 'i' obtained for the two types of adsorption sites and $K_{L1,i}$ and $K_{L2,i}$ (L g^{-1}) are the respective Langmuir equilibrium constants for component 'i'.

The parameters related with the energy of adsorption in Langmuir (K_L) and Bi-Langmuir models (K_{L1} and K_{L2}) were estimated considering the Van't Hoff equation:

$$K_x = K_x^o \exp\left(-\frac{\Delta H_x}{RT}\right)$$ **Equation 3.11**

where K_x (L g^{-1}) corresponds to the energy of adsorption parameters of Langmuir (K_L) and Bi-Langmuir isotherm (K_{L1} and K_{L2}) models and K_x^o (L g^{-1}) is the respective equilibrium constant (K_L^o, K_{L1}^o and K_{L2}^o), ΔH_x (kJ mol^{-1}) is the respective adsorption enthalpy (ΔH_L, ΔH_{L1} and ΔH_{L2}), *R* is the ideal gas constant (kJ mol^{-1} K^{-1}) and T is the absolute temperature (K). The values obtained for these parameters are summarized in Appendix A.

The extended Bi-Langmuir model developed by Butler and Ockrent (42) for Langmuir isotherm was applied:

$$q_{i,e} = \frac{q_{m1,i} K_{L1,i} C_{i,e}}{1 + \sum_{j=1}^{NC} K_{L1,j} C_{j,e}} + \frac{q_{m2,i} K_{L2,i} C_{i,e}}{1 + \sum_{j=1}^{NC} K_{L2,j} C_{j,e}} \qquad \textbf{Equation 3.12}$$

It was considered $q_{m1,i}$, $q_{m2,i}$, $K_{L1,i}/K_{L1,j}$ and $K_{L2,i}/K_{L2,j}$ values obtained from the fit of the Bi-Langmuir model to the adsorption equilibrium data of the pure component studies. This model takes into consideration the same assumptions mentioned above for the Bi-Langmuir isotherm and that all adsorptive sites are equivalent and each site holds only one molecule.

The Freundlich isotherm (43) is an empirical equation that describes the adsorption process on heterogeneous surfaces. This model assumes the existence of different adsorption energies grouped into patches of the same magnitude, which are independent and do not interact with each other (44). The formation of multilayers of adsorbed molecules in the Freundlich model can be expressed by the following equation:

$$q_{i,e} = K_{F,i} C_{i,e}^{1/n} \qquad \textbf{Equation 3.13}$$

where $K_{F,i}$ ((g $g^{-1}_{\text{dry resin}}$) (L g^{-1})$^{1/n}$) is the constant indicative of the relative capacity of the adsorbent for species 'i' and n is the correspondent Freundlich exponent (dimensionless). When n is higher than 1 it indicates a favourable adsorption. K_F and n are empirical constants that indicate the curvature and steepness of the isotherm.

Freundlich model is commonly used to explain the adsorption of organic compounds from aqueous streams onto activated carbon (44).

The isotherm parameters were determined by least-squares fitting of the data through minimizing the sum of the squared residuals (SSR) between the experimental data points and the estimated values obtained by the model.

The isosteric enthalpy of adsorption, $\Delta H_{isosteric}$ (kJ mol^{-1}), for vanillin, syringaldehyde, vanillic acid and syringic acid from aqueous solutions was calculated by means of the equilibrium data obtained at different temperatures with the *Clausius-Clapeyron* equation (41, 45):

$$\frac{\Delta H_{isosteric}}{RT^2} = \left[\frac{\partial(\ln C_{i,e})}{\partial(T)} \right]_{q_{i,e}} \qquad \textbf{Equation 3.14}$$

where R (kJ mol^{-1} K^{-1}) is the ideal gas constant, T (K) is the absolute temperature.

This equation is derived from the *Gibbs-Helmholtz* equation at temperature *T* considering that: 1) at equilibrium, the chemical potentials of the solute in the bulk liquid and adsorbent phases are equal; 2) the activity of the solute on the adsorbent phase remains constant with temperature change if the amount adsorbed is kept constant and 3) the solution exhibits an ideal behaviour and thus, the activity of the solute is equal to the concentration of solute in the bulk liquid phase, valid for dilute solute concentration in the mobile phase (45).

Considering that $\Delta H_{isosteric}$ is independent of the temperature, it corresponds to the slope of the plot of the isostere $ln\ C_{i,e}$ vs $1/T$ for different loading amounts ($q_{i,e}$).

3.3.2. Fixed bed modelling

The mathematical model used to predict the breakthrough curves of each phenolic compound includes a mass balance considering the following assumptions: axially dispersed plug flow, intraparticle mass transfer resistance expressed with the linear driving force model (46), no temperature gradients, constant porosity along the bed and no radial gradients within the bed.

The mathematical model encompasses a set of algebraic and differential equations that includes the mass balance for the liquid phase, the equilibrium isotherm between the fluid and the solid phases, the Danckwerts boundary conditions and the mass transfer between the liquid and solid phases.

The mass balance equation of species '*i*' in the liquid phase in a bed volume element is expressed by the following equation, valid for dilute solutions:

$$D_{ax}\frac{\partial^2 C_i(z,t)}{\partial z^2}-u_i\frac{\partial C_i(z,t)}{\partial z}-\frac{\partial C_i(z,t)}{\partial t}-\left(\frac{1-\varepsilon_b}{\varepsilon_b}\right)f_h\ \rho_{app}\frac{\partial q_i(z,t)}{\partial t}=0 \qquad \textbf{Equation 3.15}$$

where D_{ax} ($m^2\ min^{-1}$) is the axial dispersion coefficient, C_i ($g\ L^{-1}$) is the concentration in the bulk fluid phase for the species *i*, u_i is the interstitial velocity ($m\ min^{-1}$), q_i ($g\ g^{-1}_{dry\ resin}$) is the average adsorbed phase concentration of species '*i*' in the adsorbent particles, *z* (m) and *t* (min) are the axial position and time variables, respectively, and '*i*' concerns the solute studied (e.g. vanillin, syringaldehyde, vanillic acid and syringic acid).

The Danckwerts boundary conditions were applied to define the boundary conditions of the mass balance equation:

$$z = 0 \rightarrow D_{ax}\left.\frac{\partial C_i(z,t)}{\partial z}\right|_{z=0} = u_i\left[C_i(0,t) - C_{i,feed}\right] \quad \textbf{Equation 3.16}$$

$$z = L \rightarrow \left.\frac{\partial C_i(z,t)}{\partial z}\right|_{z=L} = 0 \quad \textbf{Equation 3.17}$$

The following initial conditions, of a clean / fully regenerated bed, were considered:

$$C_i(z,0) = 0 \quad \textbf{Equation 3.18}$$

$$q_i(z,0) = 0 \quad \textbf{Equation 3.19}$$

The LDF model was applied to estimate the contribution of mass transfer resistances. This expression is obtained considering a parabolic concentration profile within a spherical particle and it indicates that the rate of adsorption is proportional to the driving force (difference between adsorbed phase concentration in equilibrium with the bulk fluid concentration and the average adsorbed phase concentration in the particle) still required to reach equilibrium:

$$\frac{\partial q_i(z,t)}{\partial t} = k_{LDF}\left[q_i^*(z,t) - q_i(z,t)\right] \quad \textbf{Equation 3.20}$$

where, q_i^* (g $g^{-1}_{dry\ resin}$) is the adsorbed phase concentration in equilibrium with the bulk concentration at a certain time and position and k_{LDF} (min^{-1}) is the LDF kinetic rate constant.

k_{LDF} was estimated by Equation 3.21 and considers homogeneous particle (47):

$$k_{LDF} = \frac{\Omega D_{pe,i}}{f_h \rho_{app} r_p^2 \frac{dq_i^*}{dC_i}} \quad \textbf{Equation 3.21}$$

where r_p (m) is the radius of the adsorbent particle, $D_{pe,i}$ (m^2 min^{-1}) is the effective pore diffusivity, Ω (dimensionless) is the LDF factor equal to 15 considering spherical particles, $\frac{dq_i^*}{dC_i}$ is the slope of the adsorption equilibrium isotherm and q_i^* (g $g^{-1}_{dry\ resin}$) is the adsorbed phase concentration in equilibrium with the bulk concentration at time *t* in the position *z*. In the same way as Žabková *et al.* (19), mass transfer coefficients were calculated using the slope of the chord ($\Delta q/\Delta C$).

The axial dispersion in the packed bed was estimated by the following expression, using the experimental *Peclet* number obtained (37):

$$Pe = \frac{u_i L_b}{D_{ax}}$$ **Equation 3.22**

The effective pore diffusivity $D_{pe,i}$ (m^2 min^{-1}) was calculated by the following expression (48):

$$D_{pe,i} = \frac{\varepsilon_p D_{m,i}}{\tau}$$ **Equation 3.23**

where $D_{m,i}$ (m^2 min^{-1}) is the molecular diffusivity of solute '*i*' in the solvent and τ is the tortuosity factor (estimated by the Wakao and Smith model (49), corresponding to the inverse of the particle porosity).

$D_{m,i}$ was estimated for each solute by the Wilke-Chang correlation (48, 50):

$$D_{m,i} = 4.44 \times 10^{-10} \frac{T\sqrt{\phi M}}{\mu V_{m,i}^{0.6}}$$ **Equation 3.24**

where ϕ is the association factor of the solvent, which accounts for solute-solvent interactions (Wilke and Chang [50] suggest an association factor of 2.6 when the solvent used is water), *M* (g mol^{-1}) is the molecular weight of the solvent, μ (cP) is the viscosity of the solvent, $V_{m,i}$ (cm^3 mol^{-1}) is the molar volume of solute at its normal boiling point estimated by the simple additive method proposed by Partington (51).

The model equations 3-15 to 3-24 were solved numerically with gPROMS (General Process Modelling System, version 3.7.1) using one of its integrated solvers, DASOLV, and discretizing the axial domain using orthogonal colocation method on finite elements over 20 elements with third order polynomials in each element. The solvers used in the simulations consider an absolute tolerance of $1x10^{-5}$. The mathematical model contains a system of partial differential and algebraic equations (PDAEs).

3.4. Results and discussion

3.4.1. Physical and chemical characterization of the resins

SP700 (batch number 2A507) and XAD16N (batch number SLBC8020V) were characterized as described in 3.2.4. In general, the values found in this work for the physical and chemical properties were similar to those reported in literature or given by the supplier, as summarized in Table 3.1.

Table 3.1 Physical-chemical properties of the styrene-divinylbenzene resins SP700 and XAD16N given by the supplier, experimentally obtained and found in literature

	Suppliers information		**This work**		**Reported in literature**	
	SP700	**XAD16N**	**SP700**	**XAD16N**	**SP700**	**XAD16N**
ρ_s ($g_{dry\ resin}\ L^{-1}_{dry\ resin}$)	-	-	1294	1096	-	-
ρ_{app} ($g_{wet\ resin}\ L^{-1}_{wet\ resin}$)	1010	1020	1012	988.5	-	-
Moisture content (%)	60-70	-	68.2	67.0	-	-
V_{pores} (mL g^{-1})	2.3	1.82	2.07	1.74	2.05[52]	-
ε_p	0.81	0.73	0.73	0.66	-	-
d_p (μm)	Average 450	Range 560-710	483	727	-	635[53] 750[54]
a_s ($m^2\ g^{-1}$)	1200	800	-	-	1160[52]	-
r_{pore} (Å)	90	100	-	-	35[52]	-

Moisture determination was repeated 6 times and the average value obtained for SP700 and XAD16N resins was 68.2% (± 0.5%) and 67.0% (± 0.7%), respectively. A volume ratio of dry to wet resin of 0.92 $mL_{dry}\ mL^{-1}_{wet}$ was obtained for SP700 and of 0.86 $mL_{dry}\ mL^{-1}_{wet}$ for XAD16N.

The study of particle size distribution showed the existence of particle diameters ranging from 250 μm to 850 μm for SP700 resin with an experimentally mean size of 483 μm, very close to the value of 450 μm given by supplier (Table 3.1). As for XAD16N, the particle size distribution analysis showed a wider range of particle diameters between 350 μm and 1400 μm, an interval

higher than the one reported by the supplier (Table 3.1). The mean size obtained by the laser dispersion analysis for the latter resin of 727 μm, was not in the interval of diameters given by supplier but very close to the value found in the study by Díez *et al.* (54).

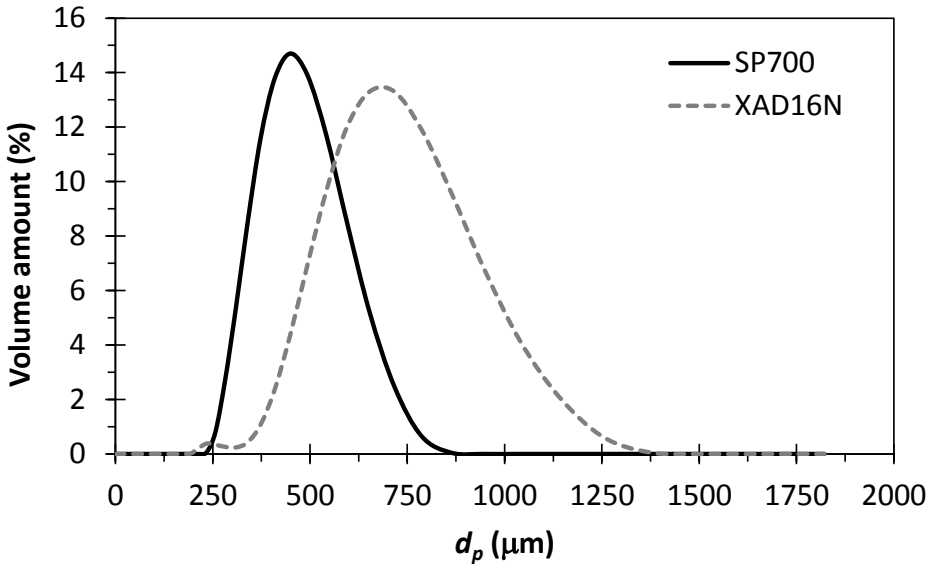

Figure 3.1 Particle size distribution of resins SP700 and XAD16N.

Helium volume was measured in triplicate and the solid (or skeletal) density obtained was 1294 (±1) $g_{dry\ resin}\ L^{-1}{}_{dry\ resin}$ and 1096 (±1) $g_{dry\ resin}\ L^{-1}{}_{dry\ resin}$ for SP700 and XAD16N, respectively.

In the mercury intrusion porosimetry analysis, the apparent density is obtained by the difference between the volume of mercury needed to fill a penetrometer before and after placing a known amount of sample. At atmospheric pressure, the mercury will resist entering in the pores with a diameter lower than 6 μm (55). Since the pressure used in this step is slightly higher (2.5 atm / 36.7 psi), some macropores might have been intruded by the mercury and thus, the apparent density may be overestimated. Nonetheless, a similar value of apparent density to the one given by the supplier was obtained for both resins (Table 3.1).

The mercury intrusion porosimetry also evaluates the diameter pore size distribution of macropores and mesopores (covering pore diameters in the range of 3.6 nm and 10.6 μm) and particle porosity.

Figure 3.2 depicts the pore diameter in function of the cumulative volume expressed in percentage and the respective differential curve of pore volume. About 69.5% and 69% of all the intruded volume for, respectively, SP700 and XAD16N, corresponded to macropores, considering that all diameters above 0.05 μm are macropores (35) and the remaining volume of 30.5% and 31% corresponded to mesopores (assuming that mesopores diameters are between 0.05 μm and 0.002 μm) (35). This led to conclude that macropores are predominant in both resins.

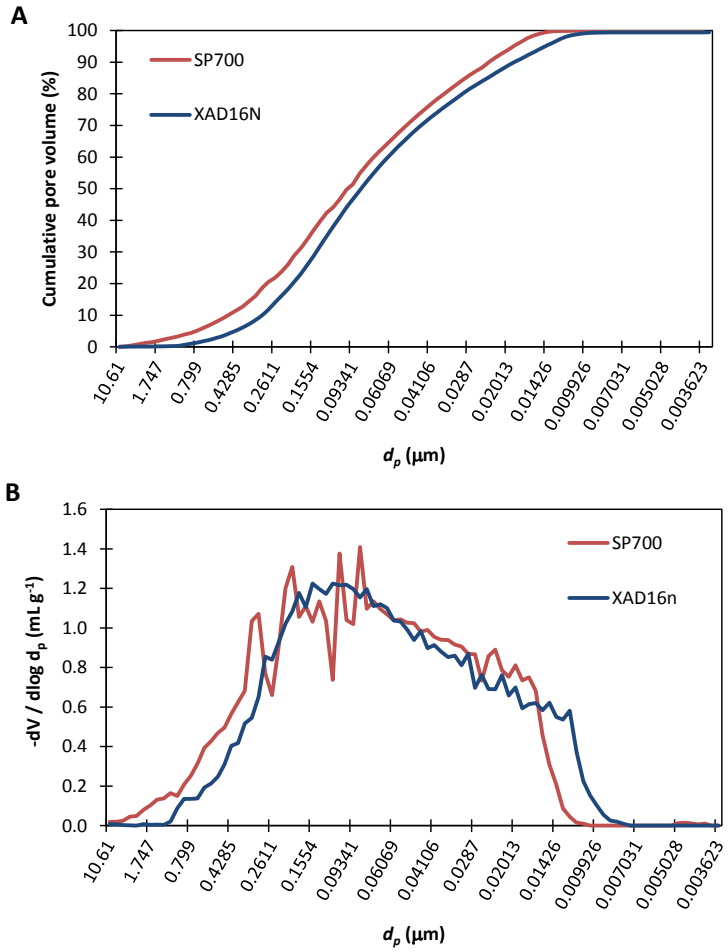

Figure 3.2 Cumulative mercury intruded volume (A) and differentical curve of pore volume (B) for SP700 and XAD16N.

Additionally, it is important to refer that the resin particles might contain pores smaller than 3.6 nm and thus some mesopores and micropores were not quantified by the mercury porosimetry analysis. This last assumption is supported by Li *et al.* (52) which stated that SP700 resin has a low proportion of micropores (<2 nm). The volume of pores found in this work (2.07 and 1.74 mL $g^{-1}_{dry\ resin}$ for SP700 and XAD16N, respectively) was slightly lower than the one estimated through Equation 3.2 using the values reported by the supplier (Table 3.1). The corresponding particle porosities obtained were of 0.73 and 0.66 $L_{pores}\ g^{-1}_{dry\ resin}$ for SP700 and XAD16N, respectively (Table 3.1).

Specific surface area given by the supplier of SP700 resin is consistent with that obtained by Li *et al.* (52) (Multipoint BET method). However, the authors reported a predominant average pore radius of 35 Å, more than one-half lower than the value given by supplier (Table 3.1).

3.4.2. Adsorption equilibrium isotherms of vanillin, syringaldehyde, vanillic acid and syringic acid in water

Adsorption equilibrium isotherms for adsorption of vanillin and syringaldehyde from aqueous solutions onto SP700 resin and XAD16N were measured and fitted to Langmuir, Bi-Langmuir and Freundlich models. Figure 3.3 and Figure 3.4 display the experimental adsorbed amounts as a function of liquid phase concentration at equilibrium for the different temperatures and the respective fitting to the models. The characteristic parameters of each model are summarized in Table 3.2. All models reasonable fit the experimental data obtained for each resin. Bi-Langmuir and Freundlich models describe the batch experiments better, in particular for equilibrium concentrations below 1 g L^{-1}. Several works performed with the adsorption of other phenolic compounds onto nonpolar resins have also shown that the Freundlich model adequately describes the adsorption process (20, 26, 56-58). Bi-Langmuir has also been applied to describe adsorption of phenol (59) and other organic compounds (60, 61).

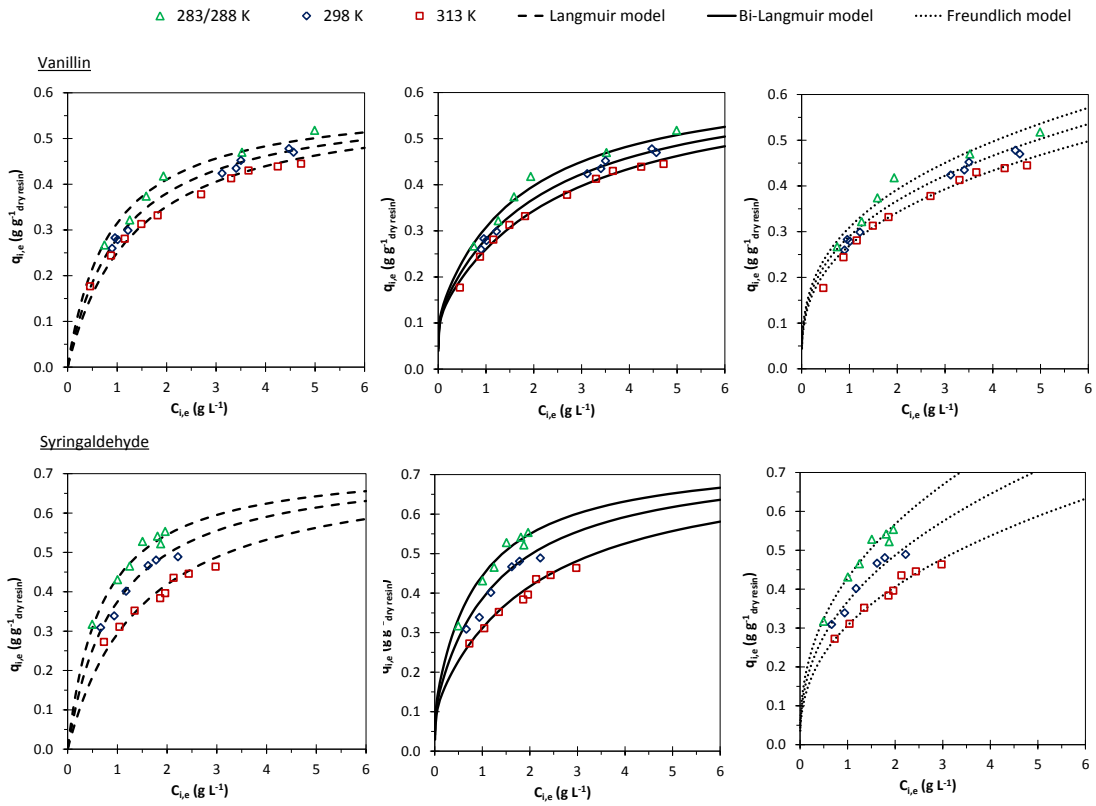

Figure 3.3 Adsorption equilibrium isotherms of vanillin and syringaldehyde in water onto the resin XAD16N at different temperatures. The dots represent experimental data, the dashed lines (- -) the Langmuir model plots, the lines (—) the Bi-Langmuir model plots and the dots (…) the Freundlich model plots.

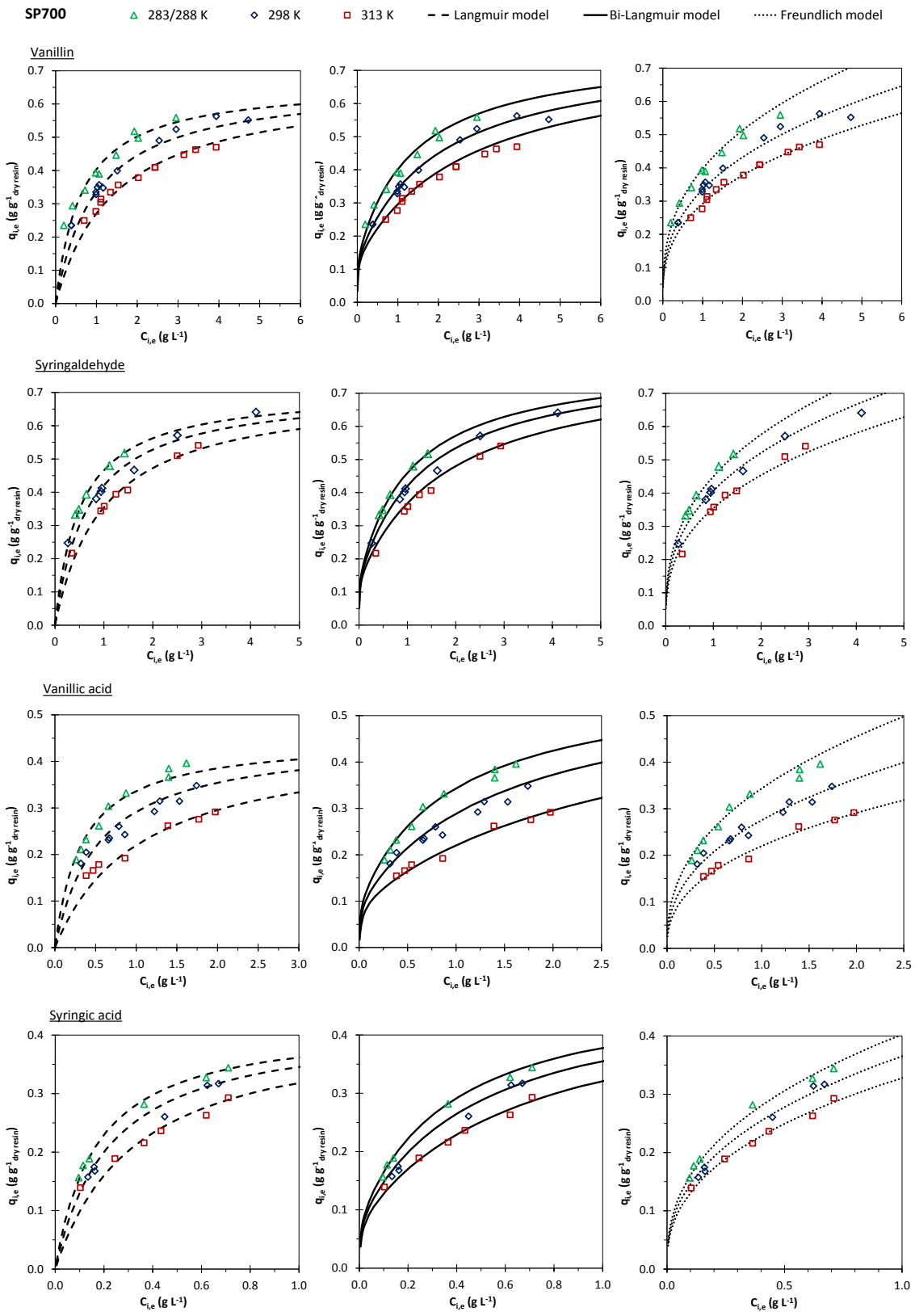

Figure 3.4 Adsorption equilibrium isotherms of vanillin, syringaldehyde, vanillic acid and syringic acid in water onto the resin SP700 at different temperatures. The dots represent experimental data, the dashed lines (- -) the Langmuir model plots, the lines (—) the Bi-Langmuir model plots and the dots (…) the Freundlich model plots.

Table 3.2 Equilibrium parameters obtained for adsorption of vanillin (V), syringaldehyde (S), vanillic acid (VA) and syringic acid (SA) onto XAD16N and SP700 resin

	V		S		SA	VA
	SP700	**XAD16N**	**SP700**	**XAD16N**	**SP700**	**SP700**
$\Delta H_{isosteric}$ (kJ mol^{-1})	-19 ± 1	-15 ± 2	-23 ± 3	-27 ± 5	-16 ± 1	-37 ± 3
Langmuir model						
$q_{m,i}$ (g g$^{-1}_{\text{dry resin}}$)	0.663	0.587	0.707	0.730	0.423	0.450
K_L^o (L g^{-1})	3.21x10^{-4}	1.12x10^{-2}	5.26x10^{-4}	8.00x10^{-5}	1.38x10^{-3}	2.05x10^{-6}
ΔH_L (kJ mol^{-1})	-20.0	-10.9	-19.7	-23.5	-20.0	-34.0
$\sum_{i=1}^{n}(q_{\exp}-q_{calc})^2$ (g g$^{-1}_{\text{dry resin}}$)^2	1.87x10^{-2}	0.32x10^{-2}	0.70x10^{-2}	0.51 x10^{-2}	0.25x10^{-2}	0.67x10^{-2}
Bi-Langmuir model						
$q_{m1,i}$ (g g$^{-1}_{\text{dry resin}}$)	0.634	0.529	0.663	0.639	0.407	0.486
$q_{m2,i}$ (g g$^{-1}_{\text{dry resin}}$)	0.131	0.116	0.139	0.113	0.0826	0.0967
K_{L1}^o (L g^{-1})	3.15x10^{-4}	8.03x10^{-3}	7.19x10^{-4}	2.17x10^{-5}	1.03x10^{-3}	1.33x10^{-6}
K_{L2}^o (L g^{-1})	5.57x10^{-2}	1.45	1.45x10^{-1}	4.85x10^{-3}	9.71x10^{-2}	1.67x10^{-4}
ΔH_{L1} (kJ mol^{-1})	-18.3	-10.0	-17.2	-25.9	-18.8	-32.5
ΔH_{L2} (kJ mol^{-1})	-18.4	-11.0	-17.3	-24.8	-19.0	-32.2
$\sum_{i=1}^{n}(q_{\exp}-q_{calc})^2$ (g g$^{-1}_{\text{dry resin}}$)^2	0.42x10^{-2}	0.20x10^{-2}	0.31x10^{-2}	0.37x10^{-2}	0.079x10^{-2}	0.30x10^{-2}
Freundlich model						
n	2.7	2.9	2.8	2.5	2.5	2.5
$K_{F,i}$ g g$^{-1}_{\text{dry resin}}$ (L g^{-1})$^{1/n}$ T1	0.3977	0.3095	0.4505	0.4292	0.4027	0.3440
$K_{F,i}$ g g$^{-1}_{\text{dry resin}}$ (L g^{-1})$^{1/n}$ T2	0.3350	0.2902	0.4076	0.3687	0.3657	0.2757
$K_{F,i}$ g g$^{-1}_{\text{dry resin}}$ (L g^{-1})$^{1/n}$ T3	0.2927	0.2699	0.3551	0.3072	0.3281	0.2200
$\sum_{i=1}^{n}(q_{\exp}-q_{calc})^2$ (g g$^{-1}_{\text{dry resin}}$)^2	0.64x10^{-2}	0.42x10^{-2}	0.34x10^{-2}	0.38x10^{-2}	0.081x10^{-2}	0.33x10^{-2}

T1: 283 K for V and 288 K for S, VA and SA; T2: 298 K; T3: 313 K

Both resins adsorb syringaldehyde in a higher extent. For instance, considering an equilibrium concentration of 1 g L^{-1} of vanillin and syringaldehyde, the respective equilibrium adsorption capacities are approximately 0.342 and 0.420 g $g^{-1}_{dry\ resin}$ (SP700) and 0.282 and 0.387 g $g^{-1}_{dry\ resin}$ (XAD16N). The maximum adsorption capacity, $q_{m,i}$, obtained with the Langmuir model for syringaldehyde is also higher than the one obtained for vanillin (about 7% for SP700 and 24% for XAD16N). Similarly, the maximum adsorption capacity, $q_{m1,i}$ obtained in the Bi-Langmuir model is also higher for syringaldehyde, in both resins (about 5% for SP700 and 21% for XAD16N). Being syringaldehyde the compound less soluble in water, these results are consistent with other studies (56, 58, 62) where it has been shown a lower adsorption for compounds showing higher solubility.

The resin SP700 was chosen to pursue with adsorption equilibrium studies with vanillic and syringic acids. The experimental adsorbed amounts at different temperatures versus the adsorbate liquid concentrations at equilibrium obtained are depicted in Figure 3.4 along with the respective Langmuir, Bi-Langmuir and Freundlich models found for each compound. In Table 3.2 it is summarized the respective characteristic parameters of each model. All three models reasonable fitted the experimental points. However, similarly to the aldehydes, the Bi-Langmuir and Freundlich models described better the experimental data, showing lower SSR.

The resin SP700 adsorbs more syringic acid than vanillic acid. This is expected since, according to the solubility experimentally determined, the syringic acid is less soluble in water than vanillic acid. Nevertheless, due to the range of equilibrium adsorption concentrations studied for each acid (related with limitations of solubility in water for each compound), the maximum adsorption capacity found for syringic acid (0.423 and 0.407g $g^{-1}_{dry\ resin}$ of $q_{m,i}$ and $q_{m1,i}$, respectively) is somewhat smaller than the one found for vanillic acid 0.450 and 0.486 g $g^{-1}_{dry\ resin}$ of $q_{m,i}$ and $q_{m1,i}$, respectively).

In Figure 3.5 it is shown the adsorption equilibrium isotherms for the four phenolics studied at 298 K. Although syringic acid is less soluble in water than its respective aldehyde, the experimental adsorbed amounts are smaller, not following the same trend observed between the aldehydes or the acids. The same behavior is noticed between vanillic acid and vanillin. This clearly demonstrates that carbonyl and carboxyl group also exerts some influence in the adsorption mechanism.

The Freundlich parameter *n* values estimated for all phenolic compounds are very similar (between 2.5 and 2.9) and indicative that the adsorption processes onto both resins are favorable. K_F is indicative of the relative capacity of the resin and decreases as following: syringaldehyde > syringic acid > vanillin > vanillic acid, following the same trend of the adsorbed amounts experimentally obtained.

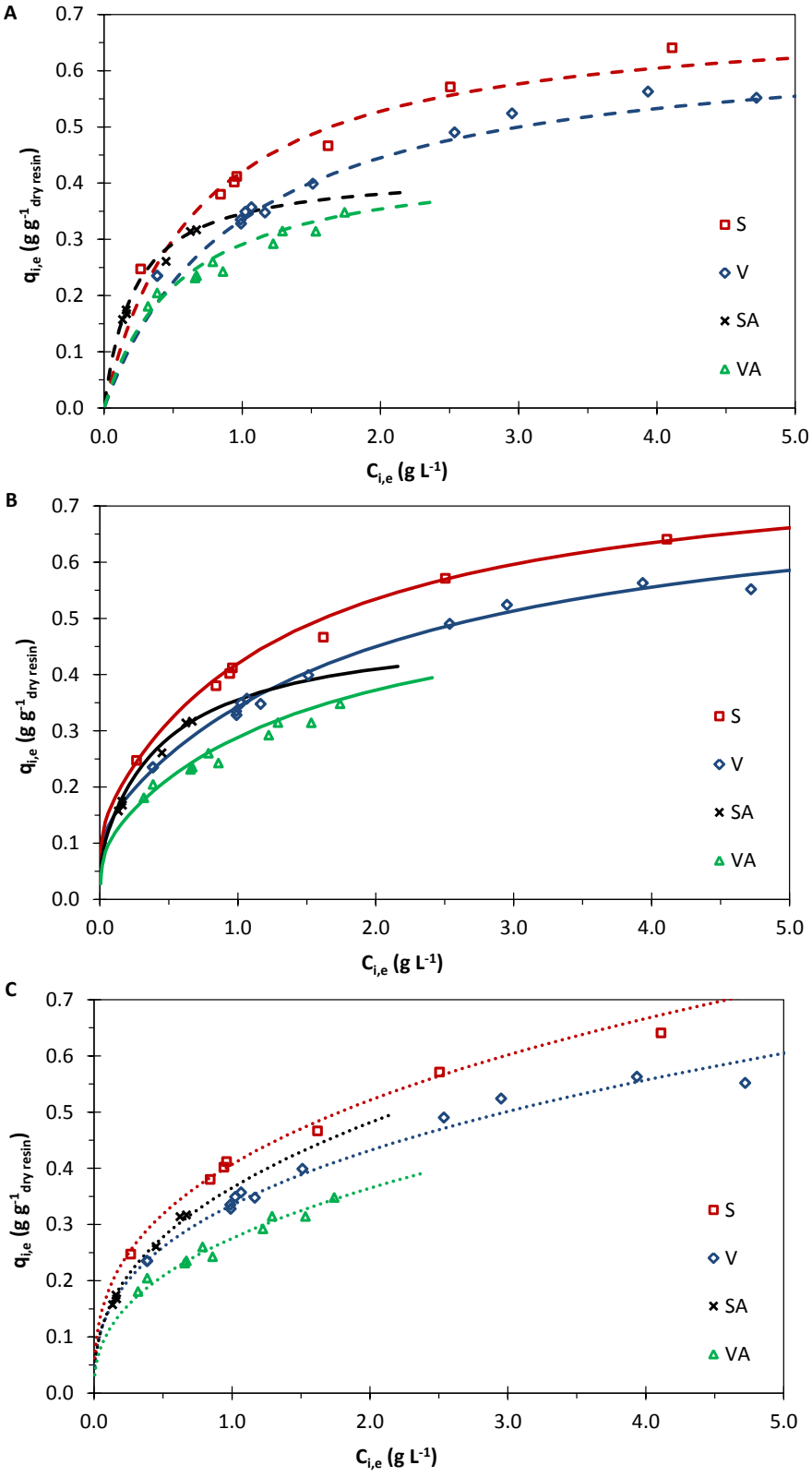

Figure 3.5 Adsorption equilibrium isotherms for V, S, VA and SA in water onto the adsorbent SP700 at 298 K. The dots represent experimental data, the dashed lines (- -) the Langmuir model plots (A), the lines (—) the Bi-Langmuir model plots (B) and the dots (…) the Freundlich model plots (C).

$K_{L,}$ K_{L1}, K_{L2} and K_F decreased with the rise of temperature (Appendix A), which is typical for exothermic processes. It was observed that the equilibrium adsorption capacity for each compound studied decreased with the increase of temperature, which denotes an exothermic process, also corroborated by the estimated value of isosteric enthalpy variation (Table 3.2). Published studies employing similar nonpolar resins to recover vanillin from aqueous solutions have also reported the same effect with temperature (19, 20).

The isosteric enthalpy of adsorption was estimated by the derived Clausius-Clapeyron relation using the experimental equilibrium data obtained. A similar order of magnitude was obtained for vanillin (-19 kJ mol^{-1}) and syringaldehyde (-23 kJ mol^{-1}) adsorption onto SP700 (Table 3.2). Some differences were found for the phenolic acids, the adsorption process for vanillic acid is more exothermic (-37 kJ mol^{-1}) than for syringic acid (-16 kJ mol^{-1}) and the aldehydes. In the case of XAD16N, the isosteric adsorption enthalpy found for syringaldehyde (-27 kJ mol^{-1}) was almost twice the value found for vanillin (-15 kJ mol^{-1}). The adsorption enthalpies estimated by the Van't Hoff equation in the determination of the parameters of Langmuir and Bi-Langmuir isotherms were very similar to the isosteric enthalpy of adsorption estimated with the experimental equilibrium data.

The values of isosteric adsorption enthalpy between -15 and -37 kJ mol^{-1} obtained (Table 3.2), indicate mainly physical adsorption onto SP700 and XAD16N resins for all studied phenolic compounds thus, the type of bonds involved in the adsorption phenomena are weak and the adsorption process can be reversed and resin easily regenerated (63). These results are also in accordance with several studies performed with phenolics adsorption onto nonpolar resins, where it is commonly stated that van der Waals interaction is the main driving force for adsorption of the molecules from the bulk solution to the adsorbent phase (26, 27, 58).

To our knowledge, there are no studies with aqueous solutions of syringaldehyde using this type of resins. Studies performed with vanillin, syringic acid and vanillic acid comprise the use of activated carbon (14-16) and synthetic cross-linked polymeric adsorbents of hydrophobic nature (19-23). It is important to note that published studies were performed with different methodologies and experimental conditions thus, special attention must be given when comparing final results.

In this work, the maximum adsorption capacities onto SP700 and XAD16N found for vanillin are higher than the ones reported in literature employing other nonpolar resins (ranging from 0.073 to 0.416 g g^{-1}). Among all, Zhang *et al.* (20) and Jin and Huang (22) reported the highest adsorption capacities of 0.416 g g^{-1} and 0.358 g g^{-1} for vanillin, respectively, employing synthetic cross-linked polymeric resins. Michailof *et al.* (14) managed to obtain maximum adsorption capacities ranging from 0.191 to 0.204 g g^{-1} using activated carbon. Žabková *et al.* (19) studied the nonpolar styrene divinylbenzene resin SP206, similar to the one used in this work but with lower surface area

(556 m^2 g^{-1}), and reported a maximum adsorption capacity of 0.115 g $g^{-1}_{dry\ resin}$. Maximum adsorption capacities found for the phenolic acids studied (Table 3.2) were also higher than the values reported in literature for adsorption onto activated carbon: for syringic acid and vanillic acid the amounts adsorbed found in literature range from 0.24 – 0.32 g g^{-1} (15, 16) and 0.056 – 0.24 g g^{-1} (14), respectively.

3.4.3. Modelling of fixed bed adsorption of vanillin and syringaldehyde in water onto SP700 resin

Fixed bed assays with aqueous solutions of vanillin and syringaldehyde were performed in a column bed of 5.6 cm length and 1 cm of diameter for a flowrate of 5 mL min^{-1}. Different feed concentrations (0.38 - 4.1 g L^{-1}) and temperatures (298 and 313 K) were studied to validate the Bi-Langmuir isotherm model obtained by equilibrium batch studies. The experimental conditions and results are summarized in Table 3.3.

Similarly, in Table 3.3 it is summarized the fixed bed studies performed with aqueous solutions of vanillic and syringic acids carried out for different feed concentrations ranging from 0.16 to 1.4 g L^{-1} and temperatures (288, 298 and 313 K) to validate the respective Bi-Langmuir isotherm models found by equilibrium batch studies. The same bed used for the dynamic studies with the aldehydes was employed and the feed flowrate was set to 5.25 mL min^{-1}.

The predicted stoichiometric times calculated by the equilibrium model by means of Equation 3.5 and expected adsorbed amounts along with the correspondent experimental values obtained by the mass balance (Equation 3.4 and Equation 3.7) are indicated in Table 3.3. The Bi-Langmuir model predicted well the experimental stoichiometric times and adsorptive capacity for the dynamic experiments performed with each compound (with SD values below 6%).

The mathematical model mentioned in section 3.3 was implemented to describe the breakthrough curves obtained. The parameters of the mathematical model, axial dispersion, molecular diffusivity and effective pore diffusivity are indicated in Table 3.4. For each experiment carried out, the k_{LDF} estimated as described in 3.3.2 are specified in Table 3.3 .

As concentration increases, the slope $\Delta q/\Delta C$ decreases resulting in higher k_{LDF} and thus, lower mass transfer resistances. Considering the experiments performed for vanillin at 298 K it is possible to observe that k_{LDF} increases linearly with the increase in concentration with a correlation coefficient R^2 of 0.9954 (Figure 3.6).

Moreover, for the 4 compounds, k_{LDF} increases with the increase in temperature (Figure 3.7). This means that the mass resistance decreases with the increase in concentration and temperature, as expected. For feed concentration of approximately 0.7 g L^{-1} at 298 K, k_{LDF} estimated for vanillic acid (0.105 min^{-1}) was almost twice the value obtained for syringic acid (0.068 min^{-1}), thus the estimated mass transfer resistance is somewhat higher for the latter compound. In general, mass transfer resistance estimated for the phenolic acids is lower than for the phenolic aldehydes, being vanillic acid the compound offering the lowest mass transfer resistance in the adsorption process.

Table 3.3 Mass transfer coefficients, predicted and experimental stoichiometric times, and adsorbed amounts of V and S for each $C_{i,feed}$ and *T*, for a column of 5.6 x 1 cm with 0.35 porosity and feed flowrate of 5 and 5.25 mL min^{-1} for the aldehydes and acids, respectively.

	$C_{i,feed}$ (g L^{-1})	*T* (K)	k_{LDF} (min^{-1})	$t_{st,pred}$ (min)	$t_{st,exp}$ (min)	*SD** (%)	$q_{ads,pred}$ (g $g^{-1}_{dry\ resin}$)	$q_{ads,exp}$ (g $g^{-1}_{dry\ resin}$)
V	0.385	298	0.035	111.2	113.5	2.1	0.231	0.235
	0.383	298	0.035	111.6	114.7	2.8	0.230	0.238
	1.02	298	0.062	63.0	63.2	0.3	0.345	0.344
	1.07	298	0.062	61.3	59.4	3.1	0.352	0.343
	3.94	298	0.149	26.3	26.4	0.4	0.553	0.554
	1.11	313	0.107	51.8	52.9	2.1	0.309	0.314
S	0.96	298	0.044	80.0	79.8	0.2	0.414	0.412
	4.11	298	0.122	29.0	29.2	0.7	0.638	0.641
	0.98	313	0.073	69.2	70.4	1.7	0.365	0.356
VA	1.40	288	0.105	48.7	47.4	2.7	0.385	0.384
	0.67	298	0.105	64.5	62.2	3.6	0.244	0.235
	1.24	298	0.151	45.1	42.4	5.9	0.315	0.296
	1.39	313	0.300	32.6	33.5	2.9	0.254	0.262
SA	0.71	288	0.054	86.8	85.7	1.3	0.348	0.344
	0.67	298	0.068	82.1	82.0	0.1	0.320	0.320
	0.16	298	0.029	196.4	194.7	0.9	0.181	0.183
	0.71	313	0.123	71.4	72.1	1.0	0.286	0.287

*SD (%) corresponds to the standard deviation between the experimental and predicted stoichiometric time, calculated with the following expression: $SD(\%) = \frac{\left|t_{st,pred} - t_{st,\exp}\right|}{t_{st,pred}} \times 100$;

Table 3.4 Summary of parameters used for simulation of V, S, VA and SA breakthroughs, for a column 5.6 x 1 cm with porosity 0.35 and feed flowrate of 5 and 5.25 mL min^{-1} for the aldehydes and acids, respectively.

Compound	T (K)	D_{ax} (m^2 min^{-1})	$D_{m,i}$ (m^2 min^{-1})	$D_{pe,i}$ (m^2 min^{-1})
V	298	$1.04x10^{-4}$	$4.95x10^{-8}$	$2.62x10^{-8}$
	313	$1.04x10^{-4}$	$7.10x10^{-8}$	$3.76x10^{-8}$
S	298	$1.04x10^{-4}$	$4.48x10^{-8}$	$2.37x10^{-8}$
	313	$1.04x10^{-4}$	$6.42x10^{-8}$	$3.40x10^{-8}$
VA	288	$1.09x10^{-4}$	$3.65x10^{-8}$	$1.93x10^{-8}$
	298	$1.09x10^{-4}$	$4.82x10^{-8}$	$2.55x10^{-8}$
	313	$1.09x10^{-4}$	$6.91x10^{-8}$	$3.66x10^{-8}$
SA	298	$1.09x10^{-4}$	$3.97x10^{-8}$	$2.11x10^{-8}$
	313	$1.09x10^{-4}$	$6.27x10^{-8}$	$3.32x10^{-8}$

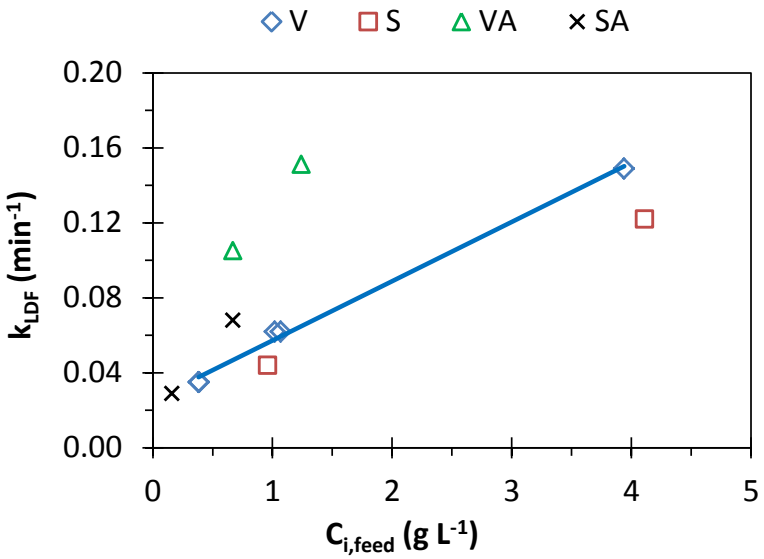

Figure 3.6 Representation of k_{LDF} vs feed concentration for V, S, VA and SA (in aqueous solution) for experiments at 298 K. The line represents the linear regression for V.

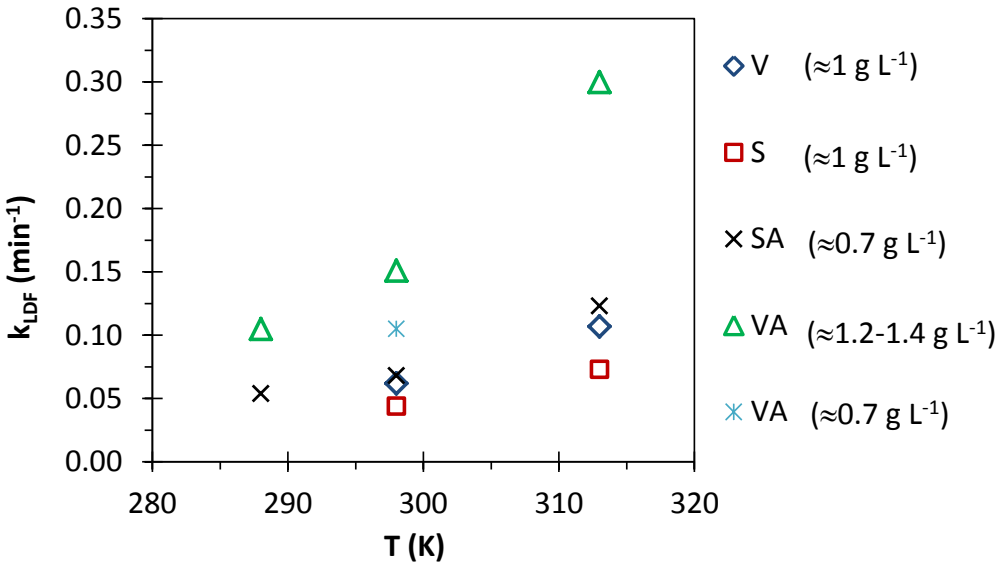

Figure 3.7 Representation of k_{LDF} vs feed concentration for V, S VA and SA (in aqueous solution) for different temperatures.

Figure 3.8 and Figure 3.9 show the experimental and predicted concentration histories for adsorption of vanillin and syringaldehyde in aqueous solution onto SP700 performed at 298 K. Similarly, in Figure 3.10 it is shown the experimental breakthrough curves together with the predicted behaviour obtained with vanillic and syringic acids for the same temperature of 298 K and using the same bed used for the aldehydes.

The predicted behaviours demonstrate that the mathematical model considered is adequate to describe the fixed bed experiments performed. In general, the equilibrium data successfully described the breakthrough curves at 298 K.

Moreover, it is possible to observe that, in general, for the acids, the k_{LDF} should be somewhat smaller. Additionally, for experiments performed with vanillin for feed concentration of 0.38 g L^{-1}, the k_{LDF} estimated should also be somewhat smaller in order to predict better the transient concentration history at column outlet observed.

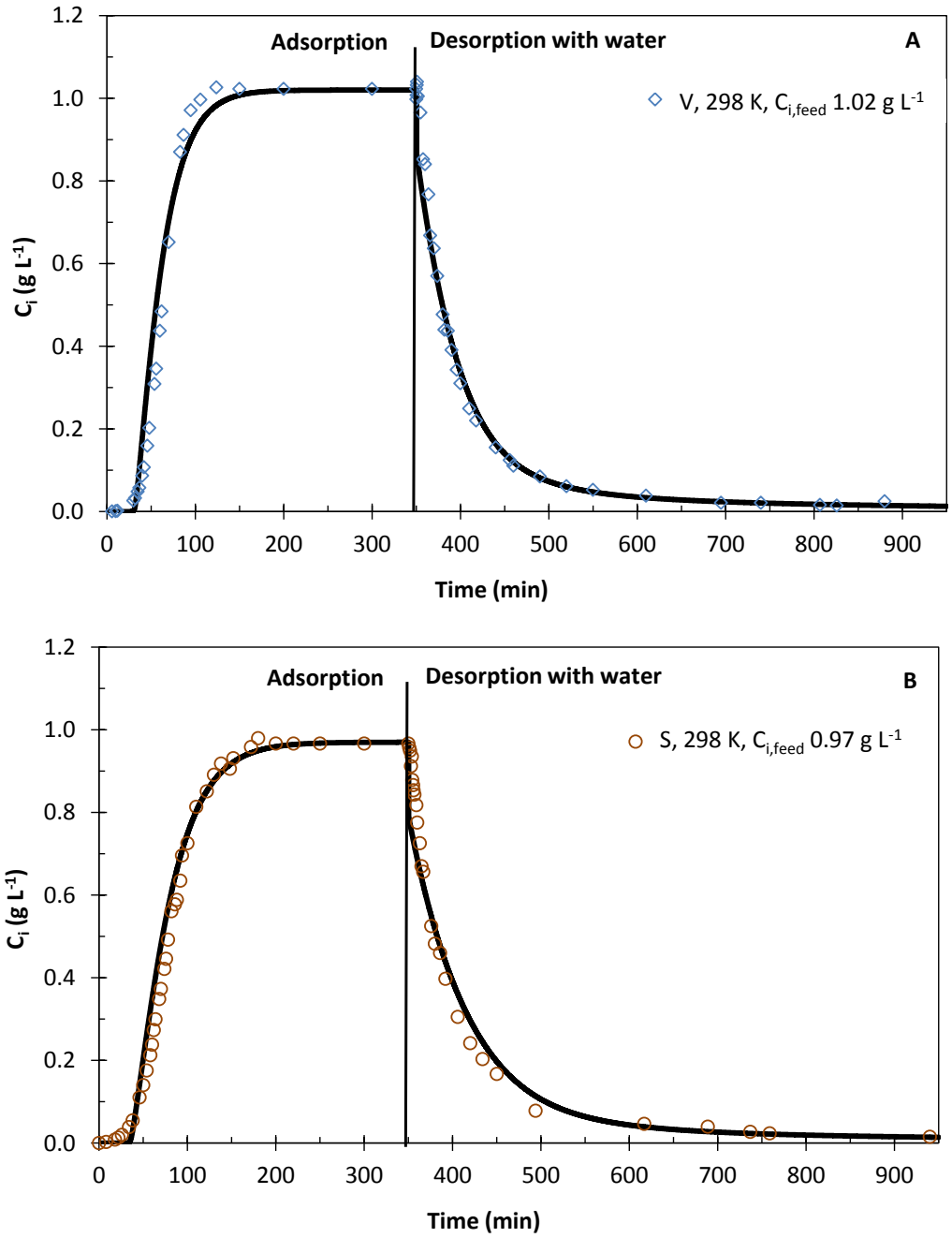

Figure 3.8 Concentration of V (A) and S (B) versus time at the adsorption column outlet. Conditions: feed of approximately 1 g L^{-1} onto the SP700 resin and desorption with water at 298 K, feed flowrate 5 mL min^{-1}, in a column of 5.6 x 1 cm and porosity 0.35: points correspond to the experimental values, the lines (—) the simulations obtained with Bi-Langmuir isotherm. The axial dispersed plug flow model with LDF approximation was used to fit the experimental breakthrough curves.

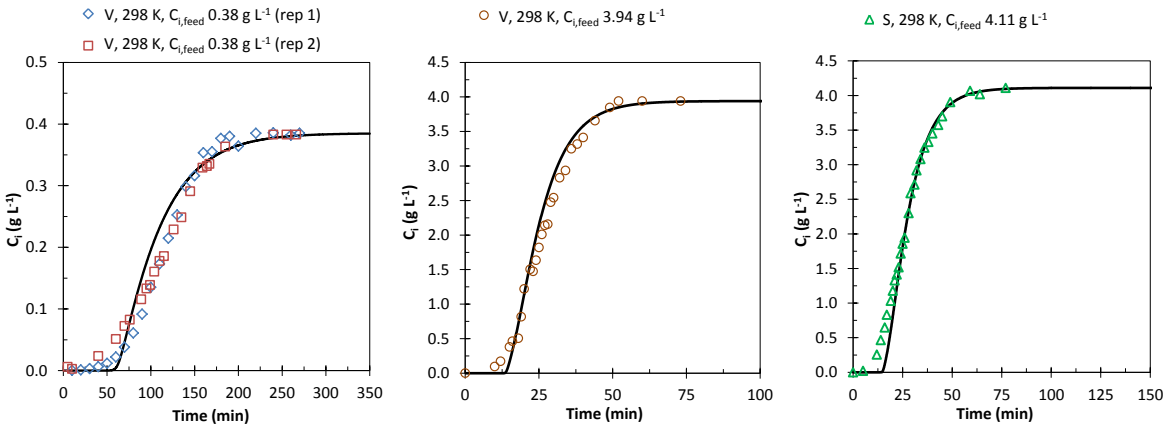

Figure 3.9 Concentration of V and S versus time at the adsorption column outlet. Conditions: column with SP700 resin for different feed concentrations at 298 K and feed flowrate of 5 mL min^{-1}, in a column of 5.6 x 1 cm and porosity 0.35: points correspond to the experimental values, the lines (—) to the mathematical modelling with Bi-Langmuir isotherm. The axial dispersed plug flow model with LDF approximation was used to fit the experimental breakthrough curves.

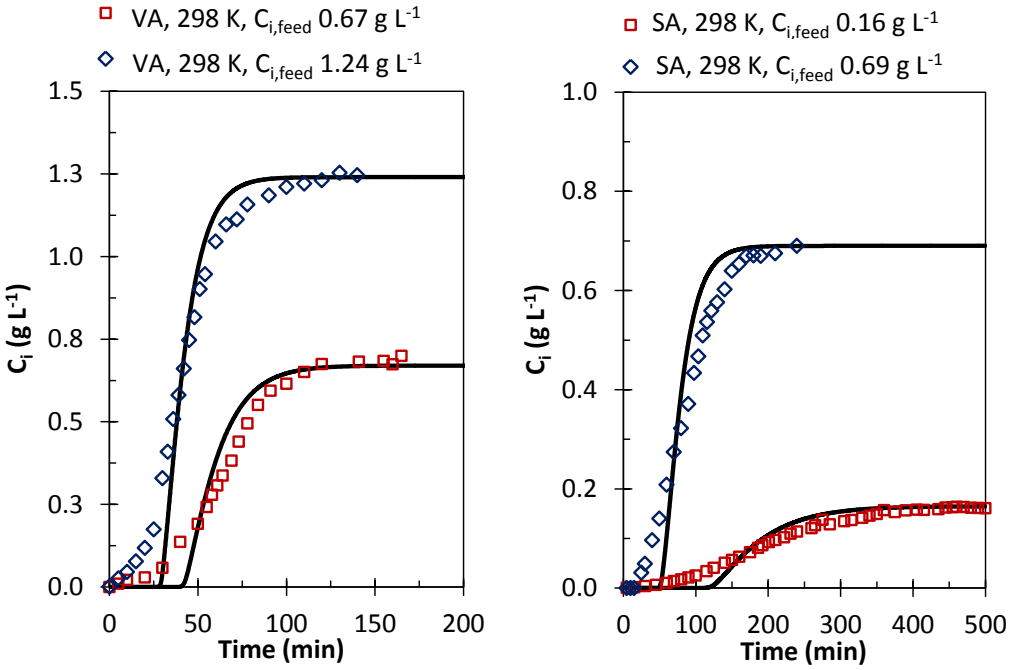

Figure 3.10 Concentration of VA and SA versus time at the adsorption outlet. Conditions: column with SP700 resin for different feed concentrations at 298 K and feed flowrate of 5.25 mL min^{-1}, in a column of 5.6 x 1 cm and porosity 0.35: points correspond to the experimental values, the lines (—) to the mathematical modelling with Bi-Langmuir isotherm. The axial dispersed plug flow model with LDF approximation was used to fit the experimental breakthrough curves.

In batch equilibrium adsorption experiments it was observed that the adsorption capacity was slightly higher for syringaldehyde than vanillin. This trend was also observed with fixed bed studies, for feed concentrations of 1 g L^{-1} and 4 g L^{-1}. The experimental adsorbed amounts given in Table 3.3 for syringaldehyde were 13 to 20 % higher than the adsorbed amounts obtained for vanillin experiments, regardless of the selected temperature.

In the particular case of vanillin and syringaldehyde adsorption at 298 K and feed concentration of approximately 1 g L^{-1} shown in Figure 3.8, the adsorbed amount of syringaldehyde (0.412 g $g^{-1}_{dry\ resin}$, given in Table 3.3) was about 20% higher than that for vanillin adsorption at the same experimental conditions (0.343-0.344 g $g^{-1}_{dry\ resin}$, given in Table 3.3). Additionally, the experimental adsorbed amount and stoichiometric time obtained for each compound, satisfactorily matched the predicted values (Table 3.3). The stoichiometric time prediction standard deviations (SD) were below 3% (Table 3.3).

Desorption studies with water were performed for the experiments with vanillin and syringaldehyde adsorption at 298 K and feed concentration of 1 g L^{-1}. After eluting 9 hours with the feed flowrate and temperature used for the adsorption (approximately 1750 BV), about 83-85 % of the adsorbed amount of vanillin and syringaldehyde was desorbed. As it can be seen from Figure 3.8, the shape of the desorption curve is different from the adsorption curve because of the non-linearity of the adsorption equilibrium. Additionally, the Bi-Langmuir satisfactorily predicted the experimental desorption points.

It is important to notice that desorption studies performed with water were considerably time-consuming and led to a high dilution of the final solution obtained. In order to obtain a more feasible desorption process other solvents must be applied when the recovery of vanillin and syringaldehyde is envisaged. Considering this, existing literature shows the advantage of employing organic solvents as eluting agent (13, 20, 21, 64-66). Wang *et al.* (13, 64) demonstrated that about 95-96 % of vanillin and syringaldehyde could be desorbed from the nonpolar D101 resin with 1.3 bed volumes of ethyl acetate. The advantage of using ethanolic solutions to desorb phenolic compounds from polymeric resins has also been shown in several works (20, 21, 65, 66) and was summarized in Chapter 2 – state of the art (section 2.5.4.1). Existing literature shows high recoveries employing aqueous ethanolic solutions with ethanol concentrations higher than 80%.

Figure 3.11 shows the experimental and model predicted monocomponent breakthrough curves of the experiments performed with vanillin and syringaldehyde for a feed concentration of approximately 1 g L^{-1} at 313 K. It is observed that syringaldehyde is adsorbed in a higher amount than vanillin, as also verified for the 298 K experiments. As expected, the adsorbed amount of these compounds at 313 K was smaller than at 298 K (Table 3.3) due to the exothermic nature of the adsorption process onto SP700. Previous equilibrium batch experiments showed that the adsorption capacity was negatively affected by the increase of temperature.

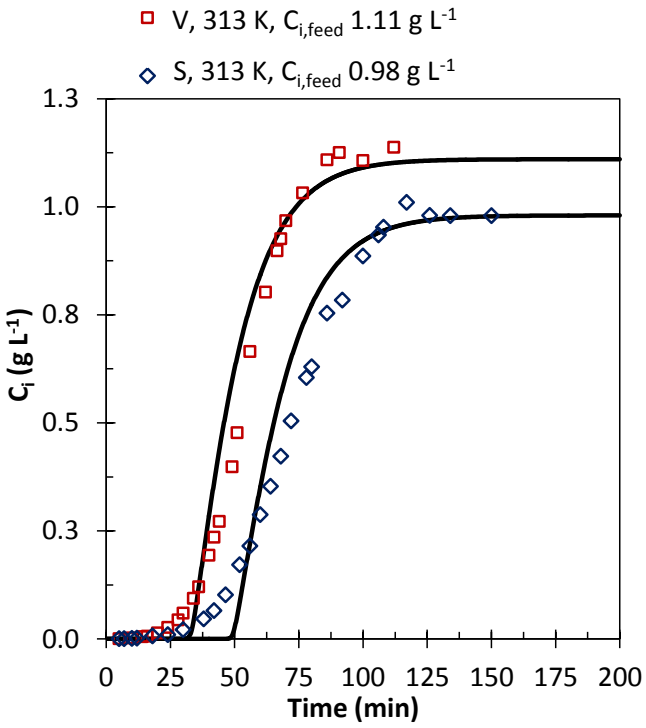

Figure 3.11 Concentration of V and S versus time at the adsorption outlet. Conditions: Feed of approximately 1 g L^{-1} onto the SP700 resin at 313 K and feed flowrate of 5 mL min^{-1}, in a column of 5.6 x 1 cm and porosity 0.35: points correspond to the experimental values, the lines (—) to the mathematical modelling with Bi-Langmuir isotherm. The axial dispersed plug flow model with LDF approximation was used to fit the experimental breakthrough curves.

Figure 3.12 shows the breakthroughs performed for vanillic and syringic acids at 288 K and 313 K where it is possible to observe that the adsorptive capacity decreases with the increase of temperature, also observed for batch experiments and in agreement with the expected exothermic nature the adsorption process.

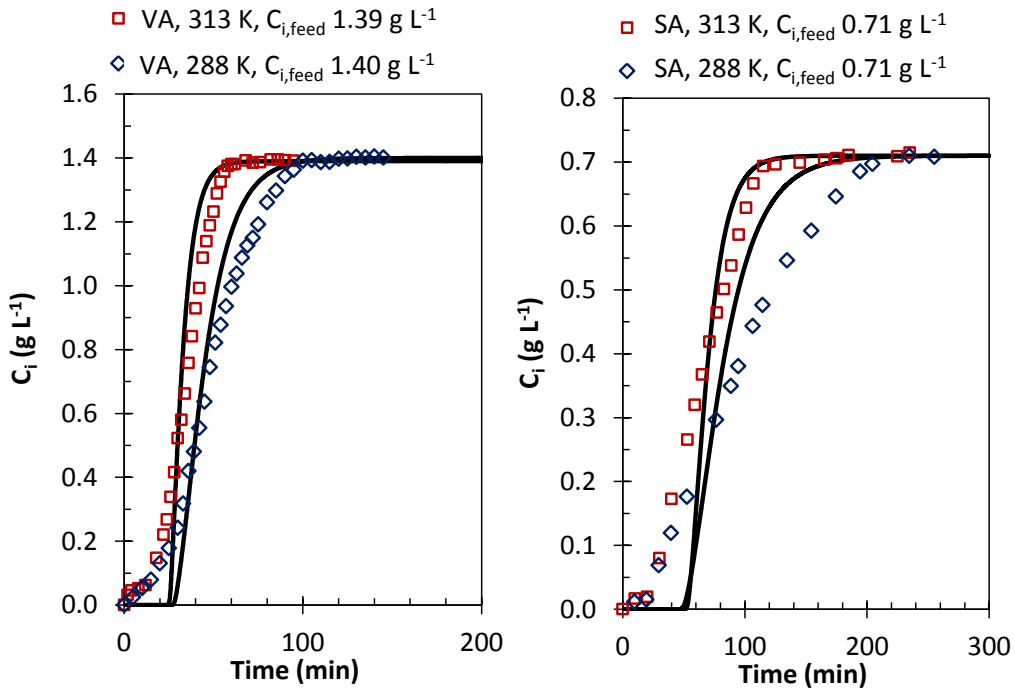

Figure 3.12 Concentration of VA and SA versus time at the adsorption outlet. Conditions: column with SP700 resin for different feed concentrations at 288 or 313 K and feed flowrate of 5.25 mL min^{-1}, in a column of 5.6 x 1 cm and porosity 0.35: points correspond to the experimental values, the lines (—) to the mathematical modelling with Bi-Langmuir isotherm. The axial dispersed plug flow model with LDF approximation was used to fit the experimental breakthrough curves.

Comparatively to desorption with water, the main benefit of using ethanolic solutions to recover the phenolic compounds is the shorter desorption times needed which results in less eluent consumption and simultaneous sample concentration. For these reasons, ethanol:water (90:10, % V/V) solution was chosen to perform further desorption studies and will be detailed in Chapter 4.

3.4.4. Multi-component adsorption studies

Binary adsorption studies with vanillin and syringaldehyde onto SP700 resin were performed in order to assess competition phenomena among themselves. The extended Bi-Langmuir model was applied to describe the local binary equilibria.

Binary batch equilibrium adsorption studies with vanillin and syringaldehyde were performed at 298 K employing different amounts of resin and starting from a feed solution containing 2.12 g L^{-1} and 2.62 g L^{-1}, respectively. In Figure 3.13-A it is shown the experimental adsorbed amounts obtained for each compound and the respective adsorbed amounts predicted with the extended Bi-Langmuir model. Table 3.5 summarizes the equilibrium concentrations achieved and the respective experimental and predicted adsorbed amounts. It is possible to observe that this model successfully describes the adsorption of vanillin in the presence of a similar amount of syringaldehyde, or vice-versa, with deviation values below 6%.

One fixed bed assay was performed with an aqueous solution containing 1.16 g L^{-1} and 1.09 g L^{-1} of vanillin and syringaldehyde, respectively. The mixture was loaded onto the same column bed used in the pure component experiments at 298 K and feed flowrate of 5 mL min^{-1}. Figure 3.13-B portrays the experimental and predicted values by the extended Bi-Langmuir model. Table 3.6 summarizes the respective experimental adsorbed amounts and the predicted ones with the extended Bi-Langmuir model. Likewise to the studies performed in batch, the extended Bi-Langmuir model reasonably predicts the adsorption capacity obtained for each compound.

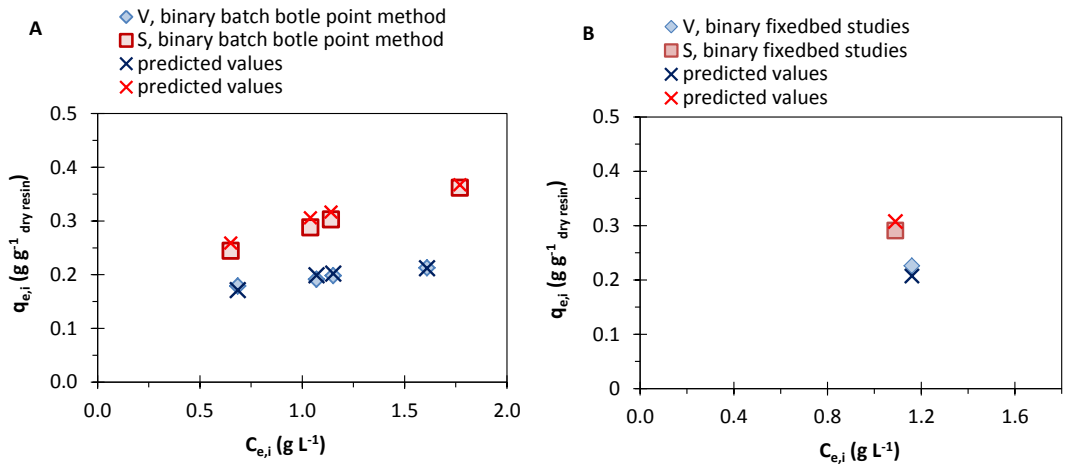

Figure 3.13 Binary V and S experimental adsorbed amounts obtained for different equilibrium concentrations in A. batch and B. dynamic adsorption studies and, the respective adsorption amount predicted with the extended Bi-Langmuir model.

Table 3.5 Equilibrium concentrations, experimental adsorbed amounts and predicted adsorbed amounts with the extended Bi-Langmuir model for binary batch equilibrium adsorption experiments employing different amounts of SP700 resin starting with a feed solution containing 2.12 g L^{-1} of V and 2.62 g L^{-1} of S at 298 K

$C_{e,i}$ g L^{-1}		$q_{ads,exp}$ g $g^{-1}_{dry\ resin}$		$q_{ads,pred}$ g $g^{-1}_{dry\ resin}$		%SD*	
V	S	V	S	V	S	V	S
0.68	0.65	0.179	0.245	0.171	0.259	4.3	5.5
1.15	1.14	0.198	0.303	0.202	0.317	2.0	4.3
1.61	1.77	0.213	0.362	0.212	0.367	0.3	1.5
1.07	1.04	0.191	0.288	0.199	0.306	4.0	5.9

*SD (%) corresponds to the standard deviation between the experimental and predicted adsorbed amounts, calculated with the following expression: $SD(\%) = \frac{\left|q_{ads,pred} - q_{ads,\exp}\right|}{q_{ads,pred}} \times 100$.

Table 3.6 Experimental and predicted adsorbed amounts for binary fixed bed adsorption experiments at 298 K, feed flowrate of 5 mL min^{-1}, SP700 bed with 5.6 x 1 cm and porosity 0.35

		$C_{i,feed}$ g L^{-1}	$q_{ads,exp}$ g $g^{-1}_{dry\ resin}$	$q_{ads,pred}$ g $g^{-1}_{dry\ resin}$	%SD*
Binary system	V	1.16	0.226	0.207	9.1
	S	1.09	0.291	0.308	5.4

*SD (%) corresponds to the standard deviation between the experimental and predicted adsorbed amounts, calculated with the following expression: $SD(\%) = \frac{\left|q_{ads,pred} - q_{ads,\exp}\right|}{q_{ads,pred}} \times 100$.

Figure 3.14 shows the experimental and predicted transient concentration histories of each phenolic aldehyde for the binary fixed bed experiment performed. The concentration histories of each compound is described with the history obtained by the previously described mathematical model comprising the extended Bi-Langmuir model for the multi-component equilibrium prediction, linear driving force approximation to describe the intraparticle mass transfer resistance, no radial and temperature gradients and constant porosity along the bed. The mass resistance estimated for this bi-component experiment is somewhat higher than the one experimentally observed.

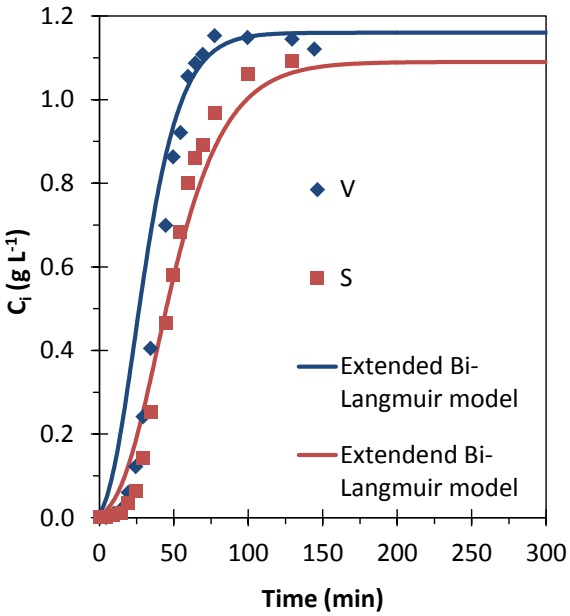

Figure 3.14 Concentration histories obtained for adsorption onto SP700 resin of a binary system containing V (1.16 g L^{-1}) and S (1.09 g L^{-1}), feed flowrate 5 mL min^{-1}, in a column of 5.6 x 1 cm and porosity 0.35: points correspond to the experimental values and the lines to the simulations obtained considering the axial dispersed plug flow model with LDF approximation and the extended Bi-Langmuir model ($k_{LDF,V}$ 0.116 min^{-1} and $k_{LDF,S}$ 0.066 min^{-1}).

In order to evaluate the influence of pH value change on the adsorption of vanillin, syringaldehyde, vanillic acid and syringic acid, two four-component fixed bed adsorption experiments onto a bed of SP700 were performed at 298 K and pH values of 3.5 and 6.5. Results are summarized in Appendix B. These four-component experiments allowed verifying that at pH value of 6.5 the phenolic acids are practically not adsorbed. This behavior was expected due to the *pKa* value of the phenolic acids in water be near 4. Therefore, at pH value of 6.5, it is expected that the phenolic acids are ionized and consequently, are not adsorbed by a non-polar resin.

In the perspective of employing non-polar resins to recover vanillin ad syringaldehyde from real oxidized lignin streams, a pH value change can be advantageous to tune the adsorption process towards the preferential adsorption of the phenolic aldehydes in detriment of other phenolic acids present with lower *pKa*.

3.5. Conclusions

Adsorption studies of vanillin and syringaldehyde onto the macroporous styrene-divinylbenzene adsorbents (SP700 and XAD16N) were performed. The respective adsorption equilibrium isotherms in aqueous solutions were estimated for different temperatures. SP700 resin revealed higher adsorption capacity for vanillin and thus was selected to pursue with further batch adsorption studies with vanillic and syringic acids.

The adsorbed amounts of the phenolic compounds studied had a non-linear behavior with the equilibrium concentration and thus, equilibrium data were satisfactorily fitted to Langmuir, Bi-Langmuir and Freundlich models. The amount of each adsorbed compound decreased with the increase of temperature, thus revealing the exothermic nature of the process. Isosteric enthalpy of adsorption ranged from -15 to -37 kJ mol^{-1}, being the adsorption of vanillic acid the most exothermic process.

Regarding SP700 equilibrium adsorption studies, the amount of each compound adsorbed decreased in the following order: S > SA > V > VA. However, maximum adsorption capacity obtained with the Langmuir model followed the trend S (0.707 g $g^{-1}_{dry\ resin}$) > V (0.663 g $g^{-1}_{dry\ resin}$) > VA (0.450 g $g^{-1}_{dry\ resin}$) > SA (0.423 g $g^{-1}_{dry\ resin}$); the same trend was obtained with the Bi-Langmuir model, with maximum adsorption capacity, $q_{m1,i}$, of S (0.663 g $g^{-1}_{dry\ resin}$) > V (0.634 g $g^{-1}_{dry\ resin}$) > VA (0.486 g $g^{-1}_{dry\ resin}$) > SA (0.407 g $g^{-1}_{dry\ resin}$). The Freundlich exponent *n* was within 2.5 and 2.9, indicating that the adsorption was favorable.

Fixed bed adsorption studies for different feed concentrations and temperatures were performed for the four compounds. The transient concentration histories along time were satisfactorily described with the axial dispersed plug flow model comprising the Bi-Langmuir isotherm and the LDF approximation to represent the intraparticle mass transfer.

Vanillin and syringaldehyde desorption studies with water revealed to be a very time consuming process that greatly dilutes the desorbed phenolic compounds. Therefore, other studies towards improving desorption step with more efficient solvents will be conducted in order to find a more feasible desorption process for vanillin and syringaldehyde recovery.

Adsorption studies of the binary mixture of vanillin and syringaldehyde were successfully described employing the extended Bi-Langmuir isotherm model.

3.6. References

1. Zakzeski, J., Bruijnincx, P. C. A., Jongerius, A. L. and Weckhuysen, B. M. (2010) The catalytic valorization of lignin for the production of renewable chemicals. Chem. Rev., 110: 3552-3599.
2. Pinto, P. C. R., Borges da Silva, E. A. and Rodrigues, A. E. (2012) Lignin as source of fine chemicals: vanillin and syringaldehyde: In Biomass Conversion. Chinnappan Baskar, Shikha Baskar and Ranjit S. Dhillon. Springer Berlin Heidelberg: London, United kingdom, 381-420.
3. Rekha, K. R., Selvakumar, G. P. and Sivakamasundari, R. I. (2014) Effects of syringic acid on chronic MPTP/probenecid induced motor dysfunction, dopaminergic markers expression and neuroinflammation in C57BL/6 mice. Biomedicine & Aging Pathology, 4: 95-104.
4. Yrbas, M. d. l. A., Morucci, F., Alonso, R. and Gorzalczany, S. (2015) Pharmacological mechanism underlying the antinociceptive activity of vanillic acid. Pharmacology Biochemistry and Behavior, 132: 88-95.
5. Kumar, S., Prahalathan, P. and Raja, B. (2014) Vanillic acid: A potential inhibitor of cardiac and aortic wall remodeling in l-NAME induced hypertension through upregulation of endothelial nitric oxide synthase. Environ. Toxicol. Phar., 38: 643-652.
6. Erofeev, Y. V., Afanas'eva, V. L. and Glushkov, R. G. (1990) Synthetic routes to 3,4,5-trimethoxybenzaldehyde (review). Pharm. Chem. J., 24: 501-510.
7. Bjørsvik, H.-R. and Minisci, F. (1999) Fine chemicals from lignosulfonates. 1. Synthesis of vanillin by oxidation of lignosulfonates. Org. Process Res. Dev., 3: 330-340.
8. Burri, J., Graf, M., Lambelet, P. and Löliger, J. (1989) Vanillin: more than a flavouring agent - a potent antioxidant. J. Sci. Food Agric., 48: 49-56.
9. Logan, C. D. (1965) Cyclic process for recovering vanillin and sodium values from lignosulfonic waste liquors by ion exchange, US Patent 3197359 (27-07-1965).
10. Forss, K. G., Fremer, K. E. and Talka, E. T. (1981) Method for the isolation of vanillin from lignin in alkaline solutions, US Patent 4277626 (07-07-1981).
11. Stecker, F., Fischer, A., Kirste, A., Voitl, A., Wong, C. H., Waldvogel, S., Regenbrecht, C., Schmitt, D. and Hartmer, M. F. (2014) Method for obtaining vanillin from aqueous basic compositions containing vanillin, WO Patent 2014006108 A1 (09-01-2014).
12. Derouane, E. G. and Powell, R. A. (1987) Vanillin extraction process using large pore, high silica/alumina ratio zeolites, US patent 4652684 (24-03-1987).

13. Wang, Z., Chen, K., Li, J., Wang, Q. and Guo, J. (2010) Separation of vanillin and syringaldehyde from oxygen delignification spent liquor by macroporous resin adsorption. Clean, 38: 1074-1079.

14. Michailof, C., Stavropoulos, G. G. and Panayiotou, C. (2008) Enhanced adsorption of phenolic compounds, commonly encountered in olive mill wastewaters, on olive husk derived activated carbons. Bioresour. Technol., 99: 6400-6408.

15. García-Araya, J., Beltrán, F., Álvarez, P. and Masa, F. (2003) Activated carbon adsorption of some phenolic compounds present in agroindustrial wastewater. Adsorption, 9: 107-115.

16. Richard, D., Delgado-Núñez, M. L. and Schweich, D. (2009) Adsorption of complex phenolic compounds on active charcoal: Adsorption capacity and isotherms. Chem. Eng. J., 148: 1-7.

17. Fargues, C., Mathias, Á. L. and Rodrigues, A. (1996) Kinetics of vanillin production from kraft lignin oxidation. Ind. Eng. Chem. Res., 35: 28-36.

18. Žabková, M., Borges da Silva, E. A. and Rodrigues, A. E. (2007) Recovery of vanillin from Kraft lignin oxidation by ion-exchange with neutralization. Sep. Purif. Technol., 55: 56-68.

19. Žabková, M., Otero, M., Minceva, M., Zabka, M. and Rodrigues, A. E. (2006) Separation of synthetic vanillin at different pH onto polymeric adsorbent Sepabeads SP206. Chem. Eng. Process., 45: 598-607.

20. Zhang, Q.-F., Jiang, Z.-T., Gao, H.-J. and Li, R. (2008) Recovery of vanillin from aqueous solutions using macroporous adsorption resins. Eur. Food Res. Technol., 226: 377-383.

21. Xiao, G.-Q., Xie, X.-L. and Xu, M.-C. (2009) Adsorption performances for vanillin from aqueous solution by the hydrophobic - hydrophilic macroporous polydivinylbenzene / polyacrylethylenediamine IPN resin. Acta Phys.-Chim. Sin., 25: 97-102.

22. Jin, X. and Huang, J. (2013) Adsorption of vanillin by an anisole-modified hyper-cross-linked polystyrene resin from aqueous solution: equilibrium, kinetics, and dynamics. Adv. Polym. Tech., 32: E221-E230.

23. Samah, R. A., Zainol, N., Yee, P. L., Pawing, C. M. and Abd-Aziz, S. (2013) Adsorption of vanillin using macroporous resin H103. Adsorpt. Sci. Technol., 31: 599-610.

24. Crittenden, B. D. and Thomas, W. J. (1998) Adsorption Technology and Design. First edition, Butterworth and Heinemann: Oxford, United Kingdom.

25. Kunin, R. (1991) 1.11 Polymeric adsorbents: In Ion Exchangers. Konrad Dorfner. De Gruyter: New York.

26. Pan, B. C., Xiong, Y., Su, Q., Li, A. M., Chen, J. L. and Zhang, Q. X. (2003) Role of amination of a polymeric adsorbent on phenol adsorption from aqueous solution. Chemosphere, 51: 953-962.

27. Suresh, S., Srivastava, V. and Mishra, I. (2012) Adsorption of catechol, resorcinol, hydroquinone, and their derivatives: a review. Int. J. Energy Environ. Eng., 3: 1-19.

28. Li, A., Long, C., Sun, Y., Zhang, Q., Liu, F. and Chen, J. (2002) A new phenolic hydroxyl modified polystyrene adsorbent for the removal of phenolic compounds from their aqueous solutions. Sep. Sci. Technol., 37: 3211-3226.

29. Jiang, Z.-M., Li, A.-M., Cai, J.-G., Wang, C. and Zhang, Q.-X. (2007) Adsorption of phenolic compounds from aqueous solutions by aminated hypercrosslinked polymers. J. Envirn. Sci., 19: 135-140.

30. Huang, J., Yan, C. and Huang, K. (2009) Removal of *p*-nitrophenol by a water-compatible hypercrosslinked resin functionalized with formaldehyde carbonyl groups and XAD-4 in aqueous solution: a comparative study. J. Colloid Interface Sci., 332: 60-64.

31. Huang, J., Jin, X. and Deng, S. (2012) Phenol adsorption on an N-methylacetamide-modified hypercrosslinked resin from aqueous solutions. Chem. Eng. J., 192: 192-200.

32. Huang, J., Yang, L., Wu, X., Xu, M., Liu, Y.-N. and Deng, S. (2013) Phenol adsorption on *α,α′*-dichloro-*p*-xylene (DCX) and 4,4′-bis(chloromethyl)-1,1′-biphenyl (BCMBP) modified XAD-4 resins from aqueous solutions. Chem. Eng. J., 222: 1-8.

33. Asaoka, K., Bae, J.-Y. and Lee, H.-H. (2012) Porosity of dental gypsum-bonded investments in setting and heating process. Dent. Mater. J., 31: 120-124.

34. Pereira, C. S. M., Silva, V. M. T. M. and Rodrigues, A. E. (2009) Fixed bed adsorptive reactor for ethyl lactate synthesis: experiments, modelling, and simulation. Sep. Sci. Technol., 44: 2721-2749.

35. Ruthven, D. M. (1984) Principles of Adsorption and Adsorption Processes. John Willey and Sons: New York, United States of America.

36. Rodrigues, A. E., Levan, M. D. and Tondeur, D. (1989) Adsorption: Science and Technology. First edition, Kluwer Academic Publishers: London, United Kingdom.

37. Guiochon, G., Felinger, A., Shirazi, D. and Katti, A. (2006) Fundamentals of Preparative and Nonlinear Chromatography. second, Elsevier Academic Press: New York, United States of America.

38. Wankat, P. C. (1994) Rate-controlled separations. Blackie Academic & Professional: London, United Kingdom.

39. Langmuir, I. (1918) The adsorption of gases on plane surfaces of glass, mica and platinum. J. Am. Chem. Soc., 40: 1361-1402.

40. Graham, D. (1953) The Characterization of Physical Adsorption Systems. I. The Equilibrium Function and Standard Free Energy of Adsorption. J. Phys. Chem., 57: 665-669.

41. Guiochon, G., Felinger, A., Shirazi, D. and Katti, A. (2006) Fundamentals of Preparative and Nonlinear Chromatography. Second edition, Elsevier Academic Press: Oxford, United Kingdom.

42. Butler, J. A. V. and Ockrent, C. (1930) Studies in Electrocapillarity. III. J. Phys. Chem., 34: 2841-2859.

43. Freundlich, H. M. F. (1909) Kapillarchemie. Akademische Verlagsgesellschaft: Leipzig.

44. Duong, D. D. (1998) Adsorption Analysis: Equilibria and Kinetics. Imperial College Press: London, United Kingdom.

45. Jacobson, S., Golshan-Shirazi, S. and Guiochon, G. (1990) Measurement of the heats of adsorption of chiral isomers on an enantioselective stationary phase. J. Chromatogr. A, 522: 23-36.

46. Glueckauf, E. and Coates, J. I. (1947) 241. Theory of chromatography. Part IV. The influence of incomplete equilibrium on the front boundary of chromatograms and on the effectiveness of separation. J. Chem. Soc. (Resumed), 1315-1321.

47. Farooq, S. and Ruthven, D. M. (1990) Heat effects in adsorption column dynamics. 2. Experimental validation of the one-dimensional model. Ind. Eng. Chem. Res., 29: 1084-1090.

48. Reid, R. C., Prausnitz, J. M. and Poling, B. E. (1987) The Properties of Gases and Liquids. Fourth edition, McGraw Hill: New York.

49. Smith, J. M. (1981) Chemical Engineering Kinetics. McGraw-Hill Chemical Engineering Series: New York, United States of America.

50. Wilke, C. R. and Chang, P. (1955) Correlation of diffusion coefficients in dilute solutions. AIChE Journal, 1: 264-270.

51. Partington, S. (1949) An Advanced Treatise on Physical Chemistry, Vol. I, Fundamental Principles: the Properties of Gases. First edition: London, United Kingdom.

52. Li, A., Ma, F., Song, X. and Yu, R. (2011) Dynamic adsorption of diarrhetic shellfish poisoning (DSP) toxins in passive sampling relates to pore size distribution of aromatic adsorbent. J. Chromatogr. A, 1218: 1437-1442.

53. Dávila-Guzman, N. E., Cerino-Córdova, F. J., Diaz-Flores, P. E., Rangel-Mendez, J. R., Sánchez-González, M. N. and Soto-Regalado, E. (2012) Equilibrium and kinetic studies of ferulic acid adsorption by Amberlite XAD-16. Chem. Eng. J., 183: 112-116.

54. Díez, S., Leitão, A., Ferreira, L. and Rodrigues, A. (1998) Adsorption of phenylalanine onto polymeric resins: equilibrium, kinetics and operation of a parametric pumping unit. Sep. Purif. Technol., 13: 25-35.

55. Webb, P. A. (2001) An Introduction to the Physical Characterization of Materials by Mercury Intrusion Porosimetry with Emphasis on Reduction and Presentation of Experimental Data. Micromeritics Instrument Corp.: Georgia.

56. Souchon, I., Rojas, J. A., Voilley, A. and Grevillot, G. (1996) Trapping of aromatic compounds by adsorption on hydrophobic sorbents. Sep. Sci. Technol., 31: 2473-2491.

57. Ku, Y. and Lee, K. C. (2000) Removal of phenols from aqueous solution by XAD-4 resin. J. Hazard. Mater., 80: 59-68.

58. Wang, X. J., Zhao, J. F., Xia, S. Q., Li, A. M. and Chen, L. (2004) Adsorption mechanism of phenolic compounds from aqueous solution on hypercrosslinked polymeric adsorbent. J. Envirn. Sci., 16: 919-924.

59. Gritti, F. and Guiochon, G. (2013) Analytical Solution of the Ideal Model of Chromatography for a Bi-Langmuir Adsorption Isotherm. Anal. Chem., 85: 8552-8558.

60. van Noort, P. C. M. (2006) Gibbs free energies for dual langmuir-like adsorption onto hard carbon materials in sediment and soils. Environ. Toxicol. Chem., 25: 3125-3132.

61. Santos, M. P. S. and Rodrigues, A. E. (2015) Adsorption Equilibrium and Fixed Bed Adsorption of Aniline onto Polymeric Resin and Activated Carbons. Sep. Sci. Technol., 49: 335-344

62. Payne, G. F., Payne, N. N., Ninomiya, Y. and Shuler, M. L. (1989) Adsorption of nonpolar solutes onto neutral polymeric sorbents. Sep. Sci. Technol., 24: 457-465.

63. Bond, G. C. (1974) Heterogeneous Catalysis: Principles and Applications. Clarendon Press: Oxford, United Kingdom.

64. Li, A., Zhang, Q., Zhang, G., Chen, J., Fei, Z. and Liu, F. (2002) Adsorption of phenolic compounds from aqueous solutions by a water-compatible hypercrosslinked polymeric adsorbent. Chemosphere, 47: 981-989.

65. Kammerer, D. R., Saleh, Z. S., Carle, R. and Stanley, R. A. (2007) Adsorptive recovery of phenolic compounds from apple juice. Eur. Food Res. Technol., 224: 605-613.

66. Zhao, R., Yan, Y., Li, M. and Yan, H. (2008) Selective adsorption of tea polyphenols from aqueous solution of the mixture with caffeine on macroporous crosslinked poly(N-vinyl-2-pyrrolidinone). React. Funct. Polym., 68: 768-774.

4. Successful recovery and concentration of vanillin, syringaldehyde, vanillic acid and syringic acid with ethanol/water solution[1]

The recovery of purified fractions of vanillin (V) and syringaldehyde (S) from an oxidized lignin medium has attracted considerable attention driven by the high added value of these products and the importance of lignin valorisation processes in biorefineries. Polymeric resins with high specific area can be a viable option for the adsorption of aromatic compounds in polar solvents and desorption with less polar solvents for their recovery.

In this chapter, mono-component batch and fixed bed adsorption experiments are performed with vanillin and syringaldehyde onto SP700 resin in ethanol:water (90:10, % V/V) solutions to obtain the respective isotherm models at 298 K and 313 K. The adsorption behaviours of vanillin and syringaldehyde are described by Linear and Freundlich models.

On the perspective of the real application of SP700 resin for recovery of vanillin and syringaldehyde, fixed bed is first loaded with an aqueous solution of each compound and then desorption is performed with ethanol:water (90:10 % V/V). A similar study is performed with the correspondent model solutions of the phenolic acids: vanillic (VA) and syringic (SA) acids. More than 83% of each compound is readily desorbed within 16-20 bed volumes, yielding to final enriched solutions of each phenolic compound.

The desorption histories for vanillin and syringaldehyde at the outlet of the fixed bed are successfully described by the mathematical model comprising the equilibrium isotherms and linear driving force rate equations to describe the diffusional mass transfer inside the resin.

This work demonstrates that the adsorption of the phenolic compounds from aqueous solution onto SP700 bed and desorption with ethanol:water (90:10, % V/V) solution can be a promising approach for the recovery of these compounds from lignin oxidation mixture. The high level of concentration

[1] This chapter is based on the paper

Mota, I. F., Pinto, P. C. R., Loureiro, J. M. and Rodrigues, A. E. (2016) Successful recovery and concentration of vanillin and syringaldehyde onto a polymeric adsorbent with ethanol/water solution. Chem. Eng. J., 294: 73-82.

Mota, I. F., Barbosa, S., Pinto, P. C. R., Loureiro, J. M., Rodrigues, A. E., Adsorption of vanillic and syringic acids onto a macroporous polymeric resin and recovery with ethanol:water (90:10, % V/V) solution (draft in preparation).

achieved with this strategy and the type of solvent used is favourable for any further processing step, such as crystallization or spray drying.

4.1. Introduction

The demand for obtaining purified fractions of vanillin and syringaldehyde using greener methodologies and lower environmental impact technologies led to an increase of adsorption studies already summarized in Chapter 2. Additionally, adsorption processes are widely studied and referred to as a promising technology to recover phenolic compounds from numerous sources.

Has as already been stated in the previous chapters, the adsorption studies of phenolic compounds employing polymeric resins (1) has increased in the recent years due to their enhanced capacities of adsorption, chemical stability and inertness and, most of all, due to the fact that recovery and regeneration of these compounds can be performed all together in one step (2, 3).

Regarding the recovery of vanillin and syringaldehyde from this type of resins, it has been shown in Chapter 3 that using water as eluting agent can be very time consuming with the additional disadvantage of noteworthy compounds dilution, generating a high volume and thus, hindering the development of a feasible industrial process. The use of organic solvents can provide a good alternative to overcome this drawback.

The adsorption and desorption behavior of phenolic compounds onto polymeric adsorbents are explained by the solubility parameter. This parameter, also known as the Hildebrand solubility parameter (4), is defined as the square root of the cohesive energy density; since the cohesive energy density is obtained from the heat of vaporization, this parameter is related with the van der Waals forces holding the molecules together. In general, the Hildebrand's model follows the generic rule 'like likes like'; thus, it is expected that two solvents are miscible and have the same dissolving capabilities or one solute is soluble in a solvent if their intermolecular van der Waals attractive forces, cohesive energy density, and solubility parameter values are similar (5). Considering this, the aromatic nonpolar adsorbent will be greatly selective for aromatic adsorbates, particularly in polar solvents such as water, where the adsorbate has limiting solubility. On the other side, the best elution or regenerating solvent is that with lower solubility parameter. Therefore, acetone, methanol or ethanol can be a good choice of eluents, recovering the solute from the adsorbent with minimum volume consumption. Nonetheless, the solubility of the solute in the organic solvent acting as eluent must be high enough to allow rapid dissolution after the solvent diffusion from the adsorption sites.

Desorption studies of several phenolic compounds from polymeric resins using methanolic (3) or ethanolic (6-9) solutions have been performed and demonstrated that a concentrated final solution can be obtained since almost all of the adsorbed compounds can be recovered using few bed volumes of solvent. Some of these studies refer to vanillin desorption with ethanolic solutions. To our knowledge there are no desorption studies employing ethanolic solutions to recover syringaldehyde, vanillic acid and syringic acid from polymeric resins. Furthermore, Wang *et al.* (10) reported the recovery of 96.2% and 94.7% of vanillin and syringaldehyde, respectively, employing low volumes of ethyl ether.

In this chapter, adsorption studies of vanillin and syringaldehyde in ethanol:water (90:10, % V/V) solutions onto the macropourous polymeric adsorbent SP700 were performed for the first time. Linear and Freundlich isotherm models were established for 298 K and 313 K. Furthermore, desorption studies employing ethanol:water (90:10, % V/V) solutions as eluent were conducted for different bed loadings with aqueous and with ethanolic solutions of vanillin and syringaldehyde. Modelling of concentration histories of both compounds at the fixed bed outlet was successfully accomplished. Desorption studies employing ethanol:water (90:10, % V/V) solutions were performed for vanillic acid and syrinigc acid as well, after loading the bed with aqueous solutions of each phenolic acid.

4.2. Experimental description

4.2.1. Chemicals, adsorbents and quantification analytical method

Model solutions of vanillin (Sigma-Aldrich, purity ≥ 98%) and syringaldehyde (Sigma-Aldrich, purity ≥ 98%) were prepared with 90 % ethanol (Panreac) and 10% deionized water (% V/V) solution to obtain the adsorption equilibrium isotherms.

Results report to experiments conducted with the styrene-divinylbenzene-based synthetic resin SP700 (Mitsubishi Chemical Corporation). The resin was prepared and cleaned as previously described in Chapter 3 – section 3.2.3.

In the desorption studies employing ethanol:water (90:10, % V/V) solution, a bed of SP700 resin was previously loaded with several aqueous solutions of vanillin, syringaldehyde, vanillic acid (Sigma-Aldrich, purity ≥ 97%) and syringic acid (Sigma-Aldrich, purity ≥ 95%).

Each model solution was previously filtered through a 0.2 μm nylon membrane (Whatman®) by means of a diaphragm vacuum pump (Vacuubrand GMBH, Germany) and ultrasonic degassed (Liarre, model Starsonic 35, Italy).

The phenolic compounds were quantified by HPLC-UV using the procedure, method and equipment as described in Chapter 3 – 3.2.2.

4.2.2. Batch adsorption equilibrium studies

Adsorption equilibrium studies for vanillin and syringaldehyde solutions prepared in ethanol:water (90:10, % V/V) were performed at 298 K and 313 K employing the batch bottle point method. Different initial volumes, feed concentrations and adsorbent amounts were used: 0.06 L and 0.10 L, 0.3 to 1 g L^{-1} and, 0.2 to 10 g of adsorbent (dry weight), respectively. To ensure equilibrium, samples were shaken at 160 rpm for 72 h in an orbital shaker (Lab Companion model SI-300R). The pH (VWR model pH110) was monitored and remained constant throughout the experiments (around 4.7 for vanillin and 5.3 for syringaldehyde).

The adsorbed phase concentration of species '*i*' at equilibrium ($q_{i,e}$, g $g^{-1}_{dry\ resin}$) is calculated from a mass balance between the adsorbent and liquid phases (Equation 3.3).

4.2.3. Fixed bed adsorption and desorption experiments

Fixed bed adsorption studies were carried out in a jacketed glass column (Götec, Germany) of 11.3 cm length, 2.6 cm internal diameter and bed porosity of 0.35 (determined from tracer experiments with blue dextran). One bed volume (BV) corresponds to the bed void volume of approximately 21 mL. Vanillin and syringaldehyde solutions were fed to the column with a Smartline Pump 1000 (Knauer, Germany) at isothermal conditions guaranteed by a thermostatic bath (Lauda model E200). Different temperatures (298 and 313 K) and feed concentrations (ranging from 10 to 50 g L^{-1}) were studied at fixed feed flowrate (1.1 mL min^{-1}). The bed was preconditioned with ethanol:water (90:10, % V/V) solution before experiments.

Desorption assays were performed with ethanol:water (90:10, % V/V) solution for the same experimental conditions used in adsorption. After each run, the column was regenerated by eluting

about 48-70 BV of ethanol:water (90:10, % V/V) solution, assuring by this way the removal of any residual vanillin or syringaldehyde.

The experimental ($t_{st,exp}$, min) and predicted ($t_{st,pred}$, min) stoichiometric times were obtained by the Equations 3.4 and 3.5, considering constant feed flowrate (11, 12). For $t_{st,exp}$ determination, it was calculated the area underneath the curve of the plot $1-C_i/C_{i,feed}$ vs time, with the trapezoidal rule.

The experimental adsorbed ($q_{ads,exp}$, g $g^{-1}_{dry\ resin}$) and desorbed ($q_{des,exp}$, g $g^{-1}_{dry\ resin}$) phase concentrations were assessed from global mass balances to the adsorption and desorption steps (13) with Equations 3.7 and 3.8, respectively.

It was calculated the ratio between $q_{des,exp}$ and $q_{ads,exp}$ corresponding to the removal percentage in each adsorption/desorption cycle performed.

4.2.4. Desorption studies with ethanol:water (90:10, % V/V) for recovery of vanillin, syringaldehyde, vanillic acid and syringic acid after adsorption from aqueous solution

Desorption studies with ethanol:water (90:10, % V/V) solutions were performed after feeding a SP700 fixed bed with aqueous solutions of vanillin, syringaldehyde, vanillic acid and syringic acid.

The adsorption was performed as described in Chapter 3 – section 3.2.6 for feed concentrations ranging from 0.4 to 4 g L^{-1} for the phenolic aldehydes and from 0.16 to 1.40 g L^{-1} for the phenolic acids, achieving loadings from 0.235 to 0.641 g $g^{-1}_{dry\ resin}$ for the phenolic aldehydes and 0.181 to 0.384 g $g^{-1}_{dry\ resin}$ for the phenolic acids.

In this study a smaller jacketed glass column was used of 5.6 cm length, 1 cm of internal diameter and 0.35 of bed porosity. One bed volume (BV) corresponds to the bed void volume of approximately 1.54 mL. Desorption experiments were carried out at the same temperature and feed flowrate employed during bed loading. Desorption concentrations were monitored by HPLC-UV as described before (Chapter 3 – section 3.2.2) and the experimental desorbed phase concentration ($q_{des,exp}$, g $g^{-1}_{dry\ resin}$) was calculated with Equation 3.8. A removal percentage for each desorption run was estimated considering the ratio between $q_{des,exp}$ and $q_{ads,exp}$. After each adsorption and desorption experiment, the bed was regenerated as described in 3.2.6 employing a 0.1 M $NaHCO_3$ solution.

4.3. Mathematical modelling

4.3.1. Adsorption equilibrium modelling

Linear and Freundlich models were applied to describe the adsorption equilibrium points obtained.

In the Linear isotherm (14), the concentration in the solid phase is proportional to the concentration in the liquid phase. It is assumed that the molecules adsorbed are widely spaced over the adsorbent surface and no interference between molecules occurs. The isotherm is described by the following expression:

$$q_{i,e} = K_{Lin} C_{i,e} \qquad \textbf{Equation 4.1}$$

where K_{Lin} (L $g^{-1}_{\text{dry resin}}$) is the equilibrium distribution coefficient.

The empirical Freundlich isotherm (15), given by Equation 3.13, considers an heterogeneous adsorbent surface; it is assumed that different adsorption energies are grouped into independent patches with no interaction (16).

The isotherm parameters were obtained by least-squares fitting of results in order to minimize the sum of the squared residuals (SSR) of the difference between experimental and predicted equilibrium adsorbed phase concentrations.

4.3.2. Fixed bed modelling

The experimental fixed bed breakthrough curves were predicted by a set of algebraic and differential equations including mass balance for the liquid phase, non-linear adsorption isotherm, and mass transfer between the liquid and solid phases descried by the linear driving force (LDF) model (17).

The mass balance in the liquid phase in a bed volume element for species '*i*' is defined by Equation 3.15. It is assumed an axially dispersed plug flow model with negligible radial dispersion, isothermal operation and constant bed voidage. The Danckwerts boundary conditions (18) were applied to define the boundary conditions of the mass balance (given by Equations 3.16 and 3.17). As initial conditions, a clean bed was considered for the adsorption stage (Equations 3.18 and 3.19).

An overall effective mass transfer coefficient k_s (min^{-1}) is considered and includes intraparticle and film mass resistances. The contribution of mass transfer resistances considers the LDF approximation and is written as follows:

$$\frac{\partial q_i(z,t)}{\partial t} = k_s\left[q_i^*(z,t) - q_i(z,t)\right] \qquad \textbf{Equation 4.2}$$

where q_i^* (g g^{-1} $_{dry\ resin}$) is the adsorbed phase concentration in equilibrium with the bulk concentration at time *t* in the position *z* and q_i (g $g^{-1}{}_{dry\ resin}$) is the average adsorbed phase concentration of species '*i*' in the adsorbent particles.

The axial dispersion in the packed bed was estimated by Equation 3.22, using the experimental Peclet number (*Pe*, dimensionless) obtained (14).

k_s was estimated considering two resistances in series by means of the following expression (19, 20):

$$\frac{1}{k_s} = \frac{r_p}{3k_f}\rho_{app} f_h \frac{dq_i^*}{dC_i} + \frac{\rho_{app} f_h r_p^2 \frac{dq_i^*}{dC_i}}{\Omega D_{pe,i}} = \frac{r_p}{3k_f}\rho_{app} f_h \frac{dq_i^*}{dC_i} + \frac{1}{k_{LDF}} \qquad \textbf{Equation 4.3}$$

where k_f (m min^{-1}) is the external film mass transfer coefficient, k_{LDF} (min^{-1}) is the LDF kinetic rate constant, r_p (m) is the radius of the adsorbent particle, f_h ($g_{dry\ resin}$ $g^{-1}{}_{wet\ resin}$) is the dry particle to wet particle mass ratio, ρ_{app} ($g_{wet\ resin}$ $L^{-1}{}_{wet\ resin}$) is the particle apparent density, $D_{pe,i}$ (m^2 min^{-1}) is the effective pore diffusivity, Ω (dimensionless) is the LDF factor equal to 15 considering spherical particles, $\frac{dq_i^*}{dC_i}$ is the slope of the adsorption equilibrium isotherm (corresponding to the slope of the chord $\Delta q/\Delta C$).

k_f was obtained by the Ranz-Marshall correlation (11):

$$Sh = \frac{k_f\, d_p}{D_{m,i}} = 2.0 + 0.6 Sc^{1/3}\,\mathrm{Re}^{1/2} \qquad \textbf{Equation 4.4}$$

where Sh, Sc and Re (dimensionless) are the Sherwood, Schmidt and Reynolds numbers, respectively, d_p (m) is the particle diameter, $D_{m,i}$ (m^2 min^{-1}) is the molecular diffusivity of solute *i* in the solvent.

$D_{m,i}$ of each solute was estimated by the Wilke-Chang correlation (21, 22) as indicated in Chapter 3 by Equation 3.24. The association factor (ϕ) suggested for ethanol of 1.5 was assumed for the experiments performed with ethanol:water (90:10, % V/V).

$D_{pe,i}$ was calculated by equation 3.23 (22) and tortuosity factor was estimated by the Wakao and Smith model (23), corresponding to the inverse of the particle porosity.

The mathematical model considered was solved in gPROMS (General Process Modelling System, version 3.7.1). The system of partial differential and algebraic equations (PDAEs) was solved numerically using the DASOLV integrated solver by discretizing the axial dimension onto 100 finite elements through a second order polynomial colocation method (OCFEM).

4.4. Results and discussion

4.4.1. Adsorption equilibrium isotherms of vanillin and syringaldehyde in ethanol:water (90:10, % V/V) onto SP700 resin

Batch and fixed bed experiments onto SP700 resin were conducted with vanillin and syringaldehyde in ethanol:water (90:10, % V/V) solutions at 298 K and 313 K. Fixed bed studies will be discussed with more detail in section 4.4.2. The adsorbed phase concentrations and respective equilibrium concentrations for all the experiments are plotted in Figure 4.1. It is possible to observe that within the range of equilibrium concentrations studied, no significant variations on the adsorption capacity were observed with temperature change. Therefore it was considered that no enthalpy change was involved in the adsorption process and all experiments were combined to assess the same Linear and Freundlich isotherms for both studied temperatures. Linear regression was performed to obtain the linear isotherm and Freundlich model parameters were obtained by least-squares fitting of the data through minimizing the sum of the squared residuals between the experimental points and the estimated values.

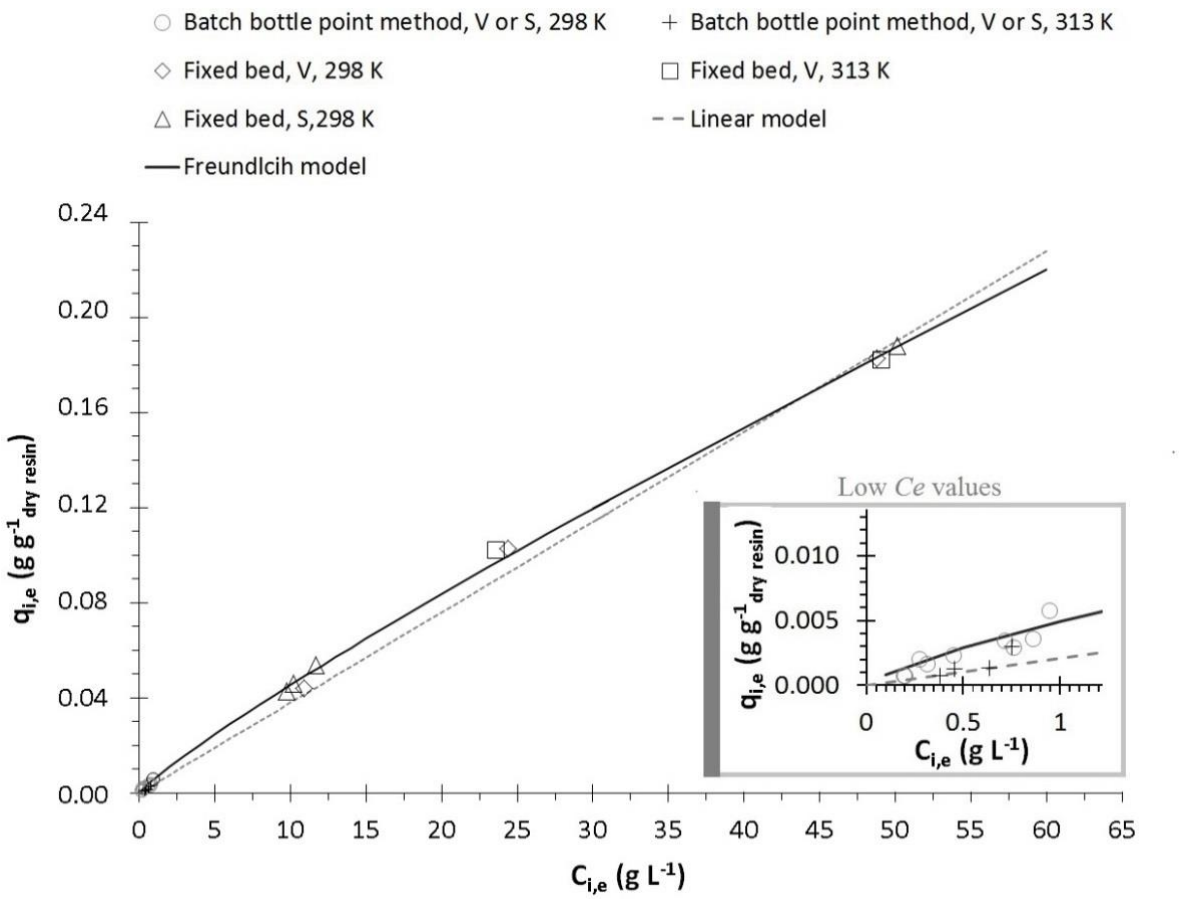

Figure 4.1 Adsorption isotherms of vanillin (V) and syringaldehyde (S) in ethanol:water (90:10, % V/V) onto the resin SP700 at 298 K and 313 K. The dots represent experimental data, the line (—) the Freundlich model plot and the dashed line (- -) the Linear model plot; V – vanillin and S - syringaldehyde.

The isotherm models obtained are plotted in Figure 4.1 and the respective parameters are indicated in Table 4.1. It is possible to observe that the adsorbed phase concentration varies almost linearly with the equilibrium concentration; however, the best fit is given by the Freundlich model. Since the adsorption is almost linear, *n* is very close to one (1.1) and inferior to that obtained for the adsorption of vanillin (*n* = 2.7) and syringaldehyde (*n* = 2.8) in aqueous solutions onto the same resin SP700. Moreover, the equilibrium constant K_F for adsorption of vanillin and syringaldehyde from ethanol:water (90:10, % V/V) are remarkably lower (Table 4.1) when compared with the equilibrium constant obtained for adsorption of vanillin and syringaldehyde from aqueous solution onto the same adsorbent (Table 3.2: K_F = 0.3350 (g $g^{-1}_{dry\ resin}$)(L g^{-1})$^{1/n}$ and K_F = 0.4076 (g $g^{-1}_{dry\ resin}$) (L g^{-1})$^{1/n}$ at 298 K, respectively).

Table 4.1 Equilibrium parameters obtained for adsorption of vanillin (V) and syringaldehyde (S) onto SP700 resin in ethanol:water (90:10, % V/V) solutions

Compound	T (K)	Model	Parameters		$\sum_{i=1}^{n}(q_{exp}-q_{calc})^2$	R^2
V or S	298 or 313	Linear	K_{Lin} (L $g^{-1}_{dry\ resin}$)	0.0038	$47.1x10^{-5}$	0.9947
		Freundlich	n	1.1	$9.93x10^{-5}$	0.9989
			K_F (g $g^{-1}_{dry\ resin}$)(L g^{-1})$^{1/n}$	0.0060		

These results meet what was experimentally observed: the adsorption of these compounds in ethanol:water (90:10, % V/V) solution was less favorable than it was in water. Therefore, in the former it is necessary higher equilibrium concentrations of each compound to reach the same adsorbed phase concentrations of vanillin or syringaldehyde in water.

Many studies have shown that polymeric resins can adsorb ethanol and other alcohols (24-30). Nielsen *et al.* (30) have shown that the higher the chain length of the alcohol, the greater is the adsorption capacity onto nonpolar resins due to the increase of the hydrophobic nature of the alcohol. Thus, the adsorptive interaction between the ethanol and the resin polymer occurring in preconditioning phase and its competitive effect with vanillin and syringaldehyde during the solution loading can partially explain the sharp decline in the adsorption capacity of these compounds when changing the solvent from water to ethanol:water (90:10, % V/V).

Moreover, the solubility of vanillin and syringaldehyde in ethanol:water (90:10, % V/V) mixture is higher than in water disfavoring the adsorption onto a resin of hydrophobic nature. In accordance, Payne *et al.* (31) have demonstrated this effect for phenol and anisole: these compounds did not adsorb onto styrene divinylbenzene resin when dissolved in hexane, but are both promptly adsorbed when the solvent is water.

When comparing the adsorption capacities of vanillin and syringaldehyde onto SP700 adsorbent dissolved in water (Table 3.2: 0.663 and 0.707 g $g^{-1}_{dry\ resin}$ for vanillin and syringaldehyde, respectively) or in ethanol:water (90:10, % V/V) solutions, one can infer that aqueous media favors adsorption and that ethanolic solutions are more suitable for desorption and recovery of the phenolic compounds.

4.4.2. Modelling of fixed bed adsorption and desorption of vanillin and syringaldehyde in ethanol:water (90:10, % V/V)

Fixed bed assays with ethanol:water (90:10, % V/V) solutions of vanillin or syringaldehyde were performed in a bed column of 11.3 cm length and 2.6 cm of diameter for a feed flowrate of approximately 1.1 mL min^{-1}. Different feed concentrations (ranging from 10 to 50 g L^{-1}) and two temperatures (298 K and 313 K) were studied with the purpose of completing batch adsorption experiments and thus, obtaining the isotherm models already discussed in the previous section. Table 4.2 summarizes the main results for each compound and condition. In general, the predicted stoichiometric times and adsorbed amounts obtained from the Freundlich model are closer to the experimental ones. This fact confirms the suitability of the Freundlich, compared with the Linear model, to describe the adsorption equilibrium data of vanillin and syringaldehyde, as previously referred.

A mathematical model considering mass balance, isotherm model and LDF approximation was implemented to describe the adsorption breakthrough curves obtained (detailed in 4.3). The parameters of the mathematical model (Reynolds, Schmidt and Sherwood numbers, axial dispersion, molecular diffusivity and effective pore diffusivity) are summarized in Table 4.3. For each experiment carried out, the overall mass transfer resistance coefficient estimated as described in section 4.3.2 is specified in Table 4.2 and accounts for the contribution of film and particle mass transfer resistances. Increasing the concentration, the slope $\Delta q/\Delta C$ decreases resulting in higher mass transfer coefficient k_s and thus, lower mass transfer resistances. Considering the experiments performed for vanillin at 298 K, through Figure 4.2 it is possible to observe the following trend: k_s increases linearly with the increase in concentration (with a correlation coefficient R^2 of 0.9721 obtained for vanillin).

Table 4.2 Mass transfer coefficients, predicted and experimental stoichiometric time, adsorbed and desorbed phase concentrations, and removal percentage for V and S in ethanol:water (90:10, % V/V) for each $C_{i,feed}$ and T (feed flowrate approximately 1.1 mL min^{-1}; bed of SP700 resin with 11.3 x 2.6 cm and porosity 0.35)

Compound	Isotherm	$C_{i,feed}$ g L^{-1}	T K	k_S min^{-1}	$t_{st,pred}$ min	$t_{st,\,exp}$ min	SD* %	$q_{ads,pred}$ g g$^{-1}_{\text{dry resin}}$	$q_{ads,exp}$ g g$^{-1}_{\text{dry resin}}$	$q_{des,exp}$ g g$^{-1}_{\text{dry resin}}$	Removal % (±4%**)
V	Freundlich	10.1	298	1.05	71.4	69.5	2.7	0.046	0.044	0.041	93
		24.4	298	1.16	66.2	68.8	3.9	0.100	0.103	0.102	99
		48.8	298	1.26	62.4	62.4	0.0	0.184	0.183	0.179	98
		23.6	313	1.76	66.6	68.6	3.0	0.097	0.102	0.089	87
		49.1	313	1.92	62.9	62.5	0.6	0.185	0.182	0.166	91
	Linear	10.1	298	1.25	62.8	69.5	10.7	0.038	0.044	0.041	93
		24.4	298	1.25	62.8	68.8	9.6	0.093	0.103	0.102	99
		48.8	298	1.25	62.8	62.4	0.6	0.185	0.183	0.179	98
		23.6	313	1.99	64	68.6	7.2	0.090	0.102	0.089	87
		49.1	313	1.99	63.4	62.5	1.4	0.187	0.182	0.166	91
S	Freundlich	9.7	298	0.95	71.6	69.5	2.9	0.044	0.043	0.044	102
		10.2	298	0.95	71.3	70.4	1.3	0.046	0.046	0.044	96
		11.7	298	0.97	71.8	73.5	2.4	0.052	0.054	0.052	96
		50.1	298	1.15	62.3	62.2	0.2	0.188	0.188	0.189	101
	Linear	9.7	298	1.14	62.8	69.5	10.7	0.037	0.043	0.044	102
		10.2	298	1.14	62.8	70.4	12.1	0.039	0.046	0.044	96
		11.7	298	1.14	64.0	73.5	14.8	0.044	0.054	0.052	96
		50.1	298	1.14	62.8	62.2	1.0	0.190	0.188	0.189	101

*SD (%) corresponds to the standard deviation between the experimental and predicted stoichiometric time, calculated with the following expression: SD (%) = $|t_{st,pred} - t_{st.exp}|/t_{st,pred}$ x 100;

** The standard deviation percentage was estimated for each experiment based upon the standard deviation calculated for $C_{i,feed}$ considering at least 4 measures and its error propagation in the adsorbed phase concentration.

Table 4.3 Parameters used for simulation of V and S breakthroughs in ethanol:water (90:10, % V/V) solutions , for a feed flowrate of 1.1 mL min^{-1} and a bed of SP700 resin with 11.3 x 2.6 cm and porosity 0.35

Compound	T K	Re	D*ax* m^2 min^{-1}	*Sc*	*Sh*	$D_{m,i}$ m^2 min^{-1}	$D_{pe,i}$ m^2 min^{-1}
V	298	0.0083	$4.98x10^{-6}$	3733	2.85	$3.23x10^{-8}$	$1.71x10^{-8}$
	313	0.0119	$4.98\ x10^{-6}$	1663	2.78	$4.99x10^{-8}$	$2.65x10^{-8}$
S	298	0.0083	$4.98\ x10^{-6}$	4126	2.88	$2.92x10^{-8}$	$1.55x10^{-8}$

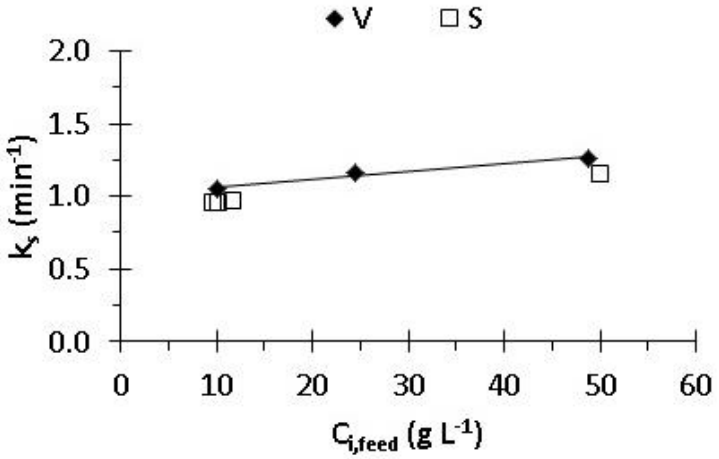

Figure 4.2 Representation of k_s vs feed concentration for V and S in ethanol:water (90:10, % V/V) solutions (298 K, feed flowrate of 1.1 mL min^{-1} and a bed of SP700 resin of 11.3 x 2.6 cm with 0.35 porosity).

Figure 4.3, Figure 4.4 and Figure 4.5 show the experimental and predicted adsorption breakthrough and desorption curves for of vanillin and syringaldehyde in ethanol:water (90:10, % V/V) solutions. Desorption experiments were performed at the same temperature as the respective breakthrough assays and employing the same solvent as the eluting solution (ethanol:water (90:10, % V/V) mixture).

Each breakthrough was modelled considering the equilibrium Linear and Freundlich isotherms obtained. A good agreement between the experimental values and the simulated breakthrough curve using the Freundlich model was found. The linear model obtained also gives a reasonable fit for the majority of experiments. As discussed previously in section 4.4.1, in the presence of ethanol:water (90:10, % V/V) the adsorption capacity varies almost linearly with the equilibrium concentration. This is the reason why the shape of the desorption curve is nearly the same as in the

experimental adsorption curve. Additionally, almost no influence of temperature in the adsorption capacity was verified, within the temperature range studied.

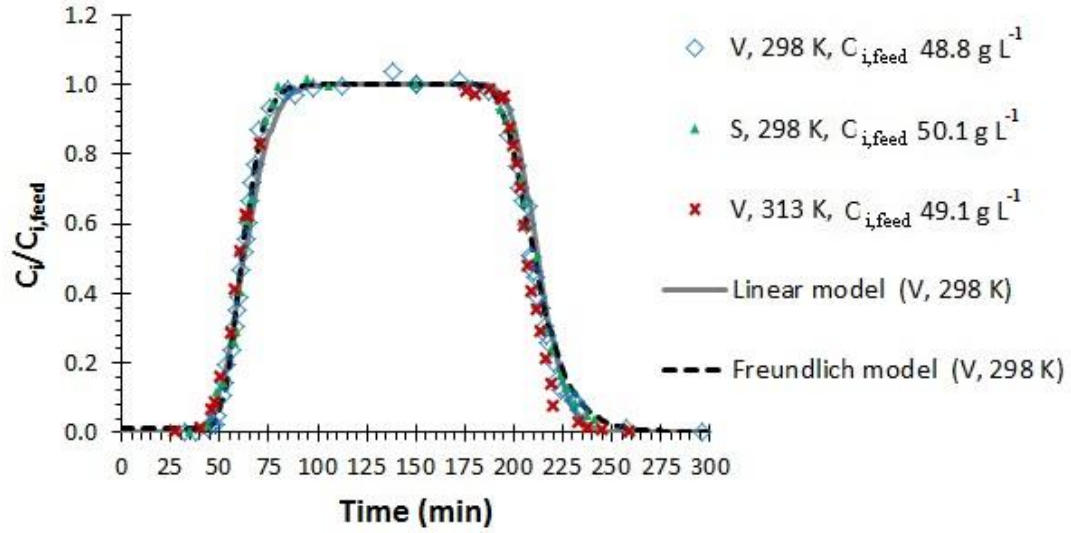

Figure 4.3 Normalized concentration of V and S versus time at the column outlet in the adsorption and desorption, both in ethanol:water (90:10, % V/V) solutions. Conditions: feed of approximately 50 g L^{-1} onto the SP700 resin at 298 K or 313 K, feed flowrate of 1.1 mL min^{-1}, in a bed of 11.3 x 2.6 cm and porosity 0.35: Points correspond to the experimental values, the line (—) the simulated mathematical model with Linear isotherm and the dashed line (- -) the simulated mathematical model with Freundlich isotherm.

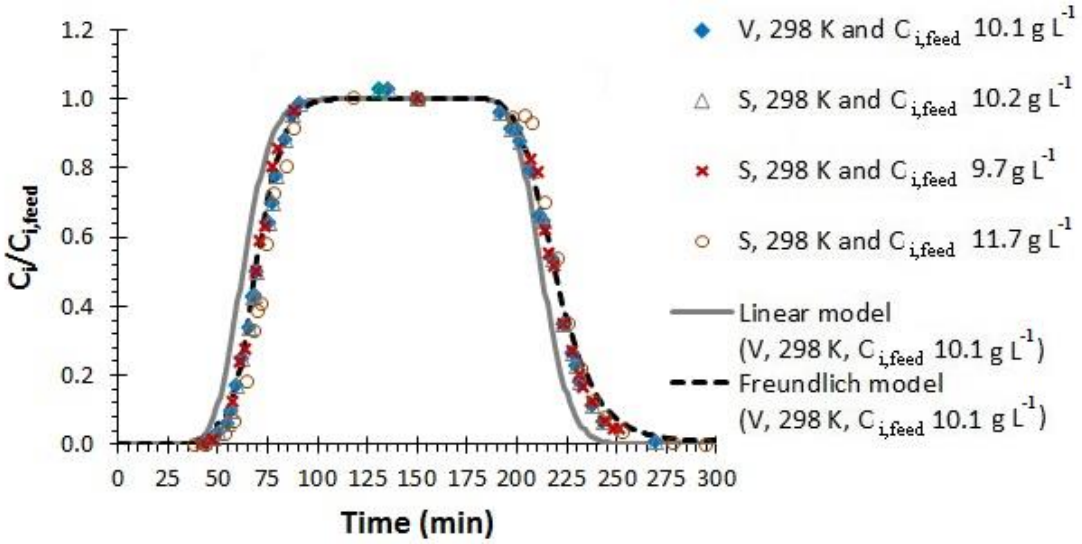

Figure 4.4 Normalized concentration of V and S in ethanol:water (90:10, % V/V) solutions versus time at column outlet in the adsorption and desorption, both in ethanol:water (90:10, % V/V) solutions. Conditions: feed of approximately 10-12 g L^{-1} onto the SP700 resin at 298 K, feed flowrate of 1.1 mL min^{-1}, in a bed of 11.3 x 2.6 cm and porosity 0.35: Points correspond to the experimental values, the line (—) the simulated mathematical model with

Linear isotherm and the dashed line (- -) the simulated mathematical model with Freundlich isotherm.

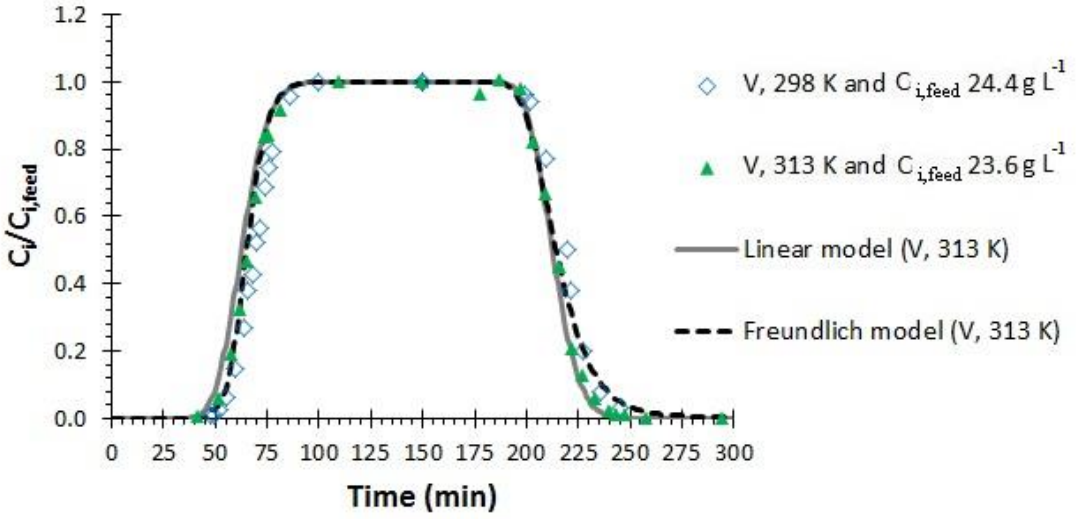

Figure 4.5 Normalized concentration of V in ethanol:water (90:10, % V/V) solutions versus time at column outlet in the adsorption and desorption, both in ethanol:water (90:10, % V/V) solutions. Conditions: feed of approximately 24 g L^{-1} onto SP700 at 298 K and 313 K, feed flowrate of 1.1 mL min^{-1}, in a bed of 11.3 x 2.6 cm and porosity 0.35: Points correspond to the experimental values, the line (—) the simulated mathematical model with Linear isotherm at 313 K and the dashed line (- -) the simulated mathematical model with Freundlich isotherm.

Table 4.2 shows the desorption percentages of the different experiments conducted for a similar desorption period of about 2 hours (approximately 6 BV). Afterwards, complete regeneration of the column proceeded by eluting the ethanol:water (90:10, % V/V) solution until no traces of vanillin or syringaldehyde were detected.

For each experiment, the removal percentage standard deviation was 4%, estimated for each experiment based upon the standard deviation calculated for $C_{i,feed}$ considering at least 4 measures and its error propagation in the adsorbed phase concentration. Therefore, for experiments with desorption amounts higher than 96% it is considered that complete recovery of the compound was achieved within 2 hours. Additionally, this explains the desorption amounts higher than 100% obtained. Errors associated with concentration measurement and inaccurate integration of the areas due to lack of experimental points can also contribute to the values of desorption amounts higher than 100%.

In general, complete regeneration of the bed was achieved for all fixed bed assays. However, for experiments conducted at 313 K complete desorption of the compounds took longer time than at 298 K. From Table 4.2, it is possible to observe that after saturating the column with a feed stream of approximately 24 g L^{-1} and desorption period of 2 h, about 87% of vanillin was recovered at 313 K assay against the 99% of vanillin desorbed at 298 K. A similar observation can be made for vanillin experiments conducted at a feed stream of 49 g L^{-1}.

4.4.3. Desorption studies with ethanol:water (90:10, % V/V) for recovery of vanillin, syringaldehyde, vanillic acid and syringic acid after adsorption from aqueous solution

The choice of the desorption solvent is very important to determine the viability of an adsorption process. The solvent must overcome van der Waals attractive forces that bind the adsorbate to the resin, and assure enough solubilization of the adsorbates after solvent diffusion to and from the adsorption site.

Previously, in Chapter 3, it was shown that desorbing vanillin and syringaldehyde from a packed bed of SP700 resin with water can be a very time consuming process and consequently, compounds are considerably diluted. Employing organic solvents as eluting agents (such as methanol, ethanol or acetone) instead of water can be of great advantage. It is known that organic solvents have a lower solubility parameter (e.g. methanol 14.5 $cal^{0.5}$ $cm^{-1.5}$, ethanol 12.7 $cal^{0.5}$ $cm^{-1.5}$, acetone 9.8 $cal^{0.5}$ $cm^{-1.5}$) than water (23.2 $cal^{0.5}$ $cm^{-1.5}$) (3, 32), which turns them more suitable solvents for elution/regeneration, when employing nonpolar resins. Ethanol can be a keen choice since it has the additional advantages of being a low-toxicity solvent widely used in perfumes and flavors and a posterior step of distillation or crystallization can be easily implemented comparatively to water, for example.

Published literature (6, 7) for similar synthetic cross-linked polymeric resins like the one used in this work has shown the advantage of employing aqueous ethanolic solutions to recover the phenolics compounds. The highest desorption amounts were achieved when employing pure ethanol or an aqueous ethanol mixture with ethanol concentration of 80% V/V. Taking this studies into consideration, a solution of ethanol:water (90:10, % V/V) was chosen to proceed with the recovery studies.

After loading a packed bed of SP700 resin with different vanillin and syringaldehyde aqueous solutions, desorption experiments were performed employing the selected eluent. Experimental conditions are summarized in Table 4.4 along with the k_s estimated by Equation 4.3 and used in the mathematical predictions of the elution histories. For this forecasts it was verified that the film mass transfer resistance had almost an equal contribution as the particle mass transfer resistance (data summarized in Table 4.4).

Table 4.4 Parameters used for simulation of V or S desorption histories employing ethanol:water (90:10, % V/V) solution after loading the bed with aqueous solutions of V and S of different $C_{i,feed}$, for a feed flowrate of 5 mL min^{-1} and a bed of SP700 resin with 5.6 x 1 cm and porosity 0.35

Compound	$C_{i,feed}$ (g L^{-1})	$q_{ads,exp}$ (g g$^{-1}_{dry\ resin}$)	T (K)	k_{LDF} (min^{-1})	k_f (min^{-1})	k_s (min^{-1})
V	0.38	0.238 0.235	298	2.02	2.55	1.13
	1.07	0.343	298	2.29	2.89	1.28
	1.11	0.314	313	3.55	4.62	2.01
	3.94	0.554	298	2.67	3.37	1.49
S	0.96	0.412	298	2.04	2.65	1.15
	0.98	0.356	313	3.18	4.23	1.82
	4.11	0.641	298	2.43	3.14	1.37

In Figure 4.6 it is depicted the experimental elution curves obtained using ethanol:water (90:10, % V/V) mixture and the predicted desorption histories according to the mathematical model presented in section 4.3 and considering Freundlich isotherm. The maximum desorption concentration occurred before 1 min elution (slightly after 3 BV), and then the concentration sharply decreased within 5 minutes. After that time, the amount of vanillin or syringaldehyde eluted was very low.

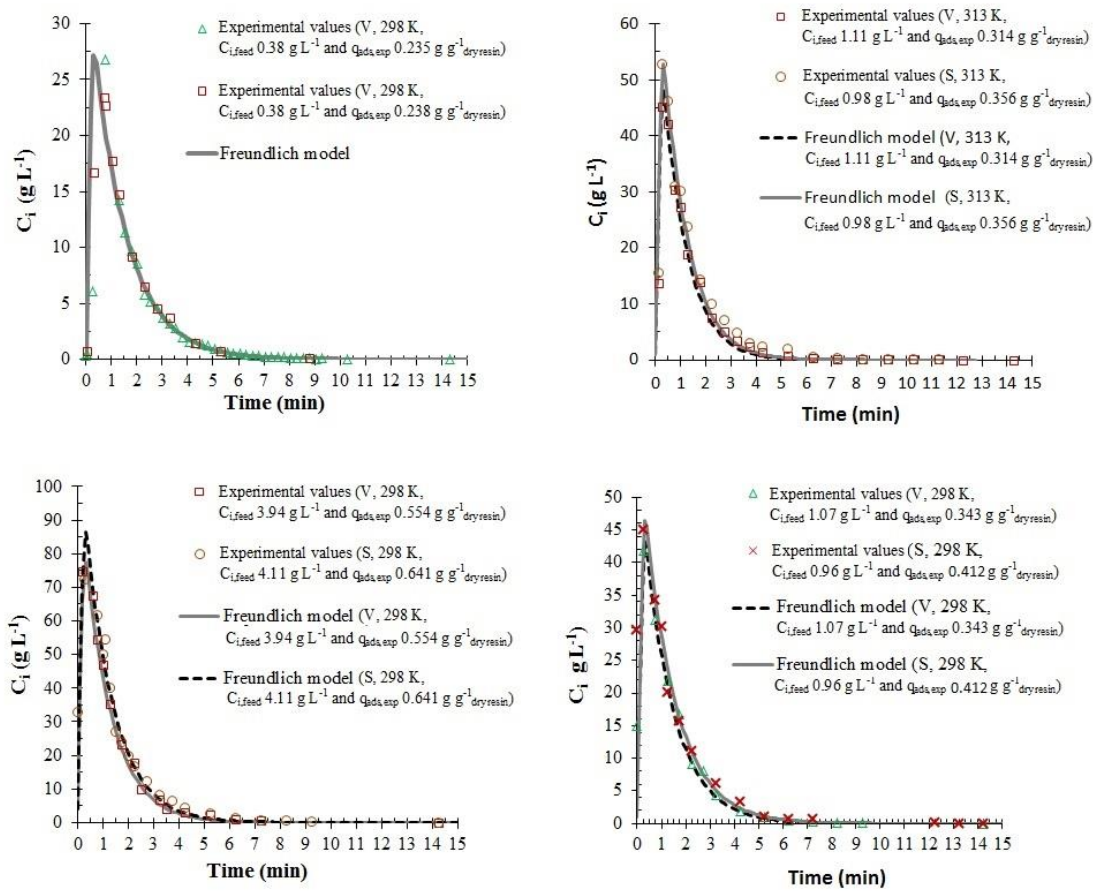

Figure 4.6 Elution histories with ethanol:water (90:10, % V/V) solution after adsorption of V or S in aqueous solution onto SP700 resin at 298 K and 313 K, feed flowrate of 5 mL min^{-1}, in a bed of 5.6 x 1 cm and porosity 0.35: Points correspond to experimental data and lines to the mathematical modelling with the Freundlich isotherm.

In general, the mathematical model fits well the experimental data. For predictions of desorption with vanillin and syringaldehyde loadings of 0.554 and 0.641 g $g^{-1}_{dry\ resin}$, respectively, the simulation predicted a maximum concentration peak near 90 g L^{-1}, somewhat higher than the experimentally detected near 75 g L^{-1}. One of the reasons that may explain these differences could be the mass transfer resistance coefficient estimation.

Table 4.5 summarizes the desorbed amounts of vanillin and syringaldehyde accomplished with eluting with 16 bed volumes employing ethanol/water (90:10, % V/V) solutions. When comparing these elution histories with the ones obtained using water as eluent, in the same conditions (Figure 3.8), it is very clear the advantage of using ethanolic solution to recover the adsorbed phenolic compounds: more than 84% of the compounds were recovered using ethanol/water (90:10, % V/V) with less than 16 bed volumes (5 minutes) against the 1750 bed volumes (9 hours of elution) used

to recover about 83-85% of the adsorbed phenolics when using water (shown in Chapter 3 – section 3.4.3).

Table 4.5 Average final concentrations for 5 minutes elution of V, S, vanillic acid (VA) and syringic acid (SA) with ethanol:water (90:10, % V/V) at feed flowrate of 5 and 5.25 mL min^{-1} for the aldehydes and acids, respectively

	T (K)	$C_{i,feed}$ (g L^{-1})	$q_{ads,exp}$ (g g$^{-1}_{dry\ resin}$)	$q_{des,exp}$ (g g$^{-1}_{dry\ resin}$)	Removal % (± 5%)	$C_{average}$ Δ5min (g L^{-1})
V	298	0.38	0.235	0.198	84	7.3
	298	0.38	0.238	0.214	90	8.1
	298	1.07	0.343	0.336	98	13.8
	298	3.94	0.554	0.498	90	25.7
	313	1.11	0.314	0.314	100	13.2
S	298	0.96	0.412	0.375	91	15.2
	298	4.11	0.641	0.609	95	24.7
	313	0.98	0.356	0.349	98	15.4
VA	288	1.40	0.384	0.317	83	11.7
	298	0.67	0.235	0.214	91	7.7
	298	1.24	0.296	0.275	93	9.9
	313	1.39	0.262	0.254	97	9.1
SA	298	0.69	0.320	0.315	98	11.2
	298	0.16	0.183	0.169	92	5.8
	313	0.71	0.287	0.280	98	10.2

$C_{average}$ Δ5min – average concentration for 5 minutes elution

With elution performed with ethanol:water (90:10, % V/V) for 16 BV: about 25 mL of solution was collected having average concentrations of nearly 8, 14 and 25 g L^{-1} according to the feed concentration studied being 0.4, 1 or 4 g L^{-1}, respectively.

Desorption studies with ethanol:water (90:10, % V/V) were performed for vanillic and syringic acids as well, after being adsorbed from aqueous solutions onto SP700 resin. Similar results as obtained for the phenolic aldehydes were obtained.

Several temperatures and initial feed concentrations were applied during the loading stage, leading to different loading amounts of the bed, ranging from 0.183 to 0.384 g g$^{-1}_{dry\ resin}$. More than 83% of vanillic and syringic acids adsorbed were recovered with 20 BV and final enriched solutions of each phenolic acid were obtained (ranging from 5.8 to 11.7 g L^{-1}). The behavior of the eluted

concentration with time for each experiment is shown in Figure 4.7. Similar desorption histories for approximately the same loading amounts were observed at 298 K and 313 K (Figure 4.7-A and -B), with a maximum concentration peak near 40 g L^{-1} for vanillic acid and near 47 g L^{-1} for syringic acid.

In Figure 4.7-C and -D it is depicted desorption histories at 298 K for two different loading amounts of vanillic acid ad syringic acid, respectively. Similarly to what was observed for the phenolic aldehydes (Figure 4.6), the maximum concentration peak increased with the increase of the loaded amount.

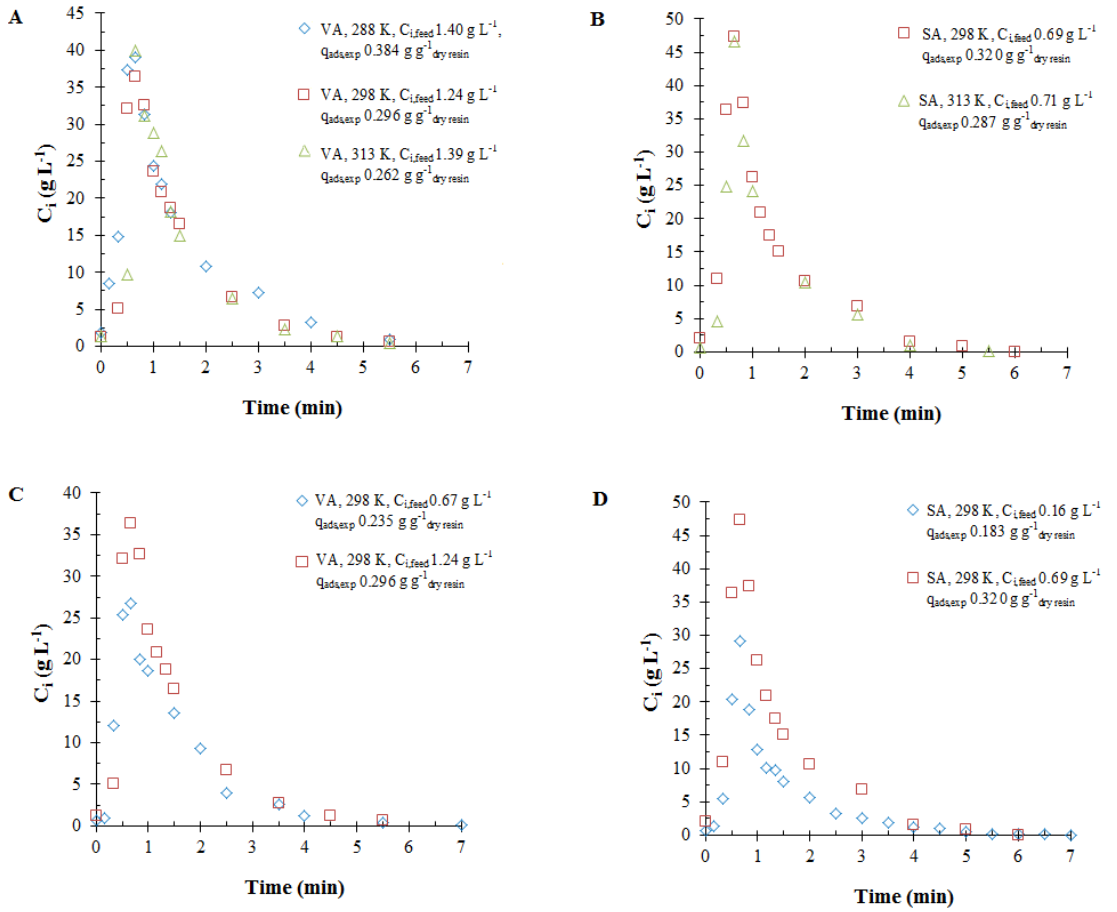

Figure 4.7 Elution profiles with ethanol:water (90:10, % V/V) solution after adsorption of vanillic (VA) - A and C - and syringic (SA) acids - B and D - in aqueous solution onto SP700 resin at different temperatures, flowrate of approximately 5.25 mL min^{-1}, in a bed of 5.6 x 1 cm and porosity 0.35: Points correspond to experimental data.

Fixed bed desorption studies revealed that SP700 can be easily regenerated and re-utilized since the phenolic compounds can be almost completely recovered, as indicated by the removal percentage

given in Table 4.5. This supports the observation already stated in Chapter 3 being an additional confirmation that the adsorption nature is mainly physical and that the adsorption process can be reversed.

The results of this work are very promising considering the application of this polymeric resin to recover vanillin, syringaldehyde, vanillic acid and syringic acid from mixtures resulting from lignin oxidation.

In addition to the high capacity of this resin for vanillin and syringaldehyde adsorption, as previously stated in Chapter 3, this work demonstrates the successful desorption of vanillin and syringaldehyde with few bed volumes of ethanolic solution with simultaneous concentration of vanillin and syringaldehyde in the final solution. This is advantageous in the perspective of the further processing steps to produce purified fractions of each phenolic compound.

Nonetheless, it is important to highlight that studies with real solutions of oxidized lignin must be carried out in order to understand the influence of other reaction products in the adsorption and desorption performance of vanillin and syringaldehyde and to evaluate the resin lifetime.

4.5. Conclusions

In this work, adsorption and desorption studies of vanillin and syringaldehyde onto SP700 resin were performed employing ethanol:water (90:10, % V/V) solutions. Adsorption equilibrium isotherms were obtained and an almost linear trend between the adsorbed phase concentration and the equilibrium liquid concentration was observed. The adsorption capacity for vanillin and syringaldehyde was negatively affected by the presence of ethanol, when compared to adsorption capacities existing in literature for aqueous medium. Experimental data were fitted to Linear and Freundlich isotherm models, concluding that the latter provided a better description of the experimental data. Freundlich isotherm constants for vanillin and syringaldehyde were 68 and 83 times smaller, respectively, in the presence of ethanol:water (90:10, % V/V) solution than for the corresponding aqueous solutions. Experiments conducted at 298 K and 313 K revealed that, within the equilibrium concentration range studied (0.3 – 50 g L^{-1}), the temperature effect was negligible for both compounds.

Fixed bed adsorption studies with vanillin and syringaldehyde in ethanol:water (90:10, % V/V) solutions were performed for different feed concentrations and temperatures. The respective breakthrough curves were successfully modelled considering the isothermal operation with the Freundlich isotherm, plug flow with axial dispersion and LDF approximation.

The advantage of loading the SP700 bed with aqueous solution of vanillin, syringaldehyde, vanillic acid and syringic acid and performing its desorption with ethanol:water (90:10, % V/V) solution was clearly stated in this work. More than 83% of recovery was accomplished with 16-20 BV, allowing obtaining enriched final solutions of each phenolic compound. For loadings between 0.183 and 0.642 g $g^{-1}_{dry\ resin}$ (corresponding to different aqueous solutions of each phenolic compound ranging from 0.16 to 4.1 g L^{-1}), final average concentration samples ranging from 5.3 and 25.7 g L^{-1} were obtained. The total regeneration of the bed is possible by extending the elution to a total of 55 bed volumes.

4.6. References

1. Soto, M. L., Moure, A., Domínguez, H. and Parajó, J. C. (2011) Recovery, concentration and purification of phenolic compounds by adsorption: A review. J. Food Eng., 105: 1-27.
2. Crittenden, B. D. and Thomas, W. J. (1998) Adsorption Technology and Design. First edition, Butterworth and Heinemann: Oxford, United Kingdom.
3. Kunin, R. (1991) 1.11 Polymeric adsorbents: In Ion Exchangers. Konrad Dorfner. De Gruyter: New York, United States of America.
4. Hildebrand, J. H. and Scott, R. L. (1950) Solubility of Non-Electrolytes. Reinhold: New York, United States of America.
5. Wypych, G. (2001) 2. Fundamental principles governing solvents use: In Handbook of solvents. George Wypych ed. ChemTec Publishing: Toronto, Canada.
6. Zhang, Q.-F., Jiang, Z.-T., Gao, H.-J. and Li, R. (2008) Recovery of vanillin from aqueous solutions using macroporous adsorption resins. Eur. Food Res. Technol., 226: 377-383.
7. Xiao, G.-Q., Xie, X.-L. and Xu, M.-C. (2009) Adsorption performances for vanillin from aqueous solution by the hydrophobic - hydrophilic macroporous polydivinylbenzene / polyacrylethylenediamine IPN resin. Acta Phys.-Chim. Sin., 25: 97-102.
8. Kammerer, D. R., Saleh, Z. S., Carle, R. and Stanley, R. A. (2007) Adsorptive recovery of phenolic compounds from apple juice. Eur. Food Res. Technol., 224: 605-613.
9. Zhao, R., Yan, Y., Li, M. and Yan, H. (2008) Selective adsorption of tea polyphenols from aqueous solution of the mixture with caffeine on macroporous crosslinked poly(N-vinyl-2-pyrrolidinone). React. Funct. Polym., 68: 768-774.

10. Wang, Z., Chen, K., Li, J., Wang, Q. and Guo, J. (2010) Separation of vanillin and syringaldehyde from oxygen delignification spent liquor by macroporous resin adsorption. Clean, 38: 1074-1079.

11. Ruthven, D. M. (1984) Principles of Adsorption and Adsorption Processes. John Willey and Sons: New York, United States of America.

12. Rodrigues, A. E., Levan, M. D. and Tondeur, D. (1989) Adsorption: Science and Technology. First edition, Kluwer Academic Publishers: London, United Kingdom.

13. Wankat, P. C. (1994) Rate-controlled separations. Blackie Academic & Professional: London, United Kingdom.

14. Guiochon, G., Felinger, A., Shirazi, D. G. G. and Katti, A. M. (2006) Fundamentals of Preparative and Nonlinear Chromatography. Second edition, Elsevier Academic Press: Oxford, United Kingdom.

15. Freundlich, H. M. F. (1909) Kapillarchemie. Akademische Verlagsgesellschaft: Leipzig.

16. Duong, D. D. (1998) Adsorption Analysis: Equilibria and Kinetics. Imperial College Press: London, United Kingdom.

17. Glueckauf, E. and Coates, J. I. (1947) 241. Theory of chromatography. Part IV. The influence of incomplete equilibrium on the front boundary of chromatograms and on the effectiveness of separation. J. Chem. Soc. (Resumed), 1315-1321.

18. Danckwerts, P. V. (1953) Continuous flow systems. Chem. Eng. Sci., 2: 1-13.

19. Farooq, S. and Ruthven, D. M. (1990) Heat effects in adsorption column dynamics. 2. Experimental validation of the one-dimensional model. Ind. Eng. Chem. Res., 29: 1084-1090.

20. Silva, J. and Rodrigues, A. E. (1997) Fixed-Bed Adsorption of n-Pentane/Isopentane Mixtures in Pellets of 5A Zeolite. Ind. Eng. Chem. Res., 36: 3769-3777.

21. Wilke, C. R. and Chang, P. (1955) Correlation of diffusion coefficients in dilute solutions. AIChE Journal, 1: 264-270.

22. Reid, R. C., Prausnitz, J. M. and Poling, B. E. (1987) The Properties of Gases and Liquids. Fourth edition, McGraw Hill: New York.

23. Smith, J. M. (1981) Chemical Engineering Kinetics. McGraw-Hill Chemical Engineering Series: New York, United States of America.

24. Zhou, J., Wu, J., Liu, Y., Zou, F., Wu, J., Li, K., Chen, Y., Xie, J. and Ying, H. (2013) Modeling of breakthrough curves of single and quaternary mixtures of ethanol, glucose, glycerol and acetic acid adsorption onto a microporous hyper-cross-linked resin. Bioresour. Technol., 143: 360-368.

25. Nielsen, D. R. and Prather, K. J. (2009) In situ product recovery of n-butanol using polymeric resins. Biotechnology and Bioengineering, 102: 811-821.

26. Lin, X., Wu, J., Fan, J., Qian, W., Zhou, X., Qian, C., Jin, X., Wang, L., Bai, J. and Ying, H. (2012) Adsorption of butanol from aqueous solution onto a new type of macroporous adsorption resin: Studies of adsorption isotherms and kinetics simulation. J. Chem. Technol. Biotechnol., 87: 924-931.

27. Groot, W. J. and Luyben, K. C. A. M. (1986) In situ product recovery by adsorption in the butanol/isopropanol batch fermentation. Appl. Microbiol. Biotechnol., 25: 29-31.

28. Delgado, J. A., Águeda, V. I., Uguina, M. A., Sotelo, J. L., García, A., Brea, P. and García-Sanz, A. (2013) Separation of ethanol–water liquid mixtures by adsorption on a polymeric resin Sepabeads 207®. Chem. Eng. J., 220: 89-97.

29. Nielsen, L., Larsson, M., Holst, O. and Mattiasson, B. (1988) Adsorbents for extractive bioconversion applied to the acetone-butanol fermentation. Appl. Microbiol. Biotechnol., 28: 335-339.

30. Nielsen, D. R., Amarasiriwardena, G. S. and Prather, K. L. J. (2010) Predicting the adsorption of second generation biofuels by polymeric resins with applications for in situ product recovery (ISPR). Bioresour. Technol., 101: 2762-2769.

31. Payne, G. F., Payne, N. N., Ninomiya, Y. and Shuler, M. L. (1989) Adsorption of nonpolar solutes onto neutral polymeric sorbents. Sep. Sci. Technol., 24: 457-465.

32. Ruoff, R. S., Tse, D. S., Malhotra, R. and Lorents, D. C. (1993) Solubility of fullerene (C60) in a variety of solvents. J. Phys. Chem., 97: 3379-3383.

5. Membrane separation of oxidized industrial kraft liquor[1]

From the point of view of sustainability of lignocellulosic based biorefineries, membrane and adsorption processes are promising technologies to be combined after production of sodium salts of vanillin and syringaldehyde by chemical oxidation of lignin.

This chapter addresses a membrane fractionation study of an oxidized industrial kraft liquor (IKL). A three stage fractionation sequence is performed with 50, 5 and 1 kDa molecular weight cut-off membranes to study the productivity of each membrane and the respective retention coefficients to total solids, ashes and low molecular weight phenolates quantified by HPLC.

The main goal of this fractionation sequence is to obtain a final stream depleted in the higher molecular weight compounds and richer in the lower ones (e.g. vanillin, syringaldehyde). Gel permeation chromatography analysis is conducted to help understanding the influence of each membrane stage in the molecular weight distribution of the compounds.

Permeate fluxes and concentration of the different families of solutes in the permeate and retentate streams are monitored. Cleaning efficiency of each membrane is evaluated employing 0.1 NaOH solution. The contribution of reversible and irreversible fouling for flux decline is analyzed by applying the resistances-in-series approach.

[1] The following paper is in preparation

Mota, I. F., Pinto, P. C. R., Ribeiro, A. M., Loureiro, J. M., Rodrigues, A. E. Downstream processing of an oxidized industrial kraft liquor by membrane fractionation for vanillin and syringaldehyde recovery (in preparation).

5.1. Introduction

In the perspective of lignin valorization, ultrafiltration (UF) or nanofiltration (NF) are promising membrane separation technologies to recover the low molecular weight phenolic compounds of interest from the reaction medium of depolymerized lignin (1-3). Besides having the particularity of being easily integrated after the oxidation process, membrane separation constitutes a good alternative over other methods (e.g. LLE, evaporation, distillation) since it is an environmentally friendly technology with lower energy requirements, good physical and chemical stability, reproducible performance and selectivity (4). The key bottlenecks to overcome in membrane separation processes are the careful selection of the membranes (e.g. cut-off, material and configuration) and operating variables in order to tune the process towards obtaining the desired retention levels while assuring an efficient utilization of the membranes with longer longevity and acceptable productivities.

This technology is already widely applied in wastewater treatment, food processing, chemicals recovery, and biotechnology and pharmaceutical industries (4-7). Several efforts at innovating with new membrane materials and process technologies to improve membrane processes performance and profitability are also found in literature (8-10). Furthermore, membrane technology application in lignocellulosic-derived streams has been the subject of many studies for lignin fractionation or concentration and recovery of hemicellulose or inorganic chemicals (e.g. sodium hydroxide) (11-17). UF is the most extensively separation process studied; however, NF has also been applied by some authors and proved to be beneficial to separate, for example, hemicelluloses from lignin with reasonable costs (16, 18). Regarding lignin concentration, UF has been successfully implemented in order to reduce reagents consumption during lignin isolation (19).

To our knowledge there are only two studies applying pressure driven processes aiming at the fractionation of oxidized lignin solutions and recovery of the high added value monomers. One of these studies encompasses the UF of a synthetic mixture of lignin/vanillin (2) and is focused on the influence of membrane cut-off and process variables pH, temperature and feed concentration on membrane productivity and vanillin recovery. A second study applies NF to a lignin oxidized medium after being extracted with ethyl acetate (3) and evaluates its performance in separating the monomers from the other higher molecular weight fractions of lignin oxidation products. Main achievements and results of these studies have already been summarized in the state of the art (Table 2.9). Both studies are important in the evaluation of the suitability of this technology in the recovery/concentration of compounds of interest and to understand the influence of the type of membrane and operating conditions.

In membrane processes, two distinct and, at the same time, valuable streams can be obtained from the oxidized lignin reaction medium: an enriched solution with simple phenolic compounds with high added value (e.g. vanillin and syringaldehyde) collected in the permeate stream and a concentrated solution in the retentate stream with higher fractions of depolymerized lignin with great potential for the production of lignin-based polymers (2, 20-22). In order to obtain purified fractions of vanillin and syringaldehyde from the permeate stream, the inclusion of other purification treatments such as ion-exchange, adsorption and crystallization have been suggested (1, 23, 24).

In membrane separation processes, flux decline is a major concern and it is important to understand the key factors influencing membrane productivity in order to develop an economical feasible process.

A typical evolution of flux with time can be described in 3 phases: 1) initial accentuated drop of flux; 2) long-term gradual decrease of flux and 3) reaching of a steady-state flux (4, 25). The initial accentuated drop of flux is mainly attributed to osmotic pressure mechanism happening in the first seconds of operation. The solute buildup at membrane surface will increase and the concentration boundary layer is established. After that the flux will decrease more gradually, the membrane surface concentration remains the same, while the thickness of the polarized layer rises progressively until reaching a steady state, dependent on the hydrodynamic conditions (25-27).

Concentration polarization due to solute buildup at the membrane surface and fouling problems like pore blockage and solute adsorption, are the major factors responsible for flux decline during operation with complex solutions, such as the case of depolymerized lignin solutions (4, 9). Membrane fouling is a consequence of concentration polarization and is intrinsically related with the chemistry of the membrane surface and solute that determines the type of solute-membrane and solute-solute interactions. The former will be responsible for fouling by adsorption of solute on the membrane surface (electrostatic attractions/repulsions) and the latter influences fouling caused by solute aggregation in solution and/or to molecules already adsorbed on the surface of the membrane.

The concentration polarization phenomena can be minimized by establishing the best set of operating conditions that reduce its effects such as equipment design, transmembrane pressure (TMP) applied, temperature, flowrate and feed concentration (4). Besides the manipulation of the operating parameters, the use of electric fields (10) or modification of membrane surface chemistry (8) are also some of the methods that could be applied to reduce concentration polarization phenomena and control fouling.

Concentration polarization is considered as a reversible process. According to the type of solute-membrane interactions, membrane fouling can be classified as reversible or irreversible process. The additional reversible and irreversible resistances responsible for the decrease of permeate flux can be assessed performing a physical cleaning (rinsing with solvent without TMP) and measuring the permeate flux to water after cleaning. Irreversible fouling will be responsible for the decrease of the original membrane permeability and, if it is not significant, the membrane permeability can be restored with chemical cleaning (e.g. employing NaOH solutions).

In this work a fractionation sequence of an oxidized industrial kraft liquor (IKL) solution was studied for the first time, employing different tubular ceramic membranes with 50, 5 and 1 kDa molecular weight cut-offs. This solution contains depolymerized lignin and low molecular weight phenolics such as vanillin, syringaldehyde, among others. The evolution of permeate flux was monitored in each stage and a resistance-in-series model was used to analyze and quantify the fouling formation. Moreover, each permeate and retentate stream was characterized regarding total non-volatile solids content (TS), ashes and total low molecular weight phenolates quantified by HPLC-UV (TP), in particular the sodium salts of vanillin and syringaldehyde contents and the respective apparent rejection coefficients calculated.

5.2. Experimental description

5.2.1. Chemicals and analytical methods

A membrane fractionation sequence was conducted with an oxidized industrial kraft liquor (IKL) solution enriched in some phenolic compounds of interest. About 20 L of oxidized IKL was produced in a structured packed bubble column reactor in alkaline medium using a mixture O_2/N_2. This solution was diluted 3 times and enriched in vanillin (V, purity ≥ 98%), syringaldehyde (S, purity ≥ 98%), vanillic acid (VA, purity ≥ 97%), syringic acid (SA, purity ≥ 95%)), acetovanillone (OV, purity ≥ 98%), acetosyringone (OS, purity ≥ 97%) and *p*-hydroxybenzaldehyde (*p*-OHB, Aldrich, purity ≥ 98%), supplied by Sigma-Aldrich, in order to have the composition expected in the batch oxidation process. The final pH value of the solution was 10.1.

Different concentration NaOH (Sigma-Aldrich, purity ≥ 98%) solutions were prepared with deionized water to assess membrane fouling and to clean the membranes.

Feed, retentate and permeate streams were characterized regarding total non-volatile solids, ashes content, viscosity determined by using capillary viscometers, low molecular weight phenolate compounds quantified by HPLC-UV, and molecular weight distribution by GPC.

Total non-volatile solids (*TS*, g L^{-1}) and ash content (*ashes*, g L^{-1}) were gravimetrically determined as described elsewhere (28) with minor modifications: 0.020 L of each sample (V_{sample}, L) was added to prior dried crucibles containing sieved and calcined sand at 900 ºC. Afterwards, the crucibles were dried overnight in an oven (Venticell, MMM Group, Germany) at 105 ºC and incinerated (Eurotherm, USA) at 650 ºC for 10 hours for TS and ashes quantification, respectively. After each drying or incinerating step, samples were let to cool down in an exsicator before weighing in an analytical balance (model ABT 220-5D, Kern & Sohn GmbH, Germany) allowing to obtain the weight of the *TS* (W_{TS}, g) and *ashes* (W_{ashes}, g). *TS* and *ashes* content were determined at least in duplicate and are defined by the following equations

$$TS = \frac{W_{TS}}{V_{sample}}$$ **Equation 5.1**

$$ashes = \frac{W_{ashes}}{V_{sample}}$$ **Equation 5.2**

Ashes content (W_{ashes} per W_{TS}) was also confirmed by incinerating about 0.10-0.25 g of dried sample at 650 ºC. An average value between both determination methods was used to determine the ashes content.

Kinematic viscosities of the feed, permeate, and retentate streams were measured with 'Cannon Fenske' type capillary viscometers (COMECTA, Spain) immersed in a water bath at 25 ºC ±0.5 ºC. Two routine viscometer series were used (75 and 50) in order to ensure flow times above 200 seconds, thus enabling ignoring the correction of kinetic energy. These viscometers allow measuring kinematic viscosities from 0.8 to 6.4 cSt. The analysis procedure encompasses measuring the flow time of one sample between two marks indicated in the viscometer. The measurement was repeated three times for each sample and the kinematic viscosity (ν, cSt) determined by the following expression:

$$\nu = \kappa t$$ **Equation 5.3**

where κ (cSt s^{-1}) is the nominal constant equal to 0.004 cSt s^{-1} for viscometer series 50 and 0.008 cSt s^{-1} for viscometer series 75. The dynamic viscosity (μ, cP) is obtained as follows:

$$\mu = \nu\rho$$ **Equation 5.4**

where ρ (g cm^{-3}) is the density of the solution. The density of the solution was experimentally obtained by weighting a known volume of sample at 25 ºC. This procedure was performed in triplicate. The density corresponds to the ratio between the sample weight and the corresponding measured volume.

The total low molecular weight phenolate compounds concentration (*TP*, g L^{-1}) was determined by high performance liquid chromatography with ultraviolet detection (HPLC-UV). A Knauer HPLC system (Germany) equipped with a Smartline 5000 online degasser, a Smartline 1000 quaternary pump, and a Smartline 2600 UV-DAD was used. The analytical column was an ACE 5 C18-pentafluorophenyl group (250 x 3.0 mm, 5 µm) with a guard column of the same material. The detection wavelength was set to 280 nm and the volume of injection loop was 20 µL. Standard solutions were filtered before injection using a 0.2 µm syringe filter (VWR). Chromatograms were run at 30ºC at 0.6 mL min^{-1} using an elution gradient composed by two eluents: A) methanol:water (5:95, % V/V) and B) methanol:water (95:5, % V/V), both acidified with formic acid (0.1% V/V). The following elution gradient was used: [0-3.30] min 90% A; 6.70 min 80% A; [6.70-20] min 80% A; 35 min 50% A; 38.3 min 0% A, [38.3-41.7] min 0% A; 45 min 90% A; [45-55] min 90% A.

Before HPLC-UV analyses, samples were prepared by solid-phase extraction (SPE) in order to separate the lower molecular weight phenolic compounds from other compounds present in the oxidation mixture. SPE was performed at least in duplicate for each sample.

The procedure used is summarized in Figure 5.1 and is based in Pinto *et al.* (29) with some minor modifications. SPE was performed with Lichrolut EN (40 – 120 µm) 500 mg, 6 mL SPE cartridges (Merck) previously conditioned with 7 mL of methanol, afterwards with 15 mL methanol:water (95:5, % V/V) solution acidified with formic acid (0.1% V/V) and finally equilibrated with 15 mL water:methanol (95:5, % V/V) solution acidified with formic acid (0.1% V/V). Afterwards, each sample is diluted with ultrapure water (1:1) and acidified until pH value being lower than 2 (checked with pH strips - Merck) using a sulfuric acid solution (diluted 1:1, Panreac, purity 96%). During acidification, some precipitation occurs and thus, the acidified sample is centrifuged to separate the supernatant phase (with the low molecular weight compounds) from the precipitate phase. The supernatant is applied to the previously conditioned cartridges and the precipitate washed with 5 mL of water:methanol (95:5, % V/V) solution acidified with formic acid (0.1% V/V) and centrifuged. The new supernatant is loaded to the same cartridge and this washing step repeated two more times. To finalize the loading step, about 2 mL of the acidified water:methanol (95:5, % V/V) solution is applied to ensure that all the low molecular weight compounds are

adsorbed onto the solid phase. After that, 10 mL of acidified methanol:water (95:5, % V/V) solution is applied to recover those compounds, the sample is diluted and quantified by HPLC-UV.

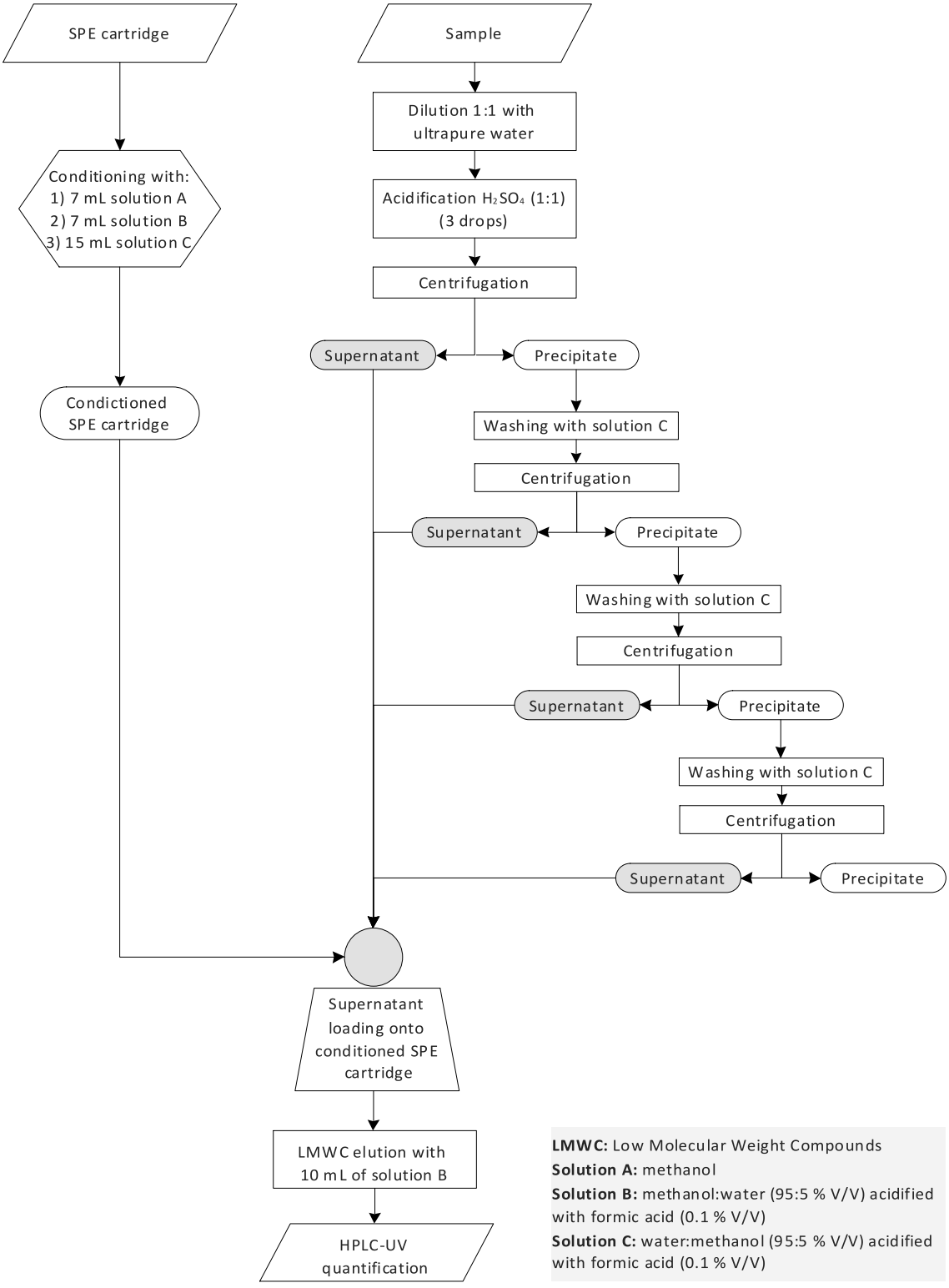

Figure 5.1 Solid-phase extraction sequence to prepare samples before being analysed by HPLC-UV.

Gel permeation chromatography (GPC) analysis was performed using the previously described HPLC system. Two Agilent gel columns of highly cross linked polystyrene/divinylbenzene with 300x7.5 mm arranged in series were used: OligoPore column with nominal particle size 3 µm, that measures molecular weights up to 3300 g mol^{-1}, and MesoPore column with nominal particle size 6 µm, that measures molecular weights up to 25000 g mol^{-1}. A guard column Oligopore 50x7.5 mm was assembled prior to the columns. The detection wavelength was set to 268 nm and the volume of injection loop was 20 µL. Separation was performed at 70 ºC and 0.8 mL min^{-1} employing an isocratic mobile phase of dimethylformamide with 0.5% LiCl (DMF).

10 polystyrene molecular weight standards with molecular weights ranging from 162 to 4910 g mol^{-1} were analyzed by GPC, preparing different solutions of approximately 5 mg mL^{-1} dissolved in the same mobile phase solvent. The following linear relationship between MW (g mol^{-1}) and retention time (t_R, min) was obtained: $LogMW = -0.1502\ t_R + 6.9745$.

Solutions of the feed and final permeates and retentates were previoulsy freeze dried and dissolved in the mobile phase solvent and filtered through a 0.2 µm syringe filter (VWR) before injection. Since samples did not dissolve completely in the DMF solution, sample preparation procedure was set after testing different concentrations of the feed solution (40-2 mg mL^{-1}) and submitting to stirring, ultrasounds and/or heating up to 46 ºC for 16-72 h. Since, no significant differences were observed in the molecular weight (MW) distribution along elution time, the conditions were set for preparing 5 mg mL^{-1} solutions stirred for 16 h.

TP standard solutions of 0.8 g L^{-1} were also analyzed in order to infer if interactions between TP and the stationary phase besides exclusion by size are happening (e.g. ion-exclusion, ion-inclusion, ion-exchange or adsorption of the solute) or interactions between the monomers themselves.

5.2.2. Equipment and experimental set-up

Experiments were performed in a set-up as shown by the schematic diagram in Figure 5.2, equipped with an ultrafiltration unit (Orelis, France) operated in cross-flow mode, a direct drive rotary vane pump (model PA1011, Fluid-O-Tech, Italy), a frequency inverter (MC07, Movitrac®B, Sew Eurodrive, Germany), inlet and outlet pressure gauges filled with glycerin (Genebre, Spain) and a rotameter (Flowtech, China). The pump used is a positive displacement unit that operates maintaining the flowrate constant throughout the process.

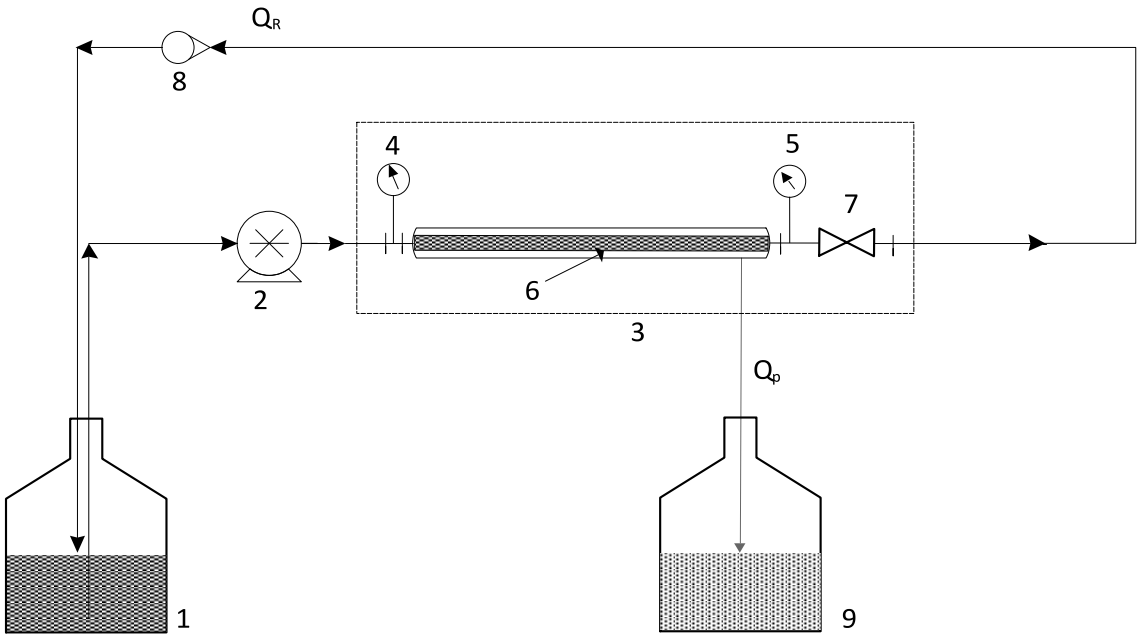

Figure 5.2 Experimental set-up schematics for cross-flow ultrafiltration in concentration mode: 1) feed vessel; 2) direct drive rotary vane pump coupled with a frequency inverter; 3) membrane module with 4) inlet pressure gauge, 5) outlet pressure gauge, 6) tubular membrane and 7) circulating valve; 8) rotameter and 9) collecting permeate vessel; Q_P: permeate flowrate; Q_R: retentate flowrate.

The ultrafiltration unit withstands maximum operating pressure and temperature of 7 bar and 80 ºC, respectively, and maximum differential pressure of 4 bar. Tubular ceramic membranes with 1 channel, 400 mm length and inside and external diameters of 6 and 10 mm, respectively, were used. The area of the membrane is 0.008 m^2. The permeate chamber holds a volume of 17 mL and the collector tube of permeate about 4 mL. Since the permeate side is open to the atmosphere there is no back pressure.

Three different molecular weight cut-off (MWCO) membranes were tested: 50 kDa (purchased from CTI, France) and 5 and 1 kDa (Filtanium^{TM}, purchased from TAMI, France). The 50 kDa MWCO membrane has a ZrO_2 active layer on a ceramic support composed with TiO_2-Al_2O_3. The 5 and 1 kDa MWCO membranes have an active layer of TiO_2 on a patented ATZ support composed with TiO_2-Al_2O_3-ZrO_2. These membranes resist to strong alkaline solutions and the maximum operating pressure is 10 bar.

5.2.3. Water membrane permeability assessment

Water permeability across the membranes were obtained by measuring deionized water permeate flowrate for different transmembrane pressures (*TMP*, Pa) at 25ºC. The *TMP* corresponds to the average between relative inlet pressure on the feed side and relative outlet pressure on the retentate side.

The permeate flux (J, $m^3\ s^{-1}\ m^2$) for each TMP is calculated as following (4):

$$J_P = \frac{Q_P}{A_m}$$ **Equation 5.5**

where Q_P ($m^3\ s^{-1}$) is the permeate flowrate measured for a certain TMP and A_m (m^2) is the membrane surface area. Assays were performed with a feed flowrate of 240 L h^{-1}.

Water permeate flux (J_w) was determined using new membranes allowing to obtain the membrane hydraulic resistance (R_m, m^{-1}) by applying the Darcy's law (4):

$$J_w = \frac{TMP}{\mu_0 R_m}$$ **Equation 5.6**

where μ_0 (Pa s) is the viscosity of water at 25 ºC.

Membrane permeability (L_p, $m^3\ s^{-1}\ m^{-2}\ Pa^{-1}$) to water is obtained from the slope of the representation J_w vs *TMP*. It represents the amount of liquid crossing the membrane per unit time, per membrane area unit and *TMP* unit. This coefficient will be used to determine the initial membrane permeability recovery in each cleaning cycle.

5.2.4. Membrane fractionation sequence

The oxidized IKL solution prepared was processed with a three stage membrane fractionation sequence as shown in Figure 5.3, starting from the highest MWCO membrane to the lowest: the permeate obtained from the first membrane processing with the 50 kDa membrane (P_{50kDa}) is treated with the 5 kDa membrane and the corresponding permeate stream obtained (P_{5kDa}) treated with the 1 kDa membrane originating a final permeate stream (P_{1kDa}). During each membrane processing, permeate and retentate (R_{50kDa}, R_{5kDa}, R_{1kDa}) samples were collected and characterized

regarding TS and TP. The molecular weight distribution by GPC was performed for feed and final retentates and permeates solutions. The permeate flux evolution with time was measured several times along processing after the permeate chamber and collector tube being filled with the permeate solution. The permeate flux at different times was calculated for specific time intervals to obtain the instantaneous permeate flux (J_p) by applying Equation 5.5.

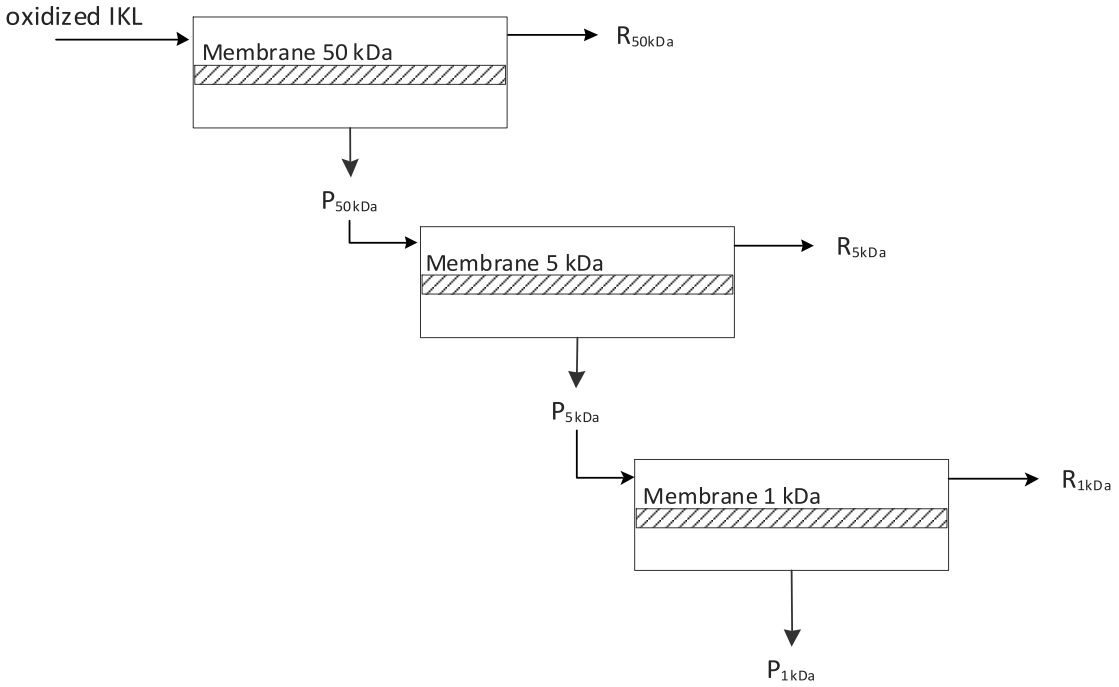

Figure 5.3 Membrane fractionation sequence of an oxidized industrial kraft liquor performed with 50, 5 and 1 kDa MWCO membranes.

The assays were performed by operating in concentration mode, at 25.5 ± 1 ºC and a fixed TMP of 1.4 bar. The retentate flowrate was approximately 120 L h^{-1} for each membrane stage. The pH value was monitored during membrane processing and remained constant throughout the process, being approximately 10.1.

In concentration mode, the retentate stream returns to the feed vessel and the permeate stream is collected to a different vessel. The 50 and 1 kDa membranes processing were performed until reaching a volume concentration factor (*VCF*) of 3 and the 5 kDa stage up to 3.4. The *VCF* corresponds to the ratio between the starting volume amount of feed solution (V_F, L) and the retentate volume amount (V_R, L) (4):

$$VCF = \frac{V_F}{V_R}$$ **Equation 5.7**

The apparent rejection coefficient (R_i) represents the fraction of solute retained by the membrane (4):

$$R_i = 1 - \frac{C_{P,i}}{C_{R,i}} \qquad \textbf{Equation 5.8}$$

where $C_{P,i}$ (g L^{-1}) is the concentration of the solute in the permeate and $C_{R,i}$ (g L^{-1}) is the concentration of the solute in the retentate. The subscript '*i*' refers to TS, ashes or TP.

5.2.5. Membrane cleaning and fouling evaluation

The membranes, system and tubing were initially washed with 0.1 mol L^{-1} NaOH solution and rinsed with deionized water until neutral pH, thus ensuring that the unit was cleaned and free from contaminants.

After processing the real oxidized lignin solution, several cleaning cycles were performed. Herein, cleaning cycles are distinguished as physical and chemical cleaning. Physical cleaning will remove the reversible component of fouling (concerning the effects of polarized concentration and solutes deposited on the membrane surface) and thus, it will allow to determine the irreversible fouling component due to pore blocking and adsorbed material. Chemical cleaning is performed to remove the irreversible foulants and evaluate the membrane cleaning efficiency by comparing the final water permeability with the initial one obtained for a non-fouled membrane. The water permeability recovery for each membrane (expressed in %) is calculated by the following expression:

$$\text{Recovery}(\%) = \frac{L_{p,after}}{L_{p,initial}} 100 \qquad \textbf{Equation 5.9}$$

where $L_{p,after}$ (L m^{-2} h^{-1} bar^{-1}) corresponds to the water permeability of the membrane after operating with the real mixture and performing the cleaning cycles and $L_{p,initial}$ (L m^{-2} h^{-1} bar^{-1}) corresponds to the initial water permeability of the membrane.

Cleaning sequence initiated with physical cleaning by rinsing the system with about 3 L of 0.001 mol L^{-1} NaOH solution and recycling with 3 L of new solution for about 30 minutes with no TMP applied at 25ºC. Afterwards, the system was rinsed again with 3 L of fresh solution and the permeate flux for different TMP measured. The water permeability obtained in this phase will be affected by the contribution of the resistance offered by the membrane and irreversible fouling. In this stage, a weak solution of NaOH was employed instead of water to avoid lignin precipitation. It is important to refer that some irreversible fouling can be removed in this stage because of the

weak alkaline solution and TMP employed during the assessment of the water permeability of the membrane and thus, the reversible fouling resistance will be somewhat overestimated.

The washing sequence continued with cycles of chemical cleaning using 0.1 mol L^{-1} NaOH solution heated up to 50 ºC and applying a TMP of 1 bar for 60 minutes. At least three cleaning cycles were performed for each membrane stage, ensuring that the maximum recovery was reached. In between each two cleaning cycles, water permeate flux was measured for different TMP. After performing the necessary chemical cleaning cycles, the system was rinsed with deionized water at TMP of 1 bar until achieving neutral pH value in the permeate stream. Then, water permeate flux was monitored once more. The membrane cleaning effectiveness is determined by comparison with the initial water permeability of the membrane (Equation 5.9). A typical cleaning temperature history is shown in Figure 5.4.

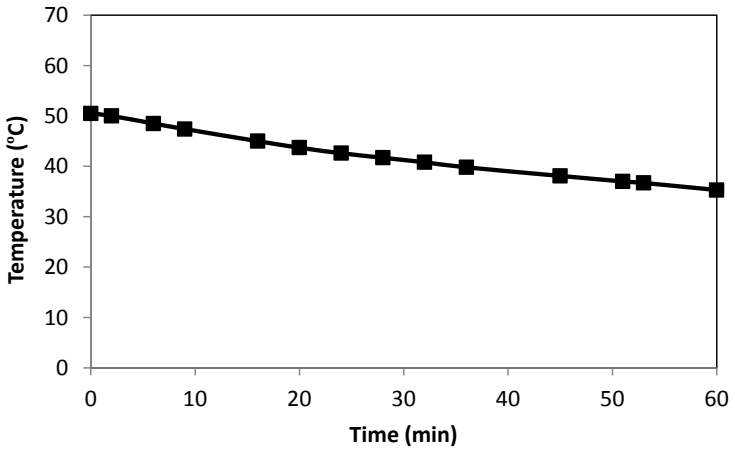

Figure 5.4 Example of evolution of temperature with time during one cleaning cycle.

It is important to note that for operation with the 50 kDa membrane, a cleaning cycle was performed after 22h of processing (1.3 VCF) and then the filtration process continued until reaching a VCF of 3.

During membrane operation with the real mixture, permeate flux declines due to concentration polarization and fouling. By applying the resistance-in-series model it is possible to quantify the contribution of the irreversible and reversible fouling during operation with real mixtures assuming that each component of the membrane fouling acts independently from any other (4):

$$J_p = \frac{TMP}{\mu_s R_T} = \frac{TMP}{\mu_s \left(R_m + R_{f,irrev} + R_{f,rev}\right)} \qquad \textbf{Equation 5.10}$$

where μ_s (Pa s) is the viscosity of the solution used in each membrane stage at 25 ºC, R_T (m^{-1}) is the total membrane resistance during membrane processing accounting for the contribution of R_m

(determined by Equation 5.6). Experimentally, the final value of permeate flux obtained during each membrane processing stage and the viscosity of the permeate solution were used to estimate R_T. $R_{f,irrev}$ was estimated immediately after physical cleaning, as explained before, considering the viscosity of water at 25ºC. $R_{f,rev}$ is obtained subtracting from R_T the contributions of R_m and $R_{f,irrev}$.

5.3. Results and discussion

5.3.1. Measurement of water permeability through the membrane

The hydraulic permeability is an intrinsic property of a non-fouled membrane very useful for assessing the membrane cleaning efficiency and determining the membrane resistance. Taking this into consideration, the water permeate fluxes through the membranes were measured for different TMP. The tubular ceramic membranes selected to perform the membrane fractionation sequence of the oxidized IKL were of 50, 5 and 1 kDa MWCO.

The permeate flux for each transmembrane pressure was calculated from Equation 5.5 and is represented in Figure 5.5. The respective permeabilities and membrane resistances are indicated in Table 5.1. As expected, it is possible to observe that the permeate fluxes increased linearly with the increase of TMP (with correlation coefficients higher than 0.9961). Moreover, the greater the MWCO, the lower is the membrane resistance and the higher is the water permeability.

Žabková *et al.* (2, 30) studied similar ceramic membranes and the membrane resistance of 5 and 50 kDa are very similar to the ones obtained in this work, being 12.22×10^{12} m^{-1} and 3.74×10^{12} m^{-1}, respectively. However, a different value was found for the 1 kDa membrane for which the authors obtained a membrane resistance of 28.06×10^{12} m^{-1}, approximately twice the value obtained in this work. Cheryan (4) stated that some differences can be found among different batches of membranes. Additionally, the authors also make reference to the fact that measurement techniques and set-up also can influence the water permeate flux.

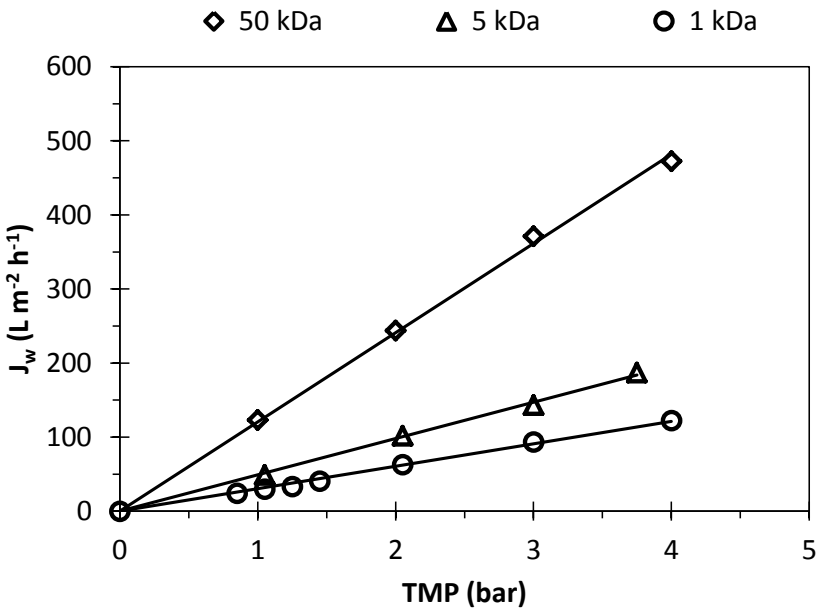

Figure 5.5 Water permeate fluxes through the membranes of 50, 5 and 1 kDa for different TMP at 25 ºC. Feed flowrate was set to 240 L h^{-1} and the surface area of each membrane is 0.008 m^2.

Table 5.1 Water permeability and membrane resistance obtained for the ultrafiltration ceramic membranes of 50, 5 and 1 kDa MW cut-off, at 25 ºC and feed flowrate set to 240 L h^{-1}

Membrane	L_P (L m^{-2} h^{-1} bar^{-1})	R_m (10^{12} m^{-1})
1 kDa	30.3	13.3
5 kDa	49.1	8.2
50 kDa	120	3.4

5.3.2. Fractionation of industrial kraft liquor (IKL) by ultrafiltration

5.3.2.1. *Permeate Fluxes*

Oxidized IKL was submitted to a fractionation sequence in concentration mode with 3 different MWCO membranes (50, 5 and 1 kDa), as shown in Figure 5.3. The sequence is divided in 3 stages. In the first stage the oxidized IKL is processed with the highest MWCO membrane of 50 kDa. After 22 h processing with this membrane, one cleaning cycle with 0.1 NaOH and rinsing with water was performed (corresponding to a VCF of 1.3) and then the filtration process continued until reaching a VCF of 3. The resulting permeate stream (P50kDa) proceeded with the second stage of the fractionation sequence employing the 5 kDa membrane. This stage was performed until a VCF of 3.4 was reached. Finally, a third stage encompassing the treatment of the latter permeate stream (P5kDa) with the 1 kDa membrane was performed. All experiments were carried out at 25 ± 3 ºC and retentate flowrate and TMP fixed to 120 L h^{-1} and 1.4 bar, respectively.

Figure 5.6 and Figure 5.7 show the permeate flux behavior with time observed during the fractionation sequence. In all membrane stages, flux decreased during operating time and it was more accentuated for the 1 kDa membrane, followed by the 50 and 5 kDa membranes. Both the 5 and the 1 kDa membranes showed a similar initial sharp decrease of flux during the first 5 hours of operation (Figure 5.8, from 26-28 to 13-16 L m^{-2} h^{-1}, VCF of 1.1), but then the flux continued decreasing steeply for the membrane of lower cut-off, up to 10 h processing (VCF 1.3), reaching a final permeate flux of 5.5 L m^{-2} h^{-1}. An attempt to explain this observed trend will be discussed below when analyzing the contribution of the different resistances to flux decline. For a similar time of operation, a final VCF of 3.4 and 3.0 was achieved for the 5 and the 1 kDa membranes, respectively, and the final permeate flux for the 5 kDa was almost double of the flux obtained for the 1 kDa membrane.

As for the 50 kDa membrane, in Figure 5.6 it is observed a sharp decrease of the initial permeate flux during the first 2.5 hours of operation from 32 to 23 L m^{-2} h^{-1} (corresponding to a VCF of 1.034) and then slowly decreased to 18 L m^{-2} h^{-1} during 22 hours of operation (VCF of 1.3). After that time, one cleaning stage with 0.1 mol L^{-1} NaOH was performed in an attempt to continue processing with higher fluxes. Although 92% of the initial water flux was readily recovered, when resuming the membrane processing, flux rapidly decreased from 22 to 17 L m^{-2} h^{-1} in one hour and reached a final flux of 9.7 L m^{-2} h^{-1} after a total time of operation of 72.6 h. Since no advantages were observed by including a cleaning stage, this procedure was not repeated for the other stages.

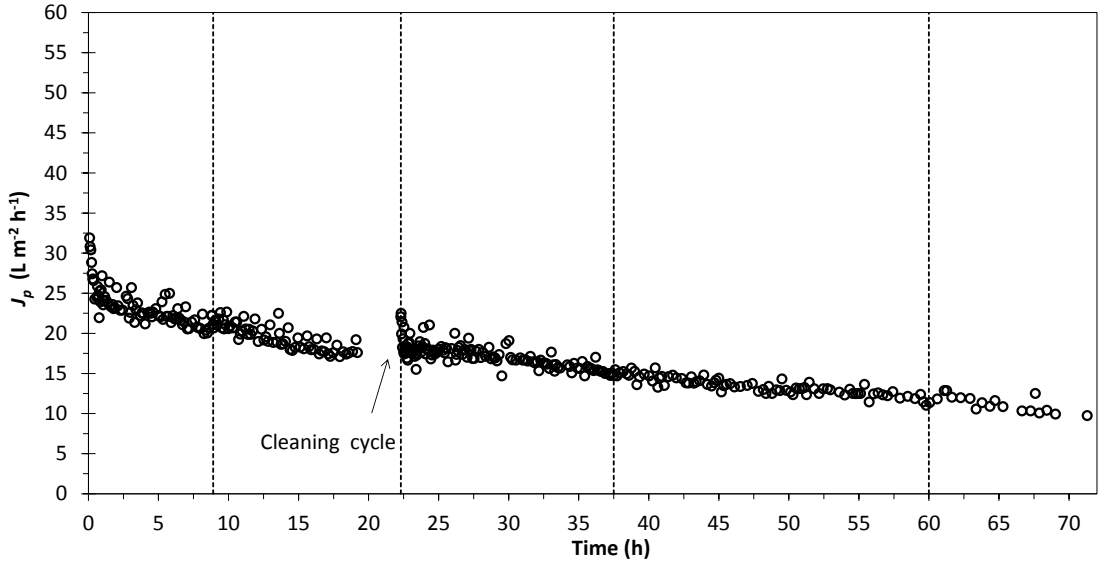

Figure 5.6 Permeate flux behaviour with operating time during processing of an oxidized IKL solution in concentration mode with the 50 kDa MWCO membrane. Feed solution containing 86.5 g L^{-1} of TS and 2.399 g L^{-1} of TP. Transmembrane pressure of 1.4 bar, flowrate 120 L h^{-1} at 25 ± 3 ºC and pH 10.1. VCF of 3. The dashed lines correspond to the time when operation was stopped/resumed.

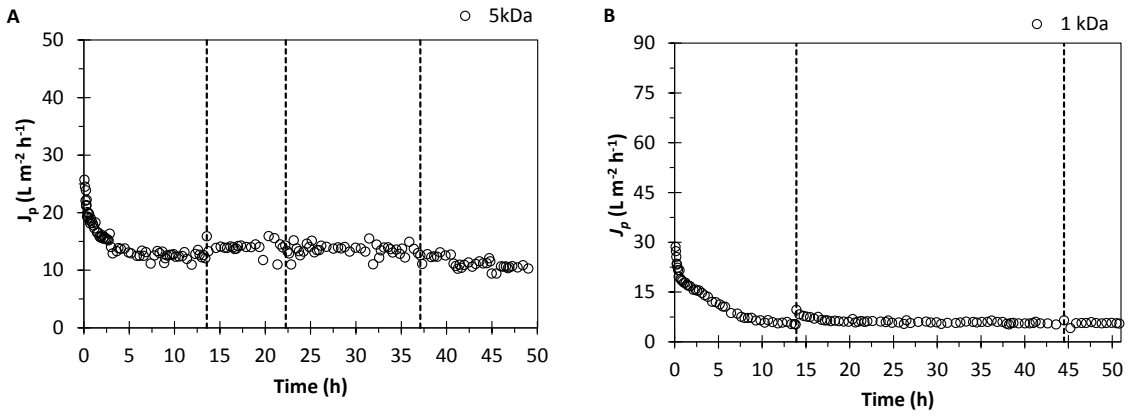

Figure 5.7 Permeate flux behaviour with operating time obtained for processing with 5 kDa (A) and 1 kDa (B) MWCO membranes in concentration mode. Feed solution of 5 kDa processing is composed with 75.3 g L^{-1} of TS and 2.379 g L^{-1} of TP. Feed solution of 1 kDa processing is composed with 64.0 g L^{-1} of TS and 2.219 g L^{-1} of TP. Transmembrane pressure of 1.4 bar, flowrate 120 L h^{-1} at 25 ± 3 ºC and pH 10.1. VCF of 3.4 (5 kDa) and 3 (1 kDa). The dashed lines correspond to the time when operation was stopped/resumed.

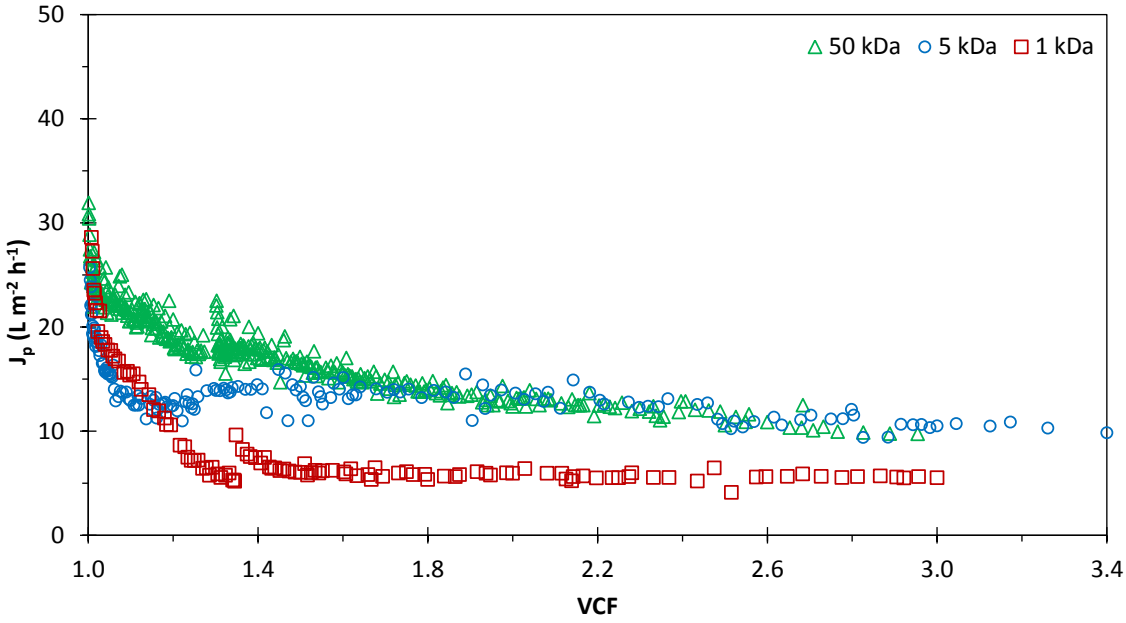

Figure 5.8 Permeate flux as a function of the VCF applied to each membrane.

Flux reduction with time is attributed to several phenomena such as the decrease in the driving force due to osmotic pressure increase, resistance of the concentration polarization boundary layer, resistance due to formation of a gel layer and resistance by fouling of the membrane caused by pore clogging and adsorption (4). Fouling formation depends of the solute-membrane and solute-solute interactions and solute characteristics and will be discussed in 5.3.2.3.

Several studies employed with black liquor have demonstrated that the polarized layer deposition phenomenon play an important role in limiting flux during operation (31). Žabková *et al.* (2) applied model lignin/vanillin solutions (60/2-6 g L^{-1}) onto 1, 5 and 15 kDa MWCO tubular ceramic membranes and identified that resistance by polarization was the main factor contributing for the flux decline observed with the 1 kDa membrane, while for the other higher cut-off membranes the decline on flux was explained by the additional formation of a gel layer.

In the particular case of this work, the permeate chamber is initially filled with air and thus the effect of the osmotic pressure is not expected in the beginning of the process. The net driving force of the flux reduction at the startup of the processing will be mainly pressure in all the three stages performed. During each membrane process, it is expected that the solutes are brought to the membrane surface by convective transport and while solvent and small particles are permeated through the membrane, larger solutes will be held by the membrane; hence, solutes will accumulate on the membrane surface increasing the concentration near the membrane surface. The concentration boundary layer is established and, eventually, a gel layer can be formed which results in an additional resistance to permeation, due to the increase of resistance to solvent and increase in the local osmotic pressure and, consequently, flux will continue decreasing. Studies have referred

that gel formation is very relevant in ultrafiltration processes (2, 4). Usually, the boundary layer is established very quickly in the beginning of operation and, afterwards, a gel layer is gradually formed in between this boundary layer and the membrane (26).

Throughout the process, bulk concentration will increase with time since operation took place in concentration mode. Therefore, the solution properties change with time affecting the hydrodynamic conditions and, hence, osmotic pressure and concentration at membrane surface will change accordingly, originating a long term flux decline due to concentration polarization. This phenomenon was more relevant for the membrane with the highest MWCO (50 kDa) where bulk concentration was higher. In this stage, the permeate flux continuously decreased as consequence of the polarized layer resistance still being established due to bulk concentration increase and, thus, constituting the main contributor for flux decline. This was also observed for the second stage with the 5 kDa membrane, although not as relevant as in the first stage.

In the last stage with the 1 kDa membrane, permeate flux did not change significantly with time after 20 hour processing, indicative that the formation of a gel layer might be established, where solute concentration reached its maximum. In this case, the convective transport through the membrane is almost counterbalanced with back diffusion of solute into the bulk solution and, thus, flux decline is not very pronounced.. Since operation took place in concentration mode, one may say that the increase in the bulk concentration with operating time had no noticeable effect on flux and that diffusion and convective phenomena remain counterbalanced.

Table 5.2 summarizes membrane productivities for some VCF achieved, as well as the respective permeate fluxes observed. Besides the influence of the MWCO of the membranes used, the decrease of TS content during the fractionation sequence study will also influence flux decline. On one hand, the flux decrease extent during processing, $\frac{J_{P,(t=0.1h)} - J_{P,final}}{J_{P,(t=0.1h)}}$, becomes more significant for the membrane with the lowest MWCO. On the other hand, comparing the initial flux observed during processing with the respective water fluxes obtained for an non-fouled membrane, $\frac{J_w - J_{P,(t=0.1h)}}{J_w}$, the extent of flux decrease was higher for 50 kDa (61% decrease) and 5 kDa (59% decrease) and lower for 1 kDa (11% decrease).

Table 5.2 Summary of the membrane productivities and permeate fluxes achieved during ultrafiltration in concentration mode and flux reductions observed

VCF	Stage 1 50 kDa		Stage 2 5 kDa		Stage 3 1 kDa	
	t (h)	J_P L m^{-2} h^{-1}	t (h)	J_P L m^{-2} h^{-1}	t (h)	J_P L m^{-2} h^{-1}
≈1.0	≈0.08	31.91	≈0.08	25.71	≈0.10	28.60
1.5	31.6	17.14	22.2	14.28	19.9	6.03
2.0	50.3	12.35	33.8	13.64	35.7	5.96
2.5	63.4	10.56	41.0	10.71	45.2	5.90
3.0	72.6	9.74	47.0	10.50	51.9	5.54
3.4	-	-	50.0	9.85	-	-
Initial feed volume (L)	15		7		4.5	
Overall average flux (L m^{-2} h^{-1})	17.86		14.46		10.64	
Average flux in the last hours of operation (L m^{-2} h^{-1})	11.57		11.17		5.82	
Water flux (J_w) at 1.4 bar and 25 ºC (L m^{-2} h^{-1})	182		69		42	
Flux reduction $\frac{J_w - J_{P,(t\approx 0.1h)}}{J_w}$ (%)	61		59		11	
Operating flux reduction $\frac{J_{P,(t=0.1h)} - J_{P,final}}{J_{P,(t=0.1h)}}$ (%)	69		62		81	

Žabková et al (2) investigated the performance of tubular ceramic membranes with 1, 5 and 15 kDa MWCO to process different synthetic mixtures of lignin and vanillin. The effect of lignin and vanillin concentrations (5-60 and 0.5-6 g L^{-1}, respectively) and pH values (8.5 and 12.5) on membrane productivity and rejection of lignin and vanillin by each membrane were studied. The increase of pH value led to a slight decrease of permeate flux, in particular for higher lignin concentrations. Regarding the experiments performed with 60 g L^{-1} of lignin, permeate fluxes obtained with the 1 kDa (5-2.8 L m^{-2} h^{-1}) and the 5 kDa (11-13 L m^{-2} h^{-1}) cut-off membranes were considerably lower than the fluxes obtained in this work. This can be explained by the fact that Žabková et al (2) employed directly to the membranes, synthetic mixtures of lignin with higher MW (60 000 g mol^{-1}) which might have contributed to more fouling formation.

5.3.2.2. *Total solids (TS), ashes, total phenolate compounds (TP), and molecular weight distribution (MW)*

A fractionation sequence of the oxidized IKL solution prepared encompassing 3 stages was performed in concentration mode starting from the membrane with the highest MWCO to the lowest: 50, 5 and 1 kDa cut-offs (depicted in Figure 5.3). In each stage, the solution was fed in cross-flow mode under constant pressure (1.4 bar), temperature (25 ºC) and flowrate (120 L h^{-1}), over the surface of the desired membrane. The pressure gradient over the membrane forces the solvent and the desired smaller molecules (low molecular weight phenolic compounds) to go through the pores of the membrane, while the larger molecules (e.g. depolymerized lignin) are retained by the membrane and return to the feed vessel. Accordingly, the fraction going through the membrane (permeate stream) will be depleted in depolymerized lignin and richer in the desired compounds while the retentate stream will be enriched in the macromolecules that do not cross the membrane.

Regarding GPC analyses, a preliminary study was conducted with several standard solutions of typical phenolic compounds present in oxidized IKL (vanillin (V), syringadehyde (S), acetovanillone (OV), acetosyringone (OS), vanillic acid (VA), syringic acid (SA) and *p*-hydroxybenzaldehyde (*p*-OHB)) in order to confirm if the retention time was affected by different interactions with the stationary phase besides exclusion by size (e.g. ion-exclusion, ion-inclusion, ion-exchange or adsorption of the solute) or interactions between the monomers themselves (32). This has been identified as a plausible situation that can occur in GPC analyses for certain compounds because linear chain standards are usually used in calibration and cannot predict other secondary separation effects originated as, for example, from interactions with the functional groups present in the phenolic compounds (32).

For this purpose, a feed solution enriched in each standard was prepared in DMF and analyzed by GPC. The MW distributions along elution time are shown in Figure 5.9 normalized with the area under the curve. The elution times obtained were different than the ones expected for each compound (from data obtained by the analysis of several polystyrene standards), allowing to conclude that the retention time is affected with the type of phenolic compound present.

Early retention times than the ones expected were observed for all the standard phenolic compounds analyzed, which means that, probably, interaction between molecules occur or ion exclusion effect is the most pronounced interaction effect with the stationary phase and, thus, the phenolic monomers are excluded at higher rate.

Moreover, it was expected that *p*-OHB would be the last compound to be eluted but, on the contrary, it was the compound eluted at the highest rate, meaning that either molecules of *p*-OHB

interact more among themselves, or that ion exchange phenomena effect, happening simultaneously, is less pronounced than for the other compounds studied.

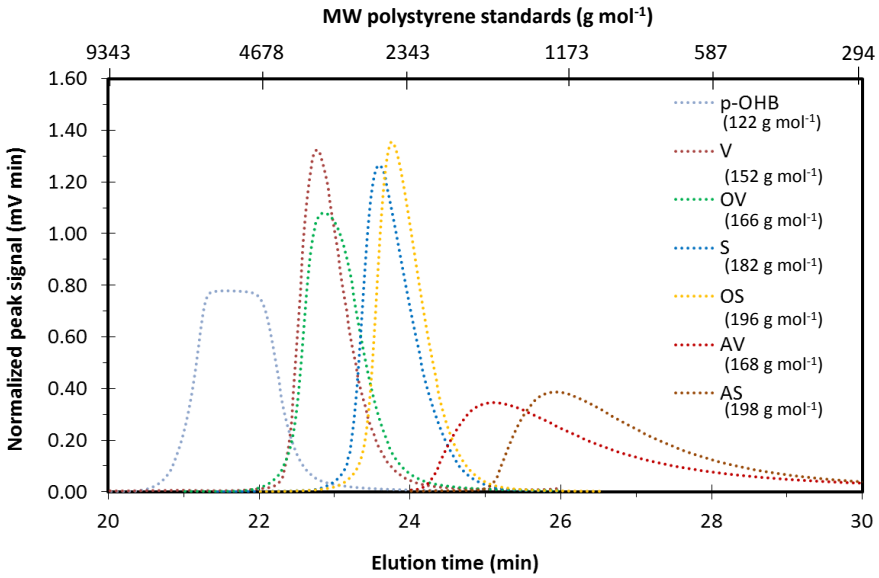

Figure 5.9 Overlaid normalized UV chromatograms obtained for standard solutions of V, S, OV, OS, VA, SA and *p*-OHB.

Taking all into consideration, GPC analyses conducted in this work will just give an indication of the molecular weight changes obtained in each fractionation stage. GPC analysis of feed and permeate and retentate streams were performed for each fractionation stage and provided the molecular weight (MW) distribution along elution time for each processing stream. The MW distributions are compared in Figure 5.10 where it is shown the peak signal normalized with the area under the curve as a function of the elution time obtained for each stream. The greater the elution time, the lower the MW of the compounds is. In Appendix C (Figure C.1) it is presented the overlaid normalized chromatograms for feed and permeates streams.

For all stages, it is possible to observe, by comparison with the feed streams of each stage (Feed, P50kDa and P5kDa), that permeates got depleted in the higher MW compounds while retentates got richer (corresponding to retention times between 12-20/22 min).

Regarding the GPC chromatograms obtained for the streams of the first fractionation sequence performed with the 50 kDa membrane, it is very clear that the group of compounds with the retention times between 22 and 25 min (i.e. near the elution times of V, S, OV and OS) went to the permeate stream and its concentration decreased in the final retentate stream obtained. With the decrease of the cut-off of the subsequent stages, this difference became smaller meaning that this family of compounds was somewhat retained with further membrane processing. This is consistent with the apparent rejection coefficient estimated for the low molecular weight phenolates and will be discussed later.

1st fractionation stage

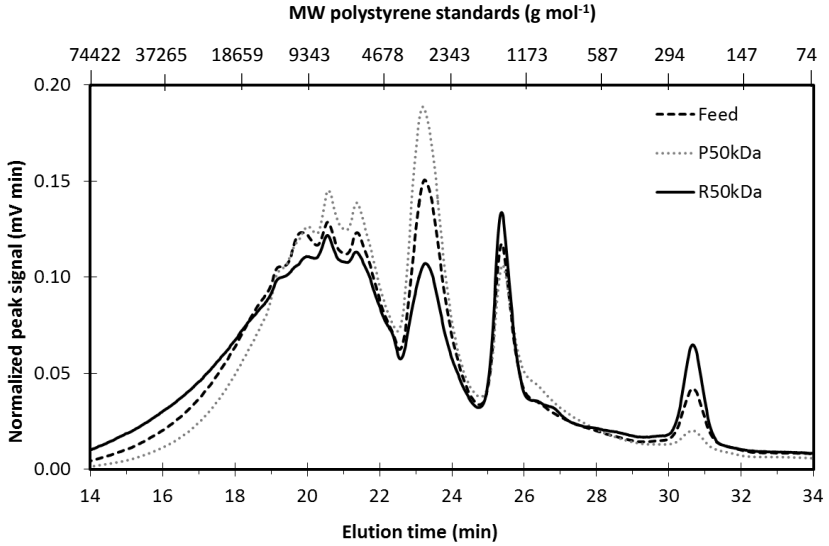

2nd fractionation stage

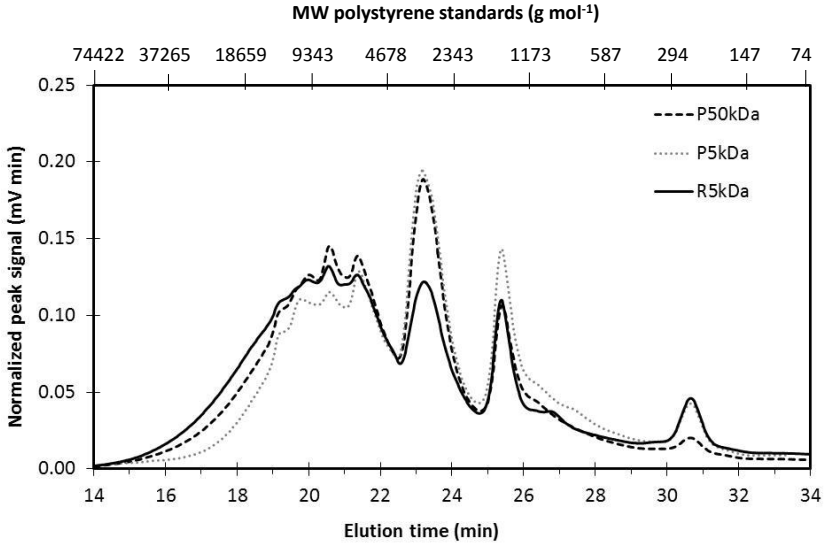

3rd fractionation stage

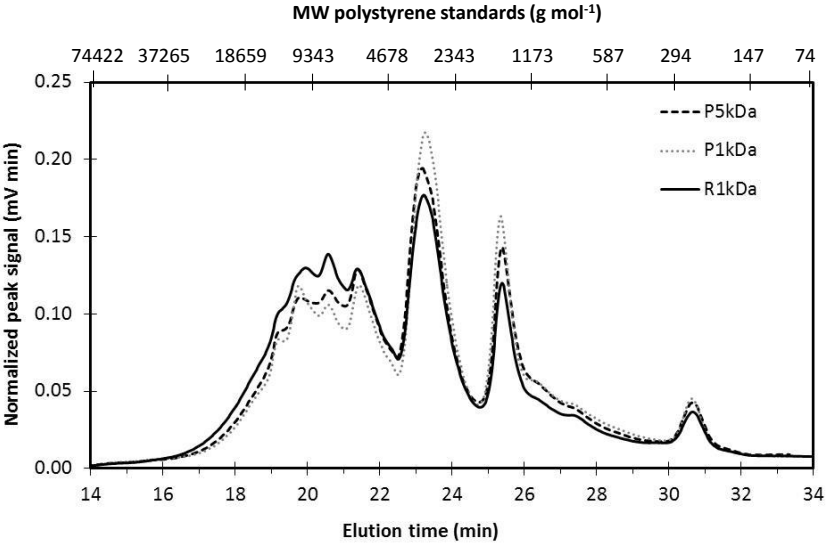

Figure 5.10 Normalized chromatograms obtained by GPC for the different streams obtained during the membrane fractionation sequence. Normalization with area under the curve.

In the perspective of V and S recovery, the main goal with this fractionation study is to concentrate the low molecular weight phenolate compounds in the permeate stream, in detriment of larger solutes included in total solids (TS) quantification (e.g. depolymerized lignin). Higher MWCO membranes will not reject much of the low molecular weight compounds, but allow the passage of larger molecules of depolymerized lignin. On the contrary, smaller MWCO membranes will allow obtaining a permeate stream purer in low molecular weight phenolates but at the cost of losing V and S that are being retained by the membrane. Therefore, besides the importance of finding the best set of operating conditions to achieve the maximum membrane productivity, a good compromise between reaching the maximum enrichment of the phenolate compounds in the permeate stream with minimal losses of material must be found, in order to find an economically feasible membrane separation process.

In Figure 5.11 are portrayed the concentration histories of TS and low MW phenolate compounds quantified by HPLC-UV (TP) in retentate and permeate streams, observed during each membrane concentration stage. The concentration evolution of TS and TP will depend on the observed rejections. Additionally, if the apparent rejection coefficient is high enough, it is expected to have a noteworthy concentration increase in the retentate with operating time or VCF increase.

Regarding TS and TP evolution with concentration time, it is possible to observe a similar trend between stages 1 and 2. In fact, although the starting concentration was different, similar apparent rejection coefficients were calculated for both concentration stages.

In stage 1, a VCF of 3 was achieved and TS in the retentate increased 1.17 times from 86.5 to 100.8 g L^{-1} and 1.15 times in the permeate stream (from 65.5 to 75.3 g L^{-1}). The apparent rejection coefficient observed increased slightly during concentration, having an average value of 23 ± 5 %. During stage 2 with a VCF of 3.4, a similar trend was observed for TS concentration in retentate stream: it increased 1.20 times from 75.3 to 90.3 g L^{-1}. However, the TS concentration in permeate stream was kept constant (65 ± 2 g L^{-1}). The apparent rejection coefficients observed increased remarkably from 13.6 to 29.1 %. The average apparent rejection observed was also within the range of the one obtained for the previous stage (21 ± 6 %).

In the last stage, performed with the membrane with the lowest MWCO, TS concentration increased 1.08 times (from 64.0 to 69.0 g L^{-1}). The TS concentration evolution with time was not as noticeable as in the previous stages, firstly because the feed stream had already been submitted to membrane processing with the 50 and 5 kDa membranes and, secondly, the apparent rejections observed during concentration were lower, increasing from 5 to 15.1 % during processing (average value of 11 ± 4 %).

Regarding TP, no retention was observed during the first stage and, thus, the concentration histories in permeate and retentate streams are basically the same (Figure 5.11). As for the second

and third stages, a somewhat lower TP rejection was observed, of 11.5% and 9.0%, respectively; thus, concentration differences in permeate and retentate streams are not as remarkable as the concentration histories observed for TS. Nonetheless, TP rejections gradually changed during concentration, reaching to average rejections towards TP of 7 ± 3 % and 11 ± 3 % for 5 and 1 kDa membranes, respectively.

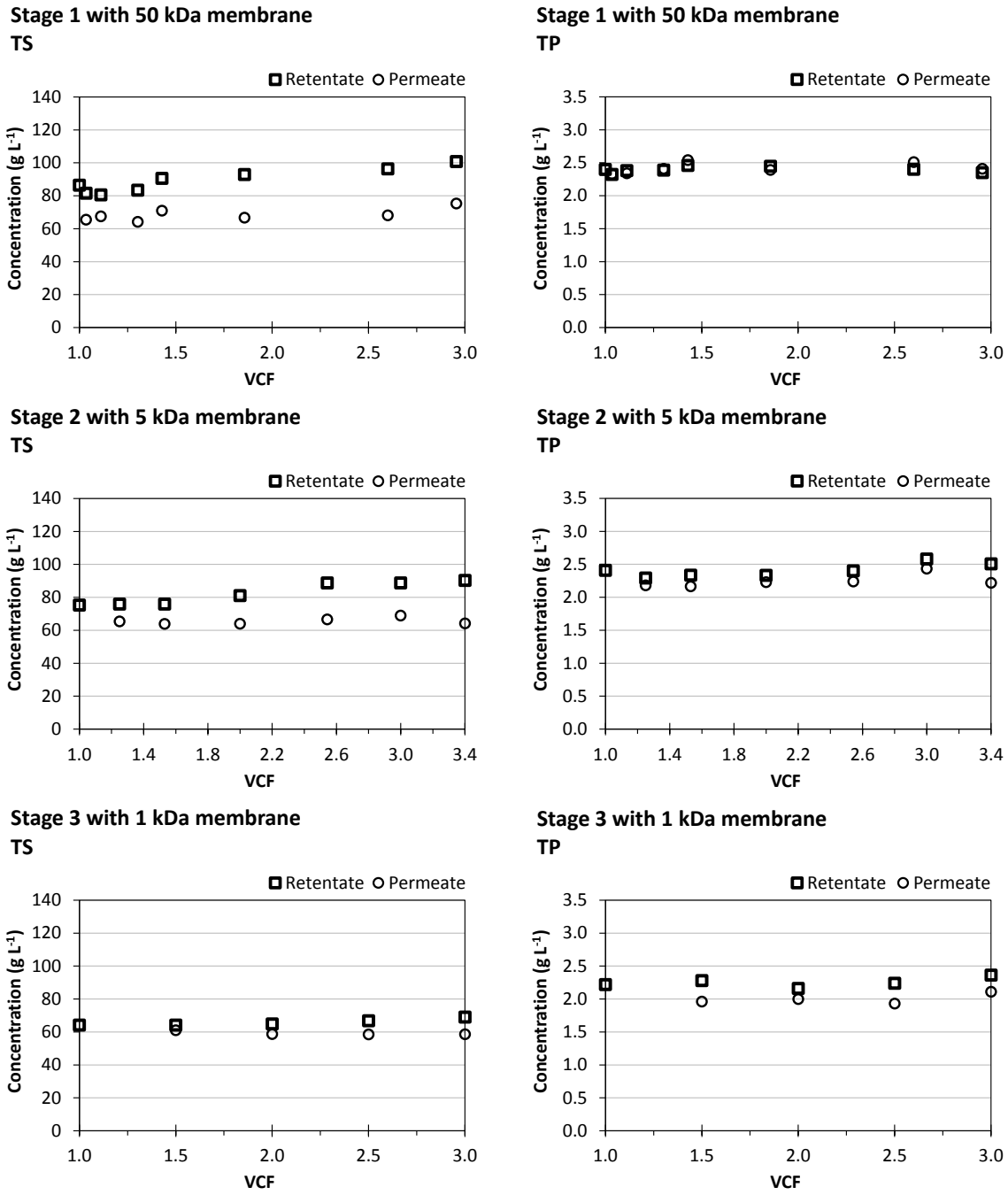

Figure 5.11 TS and TP concentration in permeate and retentate streams obtained in each membrane stage as a function of VCF.

Table 5.3 shows the concentrations of TS, ashes and TP obtained in each stream of the fractionation sequence performed with the respective final apparent rejection coefficients obtained. When comparing results, it is important to take into consideration the fact that feed concentration is different for the 3 membrane separation stages, with TS concentration decreasing along the fractionation process. The apparent rejection value for TS was approximately the same for the first two stages performed (25.3 – 29.1 %) and somewhat smaller in the last stage (15.1%).

Table 5.3 Feed, retentate and permeate compositions and apparent rejection coefficients observed for the fractionation sequence performed in concentration mode with an oxidized industrial kraft liquor at 25 ºC, flowrate of 120 L h^{-1} and 1.4 bar

Membrane		VCF	μ (cP)	TS (g L^{-1})	Ashes (g L^{-1})	TP (g L^{-1})	R_i (%) TS	Ashes	TP
50 kDa MWCO	F	3	1.24	86.5	44.8	2.399	25.3	5.0	≈0
	R		1.28	100.8	43.6	2.320			
5 kDa MWCO	F	3.4	1.03	75.3	41.4	2.379	29.1	2.6	11.5
	R		1.13	90.3	38.8	2.507			
1 kDa MWCO	F	3	0.99	64.0	37.8	2.219	15.1	3.8	9.0
	R		1.02	69.0	39.0	2.364			
	P		0.97	58.6	37.5	2.151			

F: feed stream; **R**: retentate stream; **P**: permeate stream; **VCF**: volume concentration factor; **TS**: total solids; **TP**: total phenolate compounds quantified by HPLC-UV; $\mathbf{R_i}$: apparent rejection coefficient obtained in final retentate and permeate.

Additionally, in Figure 5.12, it is shown the corresponding composition regarding ashes, TP and other compounds not quantified in this work (unk. compounds) as wt% of TS. Ashes and TP contents were slightly enriched in the permeate streams during the membrane fractionation process studies from 52 and 2.8 %W/W_{TS} to a final value of 64 and 3.7 %W/W_{TS}, respectively. The other unknown compounds can correspond to lignin-carbohydrate complexes and other phenolic compounds present in solution (33) and their composition has decreased in the permeate streams along the membrane fractionation procedure, from 45 %W/W, present in the feed stream (oxIKL), to a final value of 32 %W/W (P1kDa). This means that, probably, the majority of the compounds present in the oxIKL corresponded to higher MW compounds that were retained by the membranes or to other compounds that were rejected by the dynamic layer generated at the membrane surface.

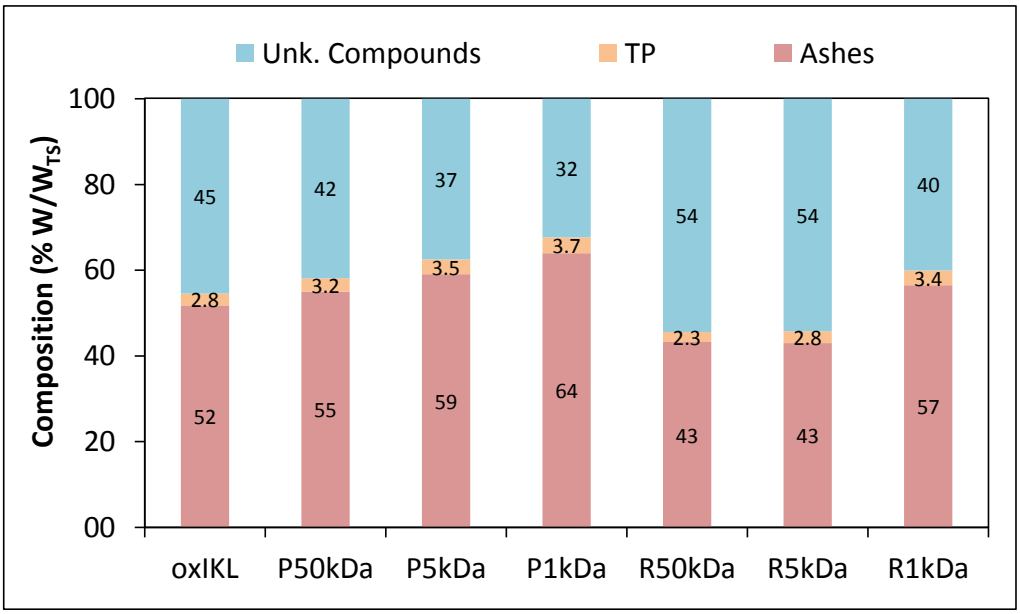

Figure 5.12 Composition (% W/W$_{TS}$) regarding ashes, TP and other compounds not quantified, for each stream obtained in the membrane fractionation sequence performed.

In Figure 5.13 it is shown the detailed composition of each stream in terms of weight of each phenolic compound identified per weight of the respective TS quantified, allowing to understand the enrichment of each phenolic monomer quantified. In general, *p*-OHB, V, OV, OS, VA and SA compositions have increased in the permeate streams between 1.1 and 1.6 times. S was the exception since its composition decreased from 9 to 7 mg g$^{-1}_{TS}$, probably due to the fact that this compound is highly susceptible to degradation.

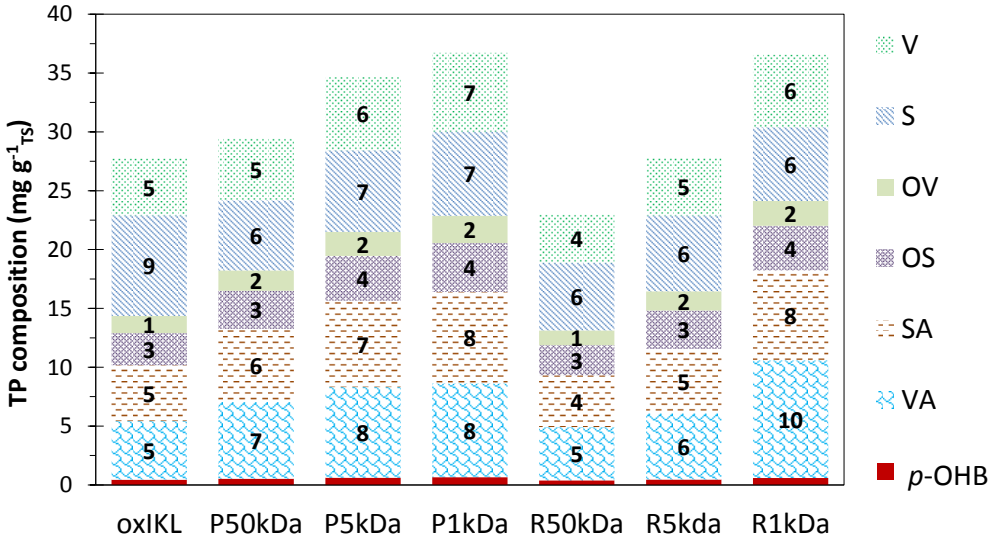

Figure 5.13 Detailed composition of the phenolate compounds quantified (V, S, OV, OS, VA, SA and *p*-OHB) expressed as mg g$^{-1}_{TS}$ for each processing stream.

The first membrane applied of 50 kDa was crucial for TP concentration in the permeate stream (P50kDa). In this first stage, about 25.3% of TS and a small amount of ashes (5%) were retained by the membrane while the TP went freely to the permeate stream. This stage led to a small enrichment of TP in P50kDa stream: starting with a feed stream containing 28 mg g^{-1} of TP, a solution with 32 mg g^{-1} of TP was obtained.

In stage 2 with the 5 kDa membrane, the TP apparent rejection was slightly higher than for stage 3 employing the 1 kDa membrane. As for the apparent rejection coefficient towards ashes, approximately the same level of retention was observed (2.6 % and 3.8 % for 5 and 1 kDa membranes, respectively)

Both stages showed the advantage of eliminating TS and some additional ashes; however, TP were also retained and, therefore, the further TP enrichment was not significant (Figure 5.13). In these last stages it was obtained 35 mg g^{-1} and 37 mg g^{-1} of TP for P5kDa and P1kDa streams, respectively.

Žabková *et al.* (2) obtained no rejections towards vanillin, processing synthetic mixtures of lignin and vanillin with ceramic membranes of 1, 5 and 15 kDa, although, the authors observed a more severe flux decline than the one observed in this work, and in the particular case of 1 kDa membrane, a significant contribution of fouling to total resistance of the membrane was obtained. Most probably, these differences are related with the fact that the depolymerized lignin solution used in this work affects the membranes differently, having impact on the apparent rejections observed towards TP.

It this work, it was clear that the first fractionation step with the membrane of 50 kDa was crucial for TP enrichment in the permeate stream. However, by proceeding with fractionation employing the 5 and 1 kDa membranes, further enrichment in TP was not very pronounced due to the observed losses of TP in the permeate stream. Therefore, it is very important to understand if the second and third stages are beneficial to the main objective of this work: obtaining purified fractions of vanillin and syringaldehyde. Since vanillin and syringaldehyde concentrations will continue with an adsorption step, the advantages of performing one, two or three membrane separation stage(s) must be evaluated.

5.3.2.3. *Cleaning effectiveness and fouling assessment*

Flux recovery is an important factor to consider when designing a membrane separation process. Therefore, water permeability recovery of each membrane was assessed regarding its initial water

permeability, obtained before treating the real oxidized lignin solutions. Physical and chemical cleaning of the membranes were conducted in order to understand the contribution of fouling formed during the processing of a real mixture.

In this work, depolymerized lignin, low molecular weight phenolic compounds and other solutes will contribute to the formation of fouling and consequently, will be responsible for the flux decline during processing. In order to obtain an economically feasible process, membrane productivities must be optimized and understanding the factors contributing for the formation of fouling is important. Fouling resistance can be distinguished in reversible and irreversible fouling. The reversible fouling is easily removed with physical cleaning, applying water or other equivalent solvent. The gel-polarized layer is assumed to be dynamic and can be considered as a reversible process. The irreversible fouling is caused by internal pore blocking or adsorption and it is usually more difficult to remove and, thus, restoring the initial permeate flux of the membrane requires more severe cleaning conditions with chemical agents and TMP.

Identifying factors affecting fouling is not easy as it depends on specific interactions between the membrane and the type of solutes present in the feed solution (4). The membrane-solute interactions will depend on properties such as charge, zeta potential, hydrophobicity, pore size, among others. Therefore, understanding in advance the membrane and solute properties could help to overcome flux limitations by choosing the best combination that avoids fouling formation. Moreover, knowing the effect of operating parameters such as temperature, differential pressure and crossflow velocity on fouling formation is also relevant.

The charge of the membrane is important to take into consideration when processing charged solutes. In the particular case of this study, it is expected to have ionized compounds in the oxidized IKL solution at the pH value of operation (≈10) (34-36). These solutions contain depolymerized lignin and other low molecular weight compounds in their sodium salt form that are expected to be negatively charged at the operating pH. Dong et al. (34) study showed that the isoelectric point for kraft lignin is 1.0 and above this pH value, the zeta potential is negative. Additionally, the p*K*a of the main low molecular weight compounds are between 4.3 and 7.9 (Table 2.1) and thus, it is expected that these compounds have negative charge in strong alkaline solutions such as the case of this work.

The most suitable membrane will be one having negative charge, since it will favour electrostatic repulsing interactions between the membrane and the ionized solutes and, thus, the membrane-solute interactions will be minimized and will not contribute for flux decline during operation. In this regard, several studies have reported that membranes with an active layer similar to the ones used in this work, of $TiO_2/Al_2O_3/ZrO_2$, have negative charges at high pH values (37-39) and, for this reason, are the most suitable membranes to treat this type of lignin solutions.

In Figure 5.14 it is portrayed the permeability recoveries accomplished by performing an initial physical cleaning and several chemical cleaning cycles. Physical cleaning allowed recovering 50%, 41% and 86% of the initial permeability observed for 50, 5 and 1 kDa membranes, respectively. It is also possible to observe that practically complete permeability recovery (> 87%) was accomplished after two/three chemical cleaning cycles. Chemical cleaning procedure can be further improved by employing higher temperatures or NaOH concentrations (e.g. 0.2 M).

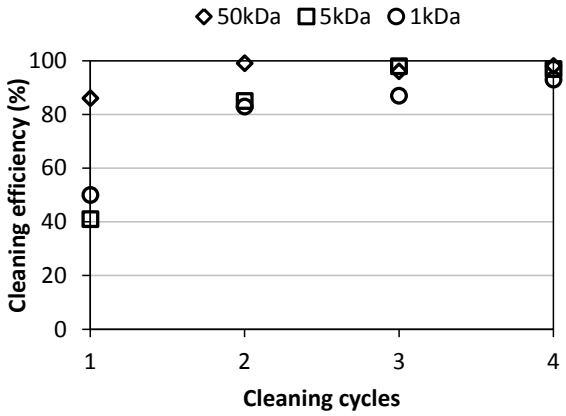

Figure 5.14 Recoveries of the initial permeability for the 50, 5 and 1 kDa MWCO membranes after processing with real oxidized mixtures and performing cleaning cycles: 1 corresponds to physical cleaning performed with no TMP pressure and 0.001 mol L^{-1} solution and the remaining cycles (2-4) to chemical cleaning with NaOH 0.1 mol L^{-1} heated up to 50 ºC.

In Žabková *et al.* (2), the initial flux recoveries were accomplished with one chemical cleaning cycle using 0.1 M NaOH solution for 6 hours, after the processing of model solutions of lignin (60 000 g mol^{-1}) and vanillin in similar tubular ceramic membranes (15, 5 and 1 kDa of MWCO). Therefore, increasing the cleaning time can also be an improvement.

It must be taken into consideration the fact that a more complex solution was used in this work, with lignin fragments of wide variety of sizes that could foul the membranes differently and increase the susceptibly of pore clogging and adsorption of the compounds on membrane surface, hindering the recovery of the initial permeability of the membranes.

The permeate flux evolution with time can be analysed by applying the resistance-in-series model (4). In Table 5.4 it is summarized the resistances values estimated for each membrane during fractionation sequence of the real oxidized lignin solutions. It is important to highlight that, although it is reasonable to assume that membrane resistance is constant during processing, the other resistances are time-dependent functions, responsible for permeate flux change over time. The contribution of the irreversible fouling usually is formed in the beginning of the process

achieving a steady state after a certain time (31). On the other hand, reversible fouling can vary during all processing time. Therefore, the fouling resistanced estimated values correspond to the maximum resistances observed.

Table 5.4 Maximum resistance achieved for each membrane with the fractionation sequence of the IKL and respective resistances of reversible and irreversible fouling

Stage	Membrane	$J_{p,final}$ (L m^{-2} h^{-1})	Resistances (10^{12} m^{-1})			
			R_T	R_f	R_{f_irrev}	R_{f_rev}
1	50 kDa	9.74	50.2	46.9	2.42	44.5
2	5 kDa	9.85	36.9	28.7	15.4	13.3
3	1 kDa	5.54	67.0	53.7	6.68	47.0

Besides the differences in the cut-off of the membranes employed and the observed flux decline in the beginning of processing, final R_T values found for each membrane are not significantly different, probably because a fractionation sequence was staged, and TS in solution were progressively removed before being applied to the next membrane. Additionally, it must be taken into consideration that the R_T value indicated for 50 kDa could be somewhat underestimated because of the chemical cleaning step performed after 22 h of processing.

Žabková *et al.* (2) determined the total resistance evolution with time for processing onto tubular ceramic membranes of 1, 5 and 15 kDa MWCO, a synthetic mixture containing 60 g L^{-1} of lignin (molecular weight 60 000 g mol^{-1}), 6 g L^{-1} of vanillin and pH value adjusted to 12.5. For the 1 kDa membrane, the authors obtained a final R_T of 35 x10^{12} m^{-1} (2), almost half the R_T observed in this work using the same membrane cut-off and an overall TS feed concentration of 64 g L^{-1}. Despite the fact that Žabková *et al.* (2) employed lignin/vanillin solutions of approximately 66 g L^{-1}, the performance differences observed are somewhat expected due to the fact that the solution employed in this work is more complex, with the presence of different solutes that can interact with each other or with the membrane in a different way, and offer additional resistances to flux permeation that model solutions do not possess. Furthermore, the wider molecular weight distribution range of the solution employed in this work can contribute for higher pore clogging propensity. It has already been mentioned above that the experimental conditions also have an important contribution to the formation of fouling and, therefore, it also must be taken into consideration the fact that flow rates, pH, TMP and VCF applied in each study are somewhat different and also can influence the fouling formed.

Concerning the 5 kDa membrane, the authors obtained R_T values near 30-33x10^{12} m^{-1} (2), not very different from the one obtained in this work employing the same cut-off. Although it is not possible to establish a straightforward comparison for the same reasons explained above about differences in composition and processing conditions, it could be expected to have higher total resistance when considering that higher bulk concentration was employed in this study (75.3 g L^{-1}) and that a wider MW distribution exists.

The change in bulk concentration and molecular sieving of solutes during the fractionation sequence influence the type of fouling generated and thus, reversible and irreversible fouling contribution to the total resistance observed in each stage can have a different relevance and could not depend directly on the cut-off of the membrane. Taking this into consideration, a resistance-in-series model was applied to determine the contribution of reversible and irreversible fouling to the total resistance observed in each stage. The respective resistance values obtained are summarized in Table 5.4.

After performing a physical cleaning cycle, the membranes initial permeability recovery was not the same, probably due to the different contribution of the irreversible fouling affecting flux, besides the intrinsic resistance of each membrane. The 1 kDa membrane stage processing exhibits irreversible fouling resistance contribution (6.68x10^{12} m^{-1}) smaller than the resistance offered by the membrane (13.32x10^{12} m^{-1}) and is in accordance with the highest permeability restoration achieved during physical cleaning (83%). The 50 kDa exhibited an irreversible fouling contribution (2.42x10^{12} m^{-1}) almost equal to its intrinsic membrane resistance (3.35x10^{12} m^{-1}) and thus, permeability recovery (58%) was smaller than the one achieved with the 1 kDa membrane. As for the 5 kDa membrane, irreversible fouling estimated (15.4x10^{12} m^{-1}) was the highest irreversible resistance estimated, affecting flux during the real solution processing and, consequently, flux recoveries accomplished with physical cleaning exhibit the lowest value (34%).

In general, the 50 kDa membrane was the one more affected by fouling (R_f/R_T of 93%), and the 5 and 1 kDa membranes were slightly less affected (78% and 80%, respectively). According to Aventosa-deLara *et al.* (40), since all R_f/R_T ratios are higher than 50%, the contribution of fouling resistance predominates over the intrinsic membrane resistance, being more noteworthy for the highest cut-off membrane studied.

Regarding the importance of the generation of reversible fouling for this fractionation sequence, the resistance caused by this component was more significant for the 50 kDa membrane ($R_{f,rev}/R_T$ of 89%), followed by the 1 kDa membrane (70%), and the 5 kDa membrane was the one having the lowest contribution (36%). This is indicative that the concentration polarization and formation of a cake layer on the 50 kDa membrane surface are the major phenomena responsible for the flux decline during operation with the 50 kDa. This partially explains the fact that flux decline never

achieved the stationary stage for this membrane and was changing with the increase of VCF. Rojas et al. (41) also observed an accentuated flux decline when processing directly an industrial black liquor with a 50 kDa ceramic membrane, never reaching the stationary stage. The authors refer to the formation of a cake layer and pore blocking as possible causes for the sharp decrease of flux observed.

Overall, since recoveries of permeate flux were almost completely accomplished for all membranes, the fouling generated during operation is easily removed allowing the re-utilization of the membranes. Nevertheless, further processing stages must be carried out to evaluate the membranes performance regarding productivities and rejection coefficients towards vanillin and syringaldehyde in successive experiments.

5.4. Conclusions

The fractionation of an oxidized IKL by 3 stages of ultrafiltration was investigated. For this purpose tubular ceramic membranes with 50, 5 and 1 kDa MWCO were employed in series and the composition of feed and retentates and permeates streams was determined regarding TS, ashes and TP. Overall, with the fractionation sequence, it was observed that TS content decreased from 86.5 g L^{-1} to 58.6 g L^{-1} while TP concentration decreased slightly less, from 2.399 g L^{-1} to 2.151 g L^{-1}. Apparent rejection coefficient values for TS of 25.3, 29.1 and 15.1 % were obtained for 50, 5 and 1 kDa MWCO membranes respectively. The 50 kDa membrane did not retain any TP, while for the other two membranes an apparent rejection coefficient of 9-12 % was obtained for both.

Optimizing the membrane process is important in order to establish the best investment in terms of membrane area, to facilitate membrane cleaning and hence to prolong its longevity. The efficiency of a membrane process is usually hindered by concentration polarization and membrane fouling. The solid buildup in the membrane boundary layer during the first minutes of operation is usually attributed to concentration polarization and is the main reason for the flux deviation from the solvent flux. After that, other mechanisms for fouling can take place due to solute-membrane and solute-solute interactions and pore clogging.

Therefore, analysis of membrane intrinsic and fouling resistances was performed and allowed understanding the importance of each component for the membranes performance during operation. The lowest cut-off membrane used (1 kDa) was the most affected one by fouling, being the reversible fouling the component most significant for the overall resistance. Consequently, flux decline for this membrane was the most pronounced of all. On the contrary, irreversible fouling

component was more important in the 5 kDa membrane operation. For the 50 kDa membrane, reversible fouling was the main reason contributing for the total resistance (93% of R_T) and the polarized layer growth was still being affected by the increase of concentration in the bulk solution, due to the operation in concentration mode.

The initial water permeate fluxes were easily accomplished within 2 to 3 cycles of chemical cleaning with NaOH 0.1 mol L^{-1} solutions allowing its further reutilization.

In this study, the advantage of treating oxidized IKL with the membrane of 50 kDa is very clear, since a permeate stream is collected having less TS and about the same TP concentration as the corresponding feed. However, the benefits of pursuing with the other membrane stages must be evaluated in the adsorption step, since simultaneously with the TS amount decrease in the permeate stream, the TP concentration was also reduced.

5.5. References

1. Borges da Silva, E. A., Žabková, M., Araújo, J. D., Cateto, C. A., Barreiro, M. F., Belgacem, M. N. and Rodrigues, A. E. (2009) An integrated process to produce vanillin and lignin-based polyurethanes from kraft lignin. Chem. Eng. Res. Des., 87: 1276-1292.
2. Žabková, M., Borges da Silva, E. A. and Rodrigues, A. E. (2007) Recovery of vanillin from lignin/vanillin mixture by using tubular ceramic ultrafiltration membranes. J. Membr. Sci., 301: 221-237.
3. Werhan, H., Farshori, A. and Rudolf von Rohr, P. (2012) Separation of lignin oxidation products by organic solvent nanofiltration. J. Membr. Sci., 423–424: 404-412.
4. Cheryan, M. (1998) Ultrafiltration and microfiltration handbook. Technomic Publishing Co., Inc: Lancaster, United States of America.
5. Jönsson, A.-S. and Trägårdh, G. (1990) Proceedings of the Symposium on Membrane TechnologyUltrafiltration applications. Desalination, 77: 135-179.
6. Girard, B., Fukumoto, L. R. and Sefa Koseoglu, S. (2000) Membrane Processing of Fruit Juices and Beverages: A Review. Crit. Rev. Biotechnol., 20: 109-175.
7. van Reis, R. and Zydney, A. (2001) Membrane separations in biotechnology. Curr. Opin. Biotechnol., 12: 208-211.
8. Susanto, H. and Ulbricht, M. (2008) Highly fouling resistant ultrafiltration membranes for water and wastewater treatments. Wa. Sci. Technol., 8: 19-24.

9. Bhattacharjee, C. and Bhattacharya, P. K. (2006) Ultrafiltration of black liquor using rotating disk membrane module. Sep. Purif. Technol., 49: 281-290.

10. Jagannadh, S. N. and Muralidhara, H. S. (1996) Electrokinetics Methods To Control Membrane Fouling. Ind. Eng. Chem. Res., 35: 1133-1140.

11. Evju, H. (1979) Process for preparation of 3-methoxy-4-hydroxybenzaldehyde, US Patent 4151207 (24-04-1979).

12. Jönsson, A.-S., Nordin, A.-K. and Wallberg, O. (2008) Concentration and purification of lignin in hardwood kraft pulping liquor by ultrafiltration and nanofiltration. Chem. Eng. Res. Des., 86: 1271-1280.

13. Toledano, A., García, A., Mondragon, I. and Labidi, J. (2010) Lignin separation and fractionation by ultrafiltration. Sep. Purif. Technol., 71: 38-43.

14. Sainio, T., Kallioinen, M., Nakari, O. and Mänttäri, M. (2013) Production and recovery of monosaccharides from lignocellulose hot water extracts in a pulp mill biorefinery. Bioresour. Technol., 135: 730-737.

15. Sevastyanova, O., Helander, M., Chowdhury, S., Lange, H., Wedin, H., Zhang, L., Ek, M., Kadla, J. F., Crestini, C. and Lindström, M. E. (2014) Tailoring the molecular and thermo–mechanical properties of kraft lignin by ultrafiltration. J. Appl. Polym. Sci., 131: 1-11.

16. Arkell, A., Olsson, J. and Wallberg, O. (2014) Process performance in lignin separation from softwood black liquor by membrane filtration. Chem. Eng. Res. Des., 92: 1792-1800.

17. Arkell, A., Krawczyk, H., Thuvander, J. and Jönsson, A. S. (2013) Evaluation of membrane performance and cost estimates during recovery of sodium hydroxide in a hemicellulose extraction process by nanofiltration. Sep. Purif. Technol., 118: 387-393.

18. Keyoumu, A., Sjödahl, R., Henriksson, G., Ek, M., Gellerstedt, G. and Lindström, M. E. (2004) Continuous nano- and ultra-filtration of kraft pulping black liquor with ceramic filters: A method for lowering the load on the recovery boiler while generating valuable side-products. Ind. Crop. Prod., 20: 143-150.

19. Uloth, V. C. and Wearing, J. T. (1988) Kraft lignin recovery: acid precipitation versus ultrafiltration. I. Laboratory test results. Pulp and paper Canada, 90: 67-71.

20. Cateto, C. A., Barreiro, M. F., Rodrigues, A. E. and Belgacem, M. N. (2011) Kinetic study of the formation of lignin-based polyurethanes in bulk. React. Funct. Polym., 71: 863-869.

21. Cateto, C. A., Barreiro, M. F. and Rodrigues, A. E. (2008) Monitoring of lignin-based polyurethane synthesis by FTIR-ATR. Ind. Crop. Prod., 27: 168-174.

22. Chahar, S., Dastidar, M. G., Choudhary, V. and Sharma, D. K. (2004) Synthesis and characterisation of polyurethanes derived from waste black liquor lignin. J Adhes. Sci. Technol., 18: 169-179.

23. Žabková, M., Borges da Silva, E. A. and Rodrigues, A. E. (2007) Recovery of vanillin from Kraft lignin oxidation by ion-exchange with neutralization. Sep. Purif. Technol., 55: 56-68.

24. Žabková, M., Otero, M., Minceva, M., Zabka, M. and Rodrigues, A. E. (2006) Separation of synthetic vanillin at different pH onto polymeric adsorbent Sepabeads SP206. Chem. Eng. Process., 45: 598-607.

25. De, S., Dias, J. M. and Bhattacharya, P. K. (1997) Short and long term flux decline analysis in ultrafiltration. Chemical Engineering Communications, 159: 67-89.

26. Bhattacharjee, C. and Bhattacharya, P. K. (1992) Prediction of limiting flux in ultrafiltration of kraft black liquor. J. Membr. Sci., 72: 137-147.

27. Aimar, P., Taddei, C., Lafaille, J.-P. and Sanchez, V. (1988) Mass transfer limitations during ultrafiltration of cheese whey with inorganic membranes. J. Membr. Sci., 38: 203-221.

28. Mota, I., Rodrigues Pinto, P. C., Novo, C., Sousa, G., Guerreiro, O., Guerra, A. R., Duarte, M. F. and Rodrigues, A. E. (2012) Extraction of polyphenolic compounds from *Eucalyptus globulus* bark: Process optimization and screening for biological activity. Ind. Eng. Chem. Res., 51: 6991-7000.

29. Pinto, P. C. R., Borges da Silva, E. A. and Rodrigues, A. E. (2010) Comparative study of solid-phase extraction and liquid−liquid extraction for the reliable quantification of high value added compounds from oxidation processes of wood-derived lignin. Ind. Eng. Chem. Res., 49: 12311-12318.

30. Žabková, M. (2006) Clean Technologies for the purification of Wastewaters: Adsorptive Parametric Pumping, Ph.D. Thesis, Chemical Engineering Department, Faculty of Engineering of University of Porto, Porto, Portugal.

31. Sridhar, S. and Bhattacharya, P. K. (1991) Limiting flux phenomena in ultrafiltration of kraft black liquor. J. Membr. Sci., 57: 187-206.

32. Lin, S. Y. and Dence, C. W. (1993) Methods in Lignin Chemistry. Springer-Verlag: London, United Kingdom.

33. Fache, M., Boutevin, B. and Caillol, S. (2016) Vanillin production from lignin and its use as a renewable chemical. ACS Sustain. Chem. Eng., 4: 35-46.

34. Dong, D. J., Fricke, A. L., Moudgil, B. M. and Johnson, H. (1996) Electrokinetic study of kraft lignin. Tappi J., 79: 191.

35. Sjöström, E., *Wood Chemistry, Fundamentals and Applications*, 1993, Academic Press, New York, United States of America.

36. Sundin, J. (2000) Precipitation of kraft lignin under alkaline conditions, Ph.D. Thesis, Department of Pulp and Paper Chemistry and Technology, Royal Institute of Technology, Stockholm, Sweden.

37. de la Rubia, Á., Rodríguez, M. and Prats, D. (2006) pH, Ionic strength and flow velocity effects on the NOM filtration with TiO_2/ZrO_2 membranes. Sep. Purif. Technol., 52: 325-331.

38. Almécija, M. C., Ibáñez, R., Guadix, A. and Guadix, E. M. (2007) Effect of pH on the fractionation of whey proteins with a ceramic ultrafiltration membrane. J. Membr. Sci., 288: 28-35.

39. Benfer, S., Árki, P. and Tomandl, G. (2004) Ceramic membranes for filtration applications - preparation and characterization. Adv. Eng. Mater., 6: 495-500.

40. Alventosa-deLara, E., Barredo-Damas, S., Zuriaga-Agustí, E., Alcaina-Miranda, M. I. and Iborra-Clar, M. I. (2014) Ultrafiltration ceramic membrane performance during the treatment of model solutions containing dye and salt. Sep. Purif. Technol., 129: 96-105.

41. Rojas, O. J., Song, J., Bullón, J. and Argyropoulos, D. S. (2006) Lignin separation from kraft black liquors by tangential ultrafiltration. Chimica e l'Industria (Italy), 88.

6. Purification of syringaldehyde and vanillin by chromatographic processes[1]

This chapter addresses the purification of an oxidized industrial kraft liquor (IKL) by chromatographic processes after being submitted to a membrane fractionation process.

The potential of adsorption onto polymeric resin SP700 has been shown in previous chapters with model phenolic compound solutions and herein a real oxidized industrial kraft liquor stream is loaded onto this resin after being treated by a membrane separation process encompassing 3 different cut-off membranes (50, 5 and 1 kDa). The final permeates P5kDa and P1kDa obtained from the second and third stages, respectively, of the fractionation sequence are loaded onto a bed packed with SP700 resin in order to evaluate if the third membrane stage with the 1 kDa membrane is important for the performance of the chromatographic process with the polymeric resin. The phenolic compounds of interest are readily eluted with an ethanol:water (90:10, % V/V) solution. Each stream is characterized regarding the total non-volatile solids, ashes and total phenolic compounds of interest quantified by HPLC-UV.

Afterwards, the potential of using supercritical fluid chromatography (SFC) technology to perform a final separation of syringaldehyde and vanillin is assessed. SFC preliminary studies with synthetic mixtures prepared with the typical phenolic compounds present in the real oxidized mixture are performed in a silica column at 150 bar and the effects of the incorporation of methanol (1-10 % V/V) or methanol containing formic acid (0.2% V/V) to the CO_2 mobile phase, of temperature (40 and 50 ºC) and of flowrate (4 and 5 mL min^{-1}), are studied to understand their influence in the chromatographic separation of the phenolic compounds regarding peak shape and selectivity. Methanol gradient methods at 3 and 5 ml min^{-1} are established with synthetic mixture at 150 bar and 40 ºC for the same silica column. Afterwards, the final eluates obtained after the adsorption/desorption studies are separated in the optimal gradient conditions found for each feed flowrate studied, thus, demonstrating the potential of applying SFC to purify phenolic compounds from oxidized IKL previously treated by membrane and adsorption processes.

---

[1] The following papers are in preparation:

Mota, I. F., Pinto, P. C. R., Loureiro, J. M., Rodrigues, A. E. Vanillin and syringaldehyde recovery from an oxidized industrial kraft liquor stream by adsorption onto a polymeric resin (draft in preparation).

Mota, I. F., Pinto, P. C. R., Loureiro, J. M., Rodrigues, A. E. Purification studies of typical phenolic compounds found in industrial kraft liquor streams by supercritical fluid chromatography (draft in preparation).

6.1. Introduction

Chromatography is a versatile separation technology suitable for the final stage of purification of added value compounds. It is becoming widely used in food industry (1-3) and for purification of compounds with pharmaceutical applications (4-6) and can be a good alternative to the traditional techniques such as distillation, extraction or crystallization.

Adsorption constitutes an interesting approach for the recovery of the phenolic compounds from the oxidized industrial kraft liquor (ILK) once it is easily integrated with the membrane separation process and it allows the separation of the phenolic compounds of interest from dilute solutions. In the particular case of *E. globulus* kraft liquors, typical solutions obtained after alkaline oxidation contain about 1.2 $\%W/W_{TS}$ of vanillin and syryngaldehyde (7). Moreover, this technology is very simple to design and scale up and combined with an adsorbent with high capacity and easy to regenerate it becomes an economically viable process (8).

The application of polymeric resins to recover phenolic compounds from different media has gained considerable relevance in the last years (9). Its use in industrial scale processes is very promising since these resins have high adsorption capacity, the phenolic compounds are easily recovered, the cost is low and regeneration is easy to accomplish (9-11). These resins are food-grade, which makes them good candidates for application in the food and pharmaceutical sectors; moreover, they are chemically stable and inert, allowing to be easily applied in diversified operating conditions. Precipitation problems can be avoided, since the pH value is maintained constant during the adsorption process (10). Moreover, these resins possess both hydrophobic and hydrophilic groups which make them advantageous for the adsorption of phenolic compounds (10).

Several studies with real complex solutions have been conducted, and demonstrated that these resins have high adsorption capacity for various phenolic compounds and they can be readily recovered using organic solutions such as acetone, ethanol or methanol (11-18). Regarding the phenolic compounds of interest in this work, most of the existing studies in polymeric resins are related with synthetic solutions of vanillin (15, 16, 19-21) and there are only few studies performed with a real mixture of oxidized lignin (22, 23). These studies also showed that the phenolic compounds of interest can be recovered with elution with organic solvents.

It has been shown in the previous Chapters 3 and 4 that the polymeric adsorbents Sepabeads SP700 and Amberlite XAD16N have high capacity of adsorption for vanillin and syringaldehyde, and that the compounds can be readily recovered with few bed volumes of an ethanolic solution leading simultaneously to the concentration of the sample. However, the main disadvantage of employing polymeric adsorbents and the main challenge to overcome is the lack of selectivity for the desired phenolic compounds since several other phenolic compounds are adsorbed as well and,

consequently, further purification processes are required to obtain a commercially high purity end product.

The final purification step is the most challenging step encountered when developing new processes or new commercial products for which high degrees of purity must be achieved. In the past, considering supercritical fluid chromatography (SFC) as a tool to achieve the desired final purities was not feasible, due to serious technical limitations encountered and lack of available know-how to overcome those limitations (24).

Nowadays, these limitations have been solved and SFC is becoming the election method for the final purification step with many advantages towards the classic preparative chromatographic methods, offering the possibility of obtaining highly purified products at kilogram scale (25) resorting to smaller amounts of solvents that will be necessary to evaporate and consequently, saving labor, time and energy costs (24, 26).

SFC is a separation technique that takes advantage of the physical and chemical properties of using supercritical fluids as the mobile phase, once they exhibit densities and dissolving capacities similar to certain liquids and, simultaneously, high diffusivity and low viscosity. Supercritical CO_2 ($scCO_2$, with supercritical conditions achieved for temperature and pressure above 31 ºC and 73.8 bar (27)) is the most common supercritical fluid used because it is inexpensive, non-toxic, non-flammable, and has lower critical parameters than most of the other fluids. Additionally, using CO_2 in preparative chromatography is very advantageous since CO_2 goes to gaseous state after depressurization and thus, highly concentrated fractions can be obtained without any additional energy to remove the solvent. This CO_2 can be captured and reintegrated in the chromatographic process.

However, $scCO_2$ has a limited solvating power with respect to polar compounds and, the use of polar organic solvents such as ethanol, methanol or 2-propanol as modifiers often helps to improve the elution of polar compounds more effectively since it helps improving the solute solubility in the mobile phase and induces changes in the chromatographic selectivity (28, 29). The addition of organic acids to the polar organic solvents as additives can also help to improve peak shape and/or solute solubility, thus influence separation efficiency and selectivity (30-33). These binary or ternary mobile phases have been intensively applied for the separation of numerous types of polar substances (30, 31, 34, 35).

SFC can be a powerful tool for the final stage of purification of vanillin and syringaldehyde from oxidized IKL. It has been extensively applied to separate several phenolic compounds from model solutions (6, 31) and from more complex natural media (32, 36, 37). However, there are not many studies employing SFC encompassing the phenolic monomers of interest in this study. It has been published very recently a SFC study covering the analysis of 11 lignin-derived phenolic

compounds including vanillin (V), syringaldehyde (S), acetovanillone (OV), acetosyringone (OS), vanillic acid (VA), syringic acid (SA) and *p*-hydroxybenzaldehyde (*p*-OHB) (38). The authors optimized an ultra-high performance SFC by choosing the most appropriate column (an high strength silica column – Acquity UPC2 HSS C18 SB, from Waters) and the best set of operating conditions among flowrate (0.5-2 mL min^{-1}), pressure (110-150 bar), temperature (40-60 ºC) and presence of different additives (citric, formic, trifluoroacetic acids) using methanol as the co-solvent incorporated to the CO_2 mobilie phase. The optimized chromatographic conditions were found to be at 60 ºC, 135 bar, 1.25 mL min^{-1}, incorporation of methanol with approximately 0.23% V/V citric acid (MeOH_ca) to the CO_2 mobile phase and detection wavelength at 280 nm. The following eluent gradient was employed: 1.5% V/V of MeOH_ca 0-2 min; 1.5-9 % V/V 2-5 min; 9% V/V 5-6 min; 9-1.5 % V/V 6-7 min. Finally, the authors have obtained a SFC method with high separation power and short analysis time. Moreover, the authors successfully applied this optimized method to a real solution containing these phenolic compounds after alkaline CuO oxidation of humic acid and extraction with ethyl acetate (38).

In this work an oxidized IKL previously processed by a membrane fractionation sequence with three different cut-off tubular ceramic membranes (50, 5 and 1 kDa) was subjected to an adsorption process employing non-polar SP700 resin. Prior to adsorption, the pH values of the permeates obtained from the second and third stages of the membrane process (P5kDa and P1kDa, respectively) were corrected with H_2SO_4 solution until a pH value of approximately 8. A complete breakthrough was performed with the P1kDa stream to evaluate the maximum adsorption capacity of each total low molecular weight phenolics quantified (V, S, OV, OS. VA, SA and *p*-OHB) by this resin and cycles of adsorption/desorption were performed with both P5kDa and P1kDa streams to investigate the regeneration of the resins and their reutilization. The monomers adsorbed were recovered by eluting with ethanol:water (90:10, % V/V) solution. Each feed stream and respective eluates were characterized regarding total non-volatile solids content, ashes and total low molecular weight phenolics quantified by HPLC-UV (TP). Composition and molecular weights distribution determined by gel permeation chromatography of each eluate are compared.

Moreover, in this work the potential of SFC to separate the typical phenolic monomers found in a real oxidized IKL mixture was also evaluated. In this way, studies were made with standard solutions of V, S, OV, OS, VA, SA and *p*-OHB to evaluate the effects of the flowrate, temperature and incorporation of methanol and formic acid to the CO_2 mobile phase in the retention behavior and separation of the target compounds. A SFC chromatographic method to separate the main phenolic compounds found in the eluates obtained (V, S, OV and OS) was established for a silica column.

6.2. Experimental description

6.2.1. Chemicals and analytical methods

Prior to adsorption, each feed stream was neutralized with H_2SO_4 solution (1:1, Panreac, purity 96%) until achieving a pH value of 7.6-8.2.

Feed and respective eluates were characterized regarding **total non-volatile solids (*TS*, g L^{-1})** and **ash content (*ashes*, g L^{-1})** by gravimetric method at 105 ºC and 650 ºC, respectively; **total low molecular weight phenolic compounds concentration** (***TP***, g L^{-1}) quantified by high performance liquid chromatography with ultraviolet detection (HPLC-UV) without performing the solid-phase extraction; **gel permeation chromatography (GPC)** analysis was also conducted. Procedures and experimental set-ups are described in Chapter 5. For HPLC-UV quantification, eluents were prepared with ultrapure water, methanol (Fluka, HPLC grade) and formic acid (Chem-Lab). For GPC analysis, *N, N*-dimethylformamid (Fluka, HPLC grade) and Lithium Chloride (Normapur®, purity ≥ 99%) were employed.

Ethanolic solution used in desorption studies is composed with 10% V/V deionized water and 90% V/V ethanol (Fluka, HPLC grade).

Standard solutions of vanillin (V, Sigma-Aldrich, purity ≥ 98%), syringaldehyde (S, Sigma-Aldrich, purity ≥ 98%), vanillic acid (VA, Sigma-Aldrich, purity ≥ 97%), syringic acid (SA, Sigma-Aldrich, purity ≥ 95%)), acetovanillone (OV, Sigma-Aldrich, purity ≥ 98%), acetosyringone (OS, Sigma-Aldrich, purity ≥ 97%) and *p*-hydroxybenzaldehyde (*p*-OHB, Sigma-Aldrich, purity ≥ 98%) were used in SFC studies in order to evaluate the potential of this technique for the final stage of V and S purification. CO_2 (99.998%) was purchased from Air Liquide (Portugal) and methanol HPLC grade (Fluka) was used as the co-solvent and the incorporation of formic acid (Chem-lab) was tested as an additive to the mobile phase.

6.2.2. Fixed bed adsorption/desorption experiments

Fixed bed experiments were performed in a jacketed glass column (Götec, Germany) of 6.3 cm length and 1 cm internal diameter, packed with a styrene-divinylbenzene resin SP700 (Mitsubishi

Chemical). Physical and chemical properties of the resin have been already detailed in Chapter 3. The bed porosity (ε) of 0.37 was determined by pulse experiments at different flowrates using blue dextran as tracer (39). One bed volume (BV) corresponds to the bed void volume of approximately 1.8 mL. The packed bed was thoroughly washed with ethanol:water (90:10, % V/V) solution and water prior to use. The fixed bed adsorption setup is depicted in Figure 6.1.

The pH value of each feed solution employed was corrected to 7.6-8.2 by adding sulfuric acid (96%) aqueous solution diluted 1:1 and fed into the SP700 resin bed with a Smartline Pump 1000 (Knauer) at 5.1 mL min^{-1} for the breakthrough experiment and at 5.4 mL min^{-1} for the cycles of adsorption/desorption performed. A fixed temperature of 25 ºC was ensured with a thermostatic water bath (Lauda). The adsorbed phenolic compounds were recovered by eluting with ethanol:water (90:10, % V/V) solution at the same operating conditions as the adsorption step. For the breakthrough experiment the line and bed was washed with water for 1 minute prior to the desorption step. Samples were collected at the column outlet, diluted and quantified by HPLC-UV. The experimental adsorbed and desorbed phase concentrations were determined from global mass balances.

In the end of each experiment, the bed was completely regenerated by eluting 45 BV of 0.1 M $NaHCO_3$ solution and rinsing with deionized water until pH 5.5 - 6.

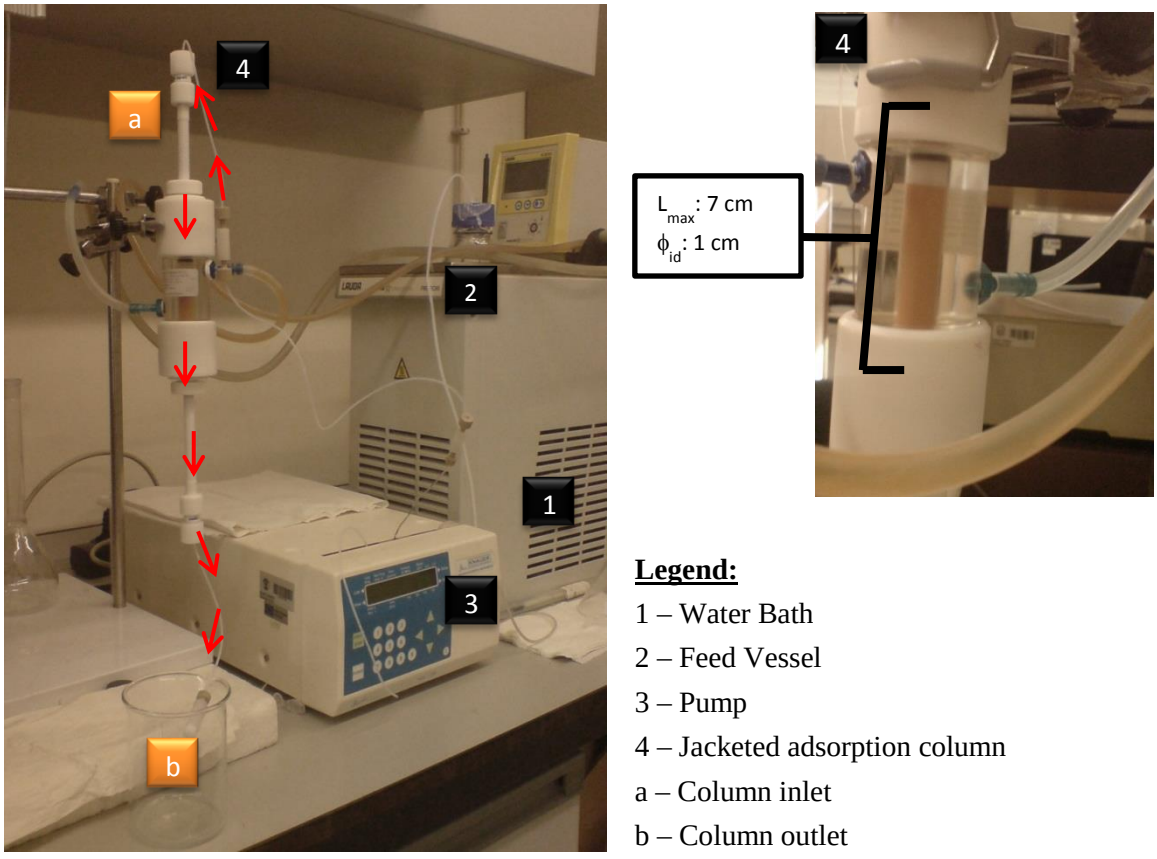

Legend:

1 – Water Bath
2 – Feed Vessel
3 – Pump
4 – Jacketed adsorption column
a – Column inlet
b – Column outlet

Figure 6.1 Fixed bed adsorption setup.

Three fixed bed experiments were performed: 1) a complete breakthrough with P1kDa as the feed stream; 2) five cycles of adsorption/desorption employing P1kDa as the feed stream and 3) four cycles of adsorption/desorption employing P5kDa as the feed stream. Each cycle includes the following sequence of steps: adsorption, washing, elution and final washing. In Figure 6.2 it is sketched the adsorption/desorption procedure performed and the sequence employed for the adsorption/desorption cycles.

A

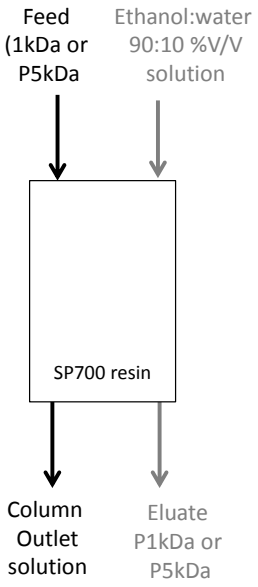

B

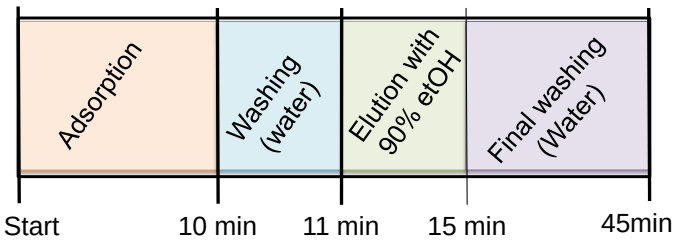

Figure 6.2 Preparative adsorption/desorption procedure: A) column packed with SP700 resin (6.3 cm of height, 1 cm of i.d., 0.37 of ε); B) Diagram of each cycle performed with P1kDa and P5kDa feed streams encompassing adsorption, washing, elution and final washing steps.

6.2.3. Supercritical Fluid Chromatography studies

SFC studies were performed in the supercritical chromatographer Thar® shown in Figure 6.3. This instrument is equipped with a column oven that holds 5 columns and can withstand temperatures between 5 ºC – 90 ºC, an auto sampler module, a fraction collector module and two delivery pumps for CO_2 and co-solvent operated between 0.5 - 15 mL min^{-1} and 0.1 - 10 mL min^{-1}, respectively. The desired flowrates are mixed in a mixer chamber and an automated backpressure regulator (ABPR) was used to control the desired flowrate. The detection is made by two detectors: diode array detector (DAD, model 2998) equipped with a high pressure flow cell and an evaporating light

scattering detector (ELSD, model 2424). The system is equipped with an automatic injector with injection volumes between 1 and 250 μL. The maximum operating pressure allowed is 300 bar. In Figure 6.4 it is portrayed a simplified diagram of the SFC equipment used. The equipment is controlled with the software ChromScope IE v1.2.

In this work it was used a Viridis^{TM} silica column of 4.6 x 250 mm and 5 μm particle size and injections of 10 μL were performed. A pressure of 150 bar was employed in all experiments and UV detection is performed at 280 nm.

The influence of temperature (40 or 50 ºC), modifier composition (methanol, 1-10 % V/V), presence of an additive (formic acid 0.2% V/V) and flowrate (5 or 4 mL min^{-1}) in the chromatographic separation was investigated with synthetic solutions aiming to understand the role of each parameter in the separation of V, S, OV, OS, VA, SA and *p*-OHB.

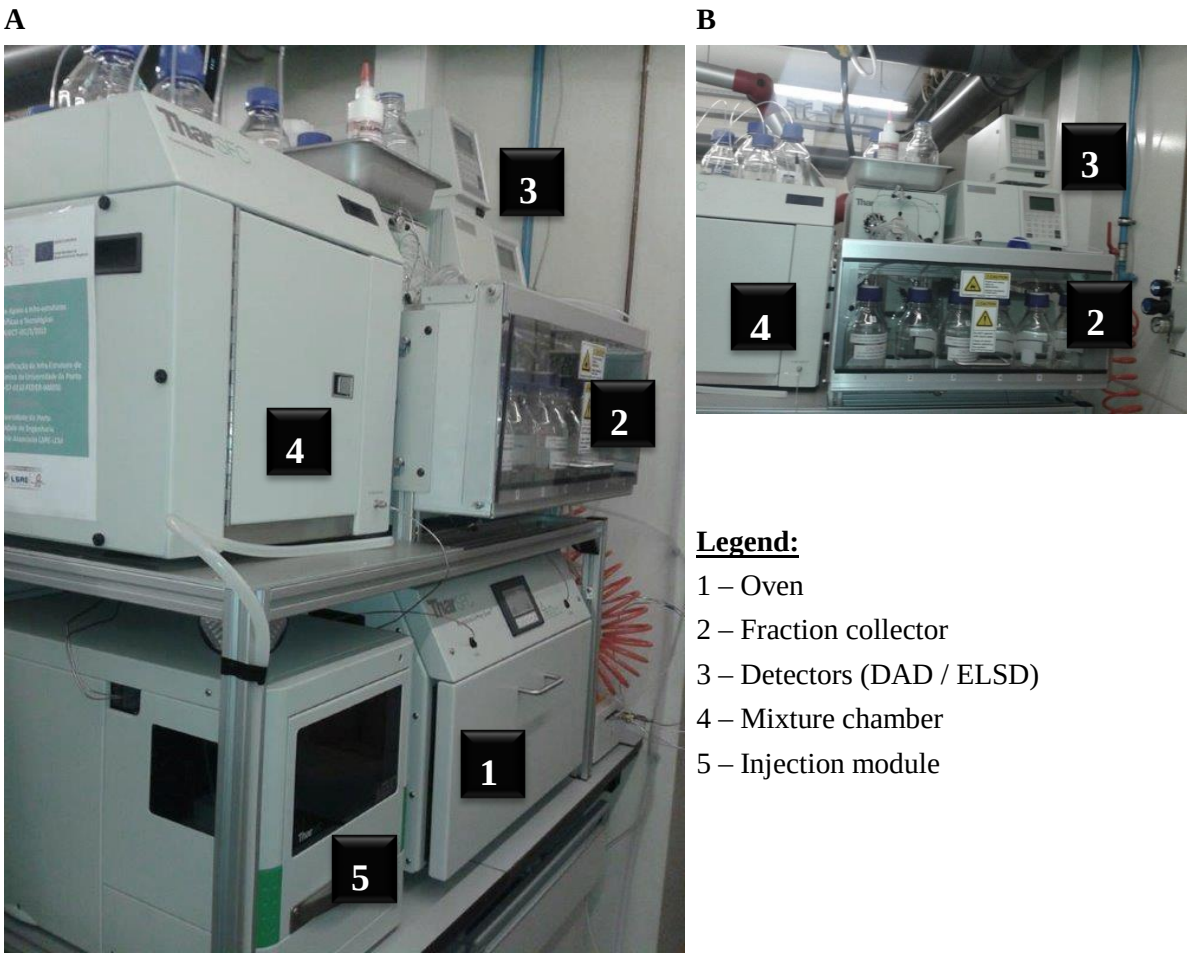

Figure 6.3 Supercritical fluid chromatography experimental setup.

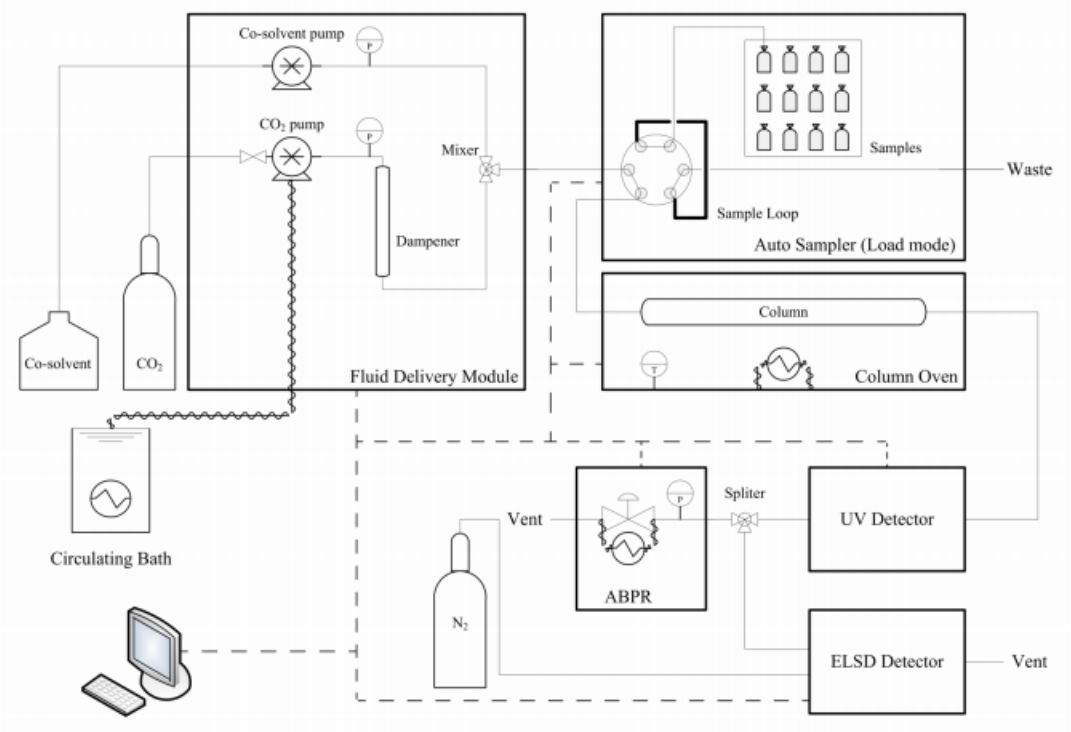

Figure 6.4 Simplified flow diagram of the supercritical fluid chromatography experimental setup used (40).

6.3. Results and discussion

6.3.1. Dynamic adsorption and desorption studies

Purification and enrichment of several natural extracts by polymeric resins have been extensively investigated (9, 14, 41-43), demonstrating the potential of this type of resins to treat solutions containing phenolic compounds. The presence of hydrophobic and hydrophilic groups in the resin turns this type of resins very attractive for the adsorption of phenolic compounds (10, 14). Moreover, adsorption processes are suitable for the recovery of compounds present in the feed stream in diluted concentration as is the case of the phenolic compounds fraction present in oxidized IKL media.

In this work, the polymeric resin SP700 was employed to treat an oxidized IKL previously submitted to a membrane fractionation sequence containing about 3 %W/W_{TS} of the phenolic

compounds quantified by HPLC-UV (TP). To our knowledge, this is the first study of adsorption employing non-polar resins aiming the V and S recovery from IKL oxidized in alkaline conditions by O_2. Existing literature reports to V and S adsorption from acidic spent liquor solutions (22, 23). Wang et *al.* (22) applied a polymeric resin to treat an oxygen delignification spent liquor in acid conditions (pH 4.5).

It has already been shown in previous Chapters that SP700 resin has good adsorption capacity for V, S, VA and SA. Taking as reference several studies published employing this type of resins to adsorb numerous different families of phenolic compounds (9), it is suggested that other phenolic compounds present in the oxidation mixture will also be co-adsorbed. Moreover, it is expected that the low MW lignin fragments will also be adsorbed (44, 45). Therefore, the main challenge to overcome when employing polymeric resins will be the lack of selectivity for V and S, since several other compounds will be co-adsorbed and co-eluted simultaneously, leading to a final product that probably requires further refining.

To overcome in some way this difficulty and taking advantage of knowing the p*K*a of some compounds present in the mixture (Table 2.1, Chapter 2), the working pH was established between 7.5-8.5 in order to avoid adsorption of the acids (VA, SA and other organic acids that might be present in solution). At this pH value, VA and SA, among other compounds, are ionized and thus will not be adsorbed. V, S, OV, OS and perhaps other low MW lignin fragments will be mostly in neutral state, and thus will be greatly adsorbed by the resin.

6.3.1.1. *Breakthrough experiment*

The final permeate stream obtained (P1kDa) pursued with an adsorption process onto SP700 resin until saturation of the bed. Afterwards, the adsorbed compounds were recovered by eluting with ethanol:water (90:10, % V/V) solution.

Figure 6.5 shows the transient concentration histories at column outlet for V, S. OV, OS, VA, SA and *p*-OHB. Since *p*-OHB is present in very low concentration, only traces of this compound were adsorbed. At the operating pH value, only traces of VA and SA were adsorbed due to the fact that these compounds are ionized at these conditions. This has already been discussed in Chapter 3 (and Appendix B), where it was shown that at pH 6.5, practically no VA and SA are adsorbed.

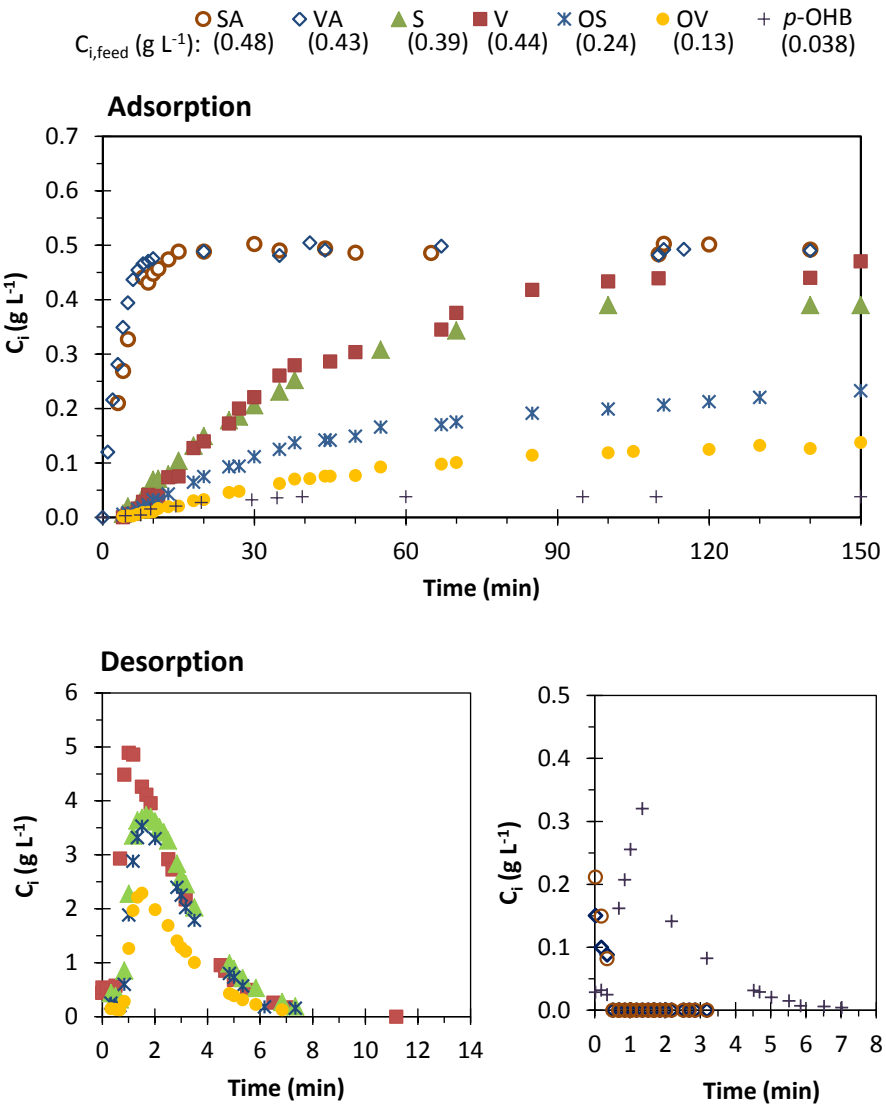

Figure 6.5 Adsorption and desorption concentration histories of V, S, OV, OS, VA, SA and *p*-OHB at column outlet. The column was packed with SP700 resin (6.3 x 1 cm, ε of 0.37) and experiments were performed at 25 ºC and feed flowrate of 5.1 mL min^{-1}.

Table 6.1 summarizes the concentration in the feed stream of V, S, OV, OS, VA, SA, *p*-OHB and TP quantified and the respective adsorption capacities and recovered percentages obtained. About 0.251 g g$^{-1}_{\text{dry resin}}$ of TP was adsorbed, being 59% V and S (corresponding to 0.147 g g$^{-1}_{\text{dry resin}}$). The remaining compounds adsorbed in this work were mainly represented by the respective V and S ketones (OV and OS).

The amount of V and S adsorbed in this work is considerably more than the maximum adsorbed amount (4.10-4.92 mg g^{-1}) reported in literature (22) employing the polymeric resin D101 to adsorb V and S from an oxygen delignification liquor, from solutions with initial feed concentrations of V and S ranging from 6.08 – 7.28 mg L^{-1}. Feed solution is composed by several phenolic compounds

and other unknown compounds that might compete with V and S for the available adsorption sites of the resin. Therefore it is expected that the V and S adsorbed amounts herein are lower than the ones obtained from mono component experiments with synthetic solutions presented in Chapter 3 (0.243 and 0.285 g $g^{-1}_{dry\ resin}$ calculated from the Bi-Langmuir equilibrium isotherm determined at 25 ºC for 0.44 and 0.39 g L^{-1} of V and S, respectively).

Table 6.1 Adsorption capacities and respective recovered amount of V, S, OV, OS, VA, SA and *p*-OHB and TP with ethanol:water (90:10, % V/V) solution. The bed (6.3 x 1 cm, ε of 0.37) was saturated with P1kDa solution onto SP700 resin at 25 ºC, 5.1 mL min^{-1}

	$C_{i,feed}$ g L^{-1}	Adsorption capacity g $g^{-1}_{dry\ resin}$	% Recovery 12 min elution	% Recovery 4 min elution
V	0.44	0.0797	81	74
S	0.39	0.0673	88	75
OV	0.13	0.0309	99	87
OS	0.24	0.0557	90	79
VA	0.43	0.0092	*	*
SA	0.48	0.0054	*	*
***p*-OHB**	0.038	0.0031	96	84
TP	2.14	0.251	83	73

*VA and SA were mostly washed out with water and only trace amounts of VA and SA were desorbed with ethanol:water (90:10, % V/V) solution.

About 81-99% of each adsorbed compound was recovered by eluting 12 minutes (34 BV) with an ethanol:water (90:10, % V/V) solution. Considering the elution with ethanolic solution for 4 minutes (11 BV), between 74-87 % of the TP adsorbed is recovered, with the advantage of obtaining a more concentrated final solution of TP since less solvent was employed. The composition of this latter eluate fraction will be detailed below in section 6.3.1.3. However, through Figure 6.5 it is possible to observe maximum concentration peaks achieved of 5 g L^{-1} for V and 4 g L^{-1} for S.

The level of recovery observed herein has also been observed in similar studies (22, 23). Wang *et al.* (22), desorbed V and S with ethyl ether and recoveries of 95-96 % were attained containing 71% of the desired aldehydes. Wu *et al.* (23) achieved 93.6% recoveries of vanillin from oxidized liquors of acidic sulphite pulping.

This experiment has contributed to demonstrate that the application of the non-ionic resin SP700 for recovering V and S from an oxidized IKL at operating pH value of 8 is achieved with great adsorption capacities. Although the pH near 7-8 was selected as a starting point, it is interesting in the future to perform a deeper study to evaluate the influence of pH in V and S adsorption in order to select the best operating pH value. Moreover, aiming the valorization of different products and enhancement of the adsorption process efficiency, it could be interesting to perform a sequential adsorption starting with pH values of 10-11 (the IKL oxidized solution as it is), followed by adsorption at pH values of 8 and 5.

6.3.1.2. *Cycles of adsorption/desorption*

Cycles of adsorption and desorption were performed aiming to evaluate the reutilization of the resin SP700 when employing real oxidized IKL previously submitted to a membrane process. In order to understand if the third stage of the membrane fractionation sequence is really needed, this study was conducted with the permeate streams obtained with the 5 kDa and 1 kDa membranes.

In Figure 6.6 it is shown the adsorption and desorption concentration histories at column outlet obtained for TP in the first cycle performed with each permeate stream abovementioned. It was possible to observe that practically the same TP concentration histories were attained in adsorption/desorption cycles performed with the different feed streams. About the same amount in TP was adsorbed in both experiments (0.063 ± 0.001 and 0.061 ± 0.001 g $g^{-1}_{\text{dry resin}}$ for P5kDa and P1kDa, respectively). Adsorption capacities obtained for V, S, OV and OS were also very similar with errors below 2% (Table 6.2).

Almost complete desorption of the TP (84 ± 2 % and 81 ± 2 % for P5kDa and P1kDa, respectively) was achieved employing the same ethanolic solution used in the experiment of saturation of the fixed bed (Table 6.2)

Five and four cycles of adsorption/desorption were performed with P1kDa and P5kDa feed solution, respectively, encompassing the steps indicated in Figure 6.2, and very similar adsorption/desorption concentration histories were obtained between cycles, demonstrating that the resin SP700 can be reutilized (at least) up to 4-5 cycles of adsorption/desorption. In Figure 6.7 and Figure 6.8 the concentration histories obtained in each cycle for V, S, OV, OS, VA and SA are overlapped. For *p*-OHB (the least adsorbed compound) and TP, the concentration histories obtained are shown in Appendix D (Figure D.1). Similarly to the recovered amounts attained in the

breakthrough experiment previously discussed, average recovery amounts are above 81%, with deviations below 6%.

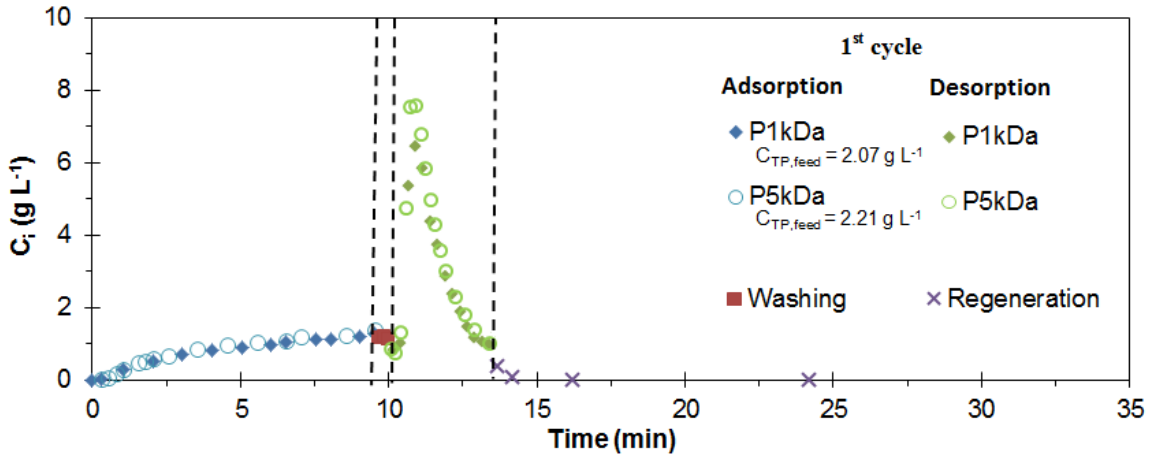

Figure 6.6 Adsorption and desorption concentration histories of TP at column outlet for the first cycle performed with P1kDa and P5kDa feed solutions. Each cycle encompassed a stage of adsorption, washing with water, elution with ethanol:water (90:10, % V/V) solution and final washing with water. The column was packed with SP700 resin (6.3 x 1 cm, ε of 0.37) and experiments were performed at 25 ºC and feed flowrate of 5.4 mL min^{-1}. TP corresponds to the overall phenolic compounds quantified by HPLC-UV (V, S, OV, OS, VA, SA and *p*-OHB).

Table 6.2 Average adsorption capacities and respective recovered amount of V, S, OV, OS and TP over five cycles of adsorption of P1kDa and four cycles for P5kDa. The bed (6.3 x 1 cm, ε of 0.37) was fed with each stream for about 10 minutes onto SP700 resin at 25 ºC, 5.4 mL min^{-1}

	P5kDa			*P1kDa*		
	$C_{i,feed}$ *g L^{-1}*	Adsorption capacity g g$^{-1}_{dry\ resin}$	% Recovery	$C_{i,feed}$ *g L^{-1}*	Adsorption capacity g g$^{-1}_{dry\ resin}$	% Recovery
V	*0.38*	0.0158 ± 0.0002	94 ± 1	0.40	0.0172 ± 0.0001	87 ± 4
S	*0.41*	0.0165 ± 0.0001	93 ± 3	0.39	0.0167 ± 0.0001	92 ± 3
OV	*0.14*	0.0063 ± 0.0002	97 ± 3	0.13	0.0060 ± 0.0001	100 ± 3
OS	*0.27*	0.0117 ± 0.0001	98 ± 2	0.25	0.0115 ± 0.0004	103 ± 6
TP	*2.21*	0.063 ± 0.001	84 ± 2	2.07	0.061 ± 0.001	81 ± 2

P5kDa $C_{i,feed}$: *p*-OHB 0.058 g L^{-1}; VA 0.49 g L^{-1}; SA 0.46 g L^{-1};

P1kDa $C_{i,feed}$: *p*-OHB 0.025 g L^{-1}; VA 0.43 g L^{-1}; SA 0.45 g L^{-1};

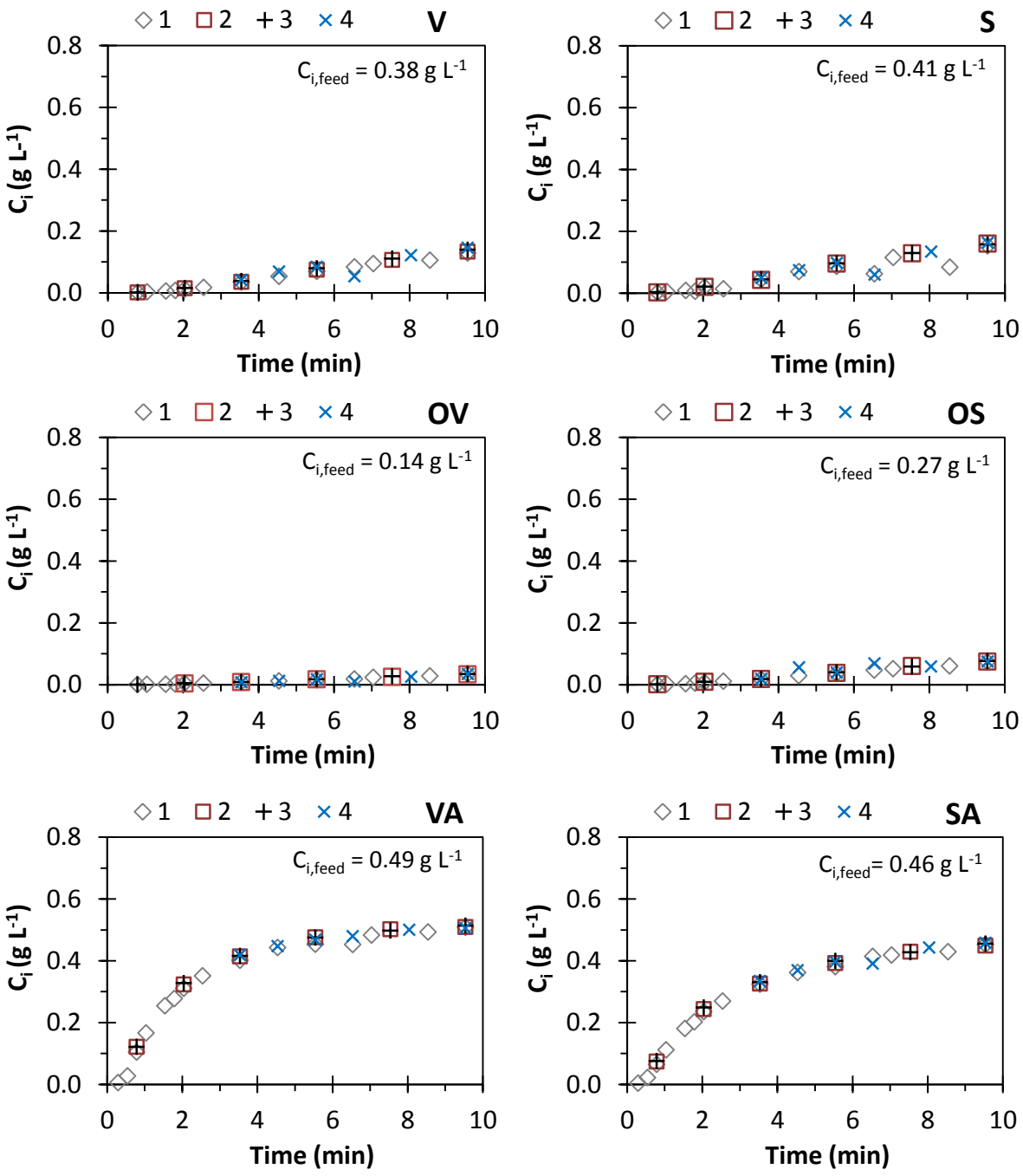

Figure 6.7 Adsorption concentration histories of V, S, OV, OS, VA and SA at column outlet for each cycle performed with P5kDa feed solution. The column was packed with SP700 resin (6.3 x 1 cm, ε of 0.37) and experiments were performed at 25 ºC and feed flowrate of 5.4 mL min^{-1}. Cycles are identified as 1- first cycle (◇), 2- second cycle (□), 3- third cycle (+) and 4- forth cycle (×).

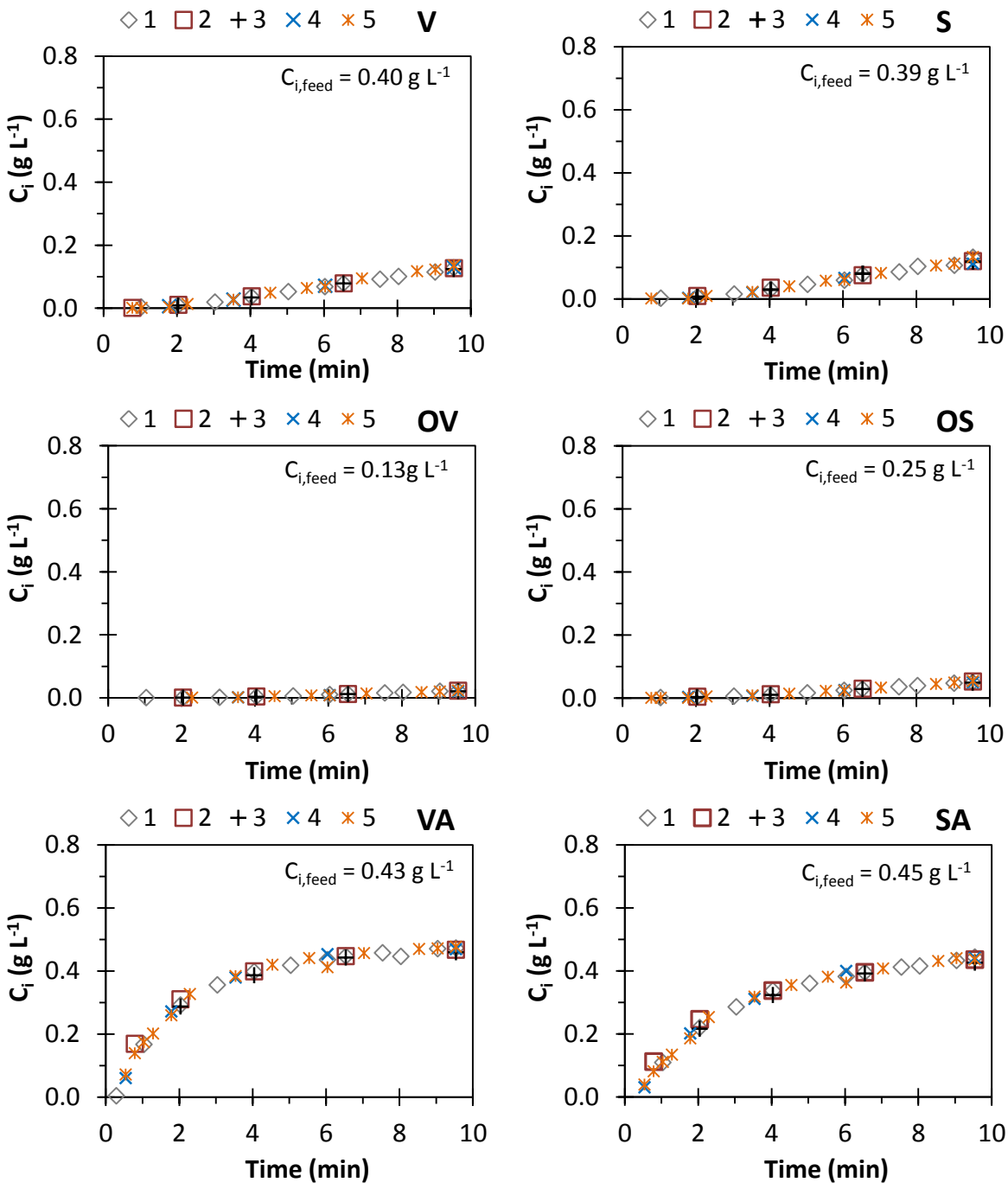

Figure 6.8 Adsorption concentration histories of V, S, OV, OS, VA and SA at column outlet for each cycle performed with P1kDa feed solution. The column was packed with SP700 resin (6.3 x 1 cm, ε of 0.37) and experiments were performed at 25 ºC and feed flowrate of 5.4 mL min^{-1}. Cycles are identified as 1- first cycle (◇), 2- second cycle (□), 3- third cycle (+), 4- forth cycle (×) and 5- fifth cycle (✳).

Average V and S adsorption capacities attained for the cycles performed with P5kDa and P1kDa are very similar and correspond to 0.0323 and 0.0339 g $g^{-1}_{dry\ resin}$, respectively. Moreover, nearly the

same TP was also adsorbed in both cycles as already mentioned, and thus, regarding each phenolic compound quantified, there are no significant differences between the P5kDa or the P1kDa permeate. Nevertheless, the decision of eliminating the third stage of the membrane fractionation sequence studied must take into account that there are other compounds not quantified that probably were adsorbed as well. Discussion about the composition of the eluates will be conducted in the next sub-section.

In Figure 6.9 it is shown the concentration histories of each eluting phenolic compound quantified by HPLC-UV observed for the first cycle performed with feed streams P5kDa and P1kDa. In Appendix D, it is shown overlaid the concentration histories obtained for the other cycles (Figures D.2 to D.4). Since the feed stream P5kDa was slightly more concentrated in TP than the P1kDa, the elution histories of V, S, O and OS are slightly higher employing the P5kDa stream.

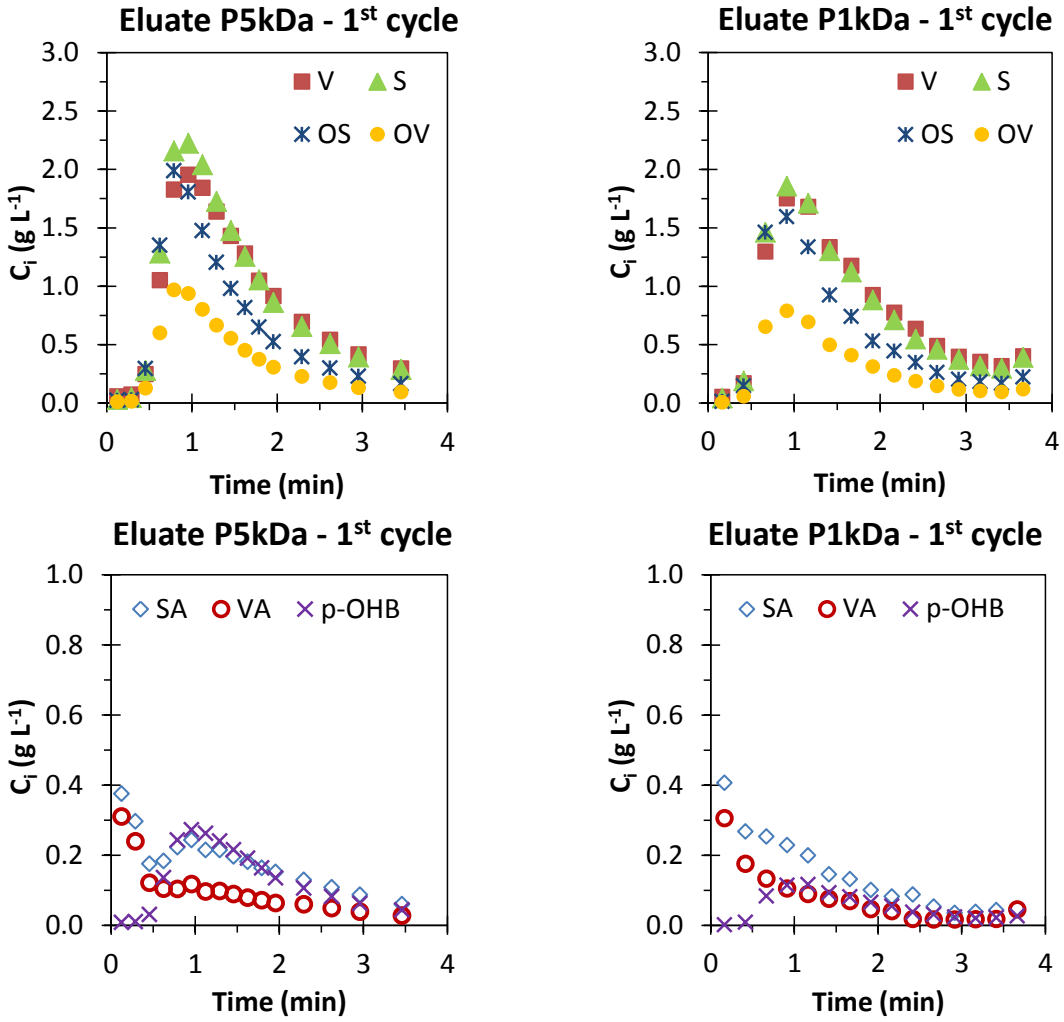

Figure 6.9 Elution concentration histories of V, S. OV, OS, VA, SA and *p*-OHB quantified for the first cycle after adsorption of feed streams P1kDa and P5kDa in a column packed with SP700 resin (6.3 x 1 cm, ε of 0.37) at the following operating conditions: 25 ºC and feed flowrate of 5.4 mL min^{-1}.

In the cycle experiments, the bed did not achieve the saturation and thus, less adsorbed amounts of TP were observed between the complete saturation of the bed experiment (0.251 g $g^{-1}_{dry\ resin}$) and the cycles performed (0.061/0.063 g $g^{-1}_{dry\ resin}$). Consequently, comparing the elution concentration with the concentration histories observed for the experiment performing complete saturation of the bed with P1kDa feed stream (Figure 6.5), more diluted eluates are obtained with lower maximum concentration values observed, around 2 g L^{-1} (Figure 6.9). In Appendix D, it is shown overlaid the concentration histories of TP obtained in each adsorption/desorption experiment performed (Figure D.5).

The advantage of performing cycles of adsorption/desorption is that almost all V and S fed onto the column are adsorbed (nearly 80%) and thus, less V and S are lost, since the bed is still retaining these compounds. Consequently the efficiency of the adsorption process is greatly improved.

6.3.1.3. *Composition of the eluates*

In Table 6.3 it is summarized the concentration of TS, ashes, TP, V, S, OV and OS assayed for each eluate obtained by collecting the solution coming out of the column for the time interval of [0.5-3.5/4[min. The eluates are: eluate P1kDa, Breakthrough (complete saturation of the bed) and eluates P5kDa, cycles and P1kDa, cycles (for adsorption/desorption cycles performed). The composition of the solution coming out of the adsorption column during feeding with P5kDa is also presented (P5kDa, column outlet). Comparing the composition of the feed (Table 5.4, Chapter 5) with the respective eluates obtained, TS has decreased significantly from 58.6 - 64.0 g L^{-1} to 7.2 – 24.6 g L^{-1}. The ashes concentration also decreased from 38 g L^{-1} to a value below 2.5 g L^{-1}. The eluate P1kDa corresponding to the complete bed saturation presents the highest TS and TP concentration. Additionally, the TP concentration has increased about 1.5 times for the eluates obtained in the cycle experiments and 4 times for the complete saturation of the bed experiment.

Moreover, through the analysis of the solution coming out of the column during adsorption cycles with P5kDa stream, it was possible to conclude that the majority of the compounds were not adsorbed onto the bed leading to a solution containing about 41.3 g L^{-1} of TS. TP concentration in this stream has decreased from 2.21 to 0.90 g L^{-1} and is mainly composed by the phenolic acids not adsorbed VA and SA, in concentrations of 0.41 and 0.33 g L^{-1}, respectively.

Table 6.3 Concentration of TS, ashes, TP, V, S, OV and OS obtained for each eluate solution collected from [0.5-3.5/4[minutes and for the column outlet during cycle adsorption experiments with P5kDa.

Concentration ($g\ L^{-1}$)	Eluate P1kDa, Breakthrough	Eluate P1kDa, cycles	Eluate P5kDa, cycles	P5kDa, column outlet
TS	24.6	7.2	9.0	41.3
Ashes	2.4	0.4	0.4	26.4
TP	9.09	3.25	3.38	0.90*
V	2.49	0.97	0.98	0.06
S	2.82	0.95	1.00	0.05
OV	1.27	0.38	0.38	0.02
OS	2.42	0.74	0.72	0.04

*VA and SA concentration is 0.41 and 0.33 $g\ L^{-1}$, respectively.

The corresponding composition regarding ashes and TP of each stream analysed are detailed in Figure 6.10, as wt% of TS. The remaining compounds not analysed in this work (unk. compounds) would correspond to other compounds present in solution such as lignin-carbohydrate complexes and other low MW lignin fractions and low MW phenolic compounds (46) that might have been adsorbed and co-eluted as well (9, 44, 45).

The aim of this characterization was to understand the level of enrichment in TP content quantified by HPLC-UV, in respect to the TS determined for each sample. The composition in terms of wt% of TS for the feed streams P5kDa and P1kDa has been already detailed in Chapter 5 (Figure 5.12). Comparing the composition of the feed steams with the corresponding eluates obtained, the content in ashes has decreased significantly from 59-65% to less than 10 $\%W/W_{TS}$. The content in TP for all the three eluates was significantly increased from 3-4 to 38-45 $\%W/W_{TS.}$ However, unk. compounds fraction corresponding to other compounds that were simultaneously adsorbed and co-eluted being also concentrated and thus, its composition also increased from 32-37% to 49-57 $\%W/W_{TS}$.

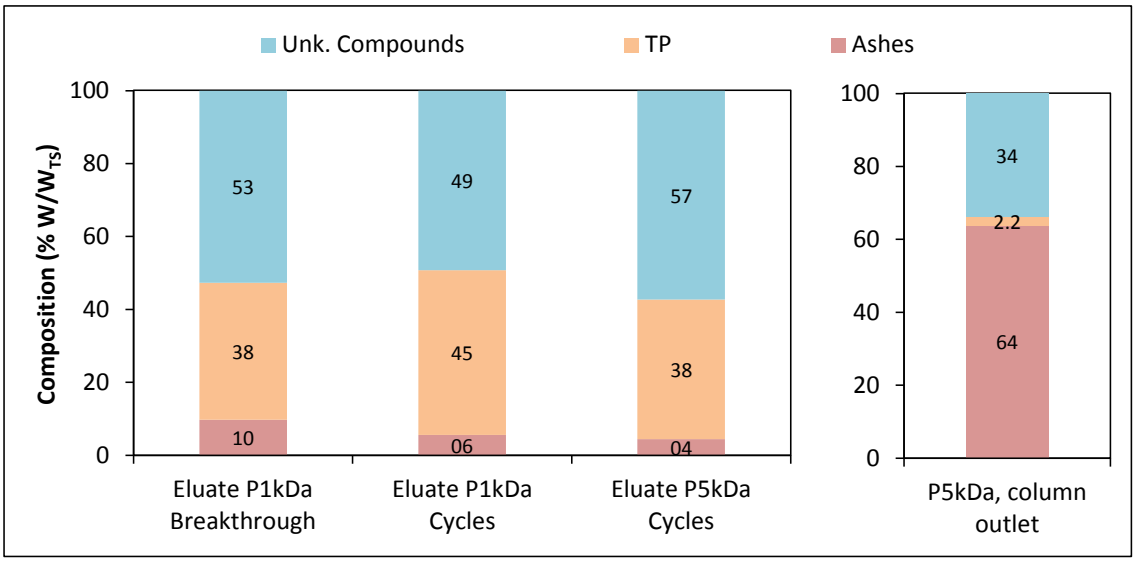

Figure 6.10 Composition (%W/W$_{TS}$) regarding ashes, TP and other compounds co-eluted not quantified for each elution stream analysed (collected for the time interval [0.5-3.5/4[minutes) and for column outlet during adsorption cycles experiments with P5kDa.

In Figure 6.11 the content of each phenolic compound quantified expressed as mg per g of TS for the feed streams employed in the adsorption/desorption studies and respective eluates are shown. The relative content of each phenolic compound quantified expressed as wt% of TP is displayed in Appendix D (Figure D.6). V and S composition increased from 11-15 mg g$^{-1}_{TS}$, present in the feed, for 216-267 mg g$^{-1}_{TS}$ (corresponding to an increase of 14-24-fold and representing about 58-59% of the TP). The remaining phenolic content obtained for the eluates corresponds mainly to OV and OS, and composition of both these compounds have increased from 6-7 mg g$^{-1}_{TS}$ to 122-156 mg g$^{-1}_{TS}$ (17-26-fold increase and representing 32-35% of the TP). Since VA, SA and *p*-OHB were adsorbed in lower amounts and thus, its composition changed from 15-17 mg g$^{-1}_{TS}$ to 4.4 mg g$^{-1}_{TS}$ for P1kDa breakthrough experiment and 29-33 mg g$^{-1}_{TS}$ for the cycle experiments.

The composition of the solution coming out of the column during cycle experiments with P5kDa was also studied (Figure 6.10). This solution was depleted in TP (2 %W/W$_{TS}$) with VA and SA (18 mg g$^{-1}_{TS}$, Figure 6.11) content being the main phenolic compounds quantified, representing 82 % of the TP. Moreover, this solution became poorer in V, S, OV and OS, representing only 18% of the TP, and strongly enriched in ashes, attaining 64 %W/W$_{TS}$. Regarding the other compounds not adsorbed (e.g. high MW lignin fragments), the P5kDa column outlet solution contains about 34 %W/W$_{TS}$.

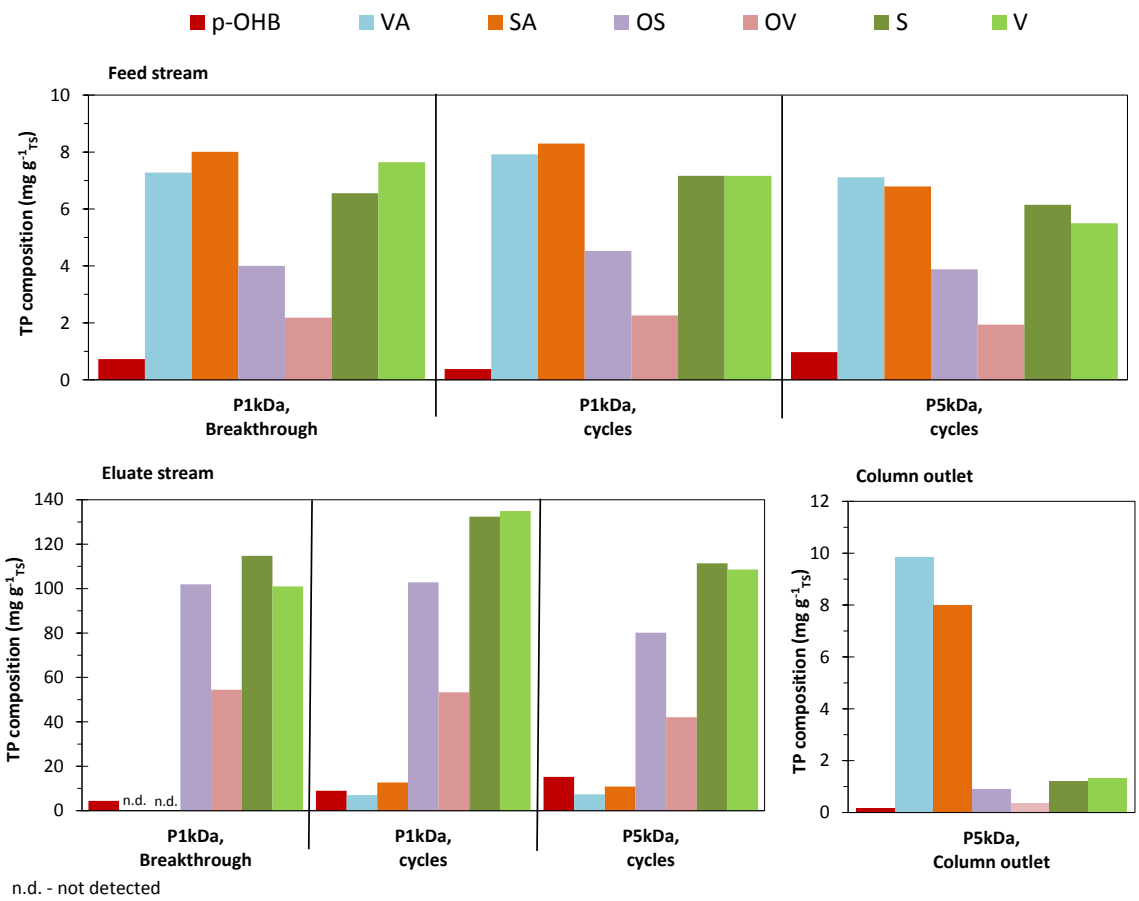

Figure 6.11 Detailed composition of the phenolic compounds quantified (V, S, OV, OS, VA, SA and *p*-OHB) expressed as mg g^{-1}_{TS} for the different feed and eluate streams obtained (collected for the time interval [0.5-3.5/4[minutes) and for column outlet solution during P5kDa adsorption cycles.

Comparing the eluate solutions obtained in the cycles study, although P5kDa eluate is slightly more concentrated in TP (3.38 g L^{-1}, Table 6.3) than the P1kDa eluate solution (3.25 g L^{-1}, Table 6.3), V and S composition in terms of mg g^{-1}_{TS} is 1.21 times more for the P1kDa eluate fraction collected (267 mg g^{-1}_{TS}) than for P5kDa (220 mg g^{-1}_{TS}). This can be partially explained by the fact that other compounds besides the TP and ashes quantified were adsorbed in more extent for P5kDa cycle experiments. It also indicates that the membrane fractionation step encompassing 3 membrane stages was somewhat beneficial to increase composition of TP in the final eluate solution obtained. Nevertheless, a third membrane stage accounts for more initial investment and operating costs and thus, the decision to include this third stage must take into consideration other variables, such as the economic aspects.

In the future, an adsorption/desorption study employing this solution as the feed stream to recover the phenolic acids (VA and SA) could be considered. These acids are known for having important

biological properties (47, 48) and a better exploitation of the oxidized IKL introduces more value to the integrated lignin oxidation and separation/purification process studied in this work.

6.3.1.4. *Composition of the eluate P1kDa along desorption time*

The concentration regarding TP, ashes and other compounds not quantified along desorption time was studied for cycles of adsorption performed with P1kDa feed solution and is summarized in Table 6.4. In Figure 6.12 it is depicted the composition in terms of $\%W/W_{TS}$ of each time fraction of P1kDa eluate collected. The main goal with this characterization was to understand if compounds co-eluted would preferentially come out of the column in the beginning of desorption and investigate TP relative content evolution along the desorption procedure (Figure 6.13).

Maximum concentration of TS, ashes and TP was found for eluate fraction collected between [0.8-1.3[minutes of desorption with ethanol:water (90:10, % V/V) solution (Table 6.4). However, considering the enrichment in TP in each fraction ($\%W/W_{TS}$) obtained, the fraction with the lowest concentration (1.26 g L^{-1}) collected for time interval [2.5-3.5[min was the richest in TP (79 % W/W_{TS}).

Table 6.4 Concentration of TS, ashes, TP, V, S, OV and OS determined for different time intervals during the elution of P1kDa cycles study

Concentration ($g\ L^{-1}$)	[0.5-0.8[min	[0.8-1.3[min	[1.3-1.8[min	[1.8-2.5[min	[2.5-3.5[min
TS	n.a.	16.1	7.9	4.6	1.6
Ashes	n.a.	1.9	1.2	0.9	0.1
TP	4.92	5.96	3.15	2.46	1.26
V	1.22	1.69	1.02	0.84	0.45
S	1.29	1.70	0.93	0.74	0.38
OV	0.62	0.74	0.36	0.27	0.13
OS	1.38	1.51	0.68	0.48	0.26

n.a. - not analysed

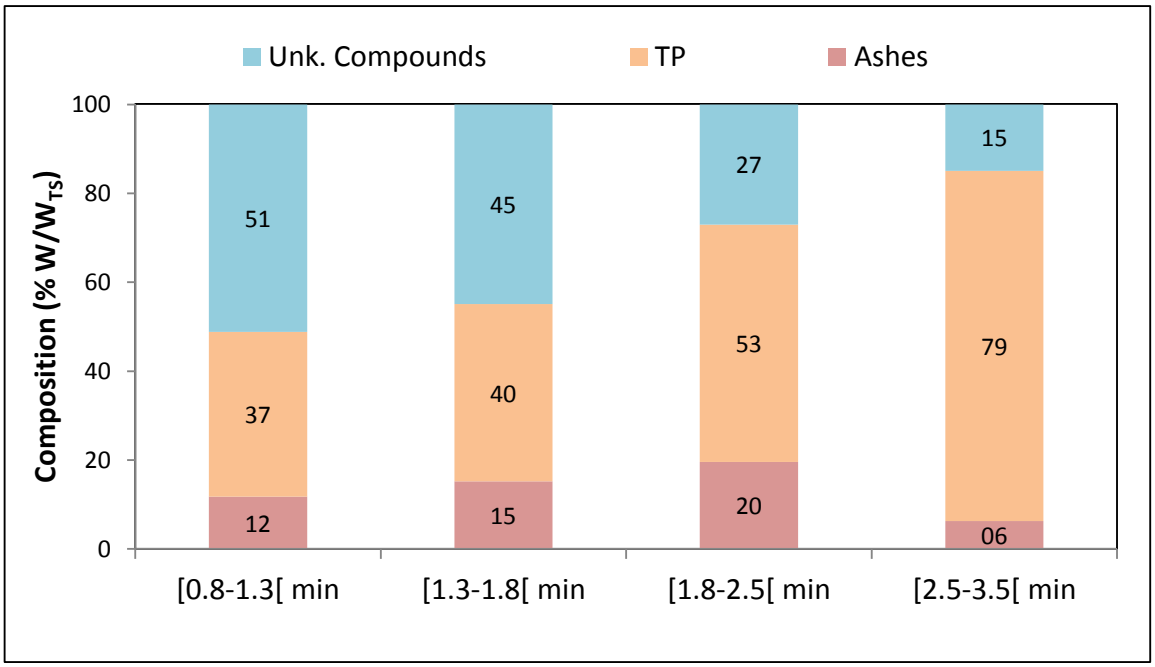

Figure 6.12 Composition (% W/W$_{TS}$) regarding ashes, TP and other compounds co-eluted not quantified for different elution time fractions of desorption for P1kDa cycle experiments.

Additionally, through Figure 6.12 it is possible to observe that the TP content has increased along time of desorption from 37 to 79 %W/W$_{TS}$ and simultaneously, the other compounds being co-eluted decreased from 51 to 15 %W/W$_{TS}$, clearly demonstrating a selective enrichment. This characterization gave the indication that the other compounds co-adsorbed (such as carbohydrates-lignin complexes, other low MW lignin fragments and TP) were mainly desorbed in the beginning of desorption procedure.

Although the last fraction collected (corresponding for the elution interval [2.5-3.5[min) is more enriched in TP (79 %W/W$_{TS}$) than the other fractions, its concentration in solution was the lowest (1.26 g L^{-1}) of all the fractions analysed, meaning that a considerable mass of TP is co-eluted in the beginning of the desorption process with the other compounds present. Therefore, the decision for the selection of the time interval to proceed with further purification steps must account for this loss in mass.

The relative V, S, OV, OS, VA, SA and *p*-OHB (expressed as wt% of TP) of each time fraction collected was determined (Figure 6.13) and it was possible to observe that the proportions between the different phenolic compounds quantified changed slightly. Along the desorption procedure, OV and OS decreased from 13% and 28% to 10% and 19%, respectively. The opposite trend was observed for V and S, where an increase of content from 25 and 26 % to 36 and 30 % was obtained, respectively. This gives an indication that probably OV and OS are desorbed in a higher rate than V and S.

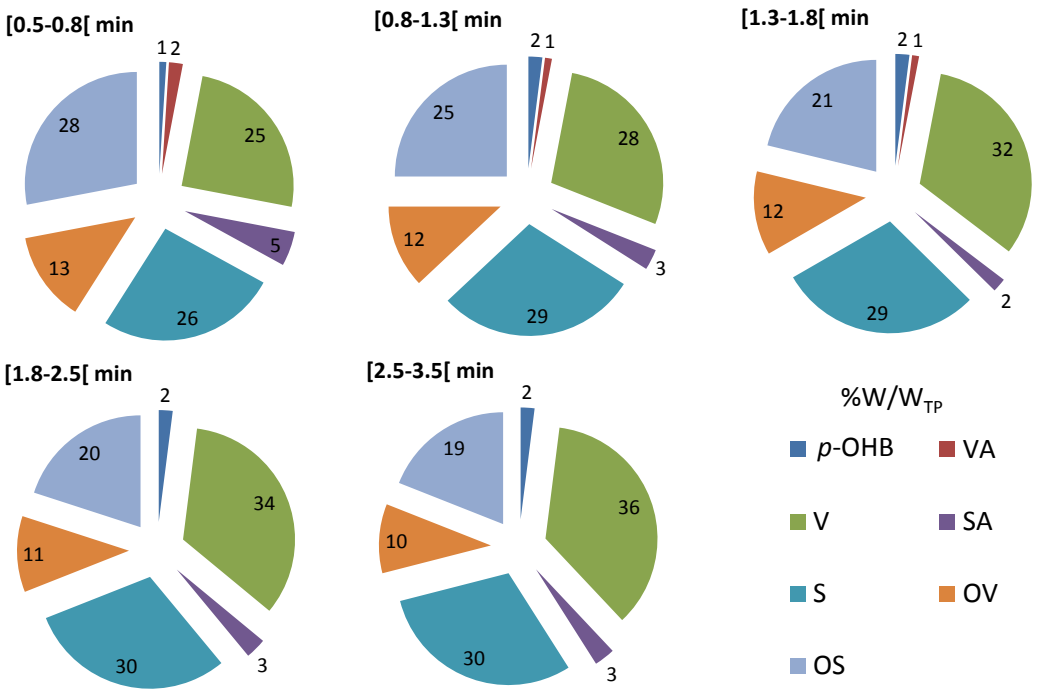

Figure 6.13 Relative V, S, OV, OS, VA, SA and *p*-OHB expressed as wt% of TP for different fractions of elution time during desorption cycle studies with ethanol:water (90:10, % V/V) solution for P1kDa.

The results of this study demonstrate the capability of adsorption/desorption to purify phenolic compounds from the oxidized IKL permeate (adsorption feed), in particular V and S. Although with some loss of these two compounds in the eluate (about 25% considering the cycles performed), the final concentration considering all the eluate collected is 1.92 and 1.98 g L^{-1} for cycles performed with P1kDa and P5kDa, respectively, with 4-6 %W/W_{TS} of ashes and 50-57 %W/W_{TS} of other unidentified compounds, corresponding to an increase of V and S purity from 1.2-1.4 % (feed stream) to 21-27 % (final eluates obtained in the cycle studies), which represents an 19.6-25.8 % increase of purity, when compared with the feed stream.

Additionally, in this study it was also demonstrated that this resin can be reused at least 4/5 times for adsorption of phenolic compounds from an oxidized IKL previously subjected to a membrane fractionation process, without losing its capacity, since most of the compounds are recovered in the elution step and complete regeneration of the bed is accomplished with water.

6.3.1.5. *Gel permeation chromatography*

Gel permeation chromatography (GPC) analysis was performed for feed streams and for the respective eluates obtained, in order to understand the differences in the molecular weight (MW) distribution profile during each adsorption/desorption study. The molecular mass distribution obtained for each stream is shown in Figure 6.14, normalized by the area under the curve.

As previously explained in Chapter 5 for GPC applied to the different streams obtained for the membrane fractionation study, GPC separates the compounds present in each sample based on molecular size allowing determining the relative MW. The greater the MW of the compound, the lower the elution time will be.

GPC is considered to be a relative method and thus, conclusions and comparison between other works/studies should be carefully done (49). Sample treatment, mobile and stationary phases influence the values/results obtained (50). As for instance, the use of different solvents can swell the stationary phase differently, consequently affecting the pore size distribution in a different manner (50). Electrostatic repulsion and solvation of the phenolic molecules can occur and thus the ionic strength of the eluent contributes also for the separation behaviour observed (50). Additionally, due to the presence of several phenolic compounds with different functional groups (e.g. hydroxyl, carbonyl, aldehyde, carboxyl), the chromatographic separation can be affected as well because of different interactions between the phenolic compounds and the stationary phase of PS-DVB such as ion exclusion, ion exchange and ion inclusion and adsorption phenomena triggered by hydrogen bonding or hydrophobic interactions between the compound and the gel (50).

In this work, different polystyrene standards were analysed by GPC in order to obtain the correlation between MW and the respective elution time. However, for the reasons explained above, the phenolic compounds will interact differently with the stationary phase, and different elution times than the ones expected will be observed. This has already been mentioned in Chapter 5 with GPC performed with some phenolic standards (Figure 5.9).

During adsorption, the low molecular weight phenolic compounds (including V, S, OV, OS and low MW lignin fragments) (44, 45, 51) present in solution will be adsorbed. Since the operating pH value was near 8, VA and SA acids will not be extensively adsorbed since experiments are being conducted in a non-polar resin and the acids are mainly ionized (since their p*K*a is around 4.3 - 4.4, indicated in Table 2.1, Chapter 2). Therefore, it is expected that the solution coming out of the column will be richer in these acids, other ionized phenolic compounds and higher MW compounds not adsorbed. This statement can be corroborated by the GPC analysis performed for the column outlet during the adsorption/desorption cycles performed with the P5kDa experiments,

depicted in Figure 6.14-B, where it can be seen that the solution coming out of the adsorption column (P5kDa column outlet) changed significantly its MW profile when compared to the respective feed and there is a predominance of compounds with higher MW (for eluting times 18-22 min) and in the acids not adsorbed (for eluting times 25-32).

A

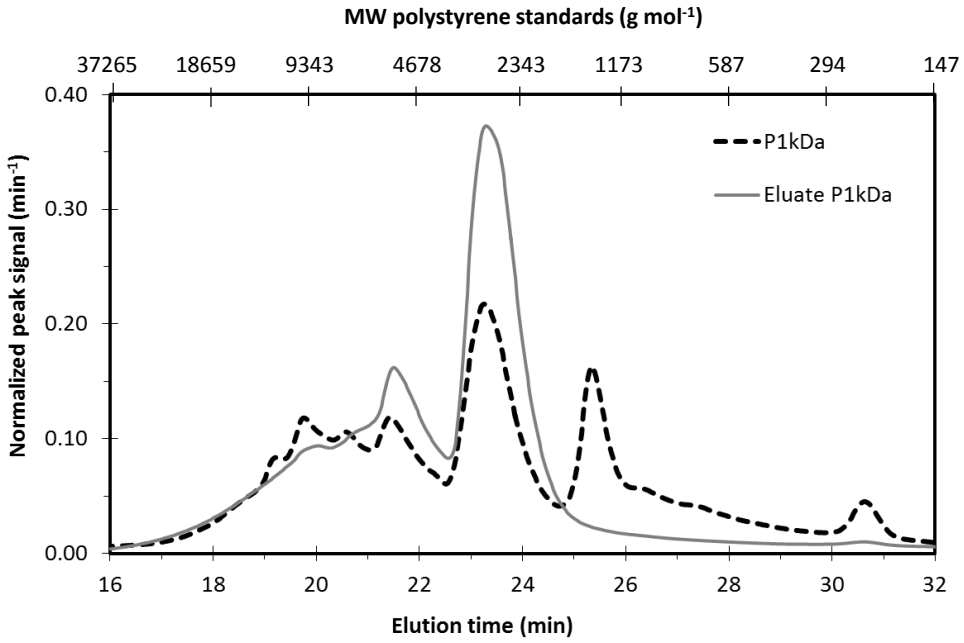

B

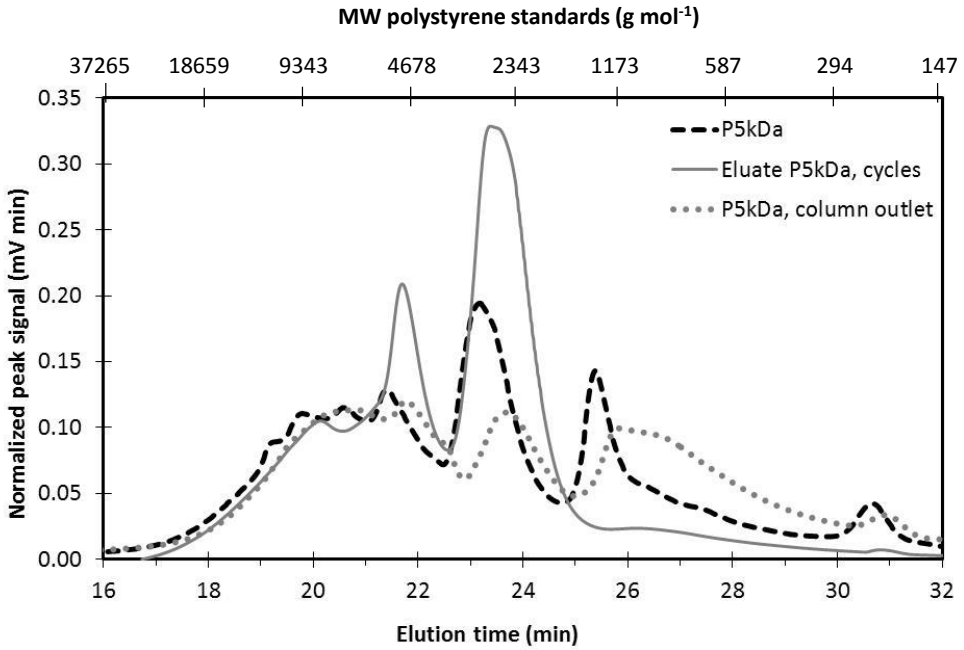

Figure 6.14 Normalized chromatograms obtained by GPC for feed streams of the adsorption process P1kDa (A) and P5kDa (B) and respective eluates. During the adsorption cycles performed with P5kDa the column outlet solution was collected and analysed as well. Normalization with area under the curve.

As can be seen through Figure 6.14, in regard to the respective feed stream, the eluates obtained after feeding the column with P1kDa and P5kDa and eluting with ethanol:water (90:10, % V/V) solution between (0.5 – 3.5/4 min.) have a completely different MW profile: the eluates have less compounds with higher MW (corresponding to elution times between 18 and 22 min), and are practically depleted of VA, SA and probably other organic acids, eluting at 30.5 min, present in solution in their ionic state. Each eluate is mainly composed with compounds eluting between 22 and 24.5 min, including V, S, OV, and OS. In Appendix C Figure C2, the normalized GPC chromatograms for all streams analysed are superimposed to better observe their differences.

GPC confirms what has already been stated above, the adsorption process refined the feed stream and thus, the eluates are depleted in compounds eluting after 25 minutes and are richer in compounds eluting between 22-25 min (the same interval of retention times observed for V and S and the respective ketones).

The elution profiles obtained for both eluates are very similar meaning that the third stage of the membrane fractionation sequence employed (discussed in Chapter 5) probably is not required since it does not enhance significantly the adsorption/desorption process regarding obtaining enriched and purified samples of V and S. Nevertheless, this decision must be made upon comparing the increment in operating costs with a third membrane stage and the gain in V and S content (already discussed in 6.3.1.3).

6.3.2. SFC studies

In supercritical fluid chromatography (SFC), to obtain a good separation of the compounds with high retention factors, selectivity and efficiency are dependent on the combination of several factors such as the type of stationary phase, presence of modifiers and additives, pressure, flowrate, temperature, sample diluent and injection volume (52). In this study the effect of methanol composition (1-10 % V/V) as the co-solvent of the CO_2 mobile phase, the incorporation of the additive formic acid (0.2% V/V), temperature (40 and 50 ºC) and flowrate (4 and 5 mL min^{-1}) were studied in order to understand their effects in the chromatographic separation of the desired phenolic compounds employing a highly polar silica column.

In order to understand the type of interaction between phenolic compounds and the silica column, typical phenolic compounds found in oxidized IKL (V, OV, S, OS, VA, SA and *p*-OHB) were analyzed by SFC and the following chromatographic conditions were employed as a starting point: 40 ºC, 150 bar, 5 mL min^{-1} and a CO_2 mobile phase containing 10% V/V methanol. The overlaid

UV signals obtained for each standard phenolic compound are shown in Figure 6.15.A, along with the respective retention times. A synthetic mixture containing all the above mentioned phenolic compounds was analyzed as well in the same chromatographic conditions (Figure 6.15.B).

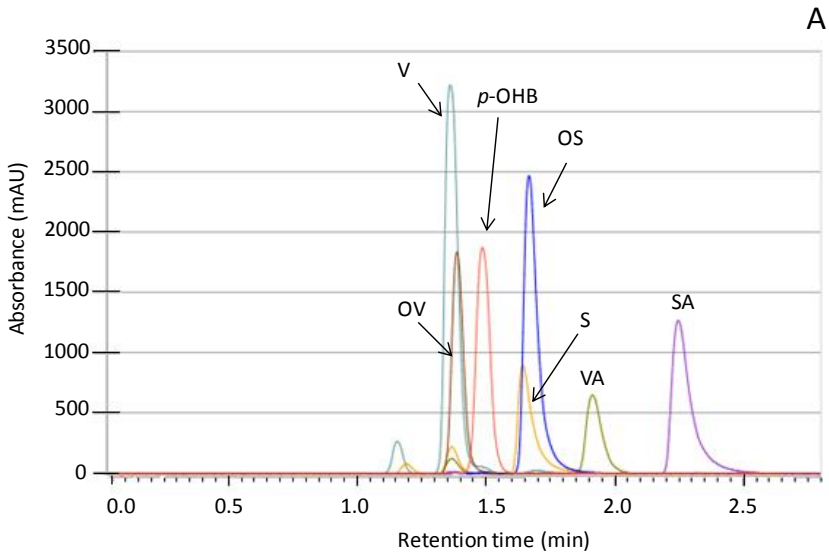

	Retention time (min)
V	1.36
OV	1.39
***p*-OHB**	1.49
S	1.64
OS	1.67
VA	1.91
SA	2.25

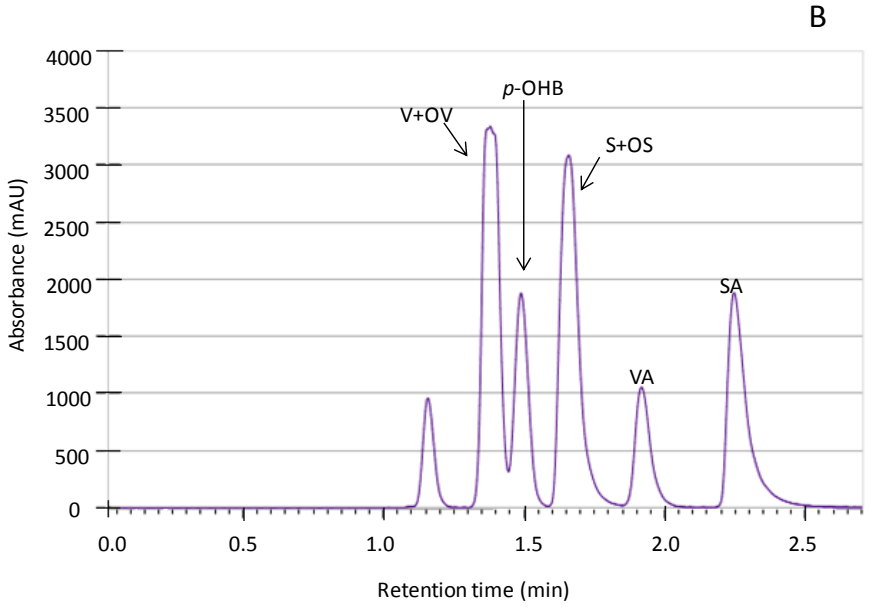

	Retention time (min)
V+OV	1.38
***p*-OHB**	1.49
S+OS	1.66
VA	1.92
SA	2.25

Figure 6.15 SFC chromatograms of standard phenolic compounds usually found in oxidized IKL medium: A) overlaid chromatograms of several standard solutions: vanillin (V, 3.38 g L^{-1}), acetovanillone (OV, 1.80 g L^{-1}), *p*-hydroxybenzaldehyde (*p*-OHB, 0.82 g L^{-1}), syringaldehyde (S, 4.22 g L^{-1}), acetosyringaldehyde (OS, 2.64 g L^{-1}), vanillic acid (VA, 1.55 g L^{-1}), syringic acid (SA, 2.64 g L^{-1}); B) synthetic mixture prepared with all the compounds: V (3.24 g L^{-1}), OV (3.36 g L^{-1}), *p*-OHB (2.16 g L^{-1}), S (2.54 g L^{-1}), OS (2.74 g L^{-1}), VA (2.04 g L^{-1}) and SA (2.56 g L^{-1}). Chromatographic conditions: 40 ºC, 150 bar, 10% V/V of methanol, 5 mL min^{-1}.

For these chromatographic conditions, it was possible to observe that the phenolic acids have interacted more with the silica stationary phase, having higher retention times. V and OV are the least retained compounds, with retention times of 1.36 and 1.39 minutes, respectively. This can be attributed to the synergic effect between the silanol groups present in the silica column and the CO_2 mobile phase applied, which led to a normal phase separation type mechanism.

Moreover, poor selectivity between V and S with their respective ketones was observed for these chromatographic conditions. However, Gaussian shape peaks were obtained for all the compounds and the analysis was performed for a very short period of time (within 3 minutes).

Comparing SFC with RP-HPLC employing the ACE 5 C18 column with a pentafluorophenyl group (250 x 3.0 mm, 5 µm) applied in this work for the quantification of the phenolic compounds (Appendix E – Figure E.1), different selectivities were found and thus, different elution orders: *p*-OHB, VA, V, SA, S, OV and OS. This is due to the different nature of the stationary phase and also to the different solubilities of the compounds in the mobile phase. This behavior was expected and has already been referred in literature (53).

6.3.2.1. *Effect of modifier and additive*

CO_2 is a very weak eluting solvent with poor solvating power and the incorporation of an organic modifier will change the eluotropic strength of the mobile phase in favour of increasing the solubility of the phenolic compounds and induce selectivity changes due to solute-mobile phase interaction changes such as hydrogen bonds and dipole-dipole interactions (28, 33). Moreover, even in the presence of a small amount of an organic modifier, the polarity of the stationary phase changes significantly since the highly polar adsorption sites on the silica column are rather masked or occupied by the solvent molecules, reducing the active sites available for the phenolic compounds interaction with the stationary phase. Therefore, it is expected that the addition of small amounts of an organic modifier will change retention and separation performances due to a change in polarity (33, 54).

In this study different compositions of methanol were added to the CO_2 mobile phase (1, 2, 5 and 10 % V/V) and Figure 6.15 and Figure 6.16 show the respective chromatograms obtained after analysing a synthetic mixture containing all the phenolic compounds of interest for each methanol composition in order to evaluate its effect on retention time, selectivity and peak shape changes.

As the methanol content is increased, the retention time is significantly reduced and Gaussian peak shapes are obtained but the separation factor between V and S with their respective ketones is

negatively affected. On the other hand, employing a CO_2 mobile phase with 1% methanol, helps improving the column selectivity but very poor peak shapes (asymmetric) are obtained, in particular for S and OS. Moreover, the detection limit of each phenolic compound is significantly decreased.

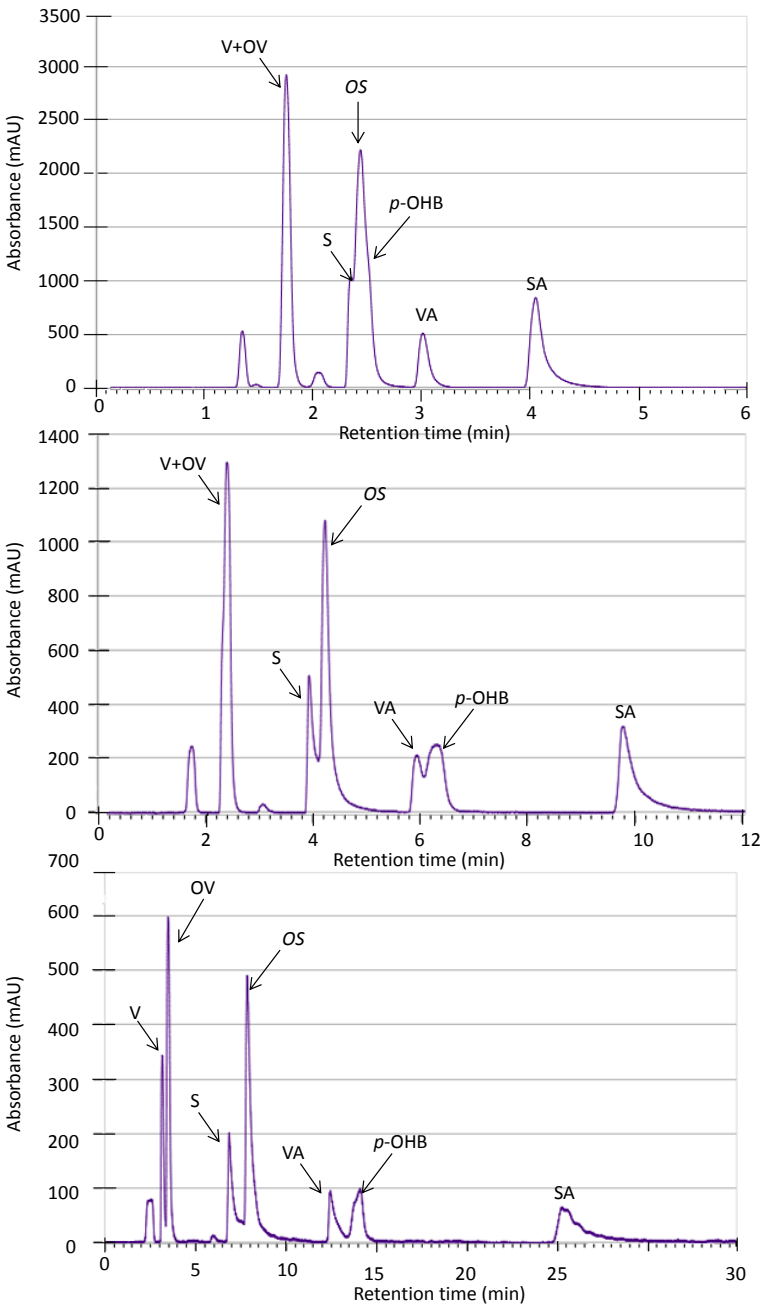

	Retention time (min)
V+OV	1.76
S	2.35
OS+*p*-OHB	2.44
VA	3.01
SA	4.05

	Retention time (min)
V+OV	2.39
S	3.92
OS	4.22
VA	5.94
***p*-OHB**	6.31
SA	9.79

	Retention time (min)
V	3.15
OV	3.48
S	6.85
OS	7.84
VA	12.44
***p*-OHB**	14.1
SA	25.24

Figure 6.16 SFC chromatograms of a synthetic mixture prepared with V (3.24 g L^{-1}), OV (3.36 g L^{-1}), *p*-OHB (2.16 g L^{-1}), S (2.54 g L^{-1}), OS (2.74 g L^{-1}), VA (2.04 g L^{-1}) and SA (2.56 g L^{-1}) for a mobile phase of CO_2 containing different amounts of modifier A) 5% V/V methanol; B) 2% V/V methanol and C) 1% V/V methanol. Other chromatographic conditions: 40 ºC, 150 bar, 5 mL min^{-1}.

Additionally, it is important to note that different amounts of methanol present in the mobile phase changed the retention times of all compounds keeping the order of elution of each compound with the exception of *p*-OHB. (Figure 6.15) *p*-OHB eluted between OV and S for 10% V/V methanol, and, decreasing the methanol composition for 5% V/V methanol, this compound eluted between OS and VA (Figure 6.16 and for more detail see Figure F.1 with the overlaid SFC chromatograms of each phenolic compound analysed at 5% V/V methanol) and for 2% V/V methanol incorporation to the mobile phase, *p*-OHB started eluting immediately after VA. This means that the eluotropic strength change of the mobile phase has induced different interaction phenomena between *p*-OHB and the stationary phase (33, 54).

The incorporation of 0.2% V/V formic acid to the methanol solution did not succeed in improving neither peak shape nor selectivity of the chromatographic process for V, S, OV and OS separation (Figure 6.17) and only delayed the retention times (e.g. for vanillin the retention time shifted from 3.26 to 3.71 min).

Sun et al. (38) were also unable to decrease peak tailing by the incorporation of formic acid (≈0.075% V/V) or trifluoroacetic acid (≈0.15% V/V) to methanol. Nevertheless, the authors manage to improve peak shape by adding citric acid (≈0.23% V/V) to methanol, obtaining more symmetrical and narrower peaks.

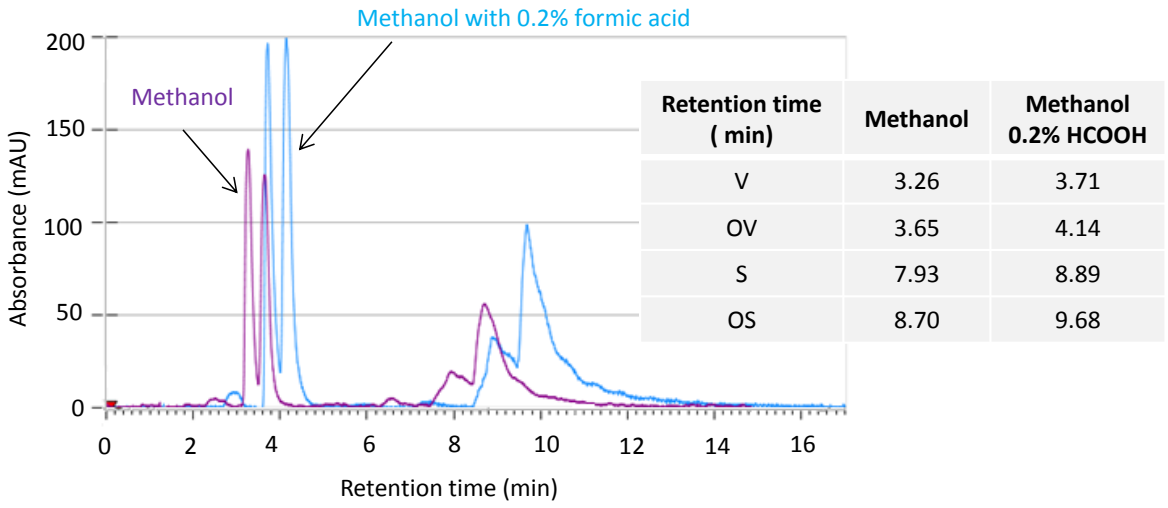

Retention time (min)	Methanol	Methanol 0.2% HCOOH
V	3.26	3.71
OV	3.65	4.14
S	7.93	8.89
OS	8.70	9.68

Figure 6.17 SFC chromatograms of a synthetic mixture of V, S, OV and OS with approximately 0.6 g L^{-1} /each for 1% V/V methanol and 1% V/V methanol containing 0.2% V/V formic acid (HCOOH). Other conditions: 40 ºC, 150 bar, 5 mL min^{-1}.

6.3.2.2. *Effect of the Temperature*

The influence of temperature on the retention time is explained by the combination of two opposite effects: the volatility and density effects. The first effect is related with the increase of the compounds volatility with temperature increase leading to lower retention times (55, 56). The second effect is regarded to the density decrease of the supercritical solvent with temperature increase and hence, solubility is decreased, leading to higher retention times. The combination of both effects determines the retention behavior of the compounds (33, 34).

Figure 6.18 shows that the retention time of the studied phenolic compounds increased with increasing temperature from 40 ºC to 50 ºC, meaning that the change of the mobile phase density was the dominant effect. Moreover, the increase in temperature slightly increased peak resolution between V and OV and S and OS but, nevertheless, the detection limit for S and OV is considerably reduced.

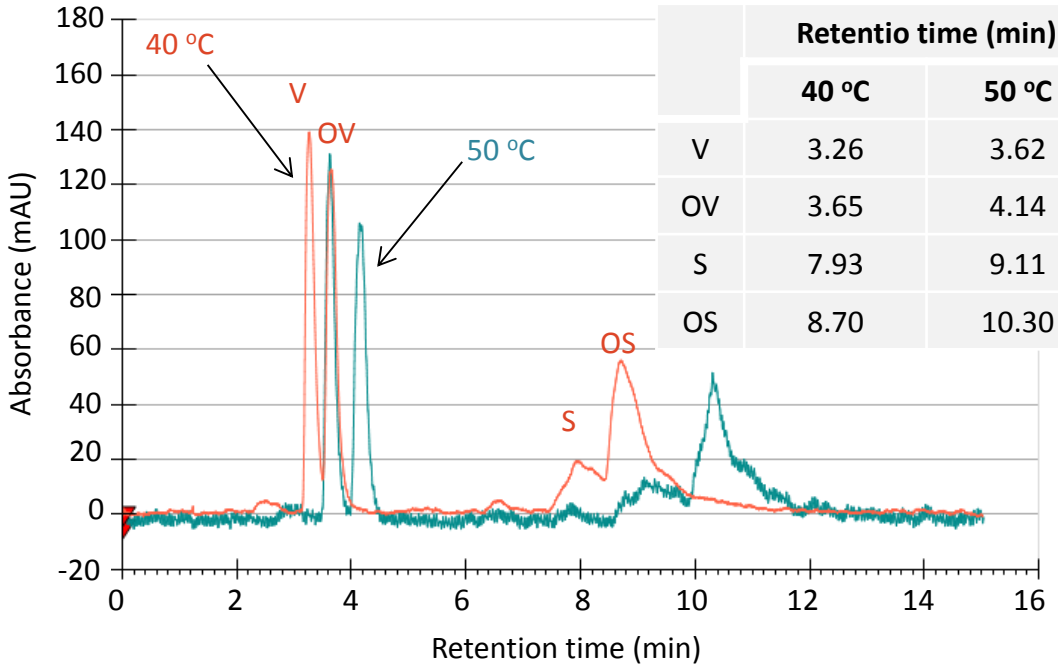

	Retentio time (min)	
	40 ºC	50 ºC
V	3.26	3.62
OV	3.65	4.14
S	7.93	9.11
OS	8.70	10.30

Figure 6.18 SFC chromatograms of a synthetic mixture of V, S, OV and OS with concentrations bellow 0.6 g L^{-1} /each for different temperatures (40 and 50 ºC). Other conditions: 5 mL min^{-1}, 150 bar, 1% V/V methanol as modifier.

6.3.2.3. *Effect of the flowrate*

In SFC systems, the flowrate has a direct impact on the analysis time without compromising peak shape due to the high diffusion coefficients when employing supercritical fluids (33). However, a flowrate change can affect the separation factor and chromatographic resolution due to modifications of the internal pressure and mobile phase density. An increase in the flowrate, increases both the internal pressure and the fluid density that will, in turn, induce a decrease in the separation factor. In the first case, the separation factor will decrease due to an apparent increase of the void volume (33) and in the second case, the separation factor will also decrease due to an increase in fluid density and thus, an increase of elution strength.

Figure 6.19 shows the chromatograms obtained for the elution of a mixture containing V, OV, S and OS at different flowrates and, besides the obvious change in the retention time, no significant changes were observed neither for peak tailing nor resolution.

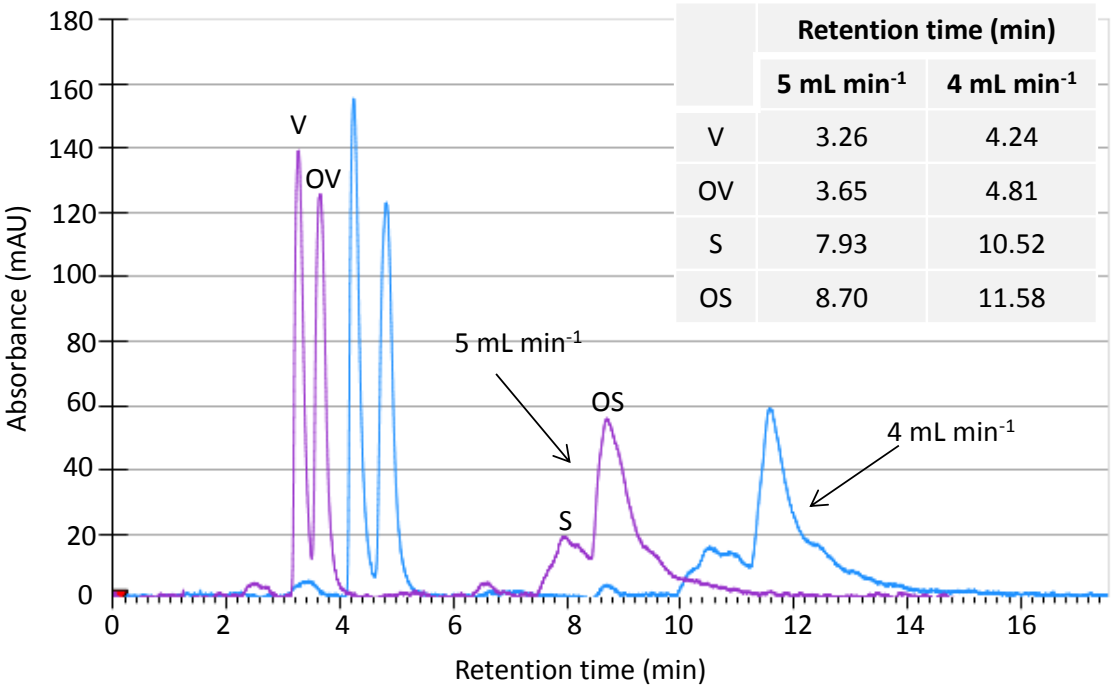

	Retention time (min)	
	5 mL min^{-1}	4 mL min^{-1}
V	3.26	4.24
OV	3.65	4.81
S	7.93	10.52
OS	8.70	11.58

Figure 6.19 SFC chromatograms of a synthetic mixture V, S, OV and OS with concentrations bellow 0.6 g L^{-1} /each for different flowrates (5 and 4 mL min^{-1}). Other conditions: 50 ºC, 150 bar, 1% V/V methanol as modifier.

6.3.2.4. *Mobile phase gradient*

Regarding the isocratic eluent studies performed, the best modifier composition obtained was for 1% V/V methanol but poorer peak shapes were obtained, in particular for S, OS, VA, SA and *p*-OHB, and more concentrated samples are needed.

The chromatographic separation of a synthetic mixture containing the phenolic compounds of interest was performed for several methanol composition gradients at 5 mL min^{-1}, 150 bar and 40 ºC in order to improve selectivity and peak shapes obtained for the 1% V/V methanol isocratic eluent employed. In the establishment of the co-solvent gradient, the chromatographic process started with 0.7% V/V of methanol to delay the elution of V and OV and thus, increase the separation factor between these compounds. Afterwards, methanol composition was gradually increased up to 2% V/V in order to elute the phenolic acids earlier with better peak shapes and then, methanol composition raise up to 5-10 % V/V methanol study in order to prepare the column for successive injections in a short period of time and promote the rapid elution of more retained compounds not studied in this work but that could be present in real and more complex samples.

In Figure 6.20A it is showed the best methanol gradient conditions found for separating V, S, OV, OS, VA, SA and *p*-OHB, taking into consideration the selectivity, peak shape and elution time observed. A methanol gradient was also established for the feed flow rate of 3 mL min^{-1} that slightly increased the separation between V and OV but the elution time of all compounds increased for 35 minutes. In Appendix F it is summarized other methanol gradients tested (Figure F.2 and Figure F.3). In Figure F.4 it is overlaid the chromatograms obtained for each phenolic compound for the best gradient found for 5 mL min^{-1}.

These preliminary tests helped to understand the influence of methanol composition, additive incorporation, temperature and flowrate in the chromatographic separation of the phenolic compounds of interest in silica columns. Among the isocratic studies, the best methanol composition in the CO_2 mobile phase found was 1% V/V. The other parameters studied (temperature, flowrate, incorporation of formic acid) did not introduce significant improvements. Some methanol gradients were tried but only increased slightly the separation between V and OV and were beneficial to elute the phenolics acids earlier with better peak shapes. More experiments should be performed in order to verify if further optimization of the chromatographic process is possible, focused, in particular, in improving V and S separation between their respective ketones. The effect of pressure should be evaluated as well as the incorporation of other additives such as citric acid.

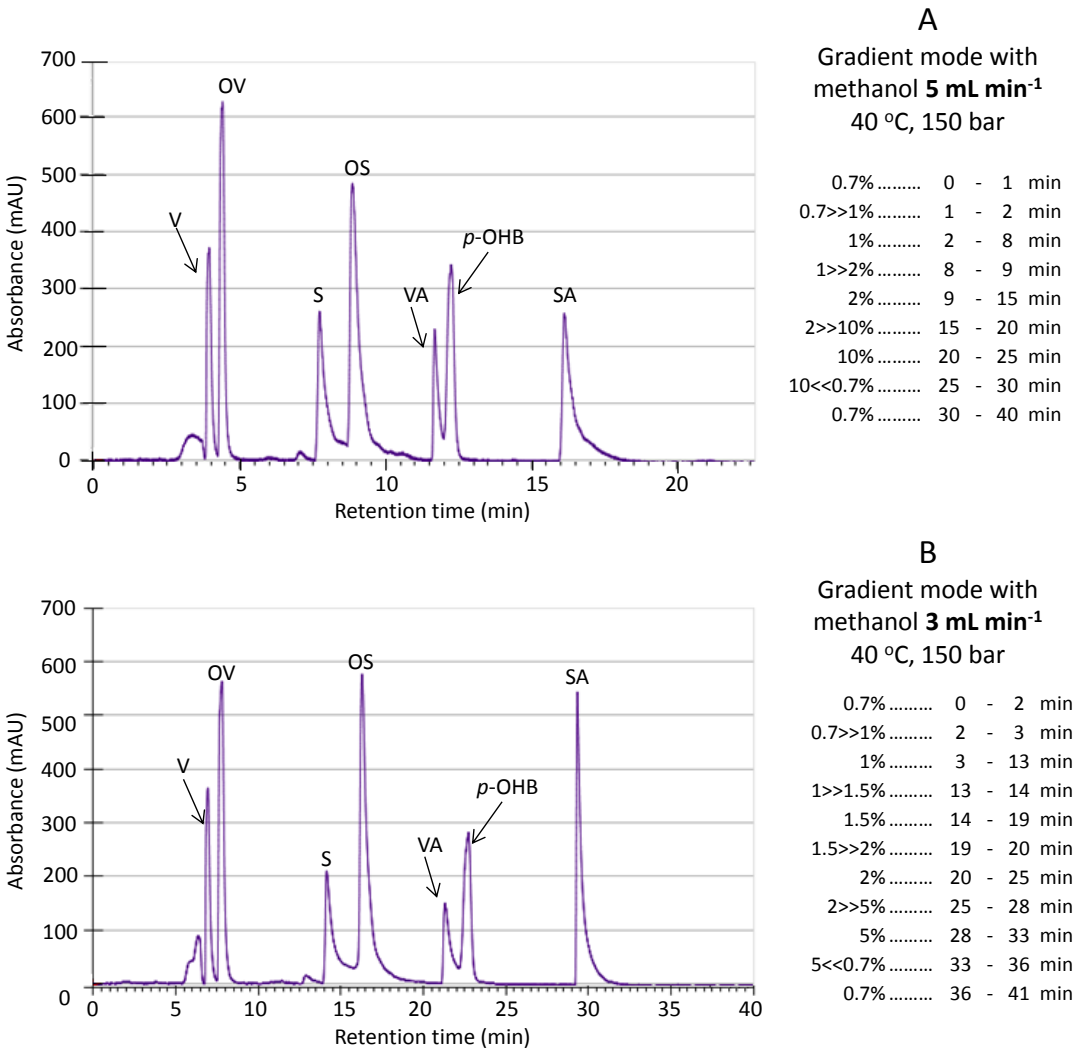

Retention time (min)	Gradient 5 mL min^{-1}	Gradient 3 mL min^{-1}
V	3.94	6.93
OV	4.39	7.78
S	7.72	14.14
OS	8.85	16.28
VA	11.66	21.31
***p*-OHB**	12.24	22.72
SA	16.26	29.34

Figure 6.20 SFC chromatograms of a synthetic mixture prepared with V (3.24 g L^{-1}), OV (3.36 g L^{-1}), *p*-OHB (2.16 g L^{-1}), S (2.54 g L^{-1}), OS (2.74 g L^{-1}), VA (2.04 g L^{-1}) and SA (2.56 g L^{-1}) for different chromatographic methods of co-solvent gradient at A) 5 mL min^{-1} and B) 3 mL min^{-1}. Other chromatographic conditions: 150 bar and 40 ºC.

6.3.3. SFC separation of the eluates produced in the adsorption of oxidized IKL permeate

The best gradient modes found at 5 and 3 mL min^{-1}, 150 bar and 40 ºC were selected to evaluate the CO_2 supercritical fluid chromatographic separation of an oxidized IKL medium previously treated by membrane and adsorption processes. Figure 6.21 and Figure 6.22 present the gradients and respective chromatograms obtained. Reasonable separation between V/OV and S/OS was achieved for both chromatographic conditions studied and very similar to the injections performed with the synthetic solutions prepared (Figure 6.20). VA and SA were not detected and *p*-OHB was detected at lower concentration than the other compounds. In fact, in previous quantification by RP-HPLC UV only trace amounts of VA, SA and *p*-OHB were present in the final eluates obtained after adsorption of the permeates P1kDa and P5kDa onto SP700 resin and desorption with ethanol:water (90:10, % V/V) solution.

This study shows the possibility of separating phenolic compounds found in oxidized IKL streams using a silica column and CO_2-based mobile phase containing methanol. The next steps will be the assessment of the effect of backpressure and other additives (e.g citric acid) on the selectivity for the phenolic compounds and peak shape. Other type of stationary phases should be evaluated by a methodical scanning of chromatography conditions.

Afterwards, the best stationary phase and chromatographic conditions found will pursue with studies at preparative scale in order to establish a SFC simulating moving bed or other multicolumn chromatography methodology employing CO_2 at supercritical conditions to purify V and S from oxidized IKL streams previously treated by membrane and adsorption processes.

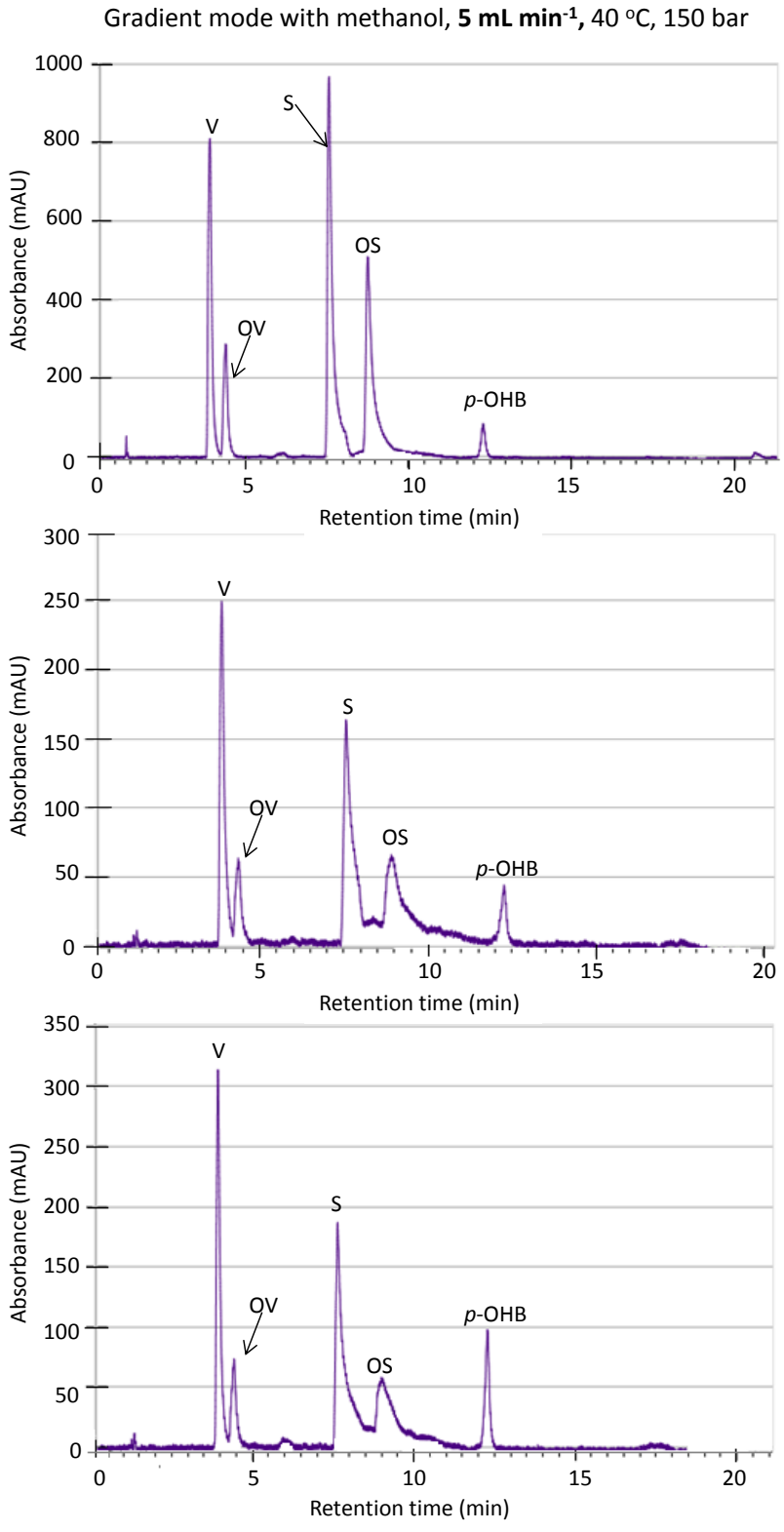

A
P1kDa,
Breakthrough

	Retention time (min)
V	3.92
OV	4.41
S	7.57
OS	8.76
***p*-OHB**	12.30

B
P1kDa,
cycles

	Retention time (min)
V	3.87
OV	4.36
S	7.56
OS	8.92
***p*-OHB**	12.27

C
P5kDa,
cycles

	Retention time (min)
V	3.93
OV	4.43
S	7.64
OS	9.00
***p*-OHB**	12.28

Figure 6.21 SFC chromatograms of the final eluates obtained: A) P1kDa, breakthrough; B) P1kDa, cycles and D) P5kDa cycles. Chromatographic conditions: 5mL min^{-1}, 150 bar, 40 ºC with the same methanol gradient mode as Figure 6.20A.

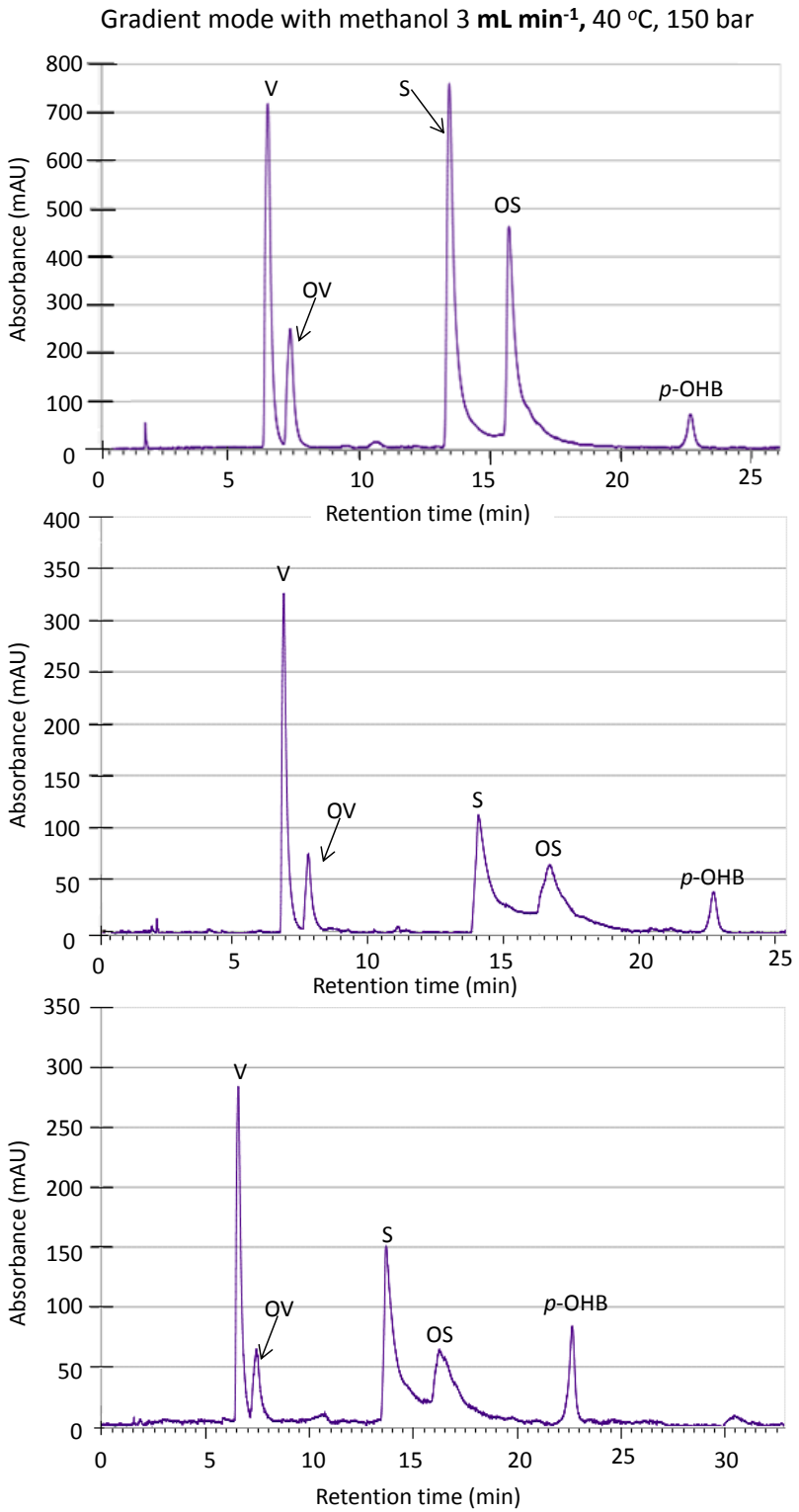

A
P1kDa,
Breakthrough

	Retention time (min)
V	6.52
OV	7.38
S	13.46
OS	15.73
***p*-OHB**	22.66

B
P1kDa,
cycles

	Retention time (min)
V	6.92
OV	7.82
S	14.08
OS	16.70
***p*-OHB**	22.74

C
P5kDa,
cycles

	Retention time (min)
V	6.55
OV	7.42
S	13.68
OS	16.24
***p*-OHB**	22.64

Methanol gradient method:

0.7%	0 - 2 min		1.5%	14 - 19 min		5%	28 - 33 min	
0.7>>1%	2 - 3 min		1.5>>2%	19 - 20 min		5<<0.7%	33 - 36 min	
1%	3 - 13 min		2%	20 - 25 min		0.7%	36 - 41 min	
1>>1.5%	13 - 14 min		2>>5%	25 - 28 min				

Figure 6.22 SFC chromatograms of the final eluates obtained: A) P1kDa, breakthrough; B) P1kDa, cycles and D) P5kDa cycles. Chromatographic conditions: 3 mL min^{-1}, 150 bar, 40 ºC with the same methanol gradient mode as Figure 6.20B.

6.4. Conclusions

The permeates P5kDa and P1kDA obtained from the oxidized IKL membrane fractionation process with the membranes 50, 5 and 1 kDa MWCO were submitted to adsorption/desorption studies employing the polymeric resin SP700 prior to a pH value correction to 7.5-8.

A complete breakthrough with the P1kDa feed stream was performed and 0.251 g $g^{-1}_{dry\ resin}$ of phenolic compounds quantified were adsorbed. At the operating pH value the phenolic acids (VA, SA) were mostly ionized and were practically not adsorbed and thus, about 93% of the adsorbed phenolic monomers correspond to V, S, OV and OS. *p*-OHB is present in the feed stream in very low concentrations, therefore it was not adsorbed in considerable amounts. About 73-87 % of the phenolic compounds adsorbed were recovered within 11 BV by eluting with an ethanol:water (90:10, % V/V) solution. A final eluate solution of 5.31 g L^{-1} of V and S was obtained, representing 215 mg g^{-1}_{TS}.

Cycles of adsorption and desorption with P1kDa and P5kDa permeates were performed aiming to evaluate the reutilization of the resin and compare the adsorption performances employing these different streams obtained from the membrane fractionation process. Each cycle encompassed adsorption, washing, desorption and final washing steps for 10, 1, 4 and 30 minutes, respectively. Final eluates composition in TS, TP and ashes was detailed and discussed.

The adsorption capacities obtained were very similar between cycles performed with both streams: 0.063 g $g^{-1}_{dry\ resin}$ and 0.061 g $g^{-1}_{dry\ resin}$ of phenolic compounds were adsorbed for experiments performed with P5kDa and P1kDa, respectively. Moreover, recoveries of 81-84 % were achieved from the desorption step and the remaining compounds were washed out in the final washing step. Therefore, it can be concluded that the resin SP700 can be efficiently reutilized up to 4-5 cycles of adsorption/desorption.

Final eluates with 1.98 and 1.92 g/L of V and S concentration were obtained, representing 220 and 267 mg g^{-1}_{TS} for P5kDa and P1kDa, respectively. The differences between employing P5kDa and P1kDa were not very significant and thus, the third membrane stage of the fractionation sequence studied was not relevant for improving the adsorption process efficiency in V and S. Nevertheless, the decision of maintaining the third membrane stage must be made upon comparing the increment in investment and operating costs with an additional membrane stage with the gain of the final eluate composition of V and S obtained. The posterior step of final refinement of the V and S solution must also be taken into consideration.

In terms of MW distribution analysed by GPC, the higher MW fractions were eliminated in the adsorption/desorption process and the most representative MW fraction encountered in each final eluate obtained corresponds to those of V, S, OV and OS.

SFC preliminary studies were performed with synthetic solutions of typical phenolic compounds present in oxidized IKL in order to evaluate its potential as final stage of V and S purification from the final eluates obtained. The effect of methanol composition (1-10 % V/V) and incorporation of formic acid (0.2% V/V) in the CO_2 mobile phase, temperature (40 and 50 ºC) and flowrate (4 and 5 mL min^{-1}) were studied in order to understand their effects in the chromatographic separation of the desired phenolic compounds regarding peak shape and selectivity.

The incorporation of methanol as the co-solvent was the most important variable studied for phenolic compounds separation in the silica column. The higher the percentage of methanol (above 1% V/V), the lower the retention times and the better the peak shapes. However, selectivity between the phenolic compounds of interest was greatly reduced with the increase of co-solvent composition. Considering studies performed in isocratic mode, the best separation between V and S with the respective ketones was achieved for a mobile phase containing 1% V/V methanol at 150 bar, 40 ºC and 5 mL min^{-1}. Nevertheless, peak tailing was considerable for S and OS. The incorporation of formic acid to the co-solvent solution only displaced the retention times for higher values and did not succeed in improving the selectivity or solve the problems associated with peak tailing. Temperature and flowrate did not bring major improvements in the chromatographic process as well. The lower the temperature and the flowrate, the lower were the retention times and peak shape and resolution was similar.

Co-solvent gradient methods starting with 0.7% V/V methanol for 5 and 3 mL min^{-1} at 150 bar and 40 ºC were established with a synthetic mixture containing V, S, OV, OS, VA, SA and *p*-OHB. Each tested gradient method encompassed a step where methanol composition reaches 5/10 % V/V in order to elute more retained compounds existing in the real oxidized IKL streams and therefore, clean and prepare the column for successive injections during operation with real mixtures. The final eluates obtained were successfully separated employing the optimal methanol gradient conditions found for 5 and 3 mL min^{-1}. At 5 mL min^{-1} the compound has eluted earlier but separation of peaks were slightly better for feed flowrate of 3 mL min^{-1}.

This is a first step towards the development of a preparative scale separation process to purify phenolic compounds from oxidized IKL previously treated by membrane and adsorption processes. More SFC studies must be carried out in order to assess if other co-solvent or incorporation of new additives (e.g. citric acid) can improve the selectivity and efficiency of the chromatographic process obtained in this study for the (analytical and preparative) separation of phenolic compounds in silica column. Moreover, other column types should also be tested and the synergic effect with chromatographic conditions systematically exploited.

6.5. References

1. Kimball, D. A. and Norman, S. I. (1990) Processing effects during commercial debittering of California navel orange juice. J. Agric. Food. Chem., 38: 1396-1400.
2. Gao, Z. P., Yu, Z. F., Yue, T. L. and Quek, S. Y. (2013) Adsorption isotherm, thermodynamics and kinetics studies of polyphenols separation from kiwifruit juice using adsorbent resin. J. Food Eng., 116: 195-201.
3. Chai, B.-h., Meng, H.-c., Zhao, Z.-g., Huang, Q. and Fu, X. (2016) Removal of color compounds from sugarcane juice by modified sugarcane bagasse: equilibrium and kinetic study. Sugar Tech, 18: 317-324.
4. De Klerck, K., Mangelings, D. and Vander Heyden, Y. (2012) Supercritical fluid chromatography for the enantioseparation of pharmaceuticals. J. Pharm. Biomed. Anal., 69: 77-92.
5. Kalogerakis, N., Politi, M., Foteinis, S., Chatzisymeon, E. and Mantzavinos, D. (2013) Recovery of antioxidants from olive mill wastewaters: A viable solution that promotes their overall sustainable management. J. Environ. Manage., 128: 749-758.
6. Desfontaine, V., Guillarme, D., Francotte, E. and Nováková, L. (2015) Supercritical fluid chromatography in pharmaceutical analysis. J. Pharm. Biomed. Anal., 113: 56-71.
7. Pinto, P. C. R., Costa, C. E. and Rodrigues, A. E. (2013) Oxidation of lignin from *Eucalyptus globulus* pulping liquors to produce syringaldehyde and vanillin. Ind. Eng. Chem. Res., 52: 4421-4428.
8. Guiochon, G., Felinger, A., Shirazi, D. G. G. and Katti, A. M. (2006) Fundamentals of Preparative and Nonlinear Chromatography. Second edition, Elsevier Academic Press: Oxford, United Kingdom.
9. Soto, M. L., Moure, A., Domínguez, H. and Parajó, J. C. (2011) Recovery, concentration and purification of phenolic compounds by adsorption: A review. J. Food Eng., 105: 1-27.
10. Crittenden, B. D. and Thomas, W. J. (1998) Adsorption Technology and Design. First edition, Butterworth and Heinemann: Oxford, United Kingdom.
11. Kammerer, D. R., Saleh, Z. S., Carle, R. and Stanley, R. A. (2007) Adsorptive recovery of phenolic compounds from apple juice. Eur. Food Res. Technol., 224: 605-613.
12. Di Mauro, A., Fallico, B., Passerini, A. and Maccarone, E. (2000) Waste water from citrus processing as a source of hesperidin by concentration on styrene−divinylbenzene resin. J. Agric. Food. Chem., 48: 2291-2295.

13. Manthey, J. A. (2004) Fractionation of Orange Peel Phenols in Ultrafiltered Molasses and Mass Balance Studies of Their Antioxidant Levels. J. Agric. Food. Chem., 52: 7586-7592.

14. Scordino, M., Di Mauro, A., Passerini, A. and Maccarone, E. (2005) Selective recovery of anthocyanins and hydroxycinnamates from a byproduct of citrus processing. J. Agric. Food. Chem., 53: 651-658.

15. Zhang, Q.-F., Jiang, Z.-T., Gao, H.-J. and Li, R. (2008) Recovery of vanillin from aqueous solutions using macroporous adsorption resins. Eur. Food Res. Technol., 226: 377-383.

16. Xiao, G.-Q., Xie, X.-L. and Xu, M.-C. (2009) Adsorption performances for vanillin from aqueous solution by the hydrophobic - hydrophilic macroporous polydivinylbenzene / polyacrylethylenediamine IPN resin. Acta Phys.-Chim. Sin., 25: 97-102.

17. Bretag, J., Kammerer, D. R., Jensen, U. and Carle, R. (2009) Evaluation of the adsorption behavior of flavonoids and phenolic acids onto a food-grade resin using a D-optimal design. Eur. Food Res. Technol., 228: 985-999.

18. Kammerer, D. R., Carle, R., Stanley, R. A. and Saleh, Z. S. (2010) Pilot-Scale Resin Adsorption as a Means To Recover and Fractionate Apple Polyphenols. J. Agric. Food. Chem., 58: 6787-6796.

19. Žabková, M., Otero, M., Minceva, M., Zabka, M. and Rodrigues, A. E. (2006) Separation of synthetic vanillin at different pH onto polymeric adsorbent Sepabeads SP206. Chem. Eng. Process., 45: 598-607.

20. Jin, X. and Huang, J. (2013) Adsorption of vanillin by an anisole-modified hyper-cross-linked polystyrene resin from aqueous solution: equilibrium, kinetics, and dynamics. Adv. Polym. Tech., 32: E221-E230.

21. Samah, R. A., Zainol, N., Yee, P. L., Pawing, C. M. and Abd-Aziz, S. (2013) Adsorption of vanillin using macroporous resin H103. Adsorpt. Sci. Technol., 31: 599-610.

22. Wang, Z., Chen, K., Li, J., Wang, Q. and Guo, J. (2010) Separation of vanillin and syringaldehyde from oxygen delignification spent liquor by macroporous resin adsorption. Clean, 38: 1074-1079.

23. Wu, X., Zhang, N.-z. and Qi, C.-h. (2003) Enrichment of vanillin with adsorbent resin in the oxidative liquorsof acidic sulphite pulping. China Pulp & Paper Industry, 24: 21.

24. Taylor, L. T. (2009) Supercritical fluid chromatography for the 21st century. J. Supercrit. Fluids, 47: 566-573.

25. Wu, D.-R., Leith, L., Balasubramanian, B., Palcic, T. and Wang-Iverson, D., *The Impact of Chiral Supercritical Fluid Chromatography in Drug Discovery: From Analytical to*

Multigram Scale (2006), retrieved from: http://www.americanlaboratory.com/ (accessed 17-01-2017).

26. Yan, T. Q. and Orihuela, C. (2007) Rapid and high throughput separation technologies—Steady state recycling and supercritical fluid chromatography for chiral resolution of pharmaceutical intermediates. J. Chromatogr. A, 1156: 220-227.

27. Winterbone, D. E. (1997) Advanced Thermodynamics for Engineers John Wiley & Sons: New York, United States of America.

28. Berger, T. A. and Deye, J. F. (1990) Composition and density effects using methanol/carbon dioxide in packed column supercritical fluid chromatography. Anal. Chem., 62: 1181-1185.

29. Molina, B. C. P. and Johannsen, M. (2010) Adsorption equilibria of benzoic acid on silica gel from supercritical carbon dioxide. J. Supercrit. Fluids, 54: 237-242.

30. Berger, T. A. and Deye, J. F. (1991) Separation of ydroxybenzoic acids by packed column supercritical fluid chromatography using modified fluids with very polar additives. J. Chromatogr. Sci., 29: 26-30.

31. Liu, Z., Zhao, S., Wang, R. and Yang, G. (1999) Separation of polyhydroxyl flavonoids by packed-column supercritical fluid chromatography. J. Chromatogr. Sci., 37: 155-158.

32. Kamangerpour, A., Ashraf-Khorassani, M., Taylor, L. T., McNair, H. M. and Chorida, L. (2002) Supercritical fluid chromatography of polyphenolic compounds in grape seed extract. Chromatographia, 55: 417-421.

33. Lesellier, E. (2009) Retention mechanisms in super/subcritical fluid chromatography on packed columns. J. Chromatogr. A, 1216: 1881-1890.

34. Berger, T. A. and Deye, J. F. (1991) Separation of phenols by packed column supercritical fluid chromatography. J. Chromatogr. Sci., 29: 54-59.

35. Ganzera, M. (2015) Supercritical fluid chromatography for the separation of isoflavones. J. Pharm. Biomed. Anal., 107: 364-369.

36. Ramírez, P., Fornari, T., Señoráns, F. J., Ibañez, E. and Reglero, G. (2005) Isolation of phenolic antioxidant compounds by SFC. J. Supercrit. Fluids, 35: 128-132.

37. Ramírez, P., García-Risco, M. R., Santoyo, S., Señoráns, F. J., Ibáñez, E. and Reglero, G. (2006) Isolation of functional ingredients from rosemary by preparative-supercritical fluid chromatography (Prep-SFC). J. Pharm. Biomed. Anal., 41: 1606-1613.

38. Sun, M., Lidén, G., Sandahl, M. and Turner, C. (2016) Ultra-high performance supercritical fluid chromatography of lignin-derived phenols from alkaline cupric oxide oxidation. J. Sep. Sci., 39: 3123-3129.

39. Pereira, C. S. M., Silva, V. M. T. M. and Rodrigues, A. E. (2009) Fixed bed adsorptive reactor for ethyl lactate synthesis: experiments, modelling, and simulation. Sep. Sci. Technol., 44: 2721-2749.

40. Santos, B. A. V., Silva, V. M. T. M., Loureiro, J. M. and Rodrigues, A. E. (2014) Adsorption of H_2O and dimethyl carbonate at high pressure over zeolite 3A in fixed bed column. Ind. Eng. Chem. Res., 53: 2473-2483.

41. Hui, Z., Jun, W., Jing, J., Ji, L., Xiuquan, L. and Dingqiang, L. (2010) Enrichment and purification of total chlorogenic acids from tobacco waste extract with macroporous resins. Sep. Sci. Technol., 45: 794-800.

42. Lin, L., Zhao, H., Dong, Y., Yang, B. and Zhao, M. (2012) Macroporous resin purification behavior of phenolics and rosmarinic acid from Rabdosia serra (MAXIM) HARA leaf. Food Chem., 130: 417-424.

43. Kim, J., Yoon, M., Yang, H., Jo, J., Han, D., Jeon, Y.-J. and Cho, S. (2014) Enrichment and purification of marine polyphenol phlorotannins using macroporous adsorption resins. Food Chem., 162: 135-142.

44. Schwartz, T. J. and Lawoko, M. (2010) Removal of acid-soluble lignin from biomass extracts using Amberlite XAD-4 resin. Bioresources, 5: 2337–2347.

45. Westerberg, N., Sunner, H., Helander, M., Henriksson, G., Lawoko, M. and Rasmuson, A. (2012) Separation of galactoglucomannans, lignin and lignin–carbohydrate complexes from hot-water-extracted Norway spruce by cross-flow filtration and adsorption chromatography. Bioresources, 7: 4501–4516.

46. Fache, M., Boutevin, B. and Caillol, S. (2016) Vanillin production from lignin and its use as a renewable chemical. ACS Sustain. Chem. Eng., 4: 35-46.

47. Rekha, K. R., Selvakumar, G. P. and Sivakamasundari, R. I. (2014) Effects of syringic acid on chronic MPTP/probenecid induced motor dysfunction, dopaminergic markers expression and neuroinflammation in C57BL/6 mice. Biomedicine & Aging Pathology, 4: 95-104.

48. Kumar, S., Prahalathan, P. and Raja, B. (2014) Vanillic acid: A potential inhibitor of cardiac and aortic wall remodeling in l-NAME induced hypertension through upregulation of endothelial nitric oxide synthase. Environ. Toxicol. Phar., 38: 643-652.

49. Brunow, G. (2005) Methods to Reveal the Structure of Lignin In Biopolymers. Martin Hofrichter and Alexander Steinbüchel, Volume 1, 89-99.

50. Lin, S. Y. and Dence, C. W. (1993) Methods in Lignin Chemistry. Springer-Verlag: London, United Kingdom.

51. Lehto, J. and Alén, R. (2012) Purification of hardwood-derived autohydrolysates. Bioresources 7: 1813–1823.

52. Nováková, L., Grand-Guillaume Perrenoud, A., Francois, I., West, C., Lesellier, E. and Guillarme, D. (2014) Modern analytical supercritical fluid chromatography using columns packed with sub-2 μm particles: A tutorial. Anal. Chim. Acta, 824: 18-35.

53. Webster, G. K. (2014) Supercritical Fluid Chromatography: Advances and Applications in Pharmaceutical Analysis. Pan Standford Publishing: Boca Raton, United States of America.

54. Janssen, H.-G., Schoenmakers, P. J. and Cramers, C. A. (1991) Effects of modifiers in packed and open-tubular supercritical fluid chromatography. J. Chromatogr. A, 552: 527-537.

55. Shi, J., Khatri, M., Xue, S. J., Mittal, G. S., Ma, Y. and Li, D. (2009) Solubility of lycopene in supercritical CO2 fluid as affected by temperature and pressure. Sep. Purif. Technol., 66: 322-328.

56. Topal, U., Sasaki, M., Goto, M. and Hayakawa, K. (2006) Extraction of Lycopene from Tomato Skin with Supercritical Carbon Dioxide: Effect of Operating Conditions and Solubility Analysis. J. Agric. Food. Chem., 54: 5604-5610.

7. Conclusions and future work

7.1. Conclusions

This work addresses the valorization of lignocellulosic rich streams for the sustainable production of value added compounds by membrane and chromatographic processes to be combined after the production of sodium salts of vanillin and syringaldehyde by alkaline chemical oxidation of lignin. In this study, synthetic solutions and one real oxidized lignin solution were employed. The most relevant conclusions obtained will be made in the following paragraphs.

Initially, the potential of polymeric resins to recover vanillin and syringaldehyde was assessed with two macroporous styrene-divinylbenzene resins: SP700 and XAD16N. Mono-component batch equilibrium adsorption studies were carried out with vanillin and syringaldehyde for different temperatures (283/288, 298 and 313 K). Bi-Langmuir isotherm model has reasonably described the equilibrium data and higher maximum adsorption capacities, $q_{m1,i}$, were obtained employing SP700 resin of 0.634 and 0.663 g $g^{-1}_{dry\ resin}$ for vanillin and syrindaldehyde, respectively. Therefore, this resin was chosen to pursue with mono-component batch adsorption studies with vanillic and syringic acids and maximum adsorption capacities, $q_{m1,i}$, of 0.486 and 0.407 g $g^{-1}_{dry\ resin}$ were obtained with the Bi-Langmuir isotherm, respectively.

Fixed bed adsorption studies were performed with mono-component solutions of vanillin, syringaldehyde, vanillic acid and syringic acid for different feed concentrations and temperatures. The prediction of the respective breakthrough curves based on an axially dispersed plug flow model comprising the adsorption equilibrium Bi-Langmuir isotherm and the linear driving force rate model to describe the intraparticle mass transfer were satisfactorily described.

Desorption studies with water demonstrated that high amounts of this eluent are needed to recover the adsorbed vanillin and syringaldehyde (about 1750 BV), constituting a limiting step in the adsorption/desorption process. In this regard, desorption studies with ethanol:water (90:10, % V/V) solution were conducted for different bed loadings with aqueous solutions of vanillin, syringaldehyde, vanillic acid and syringic acid and demonstrated to constitute a good alternative to water, where more than 83% of each phenolic compound was readily recovered with about 16-20 BV with the additional advantage of simultaneously obtaining concentrated (up to 6 times more) solutions.

Moreover, batch and fixed bed adsorption/desorption studies of vanillin and syringaldehyde in the presence of ethanol:water (90:10, % V/V) solution were performed for 298 and 313 K. The effect of temperature in the adsorption capacity was negligible. It was demonstrated that the adsorption of both aldehydes were negatively affected by the present of ethanol and almost a linear trend between the adsorbed phase concentration and the equilibrium liquid concentration was observed. The equilibrium data was satisfactorily described by Freundlich isotherm. A mathematical model considering isothermal operation with the Freundlich isotherm and plug flow with axial dispersion and linear driving force approximation predicted well the experimental breakthrough curves obtained.

A membrane fractionation sequence encompassing three tubular ceramic membranes of different molecular weight cut-off of 50, 5 and 1 kDa was successfully performed aiming the separation of the low molecular weight phenolates from the oxidation products of higher molecular weights. In each stage, two distinct fractions were obtained: the permeate, enriched in the monomeric compounds of interest, and the retentante, containing the rejected higher molecular weight compounds. This was clearly observed by the gel permeation chromatograms obtained.

Operating flux reductions of 69%, 62% and 81% were observed for membrane processing stages with 50, 5 and 1kDa membranes, respectively. The analysis of membrane intrinsic and fouling resistances indicated high flux decline for the 50 and 1kDa membranes mostly attributed to reversible fouling. On the contrary, the most detrimental contribution for flux decline of 5kDa membrane was the irreversible fouling component. Average membrane productivities in the stationary phase of 11.6, 11.2 and 5.8 L m^{-2} h^{-1} were attained for 50, 5 and 1kDa membranes, respectively. The initial water permeate fluxes were easily accomplished within 2 to 3 cycles of hot chemical cleaning with NaOH 0.1M solutions.

Each stream of the fractionation process (feed, permeates and retentantes) was characterized regarding total non-volatile solids, total phenolic compounds quantified by HPLC-UV and ashes. The fractionation sequence was effective in decreasing the total non-volatile solids content, and apparent rejection coefficients values between 29.1-15.1 % were obtained. Less than 5% of ashes were retained in all membrane stages. The 50 kDa membrane did not retain any of the phenolate compounds while, on the contrary, about 9-12 % of the phenolate compounds of interest were retained by the other two membranes. Overall, with the fractionation sequence, total solids content decreased from 86.5 g L^{-1} to 58.6 g L^{-1} with some loss in the phenolate compounds of interest, from 2.399 g L^{-1} to 2.151 g L^{-1}.

Concluding, the membrane fractionation sequence improved the phenolate content from 28 mg g^{-1}_{TS} to 32 mg g^{-1}_{TS} during the first membrane fractionation stage and achieved a content of 35-37 mg g^{-1}_{TS} after processing with the other two membranes of lower molecular weight cut-off.

The need for a fractionation sequence encompassing three membrane stages must be carefully analyzed since the gain in composition was not significant in the second and third membrane stages.

The final permeates 5 and 1 kDa were submitted to adsorption/desorption studies employing the SP700 resin at 298K after a pH value correction from 10 to 7.5-8. At this pH value, the phenolic acids were mostly ionized and thus, were not significantly adsorbed. Cycles of adsorption/desorption performed allowed to demonstrate that these resins can be reutilized up to 4-5 times. Final concentrated and enriched solutions of phenolic compounds were achieved by eluting with ethanol:water (90:10, % V/V) solution, representing 452-376 mg g^{-1}_{TS}. The major phenolic compounds quantified in the final solutions obtained were vanillin, syringaldehyde, acetovanillone and acetosyringone.

The final eluates were successfully separated with CO_2 supercritical fluid chromatography employing the best set of operating conditions previously established with synthetic solutions: 40 ºC, 150 bar, 5 and 3 mL^{-1}, and co-solvent gradient starting with 0.7% V/V.

This work can be seen as proof of concept that oxidation, membrane fractionation and adsorption processes can be integrated to treat an oxidized industrial kraft liquor (IKL) solution. In Figure 7.1 it is presented a simplified flow sheet of the separation and purification sequence implemented in this work with the respective compositions of total non-volatile solids (TS) and phenolic compounds quantified by HPLC-UV (TP) achieved in each process.

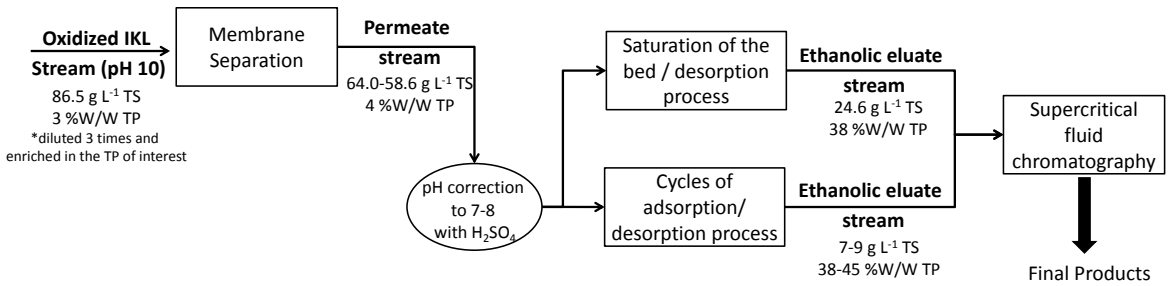

Figure 7.1 Simplified scheme of the separation and purification processes applied in this work and main composition of the streams regarding total solids (TS) and phenolate/phenolic compounds.

7.2. Future work

During the experimental development of this thesis, new research topics have emerged to investigate in a near future. Some of the future work topics arose from literature search and new scientific advances. Other future work topics are related with complementary studies to the results obtained in this thesis, thereby increase the knowledge for modelling and scale up of the membrane and chromatographic processes studied herein. In Figure 7.2 it is shown a sequence of processes that could be explored in order to further improve the separation and purification sequence studied and will be discussed in the next paragraphs.

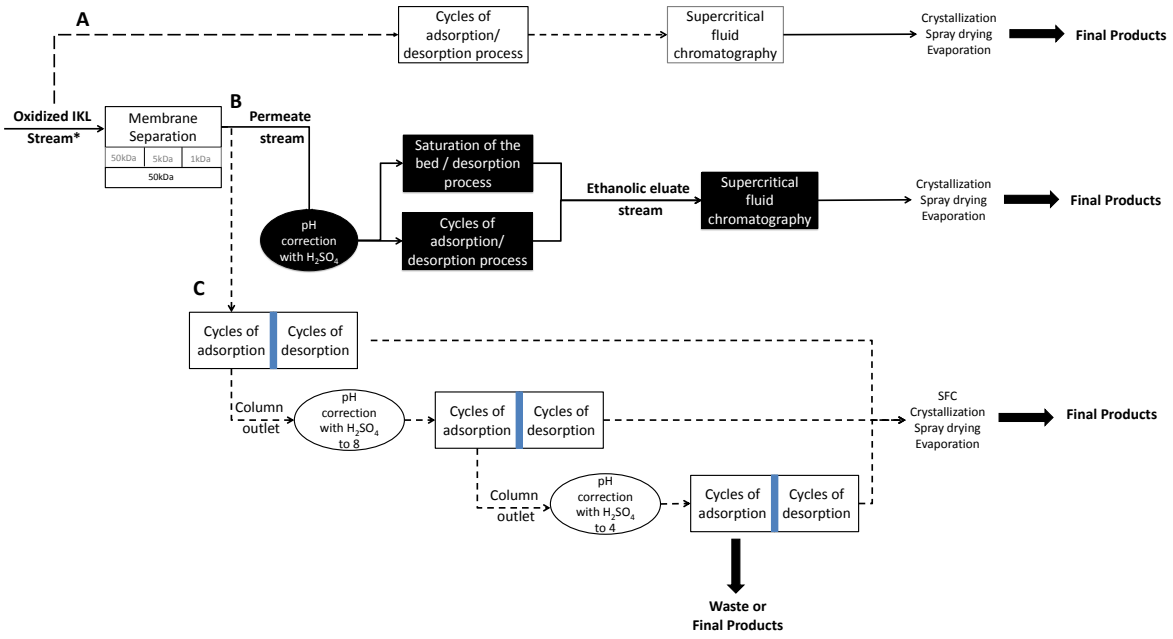

Figure 7.2 Simplified scheme of the separation and purification sequence of processes to study. The sequence studied in this work is indicated in the black box and the resin washing step with water is indicated in blue.

In order to complement the adsorption studies performed onto SP700 resin with synthetic solutions of phenolic compounds, kinetic studies must be performed in order to better describe the mass transfer phenomena. Moreover, mono-component batch and dynamic studies with other phenolic compounds (e.g. acetovanillone, acetosyringone) found in lignin oxidized medium should be conducted, as well as multi-component assays in order to find a suitable competition isotherm model to describe de adsorptive behavior.

Regarding the adsorption studies of vanillin and syringaldehyde in the presence of ethanol:water (90:10, % V/V) solution, bi-component water-ethanol adsorption experiments onto SP700 resin should be performed to evaluate the degree of ethanol adsorption by the resin employed.

Vanillin and syringaldehyde adsorption studies, employing synthetic and real oxidized lignin solutions, clearly demonstrated that the polymeric resin employed was not selective, and that other compounds were simultaneously adsorbed with the aldehydes. In the perspective of improving selectivity of the adsorption process, the use of molecular imprinted polymers (MIP) developed by using vanillin/syringaldehyde as template molecules could be an interesting approach. The design and development of MIP allow creating tailor-made adsorbents with selective properties to specific molecules by tuning the shape, size and functionality of the binding sites (1, 2). This technology has been applied in several separation processes (3-5). Studies employing methacrylate-based polymer monoliths have shown that these materials are easily prepared and functionalized with a high degree of macroporosity, being also a promising approach to pursue (6, 7).

Concerning the oxidized lignin solution submitted to adsorption/desorption studies onto SP700 resin after a membrane fractionation, although the pH near 7-8 was selected as the starting point, it is advisable to evaluate the influence of the pH in the adsorption of vanillin and syringaldehyde in order to select the best operating pH value. Moreover, aiming the valorization of different products and the enhancement of the adsorption process efficiency, it is suggested a sequential adsorption starting with pH values of 10-11 (the IKL oxidized solution as it is), followed by adsorption at pH 8 and 4, as indicated in Figure 7.2C.

Additionally, in order to investigate if cycles of adsorption/desorption could be further optimized it is required to evaluate the optimal extension of the washing step with water to observe if phenolic acids and other adsorbed compounds can be selectively removed in this step without significant loss of the aldehydes of interest.

When operating with the real oxidized lignin solution, there are several unknown compounds that compete for the adsorption sites required for vanillin and syringaldehyde such as low molecular weight fragments of lignin and other phenolic compounds, which are difficult to predict by just performing studies with synthetic solutions. Therefore, equilibrium and kinetic adsorption studies onto SP700 resin should be performed with the real oxidized lignin solution before and after being treated by a membrane separation process (as indicated in Figure 7.2 A and B/C) in order to design the most appropriate large-scale industrial chromatographic process optimized for vanillin and syringaldehyde recovery. The development of continuous or semi-continuous counter-current chromatographic processes encompassing stages of loading, washing, elution and regeneration are commonly suggested for purification of pharmaceutical compounds (8-10) and are promising approaches to be applied to oxidized lignin solutions.

Regarding the membrane separation sequence applied for the first time in this work, other approaches could be considered and results compared with those of the system of 3 membranes considered in this work. The impact of removal of one of two membrane stages, preferably 5 and 1 kDa, in the final composition could be evaluated by comparing the benefits/disadvantages gained. Therefore, the initial feed stream and the permeate obtained with the 50 kDa membrane must be fed onto SP700 resin evaluating the final eluates composition and therefore the impact of simplifying the membrane fractionation. Other intermediate molecular weight cut-offs should be tested (e.g. 100/75 or 20/15 kDa) as well.

Fouling mitigation is important to consider in membrane separation processes and thus, process conditions should be optimized to find the best combination of operating temperature, feed flowrate and transmembrane pressure that minimize fouling formation with improved membrane productivities. Moreover, it is paramount that the continuous oxidation process upstream is optimized because the degree of lignin fragmentation achieved is a detrimental aspect that influences in membrane productivity and type of fouling generated.

Gas bubbling is a classical solution that can be easily applied in order to increase the shear rate at the membrane surface and promote the removal of some fouling layers formed during operation. For this step, nitrogen could be used with the simultaneous advantage of avoiding degradation of the phenolic compounds. Introducing intermediate water backflush cleaning steps can also be an easy classical way to implement and improve the performance of the membrane process.

Membrane modification and functionalization by surface coating or grafting and incorporation of hydrophilic monomers/inorganic particles to obtain improved membrane anti-fouling properties is a promising sustainable solution to improve process performance and has been extensively studied in the last years (11-15). Moreover, employing an electrically assisted membrane process in order to reduce fouling can also be a sustainable solution to implement (16).

Concerning supercritical fluid chromatography employing CO_2, there are several aspects that should be further investigated, in order to optimize the chromatographic process and evaluate the potential of employing this technology as a final refining step in the separation and purification of oxidized lignin solutions. The following studies should be conducted: mobile phase strength modified by incorporation of solvents, such as ethanol, or by the incorporation of new additives (e.g. citric acid); optimize the operating back pressure; test other columns/stationary phases and exploited the synergic effect on selectivity, resolution and peak shape with chromatographic conditions systematically.

After choosing the most suitable stationary phase and best operating conditions, adsorption equilibria studies should be conducted. A simulating moving bed process using CO_2 as supercritical

eluent (8, 17) could be envisaged as a suitable technology to be developed for the final purification stage of vanillin and syringaldehyde.

Finally, it is important to note that there is still a considerable amount of unknown compounds present in each stream of the integrated separation and purification sequence studied. Therefore, a deeper characterization of the final permeate and eluate streams should be simultaneously conducted in order to identify the other compounds present, such as sugars, phenolic acids and other phenolic compounds.

7.3. References

1. Spégel, P., Schweitz, L. and Nilsson, S. (2002) Molecularly imprinted polymers. Anal. Bioanal. Chem., 372: 37-38.
2. Chen, L., Xu, S. and Li, J. (2011) Recent advances in molecular imprinting technology: current status, challenges and highlighted applications. Chemical Society Reviews, 40: 2922-2942.
3. Li, W. and Li, S. (2007) Molecular Imprinting: A Versatile Tool for Separation, Sensors and Catalysis: In Oligomers - Polymer Composites - Molecular Imprinting. R. G. Berger editor. Springer Berlin Heidelberg: London, United Kingdom, Volume 206, 191-210.
4. Feng, Q.-Z., Zhao, L.-X., Yan, W., Lin, J.-M. and Zheng, Z.-X. (2009) Molecularly imprinted solid-phase extraction combined with high performance liquid chromatography for analysis of phenolic compounds from environmental water samples. J. Hazard. Mater., 167: 282-288.
5. Mhaka, B., Cukrowska, E., Tse Sum Bui, B., Ramström, O., Haupt, K., Tutu, H. and Chimuka, L. (2009) Selective extraction of triazine herbicides from food samples based on a combination of a liquid membrane and molecularly imprinted polymers. J. Chromatogr. A, 1216: 6796-6801.
6. Groarke, R. and Brabazon, D. (2016) Methacrylate polymer monoliths for separation Applications. Materials, 9: 1-32.
7. Groarke, R. J. and Brabazon, D. (2016) Monolithic Materials for Bio-Separations: In Reference Module in Materials Science and Materials Engineering. Elsevier.
8. Faria, R. P. V. and Rodrigues, A. E. (2015) Instrumental aspects of simulated moving bed chromatography. J. Chromatogr. A, 1421: 82-102.

9. Ströhlein, G., Aumann, L., Mazzotti, M. and Morbidelli, M. (2006) A continuous, counter-current multi-column chromatographic process incorporating modifier gradients for ternary separations. J. Chromatogr. A, 1126: 338-346.

10. Mahajan, E., George, A. and Wolk, B. (2012) Improving affinity chromatography resin efficiency using semi-continuous chromatography. J. Chromatogr. A, 1227: 154-162.

11. Vera, M., Hessel, L. C. and Anita, B. (2014) Class II Hybrid organic-inorganic membranes creating new versatility in separations. Curr. Org. Chem., 18: 2334-2350.

12. Mustafa, G., Wyns, K., Vandezande, P., Buekenhoudt, A. and Meynen, V. (2014) Novel grafting method efficiently decreases irreversible fouling of ceramic nanofiltration membranes. J. Membr. Sci., 470: 369-377.

13. Le, N. L. and Nunes, S. P. (2016) Materials and membrane technologies for water and energy sustainability. Sustainable Materials and Technologies, 7: 1-28.

14. Mustafa, G., Wyns, K., Buekenhoudt, A. and Meynen, V. (2016) New insights into the fouling mechanism of dissolved organic matter applying nanofiltration membranes with a variety of surface chemistries. Water Research, 93: 195-204.

15. Buekenhoudt, A., Wyns, K., Mustafa, G. and Meynen, V. (2015) Method for increasing the fouling resistance of inorganic membranes by grafting with organic moieties, WO Patent 2015124784 A1 (27-08-2015).

16. Geng, P. and Chen, G. (2016) Magnéli Ti4O7 modified ceramic membrane for electrically-assisted filtration with antifouling property. J. Membr. Sci., 498: 302-314.

17. Mazzotti, M., Storti, G. and Morbidelli, M. (1997) Supercritical fluid simulated moving bed chromatography. J. Chromatogr. A, 786: 309-320.

Appendices

A.Equilibrium adsorption constants and adsorption enthalpies

In this appendix it is summarized the parameters related with the adsorption equilibrium properties and respective adsorption enthalpies estimated by the Van't Hoff equation.

Table A.1 Langmuir equilibrium parameters obtained for adsorption of vanillin (V), syringaldehyde (S), vanillic acid (VA) and syringic acid (SA) onto SP700 resin

	V		S		SA	VA
	SP700	**XAD16N**	**SP700**	**XAD16N**	**SP700**	**SP700**
Langmuir model						
$q_{m,i}$ (g g$^{-1}_{\text{dry resin}}$)	0.663	0.587	0.707	0.730	0.423	0.450
K_L^o (L g^{-1})	3.21x10^{-4}	1.12x10^{-2}	5.26x10^{-4}	8.00x10^{-5}	1.38x10^{-3}	2.05x10^{-6}
ΔH_L (kJ mol^{-1})	-20.0	-10.9	-19.7	-23.5	-20.0	-34.0
$K_{L,i}$ (L g^{-1}) T1	1.566	1.162	1.944	1.474	5.954	2.971
$K_{L,i}$ (L g^{-1}) T2	1.023	0.920	1.476	1.061	4.497	1.846
$K_{L,i}$ (L g^{-1}) T3	0.694	0.745	1.009	0.673	3.053	0.957
$\sum_{i=1}^{n}(q_{\exp}-q_{calc})^2$ (g g$^{-1}_{\text{dry resin}})^2$	1.87 x10^{-2}	0.32 x10^{-2}	0.70x10^{-2}	0.51 x10^{-2}	0.25 x10^{-2}	0.67 x10^{-2}

T1 – 283 K (V) and 288 K (S, VA, SA); T2 – 298 K; T3 – 313 K;

Table A.2 Bi-Langmuir equilibrium parameters obtained for adsorption of vanillin (V), syringaldehyde (S), vanillic acid (VA) and syringic acid (SA) onto SP700 resin

		V		S		SA	VA
		SP700	XAD16N	SP700	XAD16N	SP700	SP700
Bi-Langmuir model							
$q_{m1,i}$ (g g$^{-1}_{\text{dry resin}}$)		0.634	0.529	0.663	0.639	0.407	0.486
$q_{m2,i}$ (g g$^{-1}_{\text{dry resin}}$)		0.131	0.116	0.139	0.113	0.0826	0.0967
K^{o}_{L1} (L g^{-1})		3.15x10^{-4}	8.03x10^{-3}	7.19x10^{-4}	2.17x10^{-5}	1.03x10^{-3}	1.33x10^{-6}
K^{o}_{L2} (L g^{-1})		5.57x10^{-2}	1.45	1.45x10^{-1}	4.85x10^{-3}	9.71x10^{-2}	1.67x10^{-4}
ΔH_{L1} (kJ mol^{-1})		-18.3	-10.0	-17.2	-25.9	-18.8	-32.5
ΔH_{L2} (kJ mol^{-1})		-18.4	-11.0	-17.3	-25.8	-19.0	-32.2
$K_{L1,i}$ (L g^{-1})	T1	0.752	0.572	0.943	1.084	2.658	1.043
	T2	0.508	0.462	0.742	0.754	2.042	0.662
	T3	0.358	0.380	0.532	0.457	1.425	0.351
$K_{L2,i}$ (L g^{-1})	T1	137.8	156.0	194.6	150.1	269.5	115.5
	T2	93.0	123.3	152.8	106.1	206.5	73.6
	T3	65.2	99.6	109.5	65.7	143.0	39.5
$\sum_{i=1}^{n}\left(q_{\exp}-q_{calc}\right)^2$ (g g$^{-1}_{\text{dry resin}}$)^2		0.42 x10^{-2}	0.20 x10^{-2}	0.31 x10^{-2}	0.37 x10^{-2}	0.079 x10^{-2}	0.30 x10^{-2}

T1 – 283 K (V) and 288 K (S, VA, SA); T2 – 298 K; T3 – 313 K;

Table A.3 Freundlich equilibrium parameters obtained for adsorption of vanillin (V), syringaldehyde (S), vanillic acid (VA) and syringic acid (SA) onto SP700 resin

	V		S		SA	VA
	SP700	**XAD16N**	**SP700**	**XAD16N**	**SP700**	**SP700**
Freundlich model						
n	2.7	2.9	2.8	2.5	2.5	2.5
$K_{F,i}$ g g$^{-1}_{\text{dry resin}}$ (L g^{-1})$^{1/n}$ T1	0.3977	0.3095	0.4505	0.4292	0.4027	0.3440
T2	0.3350	0.2902	0.4076	0.3687	0.3657	0.2757
T3	0.2927	0.2699	0.3551	0.3072	0.3281	0.2200
$\sum_{i=1}^{n}\left(q_{\text{exp}} - q_{calc}\right)^2$ (g g$^{-1}_{\text{dry resin}}$)^2	0.64 x10^{-2}	0.42 x10^{-2}	0.34 x10^{-2}	0.38 x10^{-2}	0.081 x10^{-2}	0.33 x10^{-2}

T1 – 283 K (V) and 288 K (S, VA, SA); T2 – 298 K; T3 – 313 K;

B. Multi-component adsorption studies

This appendix addresses preliminary adsorption studies performed with aqueous solution containing vanillin (V), syringaldehyde (S), vanillic acid (VA) and syringic acid (SA).

In order to evaluate the influence of pH value on the adsorption of vanillin, syringaldehyde, vanillic acid and syringic acid, two four-component fixed bed adsorption experiments onto a bed of SP700 were performed as described in 3.2.6 at 298 K and pH value of 3.5 and 6.5. The extended Bi-Langmuir model was applied for both experiments. For pH value of 6.5, the phenolic acids were not adsorbed and the extended Bi-Langmuir model was successfully applied considering a binary mixture of vanillin and syringaldehyde. However this model failed to describe the experimental results performed at pH value of 3.5. It is important to highlight that due to the occurrence of some experimental drawbacks during this fixed bed study, the experiment at pH value of 3.5 must be repeated in order to confirm the results and support the conclusion that the extended Bi-Langmuir model is too simplistic to describe the complexity of the multi-component system. If a new multi-component model is to be found, it is important to perform several four-component equilibrium batch experiments as well and afterwards validate them with fixed bed experiments.

The aqueous solutions of vanillin, syringaldehyde, vanillic acid and syringic acid were prepared and loaded onto the same column bed used in the pure component experiments at 298 K and feed flowrate 5 mL min^{-1} (as described in Chapter 3, section 3.2.6). The feed composition used is summarized in Table B.1 along with the respective experimental adsorbed amount obtained for each phenolic compound. Experiments were performed at pH value of 3.5 and pH value corrected to 6.5 in order to evaluate the influence of a pH change on the adsorptive capacity. The extended Bi-Langmuir model was applied to predict the adsorbed amounts and values are given in Table B.1 and shown in Figure B.1.

Since the simplified extended Bi-Langmuir model failed to describe the fixed bed adsorption capacities obtained for each phenolic compound for experiment performed at pH value of 3.5, most probably, a more complex model accounting for additional competition effects must be applied. Nevertheless, it is important to highlight that more experiments must be carried out to confirm the adsorbed amounts experimentally obtained and also to better assess the competition behavior among the four compounds studied.

Table B.1 Experimental and theoretical adsorbed amounts obtained in multi-component (V, S, VA and SA) fixed bed adsorption experiments for different feed concentrations at 298 K, feed flowrate 5 mL min^{-1}, SP700 bed with 5.6 x 1 cm and porosity 0.35.

		$C_{i,feed}$ g L^{-1}	$q_{ads,exp}$ g g$^{-1}_{dry\ resin}$	$q_{ads,pred}$ g g$^{-1}_{dry\ resin}$	%SD*
Multi-component system (pH 3.5)	V	0.70	0.193[a]	0.085	127
	S	0.56	0.186 [a]	0.108	72
	VA	0.88	0.157 [a]	0.278	44
	SA	0.22	0.057 [a]	0.020	179
Multi-component system (pH 6.5)	V	0.48	0.137	0.128**	6.8
	S	0.67	0.302	0.285**	1.9
	VA	0.15	***	***	-
	SA	0.64	***	***	-

a) This experiment must be repeated in order to confirm the adsorbed amounts estimated due to sample deterioration.

*SD (%) corresponds to the standard deviation between the experimental and predicted adsorbed amounts, calculated with the following expression: $SD(\%) = \frac{\left|q_{ads,pred} - q_{ads,\exp}\right|}{q_{ads,pred}} \times 100$;

** value predicted considering a binary system of vanillin and syringaldehyde;

*** No adsorption of vanillic and syringic acids occurred at this pH value.

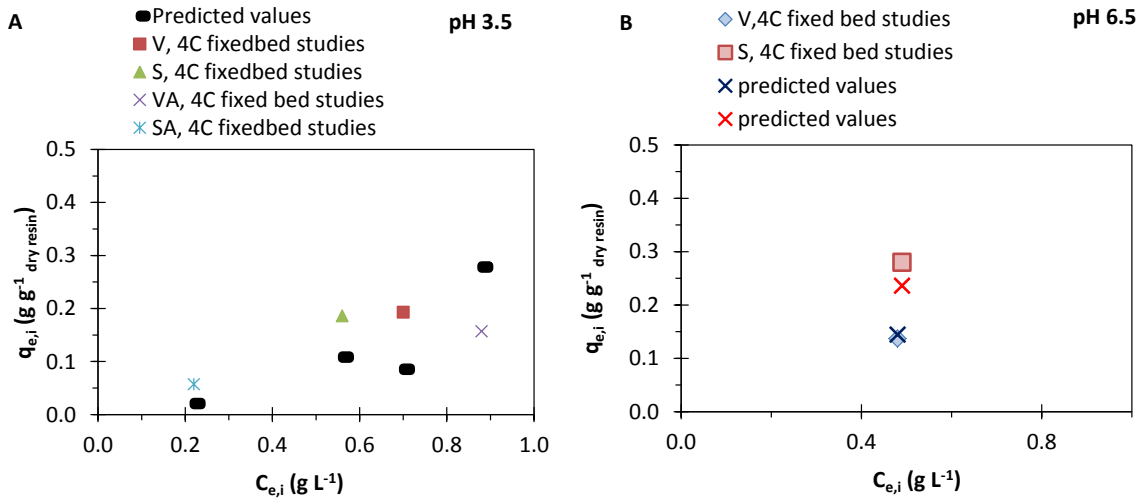

Figure B.1 Four-component (V, S, VA and SA) fixed bed adsorption studies for A) pH value 3.5 and B) pH value 7: experimental and predicted adsorption capacities obtained. Since no adsorption of VA and SA occurred, the results for these compounds are not shown in B.

In the four-component experiment performed at pH value of 6.5, the acids were not adsorbed onto the non-polar SP700 resin while vanillin and syringaldehyde were adsorbed in an equal manner as if considering a binary mixture: values predicted employing a binary extended Langmuir model were very close to the experimental values obtained – Table B.1 and Figure B.1. This behavior was expected due to the *pKa* value of the phenolic acids in water be near 4. Therefore, at pH value of 6.5, it is expected that the phenolic acids are ionized and consequently, are not adsorbed by a non-polar resin.

In Figure B.2 and Figure B.3 it is portrayed the transient concentration histories performed with the four components at pH value of 3.5 and pH adjusted to 6.5, respectively. For the latter, the mathematical model comprising the extended Bi-Langmuir model for the binary equilibrium prediction, linear driving force approximation and intraparticle mass transfer resistance, reasonably describes the experimental concentrations histories obtained.

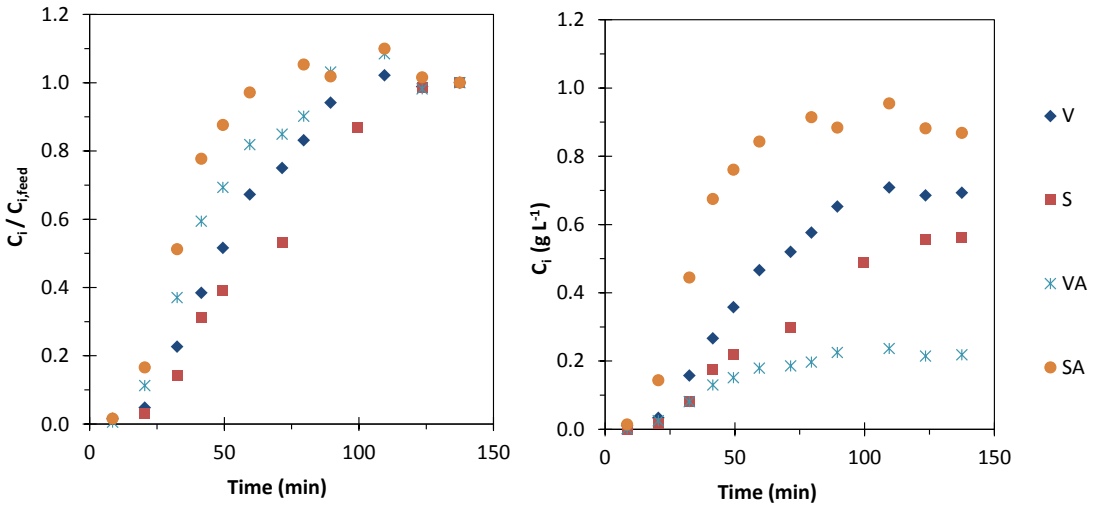

Figure B.2 Normalized concentration and concentration histories obtained for adsorption onto SP700 resin of a four-component system (V - 0.70 g L^{-1}, S - 0.56 g L^{-1}, VA - 0.88 g L^{-1} and SA - 0.22 g L^{-1}) for pH value of 3.5; feed flowrate 5 mL min^{-1}, in a column of 5.6 x 1 cm and porosity 0.35.

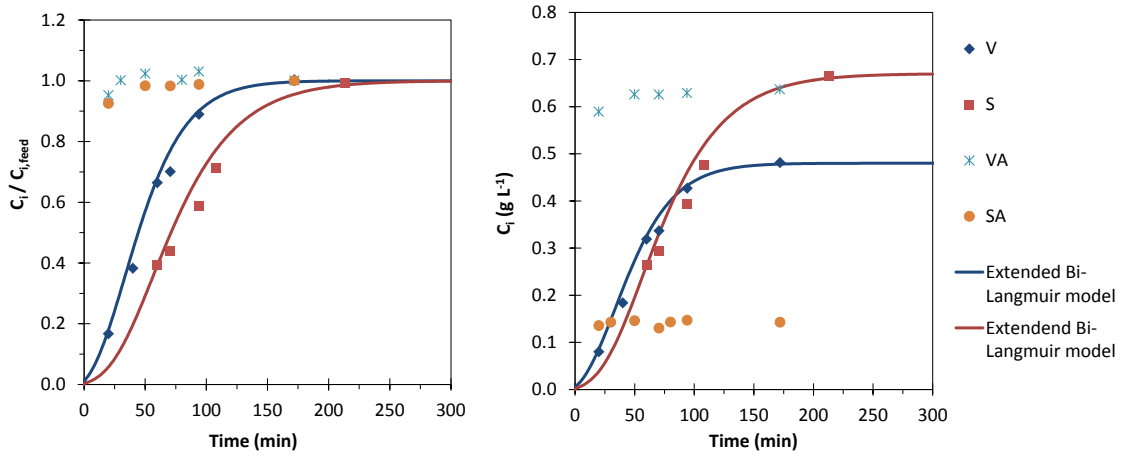

Figure B.3 Normalized concentration and concentration histories obtained for adsorption onto SP700 resin of a four-component system (V - 0.48 g L^{-1}, S - 0.67 g L^{-1}, VA - 0.15 g L^{-1} and SA - 0.64 g L^{-1}) for pH value corrected to 6.5; feed flowrate 5 mL min^{-1}, in a column of 5.6 x 1 cm and porosity 0.35: points correspond to the experimental values and the lines to the simulations obtained considering the axial dispersed model with LDF approximation and the extended Bi-Langmuir model considering a binary mixture of vanillin and syringaldehyde.

C. GPC of the different streams obtained in membrane and adsorption/desorption studies

This appendix presents some additional UV chromatograms obtained by GPC analysis of solutions obtained in membrane fractionation and adsorption studies.

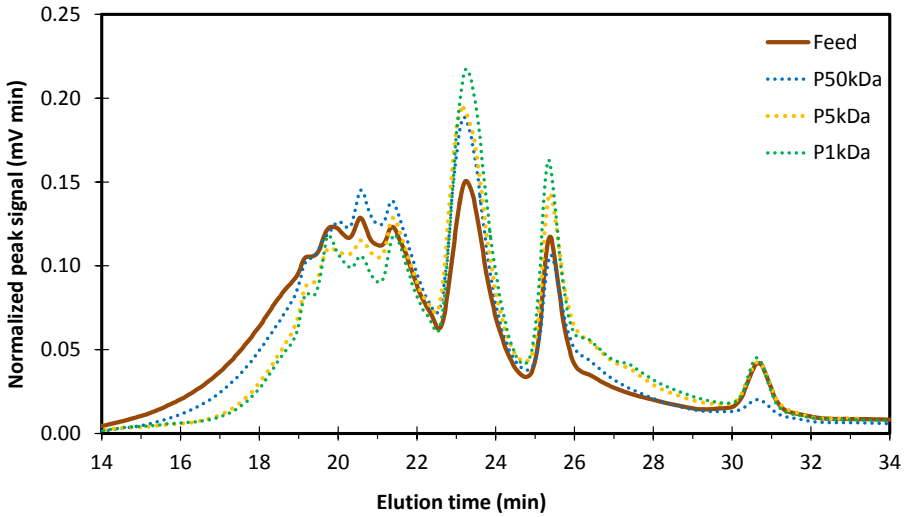

Figure C.1 UV Chromatograms obtained by GPC for oxidized IKL and permeates obtained in the membrane fractionation sequence. Normalization with area under the curve.

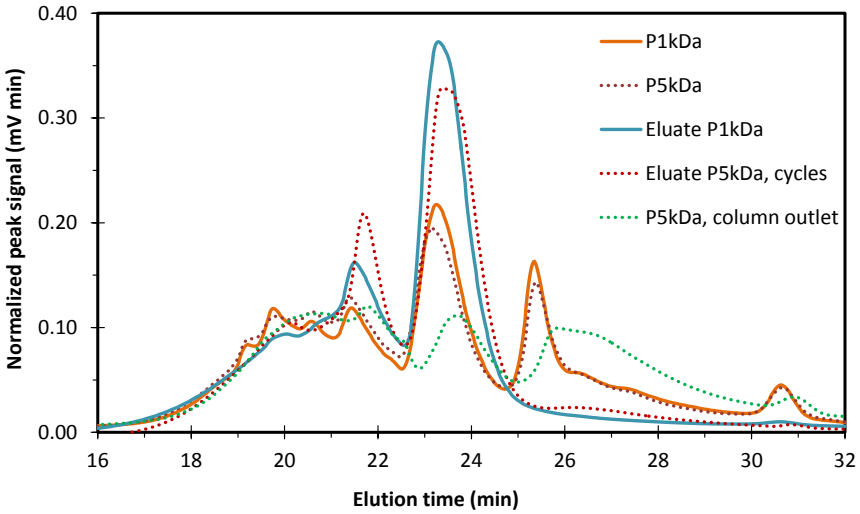

Figure C.2 UV Chromatograms obtained by GPC for the adsorption/desorption study performed: Feed stream (P1kDa and P5kDa), eluates (Eluate P1kDa, breakthrough and P5kDa, cycles) and solution coming out of the column during adsorption of P5kDa onto SP700 resin. Normalization with area under the curve.

D.Adsorption/Desorption studies

This appendix shows some additional figures to complement the Chapter 6 discussion of the adsorption/desorption cycles performed with the permeates P5kDa and P1kDa.

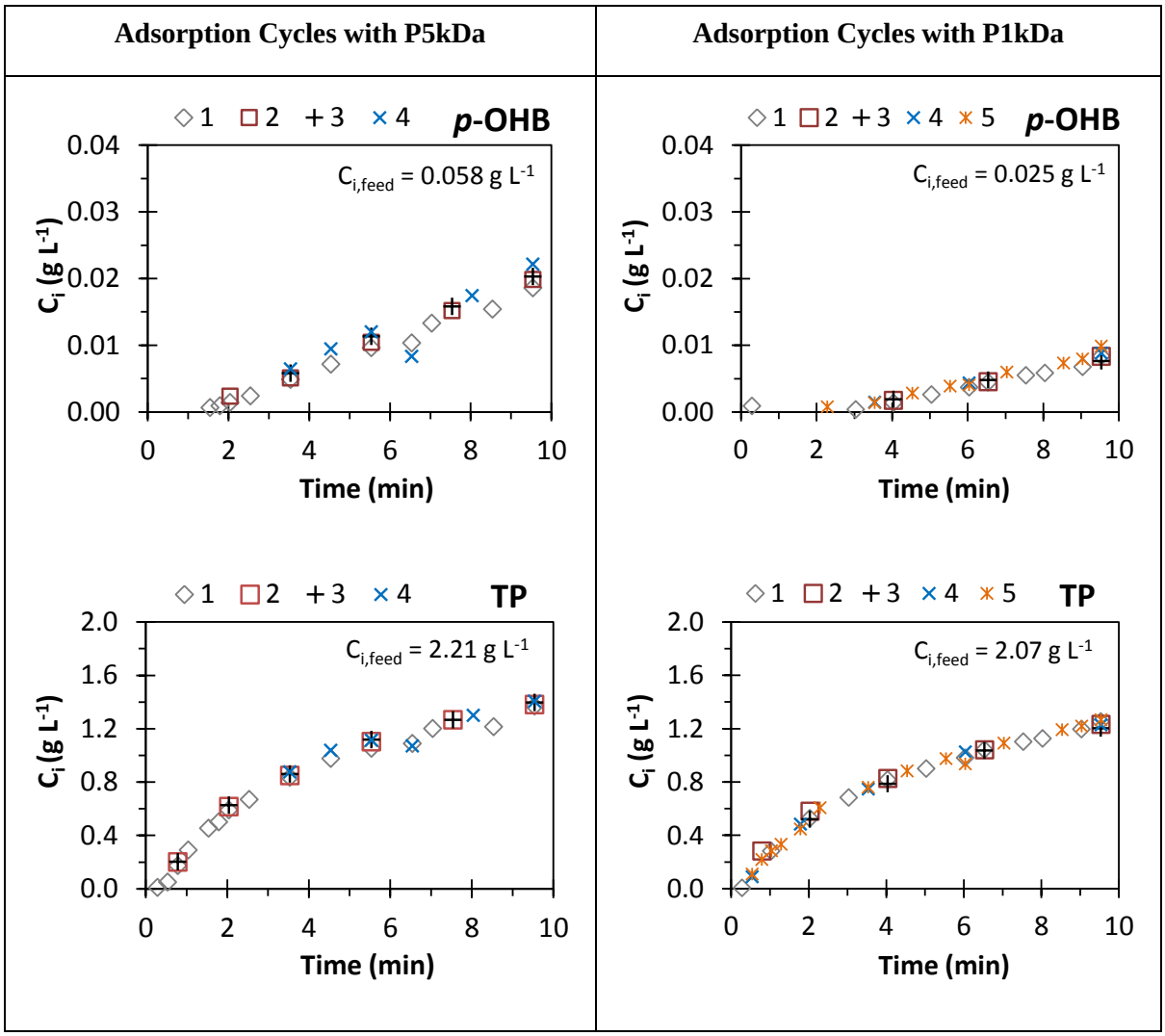

Figure D.1 Adsorption concentration histories at column outlet for each cycle performed with P5kDa and P1kDa feed solutions for *p*-hydroxybenzaldehyde (*p*-OHB) and total phenolic compounds quantified by HPLC-UV (TP). The column was packed with SP700 resin and experiments were performed at 25 ºC and feed low rate of 5.4 mL min^{-1}. Cycles are identified as 1- first cycle (◇), 2- second cycle (□), 3- third cycle (+), 4- forth cycle (×) and 5- fifth cycle (✳).

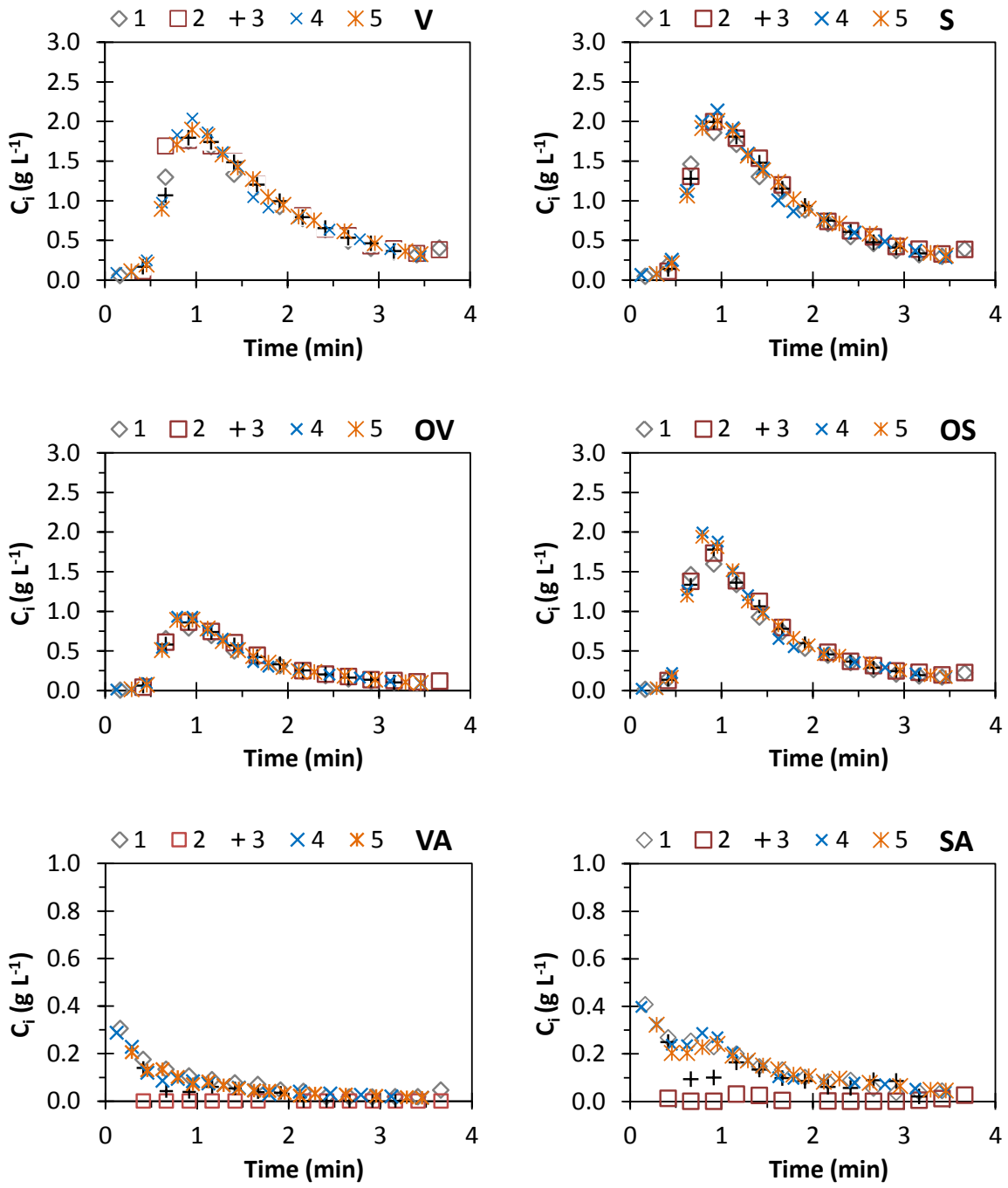

Figure D.2 Desorption concentration histories at column outlet of vanillin (V), syringaldehyde (S), acetovanillone (OV), acetosyringone (OS), vanillic acid (VA) and syringic acid (SA) for each cycle performed with P1kDa. The column was packed with SP700 resin and experiments were performed at 25 ºC and feed low rate of 5.4 mL min^{-1}. Cycles are identified as Cycles are identified as 1- first cycle (◇), 2- second cycle (□), 3- third cycle (+), 4- forth cycle (×) and 5- fifth cycle (∗).

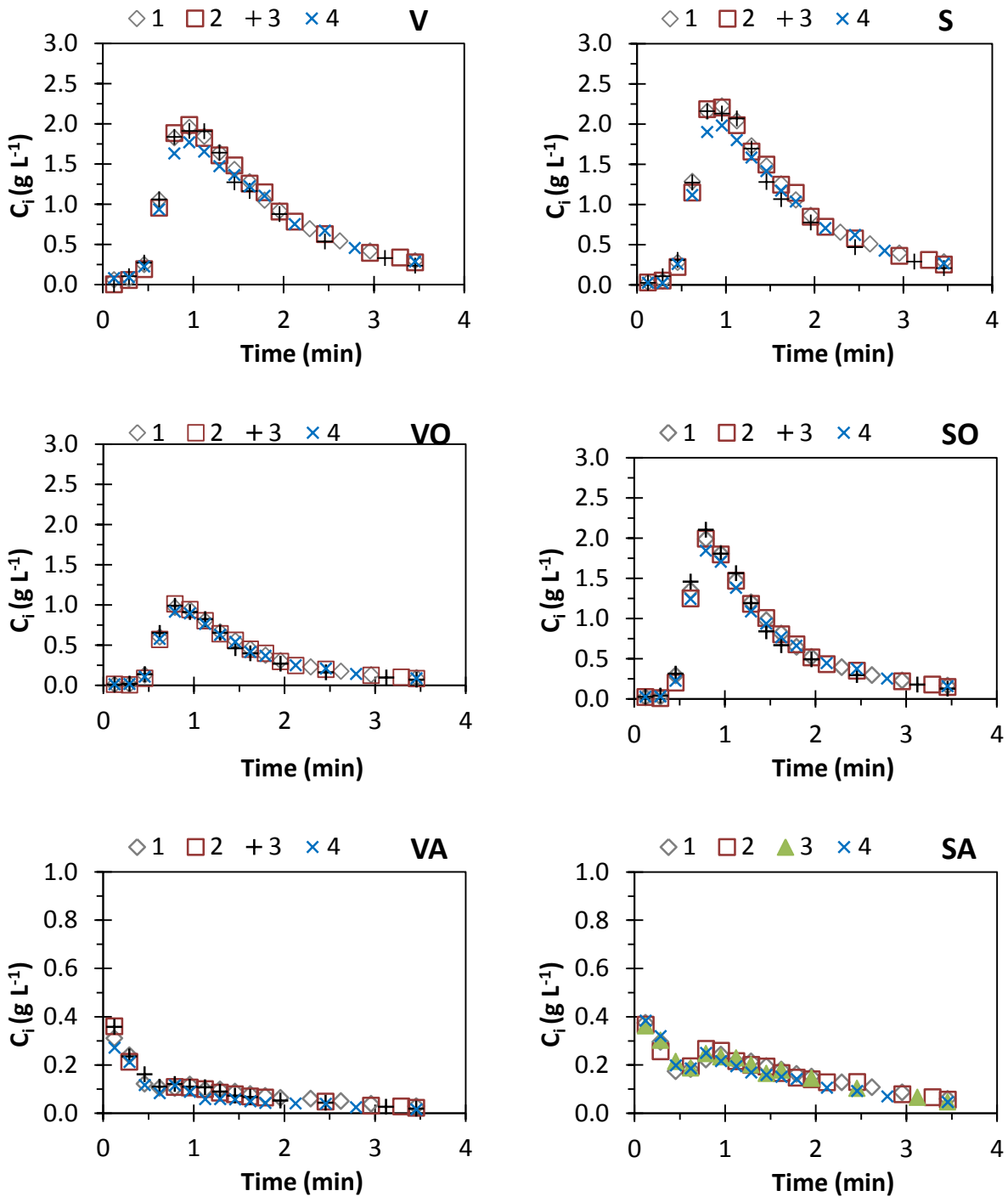

Figure D.3 Desorption concentration histories at column outlet of V, S, OV, OS, VA and SA for each cycle performed with P5kDa. The column was packed with SP700 resin and experiments were performed at 25 ºC and feed low rate of 5.4 mL min^{-1}. Cycles are identified as 1- first cycle (◇), 2- second cycle (□), 3- third cycle (+) and 4- forth cycle (×).

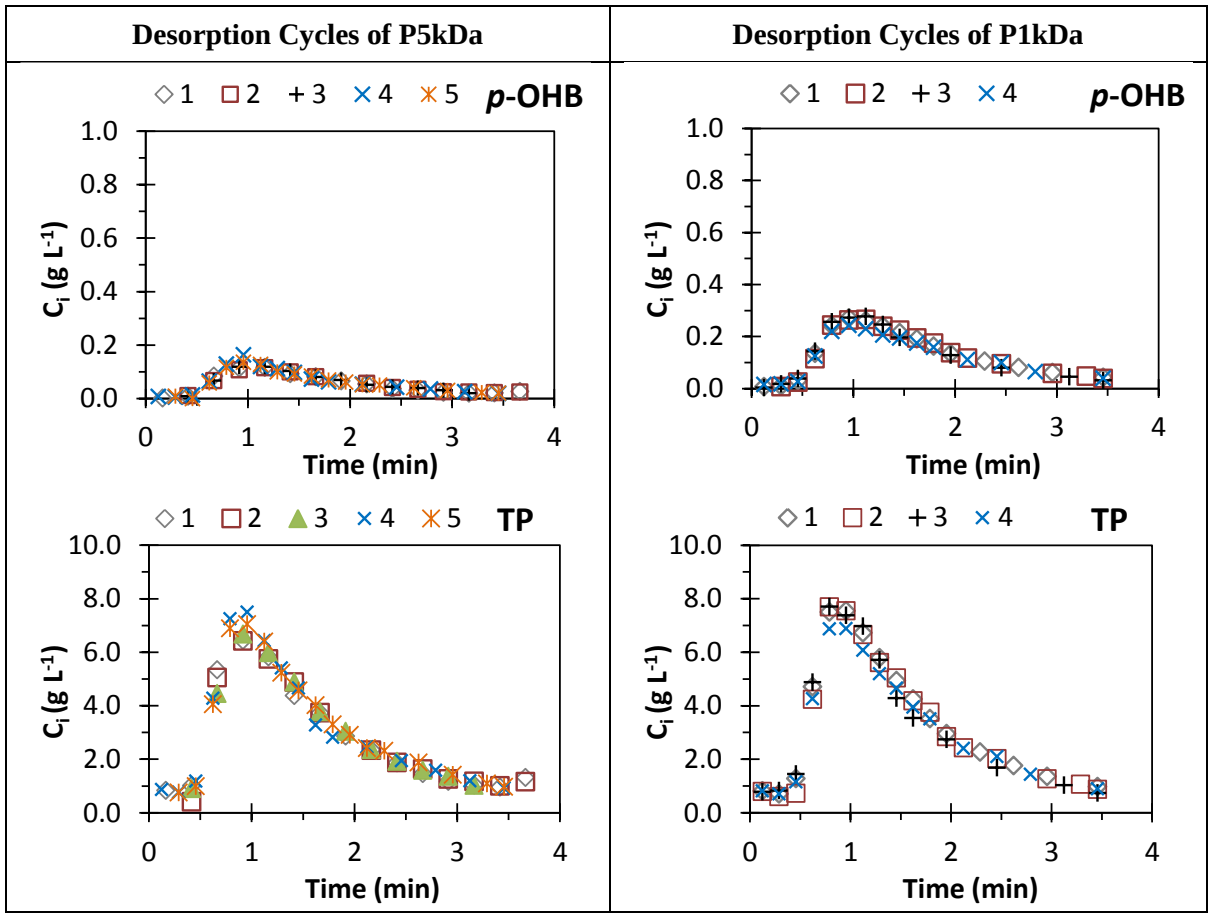

Figure D.4 Desorption concentration histories at column outlet of *p*-OHB and TP, for each cycle performed with P1kDa and P5kDa. The column was packed with SP700 resin and experiments were performed at 25 ºC and feed low rate of 5.4 mL min^{-1}. Cycles are identified as 1- first cycle (◇), 2- second cycle (□), 3- third cycle (+), 4- forth cycle (×) and 5- fifth cycle (✳).

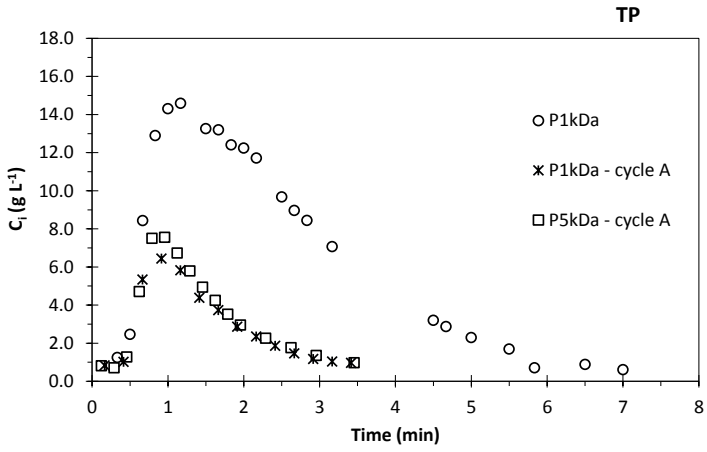

Figure D.5 Desorption concentration histories of TP for P1kDa (saturation of the bed), and for the first cycle performed with P1kDa and P5kDa. The column was packed with SP700 resin and experiments were performed at 25 ºC and feed low rate of 5.4 mL min^{-1}.

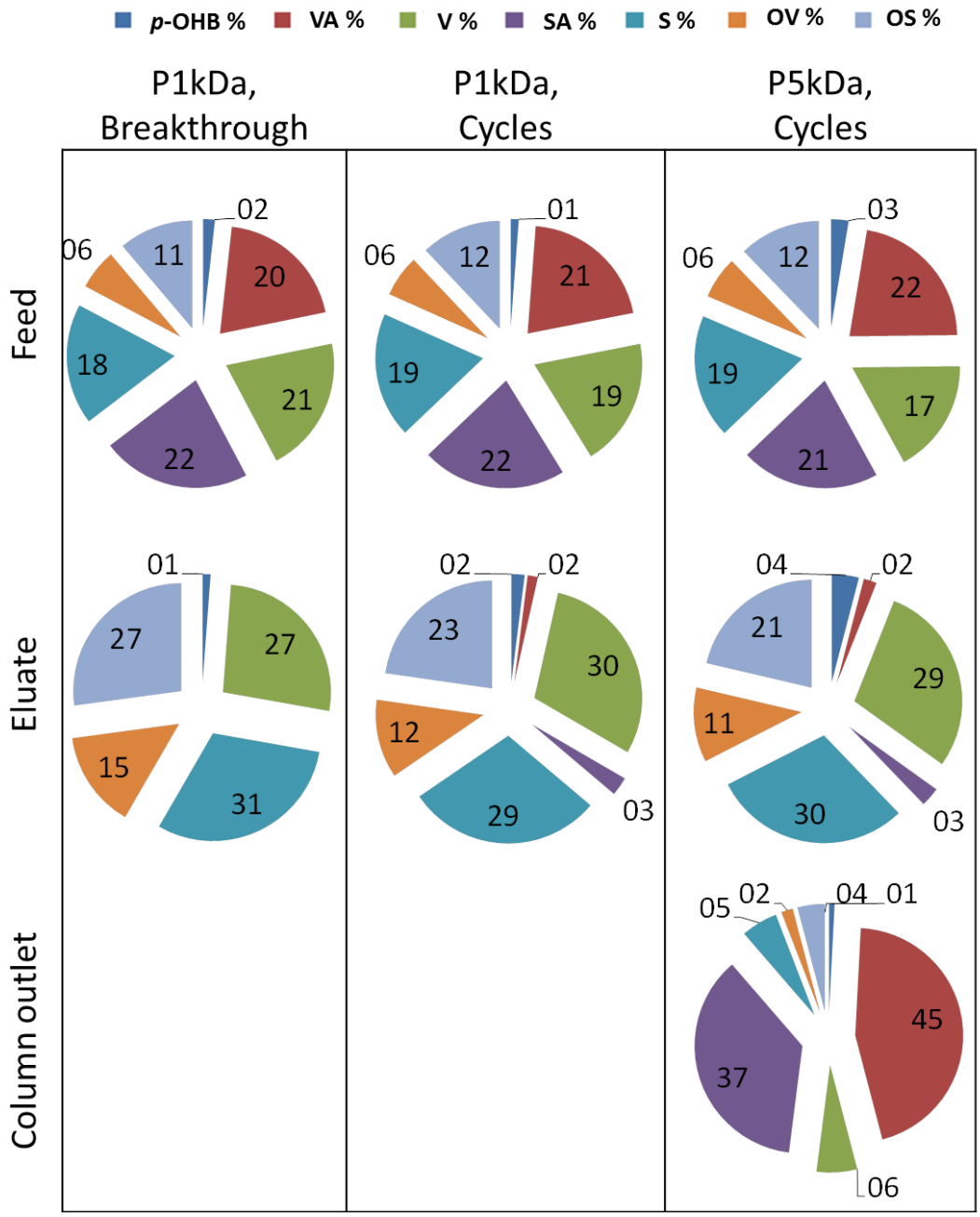

Figure D.6 Relative V, S, OV, OS, VA, SA and p-OHB expressed as wt% of TP for the different streams of the adsorption/desorption cycles studied. Only trace amount of VA and SA are present in eluate P1kDa obtained after complete saturation of the bed, and thus, not detected by HPLC-UV quantification.

E. HPLC-UV analysis of several phenolic compounds

Herein it is presented a typical RP-HPLC UV chromatogram obtained for a synthetic mixture prepared with vanillin (V), syringaldehyde (S), acetovanillone (OV), acetosyringone (OS), vanillic acid (A), syringic acid (SA) and *p*-hydroxybenzaldehyde (*p*-OHB). The analytical column used was an ACE 5 C18-pentafluorophenyl group (250 x 3.0 mm, 5 µm) with a guard column of the same material. Detection length was set to 280 nm and the volume of injection loop was 20 µL. Chromatograms were run at 30 ºC at 0.6 mL min^{-1} using an elution gradient composed is summarized in Figure E.1.

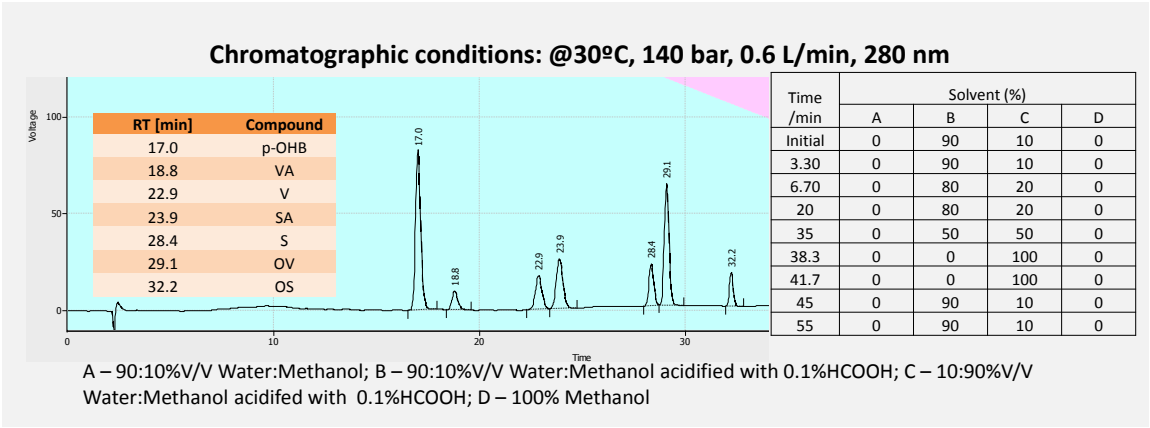

Figure E.1 UV chromatogram of a synthetic mixture prepared with V, S, OV, OS, VA, SA and p-OHB. Analysis was performed in an ACE 5 C18 column with a pentafluorophenyl group (250 x 3.0 mm, 5 µm) at 30 ºC and 6 mL min-1 with the elution gradient indicated at the right side of the chromatogram. Detection was at 280 nm. Retention time of each phenolic compound is summarized in the table indicated at the left side of the chromatogram.

F. Supercritical fluid chromatography

This appendix shows some additional figures to complement the Chapter 6 discussion about SFC studies performed for the analysis of several synthetic phenolic compounds typically found in oxidized industrial kraft liquors.

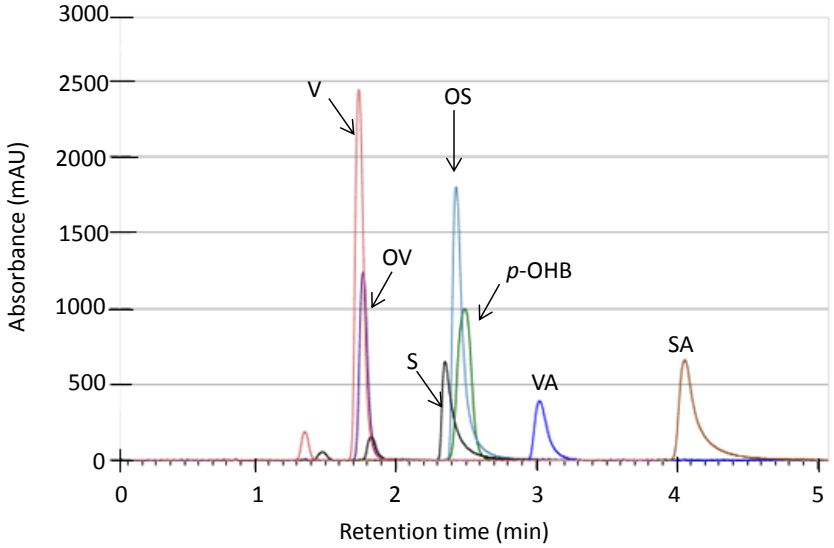

5% Methanol

	Retention time (min)
V	1.74
OV	1.77
S	2.35
OS	2.43
***p*-OHB**	2.49
VA	3.02
SA	4.06

Figure F.1 Overlaid SFC chromatograms of several standard phenolic compounds usually found in oxidized IKL medium: vanillin (V, 1.4 g L^{-1}), acetovanillone (OV, 0.74 g L^{-1}), p-hydroxybenzaldehyde (p-OHB, 1.1 g L^{-1}), syringaldehyde (S, 0.9 g L^{-1}), acetosyringaldehyde (OS, 1.6 g L^{-1}), vanillic acid (VA, 0.9 g L^{-1}), syringic acid (SA, 1.3 g L^{-1}). Other chromatographic conditions: 40 ºC, 150 bar, 5% V/V of methanol, 5 mL min^{-1}.

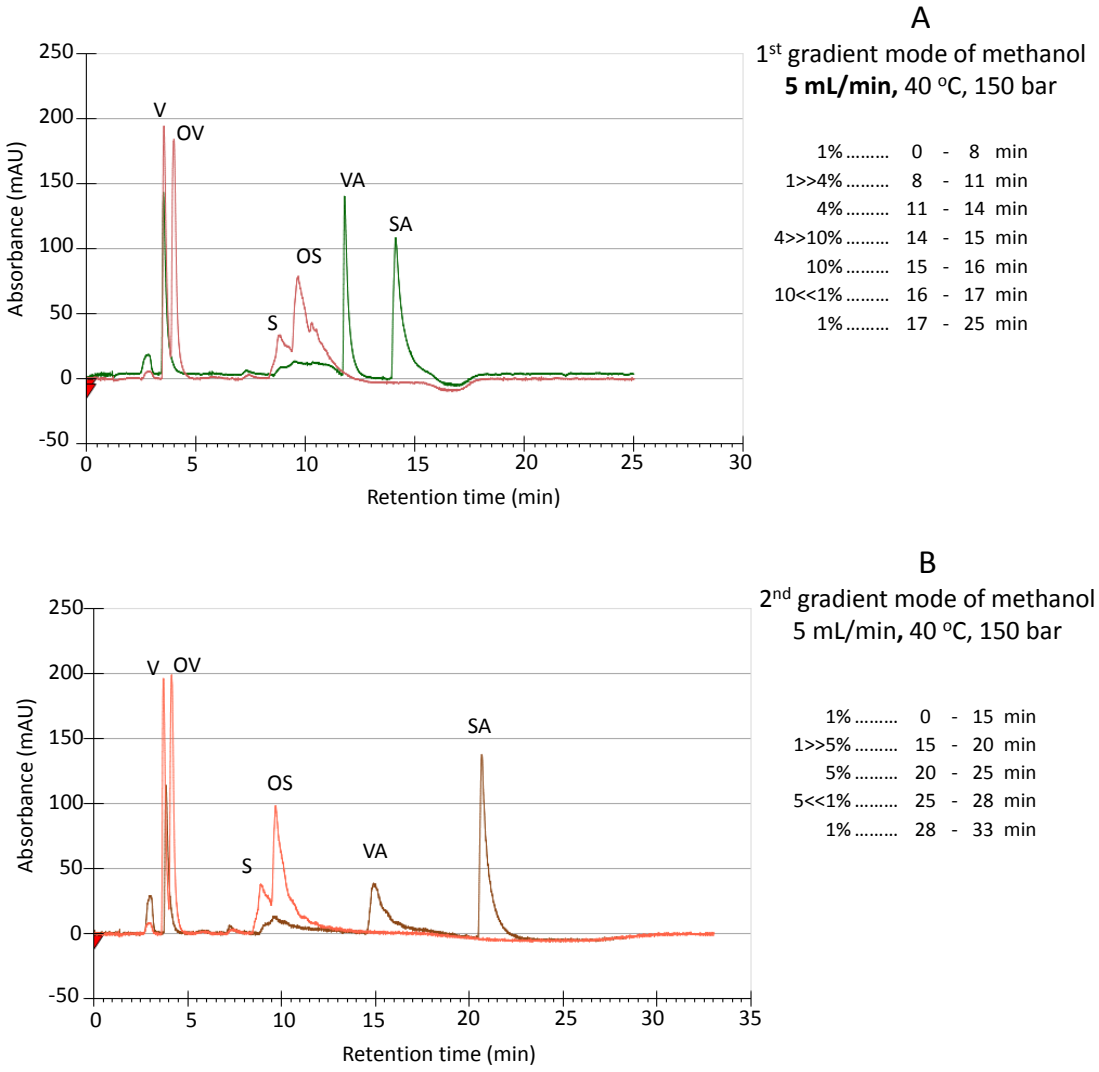

Retention time (min)	1st gradient mode		2nd gradient mode	
	Mixture 1	Mixture 2	Mixture 1	Mixture 2
V	3.54	3.52	3.71	3.84
OV	4.00	-	4.14	-
S	8.97	9.52	8.89	9.65
OS	9.68	-	9.68	-
VA	-	11.8	-	14.9
SA	-	14.12	-	20.66

Figure F.2 SFC chromatograms of synthetic mixtures with for different chromatographic methods of co-solvent gradient. Other chromatographic conditions: 150 bar, 40 °C, 5 mL min^{-1}. Concentration of each compound about 0.6 g L^{-1}.

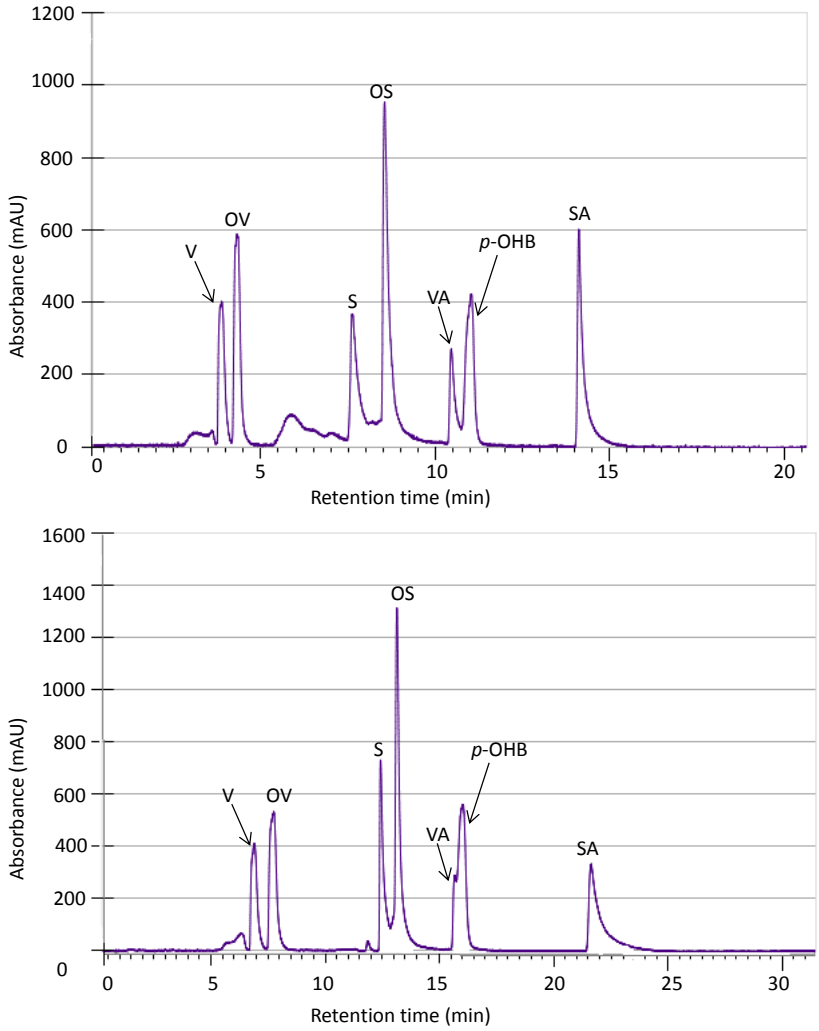

Retention time (min)	3rd gradient 5 mL/min	4th gradient 3 mL/min
V	3.88	6.90
OV	4.31	7.74
S	7.63	12.42
OS	8.55	13.14
VA	10.46	15.66
***p*-OHB**	11.03	16.03
SA	14.12	21.64

Figure F.3 SFC chromatograms of synthetic mixtures for different chromatographic methods of co-solvent gradient. Other chromatographic conditions: 150 bar and 40 ºC; 5 mL min^{-1} for the 3rd gradient mode and 3 mL min^{-1} for the 4th gradient mode. Synthetic mixture prepared with V (3.24 g L^{-1}), OV (3.36 g L^{-1}), *p*-OHB (2.16 g L^{-1}), S (2.54 g L^{-1}), OS (2.74 g L^{-1}), VA (2.04 g L^{-1}) and SA (2.56 g L^{-1}).

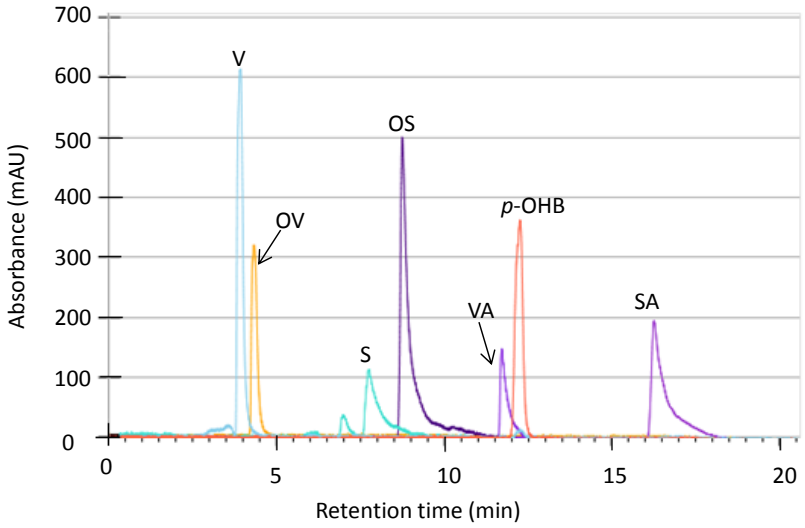

Gradient mode with methanol **5 mL min^{-1}**
40 °C, 150 bar

0.7%	0	-	1	min
0.7>>1%	1	-	2	min
1%	2	-	8	min
1>>2%	8	-	9	min
2%	9	-	15	min
2>>10%	15	-	20	min
10%	20	-	25	min
10<<0.7%	25	-	30	min
0.7%	30	-	40	min

Retention time (min)					
		OV	4.32	**VA**	11.72
		S	7.76	***p*-OHB**	12.26
V	3.92	**OS**	8.74	**SA**	16.25

Figure F.4 Overlaid SFC chromatograms of several standard phenolic compounds usually found in oxidized IKL medium: V, 1.4 g L^{-1}), acetovanillone (OV, 0.74 g L^{-1}), p-hydroxybenzaldehyde (p-OHB, 1.1 g L^{-1}), syringaldehyde (S, 0.9 g L^{-1}), acetosyringaldehyde (OS, 1.6 g L^{-1}), vanillic acid (VA, 0.9 g L^{-1}), syringic acid (SA, 1.3 g L^{-1}). Other chromatographic conditions: 40 °C, 150 bar and 5 mL min^{-1}.